

STRESS RELAXATION AND MECHANICAL PROPERTIES  
OF  
RL-1973 AND PD-200-16  
SILICONE RESIN SPONGE MATERIALS

Final Report  
Contract No. NAS1-13342  
Texas A&M Research Project - RF 3098

NASA-CR-132622) STRESS RELAXATION AND  
MECHANICAL PROPERTIES OF RL-1973 AND  
D-200-16 SILICONE RESIN SPONGE MATERIALS  
Final Report, 6 Jun. 1974 - 28 Apr. 1975  
Texas A&M Research Foundation) 181 p HC

N75-21372  
G3/24 18602  
Unclass

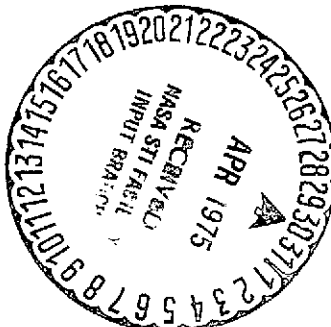
a  
**report** [REDACTED]  
from the Texas A&M  
RESEARCH FOUNDATION  
College Station, Texas

Prepared for  
National Aeronautics and Space Administration  
Langley Research Center  
Hampton, Virginia 23665

by

Texas A&M Research Foundation  
College Station, Texas 77843

April 1975



STRESS RELAXATION AND MECHANICAL PROPERTIES  
OF  
RL-1973 AND PD-200-16  
SILICONE RESIN SPONGE MATERIALS

by

D. Saylak  
J. S. Noel  
J. S. Ham  
R. McCoy

Mechanics and Materials Research Center  
Texas A&M University  
College Station, Texas 77843

Final Technical Report

on

Contract No. NAS1-13342

April 1975

National Aeronautics and Space Administration  
Langley Research Center  
Hampton, Virginia 23665

## FOREWORD

This final report was prepared by the Mechanics and Materials Research Center of Texas A&M University for the National Aeronautics and Space Administration, Langley Research Center under Contract NAS1-13342, "Stress Relaxation and Mechanical Properties of RL-1973 and PD-200-16 Silicone Resin Sponge Materials." Work reported herein was performed under the direction of Mr. A. Chapman who served as the Contracting Officer's technical monitor. Program duration was from 6 June 1974 to 28 April 1975.

The authors wish to acknowledge the contributions of the following individuals who were directly responsible for performing the program tasks and preparing this final report: Research Assistants; W. E. Conger and D. J. Fisher--Civil Engineering, N. Conrad--Aerospace Engineering. Laboratory assistance and data reduction was also provided by M. E. G. Fisher and K. Johnson.

## TABLE OF CONTENTS

	Page
FOREWORD . . . . .	i
LIST OF TABLES . . . . .	iii
LIST OF FIGURES . . . . .	iv
SYMBOLS . . . . .	vi
1.0 INTRODUCTION . . . . .	1
1.1 Purpose . . . . .	1
1.2 Scope and Objectives. . . . .	1
1.3 Background. . . . .	2
2.0 TECHNICAL PROGRAM . . . . .	4
2.1 General . . . . .	4
2.2 Materials . . . . .	4
2.3 Experimental Program. . . . .	5
2.3.1 Sample Preparation . . . . .	5
2.3.2 Apparatus. . . . .	7
2.3.3 Test Methods . . . . .	11
2.3.4 Data Reduction Procedures. . . . .	12
3.0 DISCUSSION OF RESULTS . . . . .	18
3.1 Tangent and Secant Moduli . . . . .	18
3.2 Relaxation Moduli . . . . .	23
3.3 Measurement of Glassy Transition Temperature. . . . .	32
3.4 Failure Data . . . . .	42
4.0 CONCLUSIONS AND RECOMMENDATIONS . . . . .	48
4.1 Conclusions . . . . .	48
4.2 Recommendations for Future Work . . . . .	49
REFERENCES . . . . .	51

## LIST OF TABLES

		Page
TABLE I	Tangent and Secant Shear Moduli for PD-200-16 Foam	21
TABLE II	Tangent and Secant Shear Moduli for RL-1973 Foam	22
TABLE III	Measured Thermal Properties of the Silicone Resin Sponge (SRS) Materials	41

## LIST OF FIGURES

Figure No.	Title	Page
1	Double lap shear specimen.	6
2	Cross-section of low temperature cryostat.	9
3	Typical stress relaxation trace.	13
4	Typical constant rate-to-failure trace.	14
5	Typical stress-strain curve identifying major parameters.	16
6	Initial tangent moduli observed for the PD-200-16 foam. The crosshead displacement rate was 0.05 in/min, (0.127 cm/min).	19
7	Initial tangent moduli observed for the RL-1973 foam. The crosshead displacement rate was 0.05 in/min, (0.127 cm/min).	20
8	Relaxation moduli measured for the PD-200-16 foam. The imposed strain was 1%.	24
9	Relaxation moduli measured for the PD-200-16 foam. The imposed strain was 3%.	25
10	Relaxation moduli measured for the PD-200-16 foam. The imposed strain was 5%.	26
11	Relaxation moduli measured for the PD-200-16 foam. The imposed strain was 10%.	27
12	Relaxation Moduli measured for the RL-1973 foam. The imposed strain was 1%.	28
13	Relaxation moduli measured for the RL-1973 foam. The imposed strain was 3%.	29
14	Relaxation moduli measured for the RL-1973 foam. The imposed strain was 5%.	30
15	Relaxation moduli measured for the RL-1973 foam. The imposed strain was 10%.	31
16	Schematic drawing of dilatometer.	33

LIST OF FIGURES  
(CONTINUED)

Figure No.	Title	Page
17	Curve showing the temperature measured in the dilatometer during a trial test cycle.	36
18	Curve showing the thermal strains as a function of temperature for the RL-1973, Sample 1.	37
19	Curve showing the thermal strains as a function of temperature for the RL-1973, Sample 2.	38
20	Curve showing the thermal strains as a function of temperature for the PD-200-16, Sample 1.	39
21	Curve showing the thermal strains as a function of temperature for the PD-200-16, Sample 2.	40
22	Failure shear stresses and corresponding strains observed for the PD-200-16 at the various test temperatures.	43
23	Failure shear stresses and corresponding strains observed for the RL-1973 at the various test temperatures.	44
24	The stresses at maximum load plotted against the corresponding strains for the PD-200-16.	46
25	The stresses at maximum load plotted against the corresponding strains for the RL-1973.	47

## SYMBOLS

A	shear area, mm <sup>2</sup>
G	modulus, N/m <sup>2</sup>
h	sample thickness, mm
L	sample length, mm
P	load, N
T	temperature, degrees Kelvin (K)
t	time, seconds
W	sample width, mm
$\alpha$	coefficient of thermal expansion, mm/mm/K
$\gamma$	shear strain, mm/mm or %
$\Delta$	sample deformation, mm
$\tau$	shear stress, N/m <sup>2</sup>

### Subscripts:

c	constant
g	glassy
i	initial
m	maximum or failure
o	reference
rel	relaxation
s	secant

## 1.0 INTRODUCTION AND SUMMARY

### 1.1 Purpose

The purpose of this study is to measure stress relaxation characteristics and other mechanical properties of two silicone resin sponge materials over a broad range of cold temperatures well below those anticipated during a space shuttle orbiter mission.

### 1.2 Scope and Objectives

The overall scope of the activity for this project was to furnish personnel, facilities, services, equipment and materials necessary to evaluate the stress relaxation and mechanical properties of two, government-furnished silicone resin sponge materials. Specific objectives included:

- Conduct shear stress relaxation tests at four (4) strain levels and nine (9) temperatures for each material.
- Determine failure properties at nine (9) temperatures and one (1) strain rate not to exceed  $0.005\text{ s}^{-1}$ .
- Evaluate initial tangent modulus, ultimate secant modulus, ultimate strength and strain at failure.
- Determine glass transition temperature,  $T_g$  and coefficient of linear thermal expansion,  $\alpha$ , for each material.
- Publish a final report of test results.
- Return tested samples to NASA-Langley upon completion of the work.

### 1.3 Background

The materials evaluated in this program represent candidates proposed for use as a strain-isolating layer by which the reusable surface insulation (RSI) for the space shuttle orbiter is attached to the shuttle primary structure. The brittle RSI is the baseline thermal protection system for the spacecraft and was developed to withstand severe thermal gradient of the order of 1400 K including temperatures in the cryogenic range.

Two silicone resins which have been processed into low-density sponges are under consideration for use as the strain-isolating bond material. At cryogenic temperatures the materials undergo a transition and become relatively stiff. Since the bondline temperature may remain in the cryogenic range during reentry when the orbiter is being heated, the possibility exists that the strain isolation pad may not perform its required function. To overcome this problem it may become necessary to place a sheet of high modulus material between the silicone sponge layer and the RSI to further minimize excessive induced strain. The addition of this strain arresting plate would increase the weight of the thermal protection system and hence add an additional weight penalty to the entire orbiter and its mission.

Recent work (ref. 1) involving the characterization of the mechanical behavior of silicone elastomers has shown that strain at failure may increase at certain low temperatures. It was also suggested that stiffness values might decrease as the temperature became colder. These behavioral characteristics are contrary to those normally expected in which strain capabilities decrease and moduli increase to relatively constant glassy

values. However, if these behavior characteristics can be substantiated it may be possible to eliminate the strain arresting plate and its attendant weight. The tests and results discussed in this report were designed to provide a resolution of this question.

Supportive tests to establish the linear coefficient of thermal expansion,  $\alpha$ , and glass transition temperature,  $T_g$ , were also conducted on each material to assist in the analysis of experimental results.

## 2.0 TECHNICAL PROGRAM

### 2.1 General

Stress relaxation tests were conducted by loading specimens in double-lap shear to a preselected strain level and monitoring the decay of stress with time. Before performing the test, the specimen temperature was allowed to stabilize. Time to achieve thermal equilibrium was determined by monitoring the output of a thermocouple embedded within a control specimen in the environmental chamber. The selected strain level was applied at a strain rate of  $0.002 \text{ s}^{-1}$  and was maintained for at least one hour while the specimen stress level was recorded. The specimen was then loaded to failure at  $0.002 \text{ s}^{-1}$ . Initial tangent modulus, secant modulus at failure (i.e., at maximum stress), ultimate stress and corresponding strain were determined for each test.

A total of 72 tests on each material were performed as described above; generally, two replicate tests for each condition. Each material was subjected to at least 36 test conditions including the temperatures and strain levels listed below:

Strain levels (4): 1, 3, 5 and 10 percent

Temperatures (9): 100, 125, 150, 175, 200, 225, 250,  
275 and 300 K.

### 2.2 Materials

The two foams studied in this work were silicone based formulations which the manufacturers considered to be proprietary. The General Electric material, PD-200-16, is an open-cell RTV-560 with no other additives but

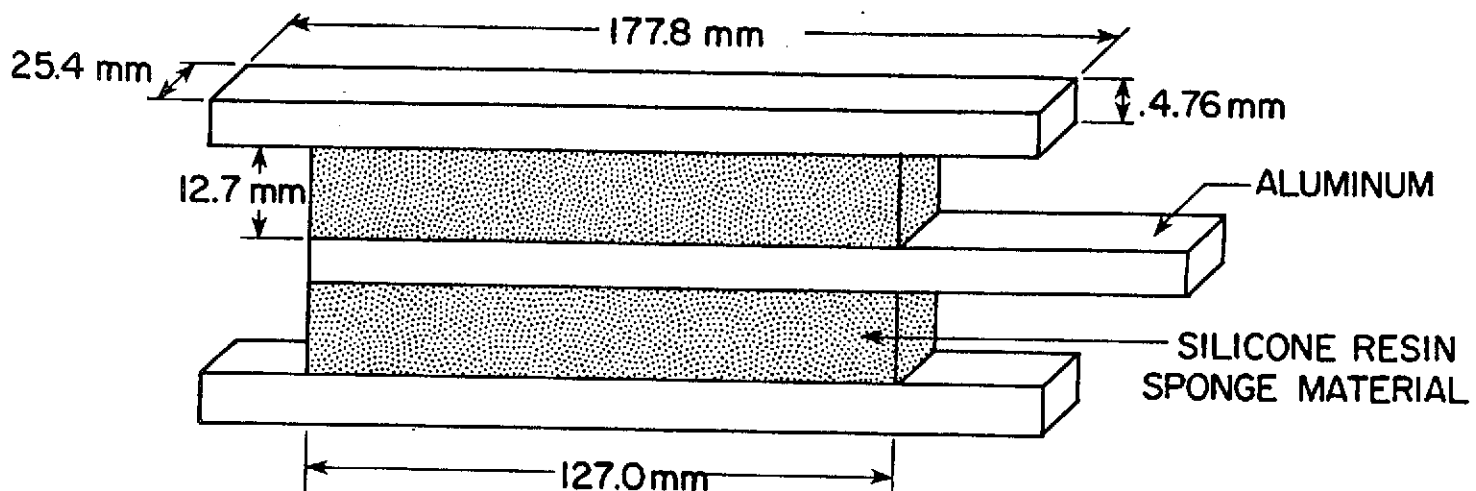
filler and blowing agent. The major constituent is poly(methylphenylsiloxane). The Raybestos Manhattan material, RL-1973, is a closed-cell foam and was also indicated to be a poly(methylphenylsiloxane) with vinyl groups crosslinked with an organic peroxide crosslinking agent. The GE material also contained crosslinking sites and a crosslinking agent which were not specified. Thus, it was impossible to distinguish between these two materials from the chemical descriptions made available (ref. 2). The above information was obtained by telephone conversations with representatives of both GE and Raybestos.

### 2.3 Experimental Program

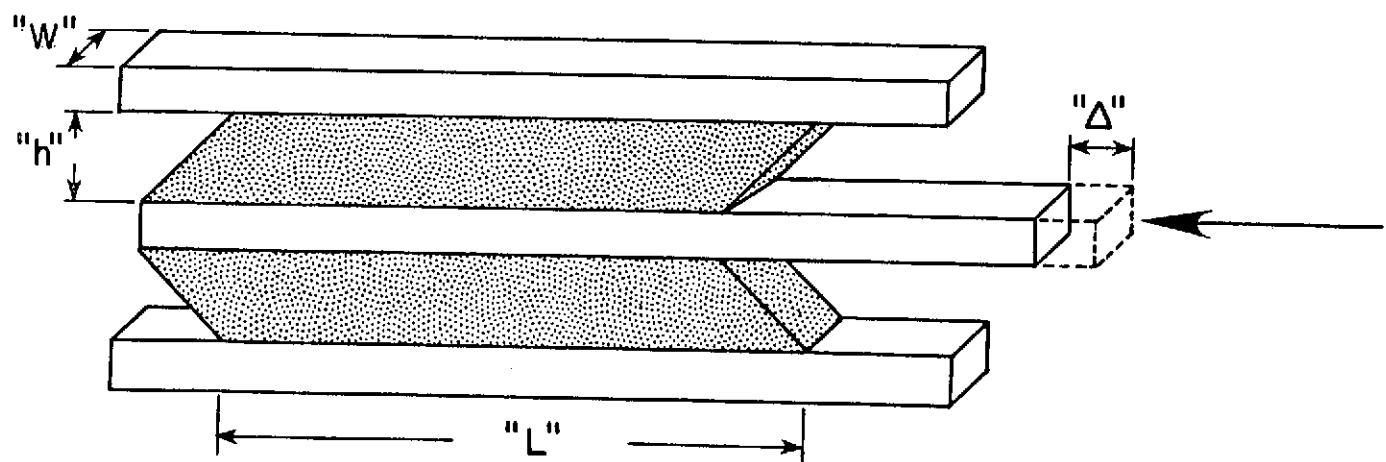
#### 2.3.1 Sample Preparation

The double-lap shear specimen consists of identical pieces of the silicone sponge material (12.7 x 25.4 x 127.0 mm) sandwiched between three aluminum platens (4.8 x 25.4 x 177.8 mm) as shown in Figure 1. The PD-200-16 and RL-1973 samples were bonded in blocks of seven or eight as needed in order to preclude the possibility of a bonding irregularity permeating the entire sample group. Before bonding, the aluminum bars were roughened by sandblasting and degreased with acetone. The bars were coated with SS-400 Primer and allowed to dry for one hour or longer. The RTV-560 adhesive was prepared in accordance with General Electric specifications (ref. 3) using dibutyl tin dilurate as a catalyst.

The aluminum bars were separated with glass slides on a clean paper sheet, and coated with a thin layer of the prepared RTV compound. Initially, dry sheets of the silicone resin foam were attached to this wet



A. UNLOADED



B. LOADED

Figure 1. Double lap shear specimen.

layer and set aside to dry. It was found that the PD-200-16 material bonded well in this manner because of its great porosity. In contrast, the RL-1973 material frequently failed to become thoroughly wetted and, consequently, formed poor bonds. It became necessary to add RTV 560 to both the RL-1973 sponge and the aluminum platen to achieve a secure bond.

After the bars and material were properly positioned and aligned, they were taped to the table to avoid slippage during curing of the adhesive. In accordance with General Electric specifications for the RTV bonding material, the samples were allowed to set for 48 hours at room temperature. They were then taken to an environmental chamber and kept at a constant temperature of 333 K and 25% R.H. for at least 72 hours to ensure complete curing of the bond. The blocks of sample were removed from the environmental chamber and the protruding RTV and silicone foam trimmed from the sides of each sample with razor blades. After the samples had cooled to room temperature, those that were to be tested at temperatures less than 275 K were individually wrapped in dessicated plastic bags to avoid moisture and placed in a freezer at 258 K. Samples used for the warmer temperatures were kept at 296 K and 55% R.H.

### 2.3.2 Apparatus

The primary piece of equipment used to perform the relaxation and failure tests was the Instron Universal Testing Machine. Forces encountered ranged from less than 4.0 N at the warmer test temperatures to more than  $20 \times 10^3$  N at the colder temperatures. At the warmer temperatures, two load cells with maximum ranges 0 to 900 N and 0 to

450 N respectively were used, while at the temperatures below the glassy transition, a 9 MN maximum load cell with a 0 to 225 N full scale maximum sensitivity was used. All loads were recorded on the 254 mm wide motor driven chart of the Instron console.

Linear variable differential transformers (LVDT's) were the primary instruments used to measure sample deformation. The LVDT's employed had a 5 mm total travel with a sensitivity of  $1.27 \times 10^{-3}$  mm per microvolt ( $\mu$ v). The LVDT's were calibrated such that 0.127 mm of deformation (1% strain) produced 1000  $\mu$ v of output. The output of the LVDT's was fed into a signal conditioner and was converted to a digital readout and printed on paper tape. When low temperature conditions caused the LVDT's to malfunction, displacement dials (with total travel of 5 mm) were substituted in their place. The deformations readings were then taken manually.

Thermocouples. All temperatures were determined and monitored by the use of copper-constantan thermocouples. The range of measurable temperatures with this type of thermocouple far exceed the 100 K to 300 K range of this testing program. By coupling the thermocouples into the same signal conditioner mentioned above, it was possible to measure a change in temperature of 0.5 K. Inherent asymmetries in the thermocouple wire allowed an absolute calibration only as close as  $\pm 3$  K.

Cold Chamber. To provide a stable thermal environment necessary to test the properties of the silicone sponge material, a low temperature cryostat was constructed (see Figure 2). The side walls of the chamber were constructed of polystyrene foam and phenolic plates formed

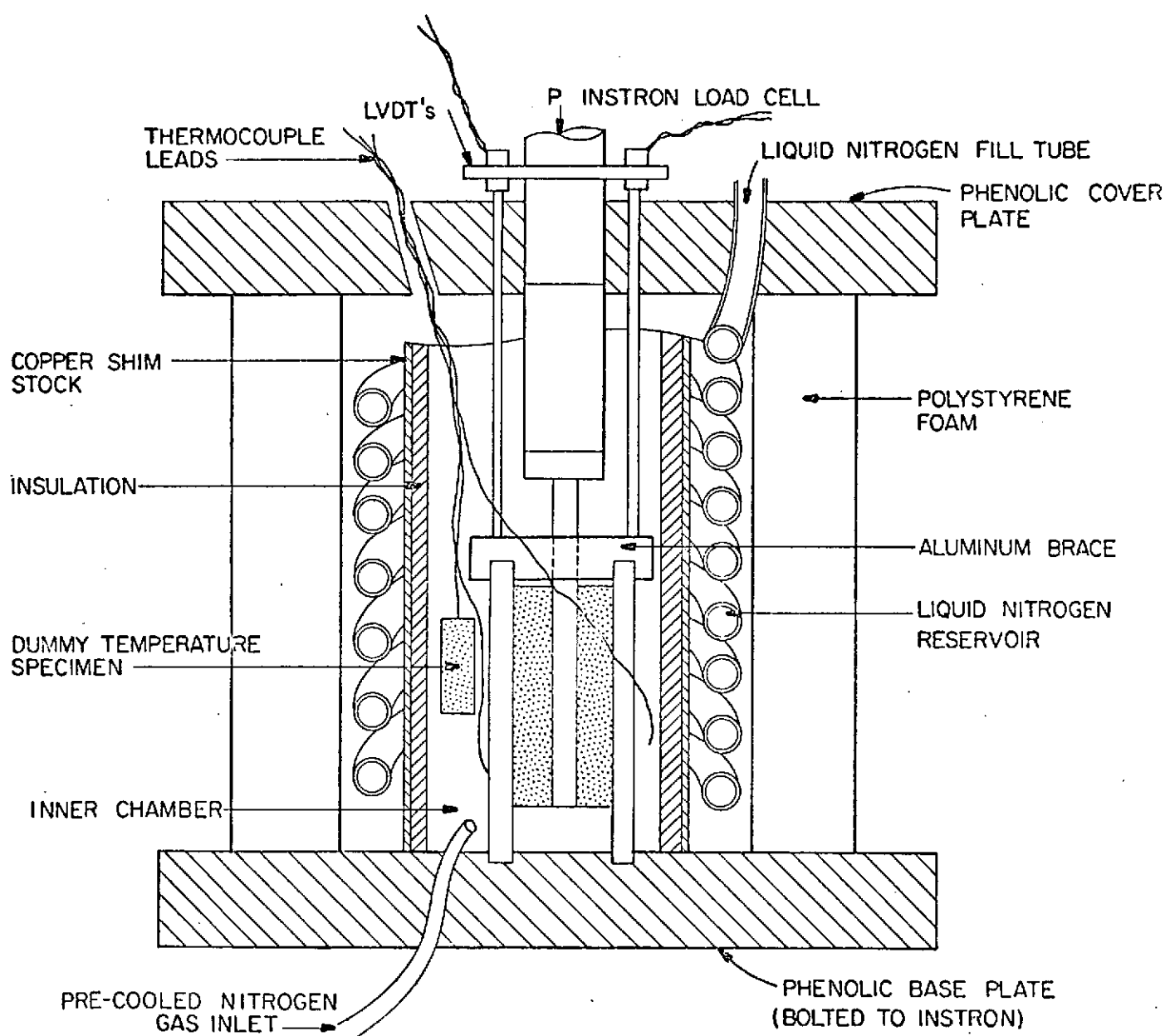


Figure 2. Cross-section of low temperature cryostat.

the base and cover. The inner chamber was constructed using thin sheets of copper shimstock which served three purposes: (1) to add high thermal conductivity in the vertical direction, (2) to avoid the formation of thermal layers within the chamber and (3) to form a reservoir surrounding the sample for the addition of liquid nitrogen into the chamber. In order to precondition the chamber, nitrogen gas, which had been pre-cooled in a liquid nitrogen bath, was introduced into the inner chamber surrounding the sample. The vapor pressure of this cool, dry gas prevented moisture from entering the apparatus and contaminating the specimen. The gas flow rate was kept low enough so as not to disturb the sample, but yet adequate to maintain a continuous circulation. To bring the chamber down to the desired test temperatures, liquid nitrogen was added as needed through a fill tube through the phenolic cover plate. To provide greater stability to the cooling process, a 4 m length of TYGON tubing, through which the liquid nitrogen was fed, was attached to the fill tube and fitted into a coil within the annular space between the chamber wall and the shimstock. Since both open ends of the tube extended outside the chamber, the liquid nitrogen did not come in contact with either the copper or the sample. The low thermal conductivity of the TYGON tubing provided a slow, stable temperature control within the cryostat.

Special walk-in environmental chambers located in the laboratory building were used to perform tests at temperatures of 250 K, 275 K and 300 K. These rooms were large enough to hold the entire test setup and their controlled temperature and humidity made the use of the cryostat described above unnecessary.

### 2.3.3 Test Methods

Before testing, all load cells, LVDT's and thermocouples were calibrated. Liquid nitrogen was poured into the thermal chamber to prepare it for the sample. An aluminum brace was affixed to the top of the sample while in the freezer in its plastic bag. After a wait of 20 to 30 minutes to allow the chamber to cool, the sample was removed from the freezer and transported to the testing apparatus. It was quickly removed from its plastic cover and set into the chamber. Three thermocouples were then inserted into the chamber, two in the space around the sample and one in a dummy sample of the material to be tested. The chamber lid was quickly set in place and the flow of nitrogen gas was initiated. The Instron crosshead was lowered until the load cell push-rod was just touching the center platen of the sample. The apparatus so assembled was allowed to sit for one to two hours to reach the testing temperature and stabilize. Liquid nitrogen was then added to the chamber reservoir as needed to lower the temperature. After approximately 40 minutes, the three thermocouples showed a stable test environment, but at least 20 minutes additional soak time was allowed for each sample. At the end of this waiting period, the LVDT's or displacement dials were attached and zeroed and the crosshead was brought down slightly to cause a slight preload on the sample (no more than one or two percent of the testing load).

To start the test, the crosshead was set in downward motion at a rate of 0.02 mm/s and halted when the desired strain level as indicated by the LVDT's was reached. Deformation, temperature and time were printed out at two minute intervals during the test while loads on the sample were recorded continuously. One of the two thermocouples hanging free in the

chamber was chosen as the reference. The use of the thermocouple in the dummy specimen was discontinued early in the program because it responded too slowly to temperature transients to permit adequate control to be maintained. Liquid nitrogen was added to the reservoir and/or the gas flow to the inner chamber adjusted as necessary to maintain a constant temperature within the chamber throughout the test.

At the end of 60 minutes of test time, the load scale on the Instron was changed and once again the crosshead was set in downward motion at a rate of 0.02 mm/s until the sample failed. Simulated Instron readouts showing typical traces of the relaxation and constant strain rate-to-failure tests are shown in Figures 3 and 4, respectively.

#### 2.3.4 Data Reduction Procedures

The calculations of shear stress,  $\tau$ , shear strain,  $\gamma$ , and shear relaxation modulus,  $G_{rel}(t)$ , for the test specimen shown in Figure 1 were based on the following relationships:

$$\tau = \frac{P}{A} \quad (1)$$

$$\gamma_c = \frac{\Delta}{h} \quad (2)$$

where:

$P$  = applied force, N

$A$  = shear area =  $W \times L$

=  $1/2 (25.4 \text{ mm} \times 127.0 \text{ mm})$

=  $1.6 \times 10^3 \text{ mm}^2$

$\Delta$  = sample deformation, mm

$h$  = thickness of silicone resin

sponge material,

= 12.7 mm

$$G_{rel}(t) = \frac{\tau(t)}{\gamma_c}$$

In addition to the shear relaxation modulus,  $G_{rel}(t)$ , mechanical behavior parameters evaluated for each test included (1) initial tangent

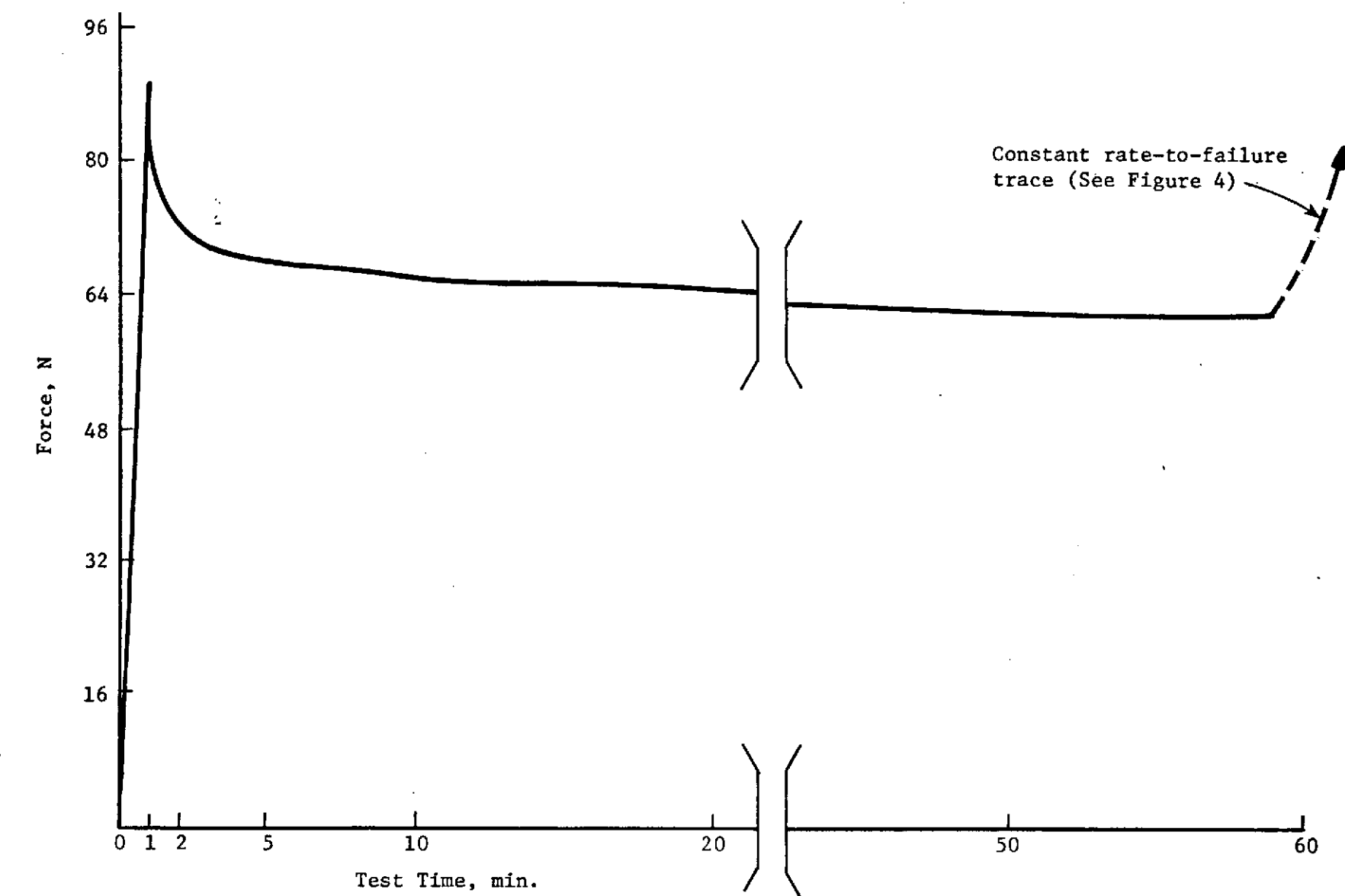


Figure 3. Typical stress relaxation trace.

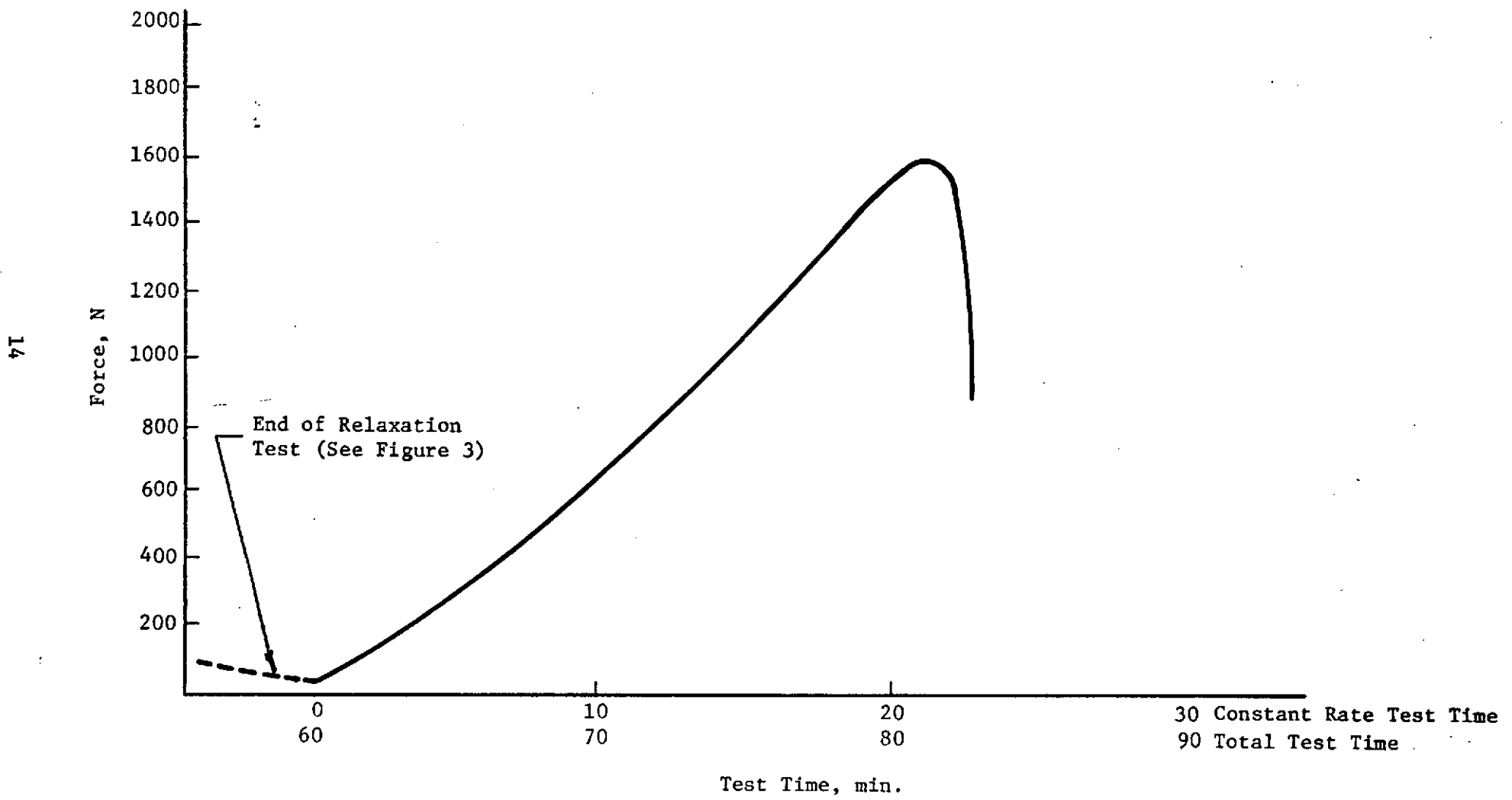


Figure 4. Typical constant rate-to-failure trace.

modulus,  $G_i$ ; (2) stress at failure,  $\tau_m$ ; (3) strain at failure,  $\gamma_m$  and (4) secant modulus at failure,  $G_s$ . The location of these parameters on a typical test curve is shown in Figure 5.

A computer program was generated to calculate these parameters. The format is given in Appendix A and tabulated values are shown in Appendix B. This program also used the Compudyne plotter which generated the stress-strain curves for each test also given in Appendix B. At least 15 points were used to generate each of these curves.

The initial tangent modulus reported herein is the average slope exhibited by the stress-strain curve prior to relaxation (as indicated by the vertical off-set in Figure 5). This was used to minimize any inconsistencies which would have been introduced by employing the slope of the stress-strain curve through the origin because of the frequent existence of a toe or positive curvature in the initial portion of the traces.

As shown in Figure 5, failure for the calculation of  $\tau_m$ ,  $\gamma_m$  and  $G_s$  was assumed to occur at the point of maximum load. The rupture point was not used because there was no way of determining how or exactly when the sample first began to tear while it was in the test chamber. To calculate the secant modulus,  $G_s$ , the final loading trace (i.e., after relaxation) was extrapolated to the strain axis with a curve drawn parallel to the original trace as shown in Figure 5. The maximum stresses and strains were then measured from that point. This procedure would not be expected to effect the failure properties since the strain levels at failure were usually large compared to those imposed during relaxation.

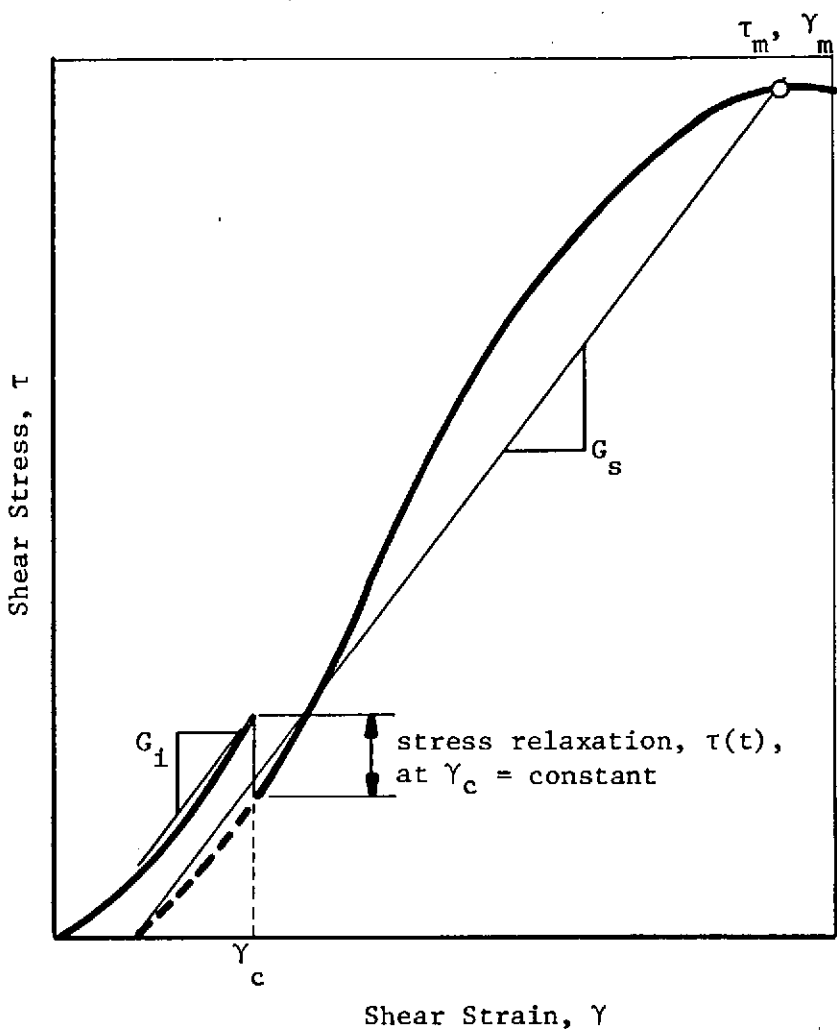


Figure 5. Typical stress-strain curve identifying major parameters.

In keeping with kinetic theory for rubbers (ref. 4) the stress and stiffness values are presented in their temperature reduced form, e.g.  $G_{\text{rel}}(T_0/T)$ , where  $T_0$  and  $T$  are the absolute values of the reference and test temperatures, respectively. This correction becomes more significant the greater the difference between  $T_0$  and  $T$ . The reference temperature,  $T_0$ , used for this correction was 300 K.

### 3.0 DISCUSSION OF RESULTS

For discussion purposes the test data for each of the two materials, PD-200-16 and RL-1973, were divided into four convenient categories: (1) tangent and secant moduli, (2) relaxation moduli, (3) thermal properties and (4) failure properties.

#### 3.1 Tangent and Secant Moduli

The values measured for the tangent modulus,  $G_t$ , and the secant modulus,  $G_s$ , are shown in Tables I and II for the PD-200-16 and RL-1973 materials, respectively. The values shown at each temperature represent the arithmetic average of the three to eight tests run at that temperature. As stated earlier, the initial tangent modulus represents the average slope exhibited by a given stress-strain curve prior to the relaxation test.

The data points plotted in the graphs of Figures 6 and 7 represent the individual test values of the tangent moduli. The tangent modulus values shown in Tables I and II, which as stated above, are averages of the measured values, served as guides for drawing the broken lines shown on the graphs. Both the tables and the figures illustrate a phenomenon that was demonstrated by nearly all the data for both materials. As the samples were cooled below room temperature they tended to remain quite more compliant (indeed PD-200-16 became more compliant). The modulus of the PD-200-16 material decreased somewhat below the room temperature values as the temperature decreased to about 175 K. With further decrease in temperature the modulus rapidly increased about two orders of magnitude.

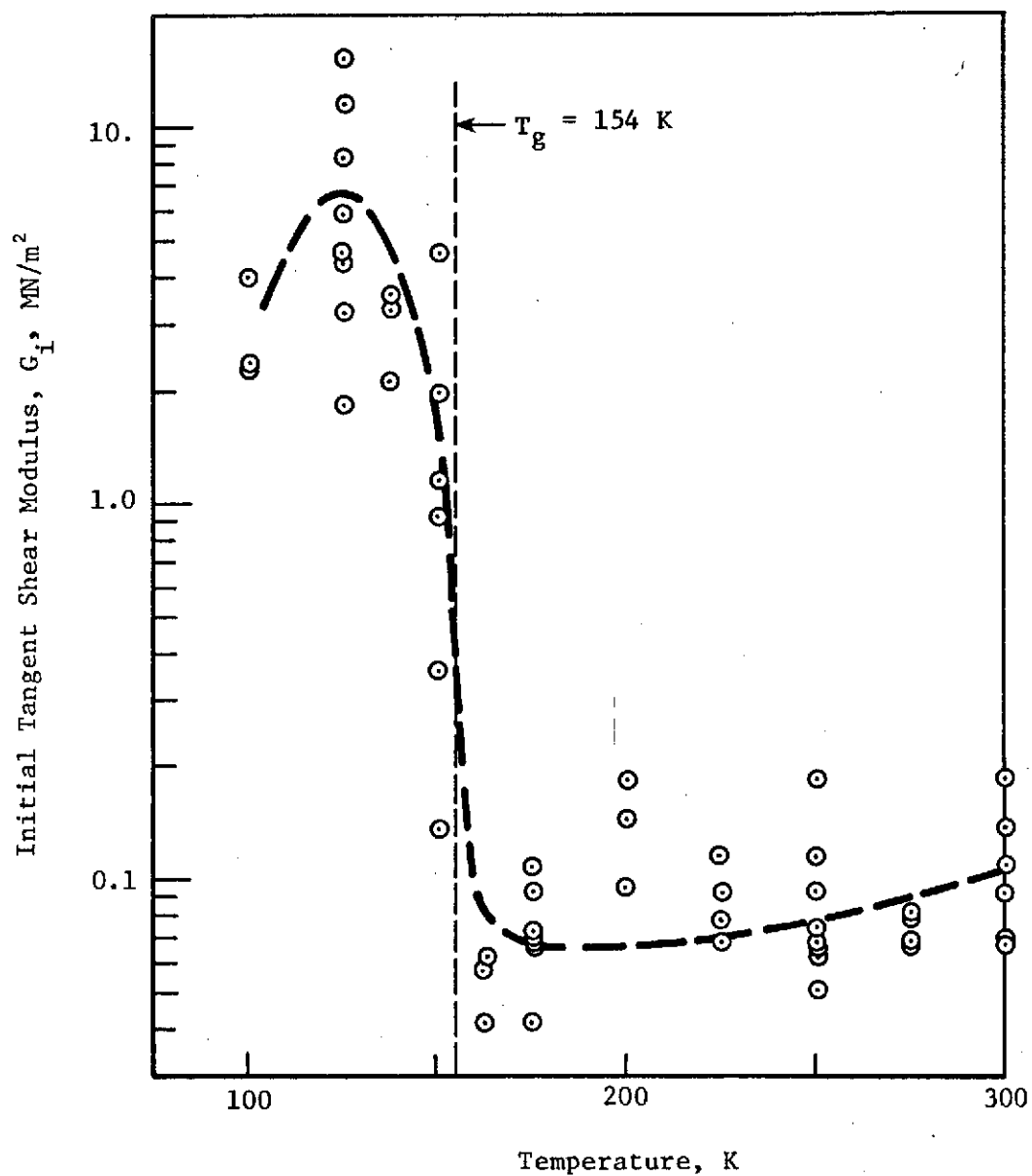


Figure 6. Initial tangent moduli observed for the PD-200-16 foam. The crosshead displacement rate was 0.05 in/min, (0.127 cm/min).

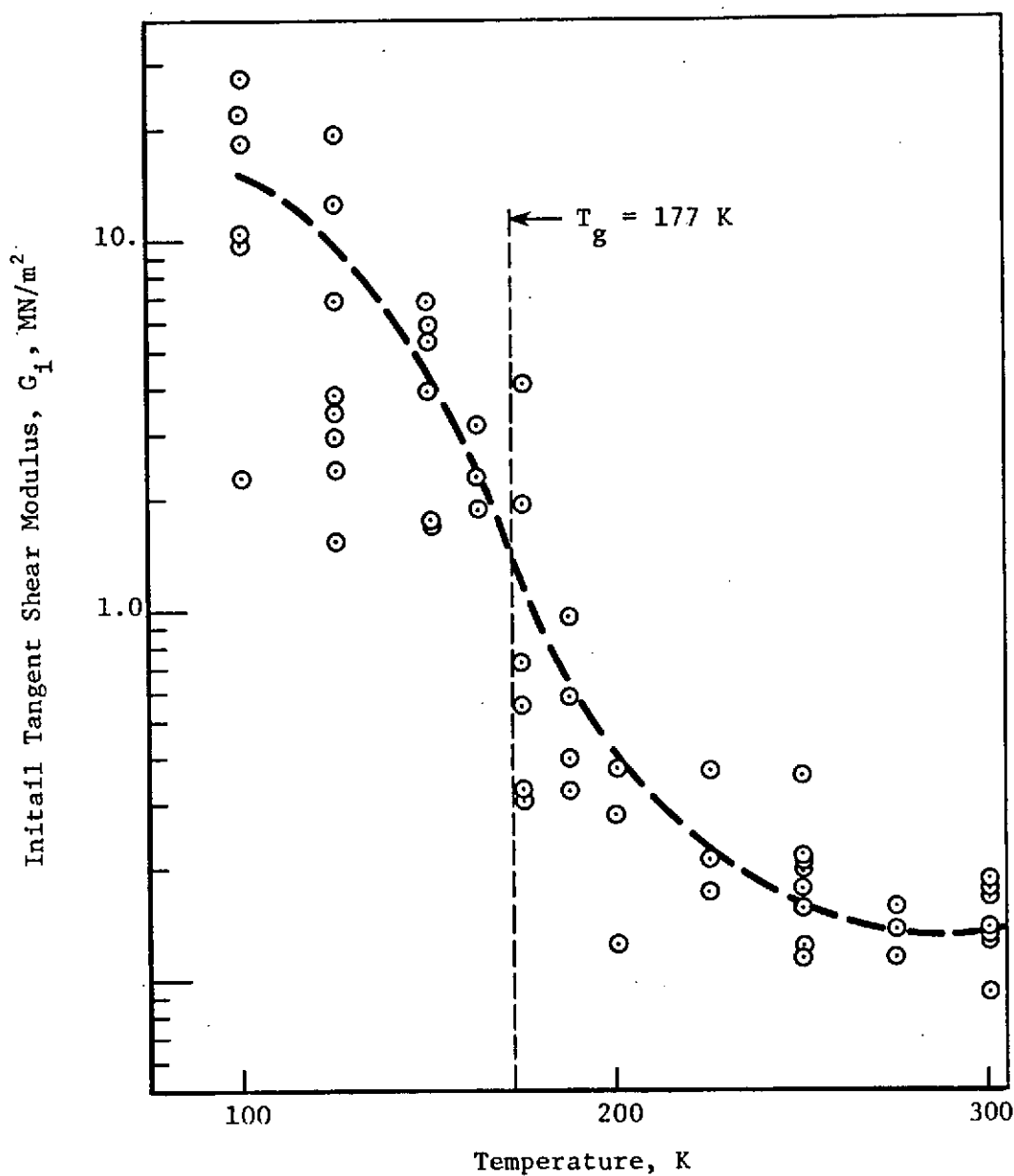


Figure 7. Initial tangent moduli observed for the RL-1973 foam.  
The crosshead displacement rate was 0.05 in/min, (0.127 cm/min).

TABLE I. Tangent and Secant Shear Moduli for PD-200-16 Foam.  
 These Moduli Represent the Averages for All Tests Run at the  
 Specified Temperature.

Test Temperature ( K )	Tangent Modulus $G_t$ (N/m <sup>2</sup> )	Secant Modulus $G_s$ (N/m <sup>2</sup> )
300	110,000	209,000
275	74,000	120,000
250	89,000	203,000
225	88,000	138,000
200*	141,000	175,000
175	74,000	242,000
163*	54,000	1,840,000
150	1,520,000	3,630,000
138*	3,000,000	10,600,000
125	7,350,000	12,900,000
100*	2,860,000	11,500,000

\*The average of three tests only.

TABLE II. Tangent and Secant Shear Moduli for RL-1973 Foam.  
These Moduli Represent the Averages for All Tests Run at the  
Specified Temperature.

Test Temperature ( K )	Tangent Modulus $G_t$ (N/m <sup>2</sup> )	Secant Modulus $G_s$ (N/m <sup>2</sup> )
300	141,000	209,000
275*	137,000	111,000
250	192,000	227,000
225	280,000	190,000
200*	256,000	418,000
188	570,000	918,000
175	1,300,000	1,910,000
163*	2,460,000	1,310,000
150	4,240,000	11,300,000
125	6,640,000	18,200,000
100	15,000,000	18,200,000

\*The average of three tests only.

At temperatures lower than 125, the stiffness of PD-200-16 decreased with further decrease in temperature as shown in Figure 6 by the curve representing the best fit of the data. The modulus of RL-1973, in contrast changed only slightly at temperatures as low as 250 K. But below 250 K the stiffness increased gradually with decreasing temperature until it reached values as high as PD-200-16.

### 3.2 Relaxation Moduli

Shear relaxation modulus is plotted versus time in Figures 8 through 11 for PD-200-16 and in Figures 12 through 15 for RL-1973. Each figure represents one imposed strain level so that four graphs are shown for each material, one for 1, 3, 5 and 10% strain. Data for at least nine temperatures ranging from 100 to 300 K are shown in each figure. In most instances two intermediate temperatures in the neighborhood of the transition temperature are also included.

As can be seen, both materials are very compliant in shear. Here as in all test the PD-200-16 could be characterized as having about half the stiffness of the RL-1973 at most temperatures. Both materials show only slight relaxation through the 60 min. test duration at both the cold and warm extremes. Only at the intermediate temperatures is there an indication of a greater slope to the log-log relaxation curve. These intermediate temperatures, interestingly enough, are near the transition temperatures identified by thermal expansion tests as described in Section 3.3 below.

No correlation between the strain level of the relaxation test and the measured relaxation modulus was observed.

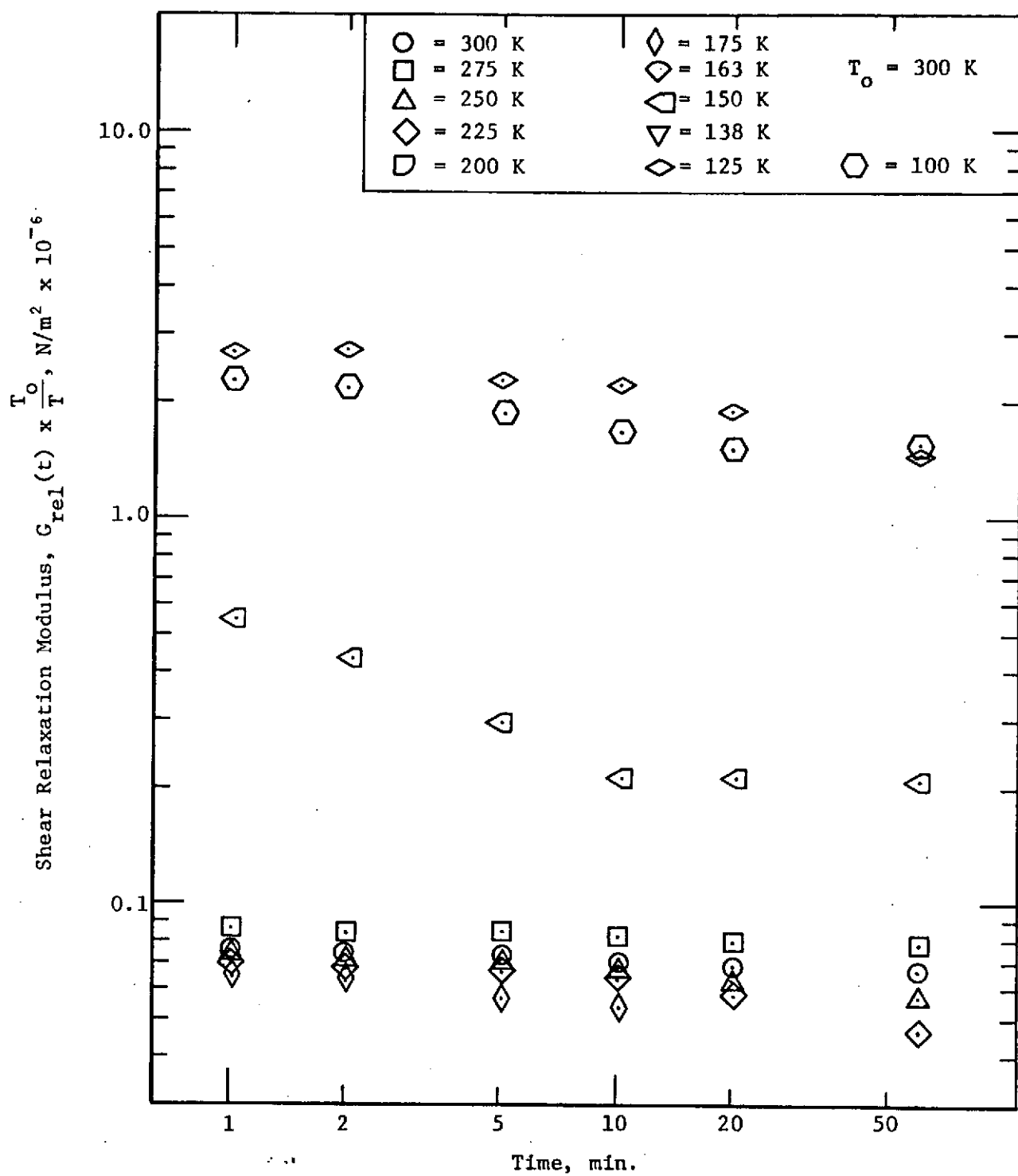


Figure 8. Relaxation moduli measured for the PD-200-16 foam. The imposed strain was 1%.

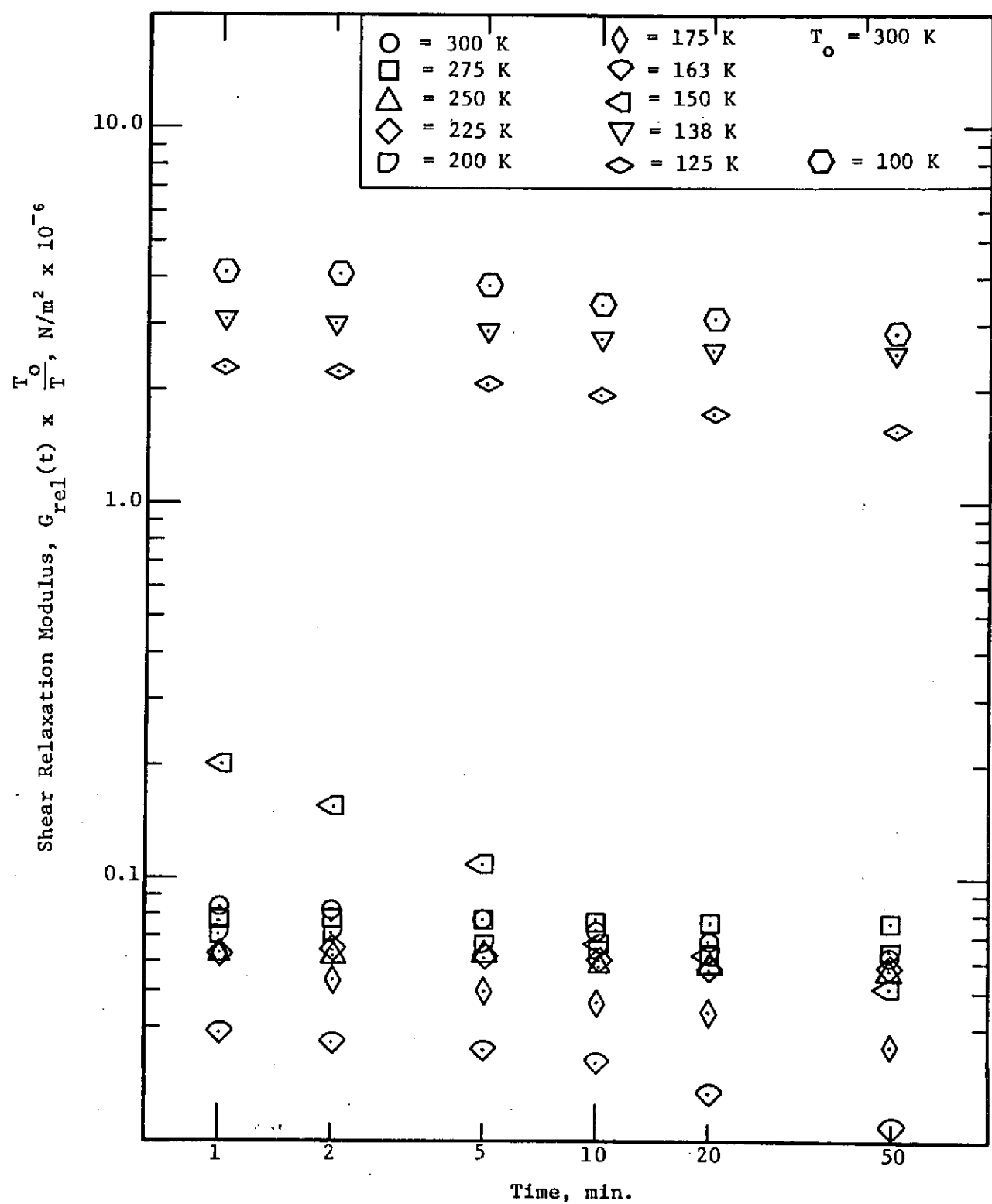


Figure 9. Relaxation moduli measured for the PD-200-16 foam. The imposed strain was 3%.

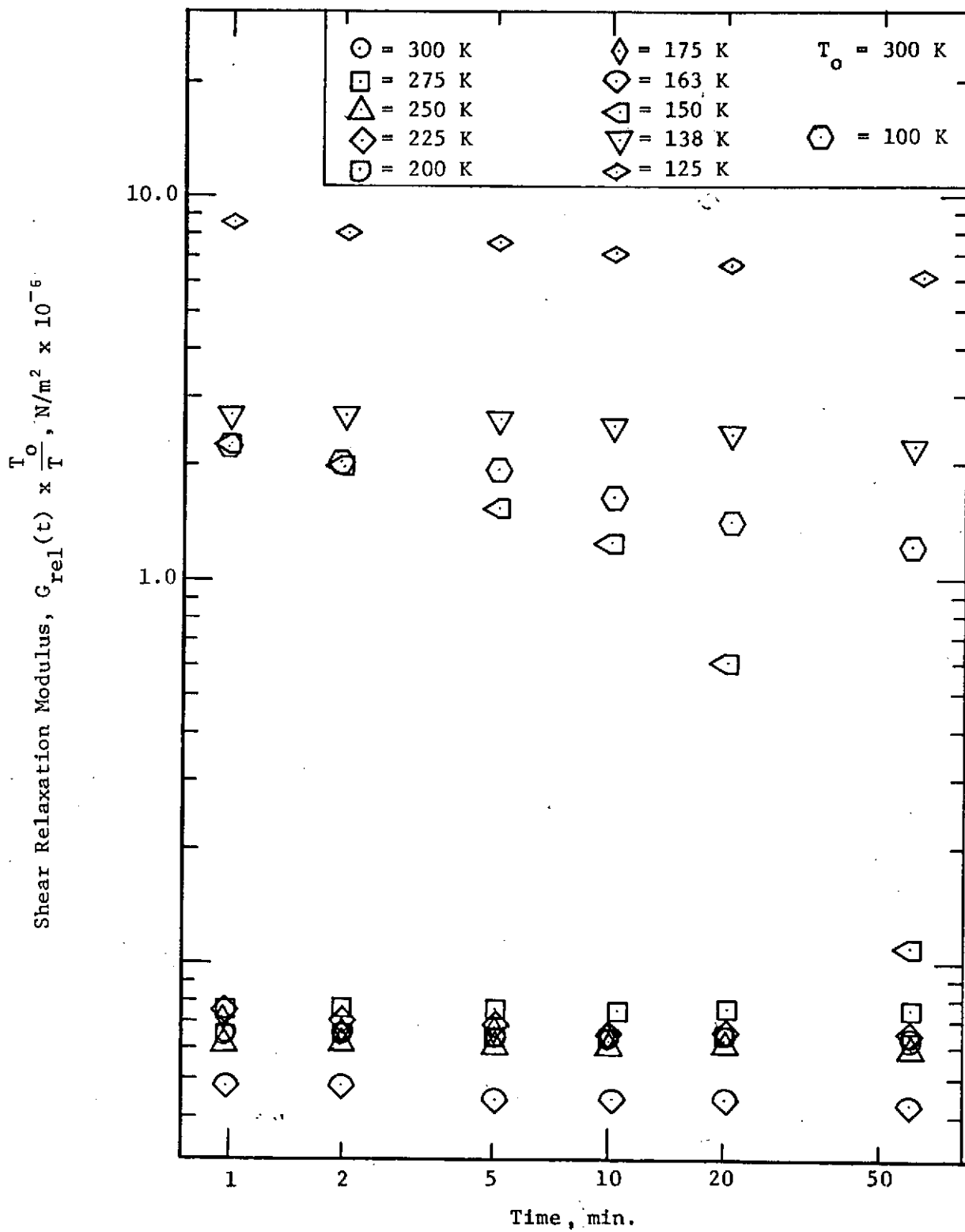


Figure 10. Relaxation moduli measured for the PD-200-16 foam. The imposed strain was 5%.

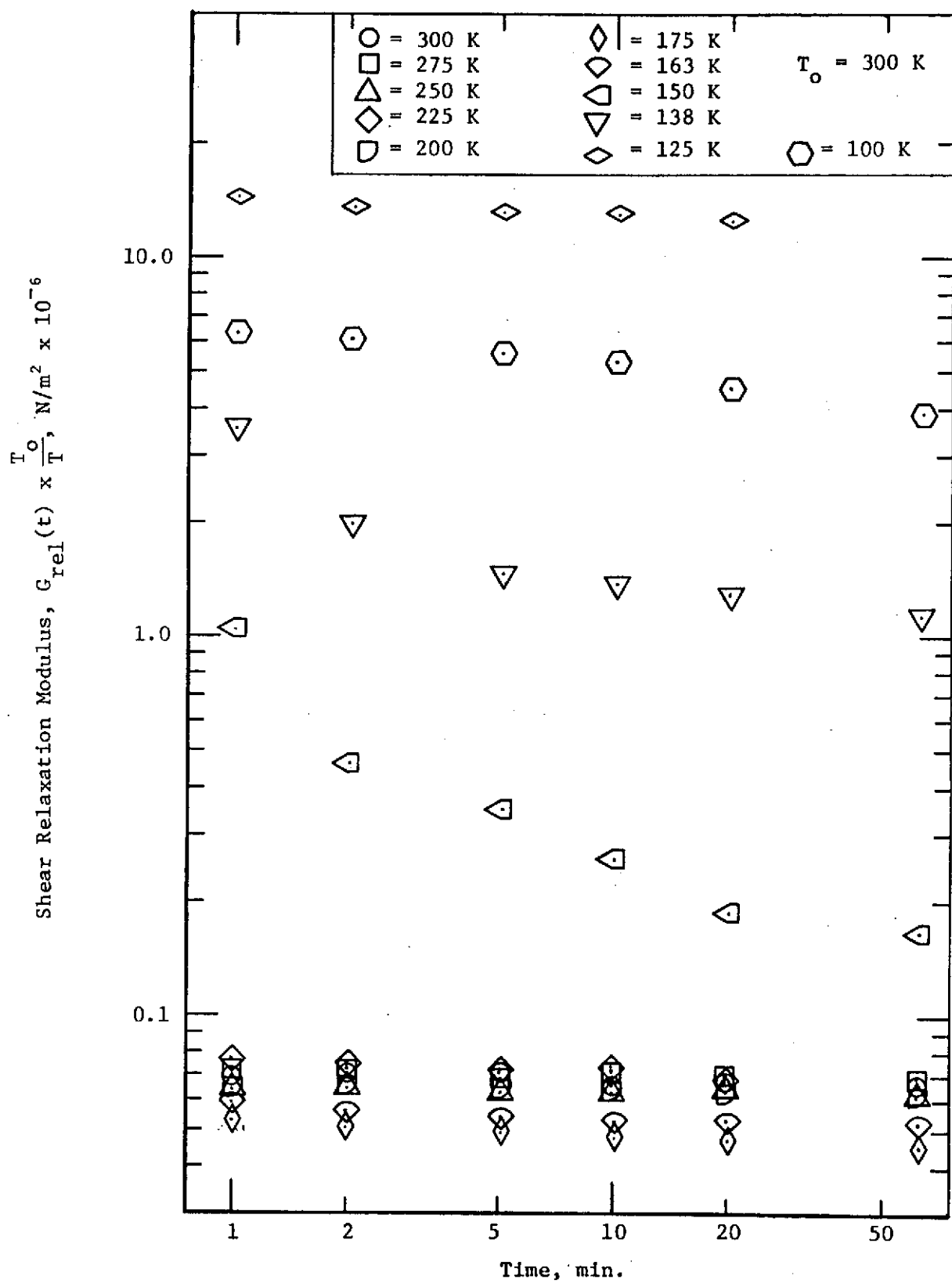


Figure 11. Relaxation moduli measured for the PD-200-16 foam. The imposed strain was 10%.

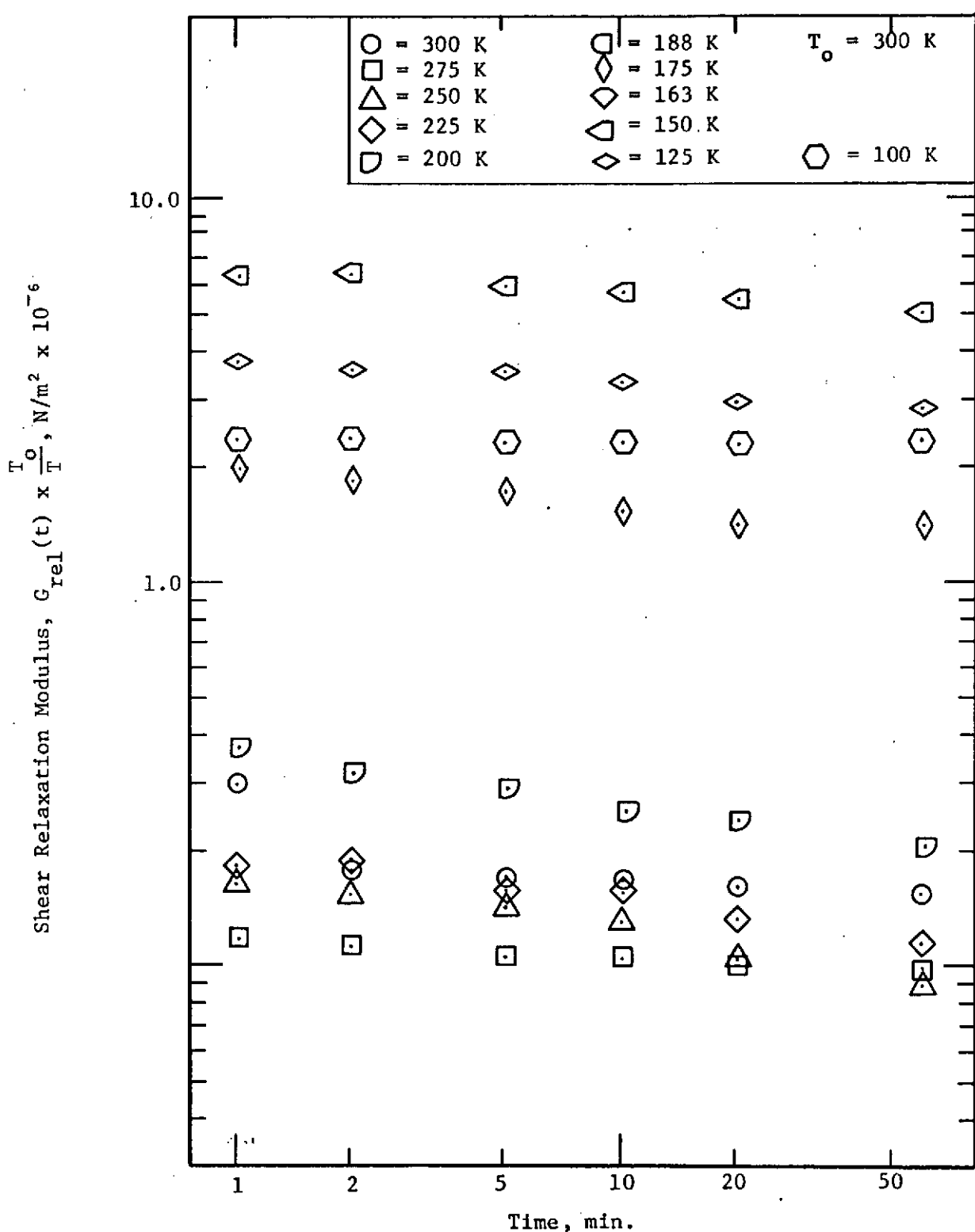


Figure 12. Relaxation Moduli measured for the RL-1973 foam. The imposed strain was 1%.

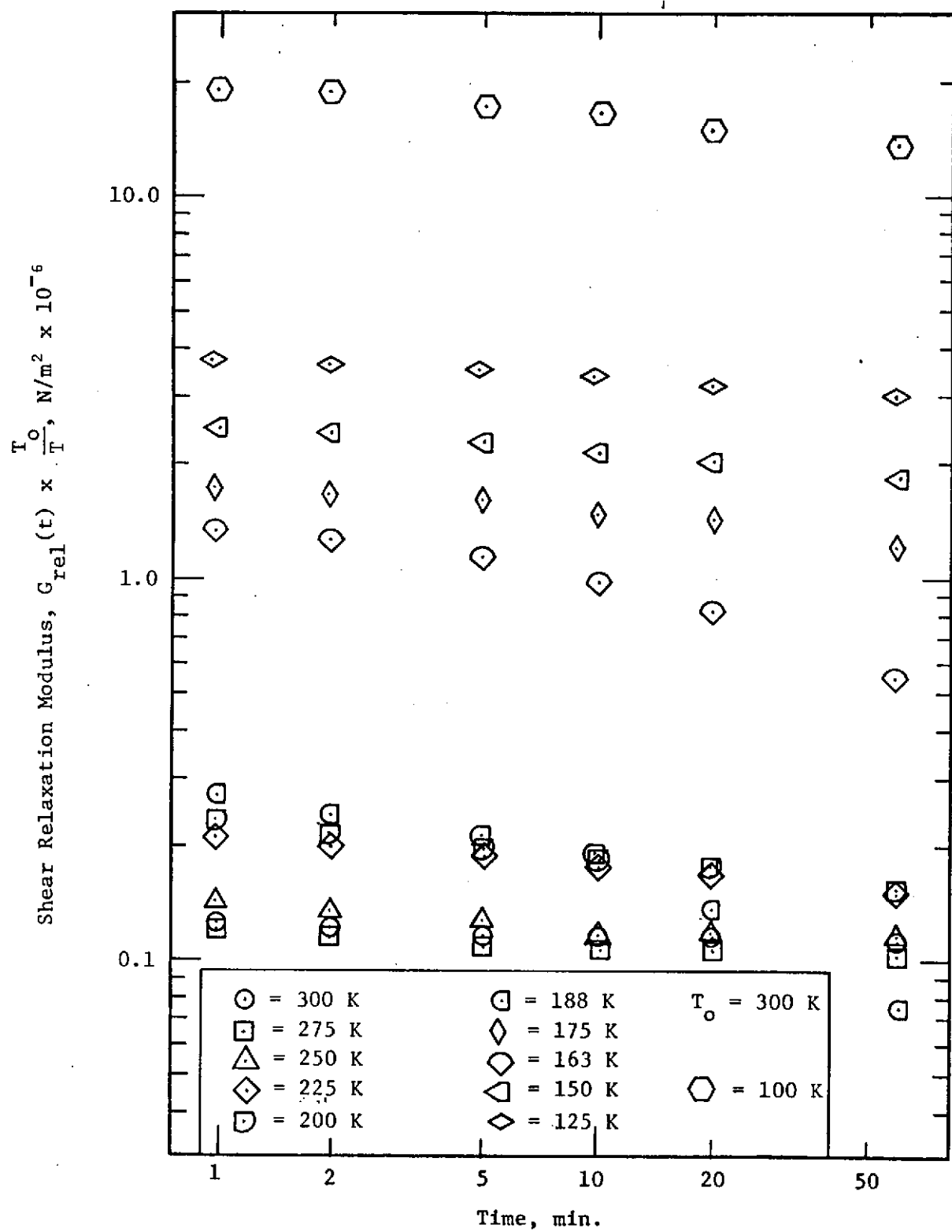


Figure 13. Relaxation moduli measured for the RL-1973 foam. The imposed strain was 3%.

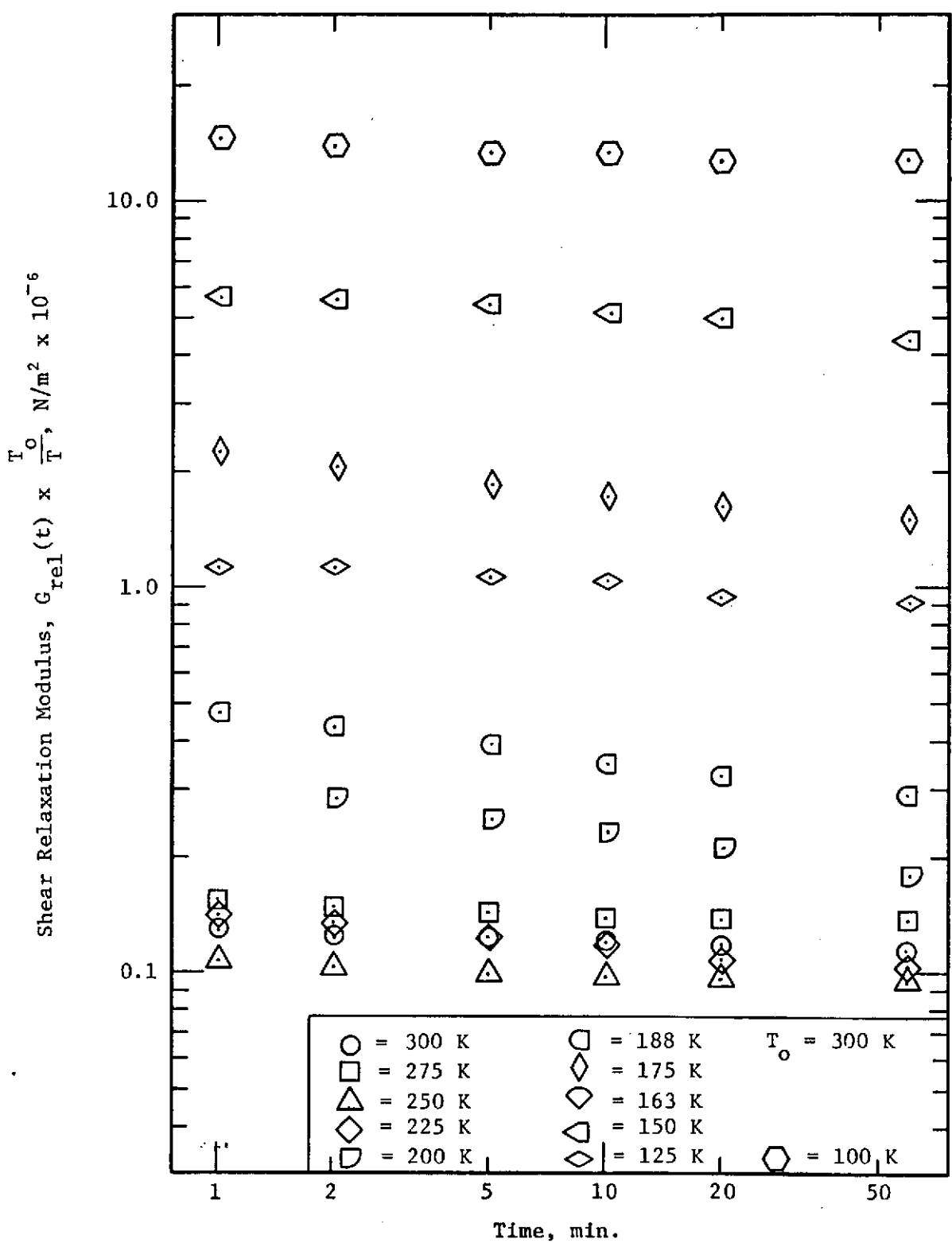


Figure 14. Relaxation moduli measured for the RL-1973 foam.  
The imposed strain was 5%.

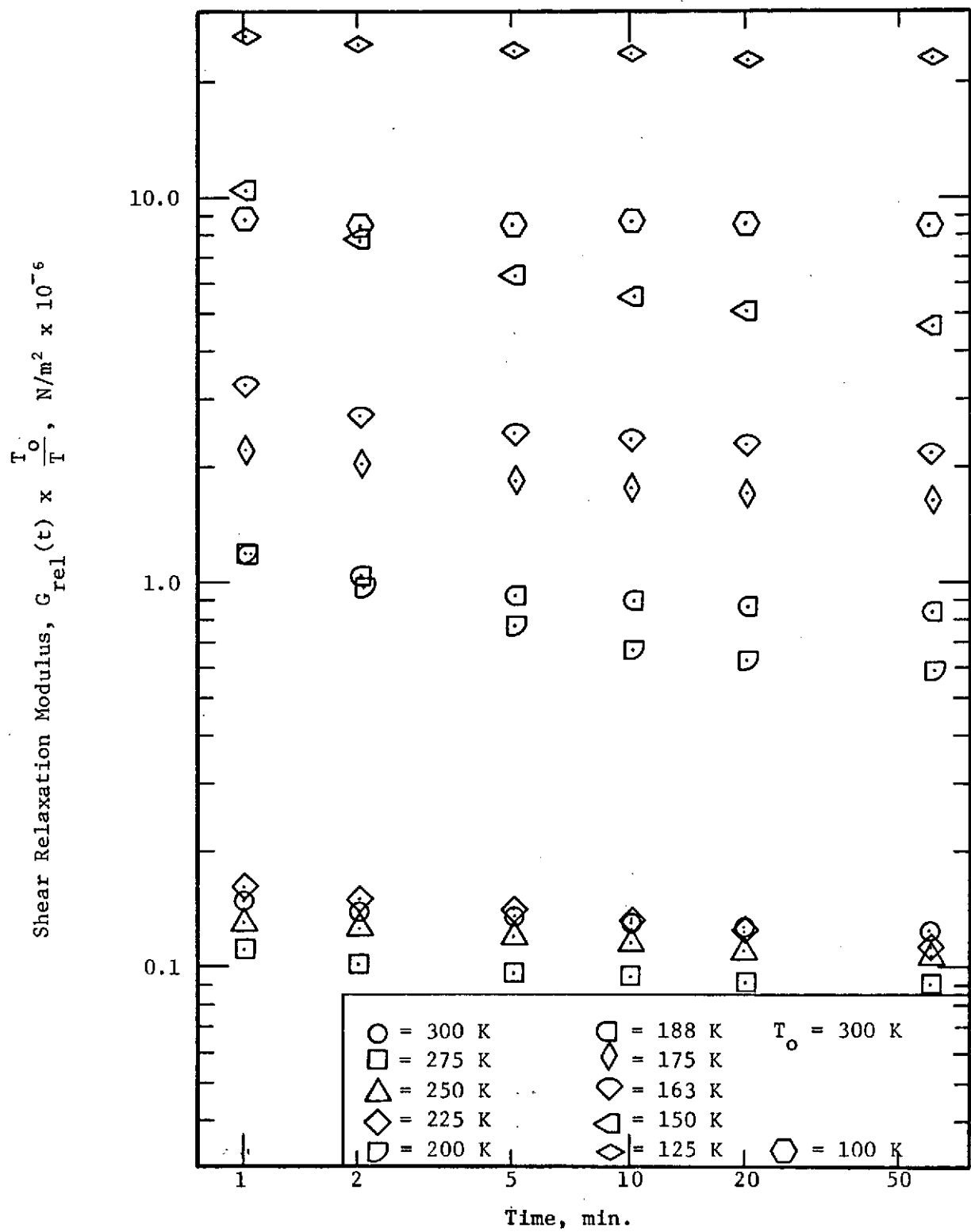


Figure 15. Relaxation moduli measured for the RL-1973 foam. The imposed strain was 10%.

The trends of the shear relaxation moduli with temperature appear to correlate exactly with those indicated by the initial tangent moduli as discussed in Section 3.1 above. Initial tangent and relaxation modulus data for the PD-200-16 exhibit the same decreasing stiffness with decreasing temperature to well below 200 K. Similarly the RL-1973 shows only a slight tendency to stiffen as temperature decreases to about 225 K.

Further, three out of four strain levels give an indication that the PD-200-16 stiffness might be decreasing at the lowest temperature (100 K). However, the great scatter inherent in the data continues to cloud this conclusion. It might be noted that two of the four figures indicate the same phenomena for the RL-1973.

### 3.3 Measurement of Glassy Transition Temperature

To measure the linear coefficients of thermal expansion,  $\alpha$ , and the glassy transition temperature,  $T_g$ , a dilatometer quite similar to that described in ASTM D 696-44 was constructed. (See Figure 16.) The apparatus is very nearly identical to that described in the JANNAF Solid Propellant Mechanical Behavior Manual (ref. 5).

The device consists of a large styrofoam solid with an oversized cavity into which a  $6 \times 10^{-3} \text{ m}^3$  stainless steel beaker is placed. The space surrounding the beaker serves as a liquid nitrogen bath which is used to cool the beaker and its contents. The beaker contains a massive

**NOTE:** Unless Otherwise Noted,  
All Dimensions Given in  
Millimeters

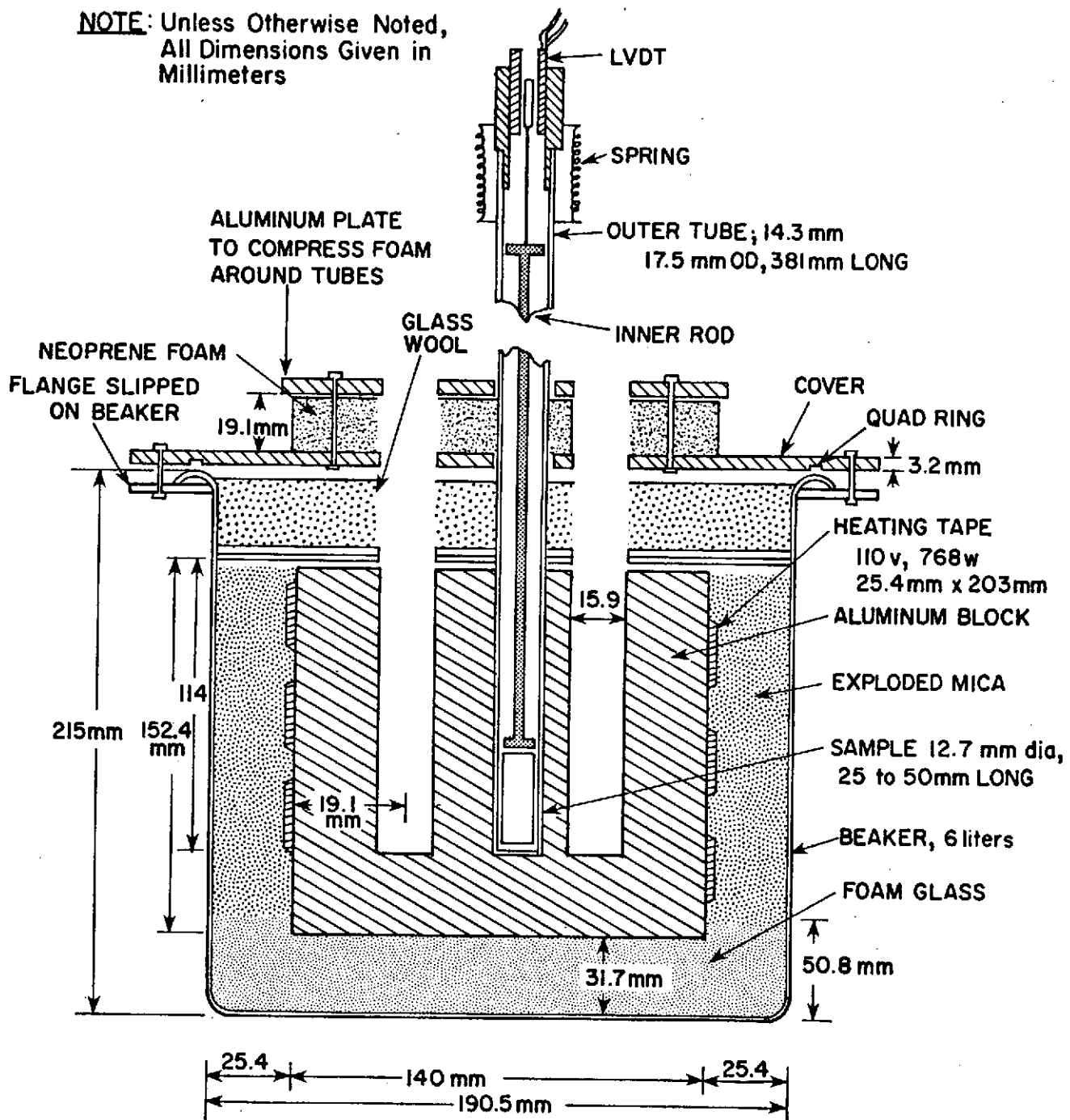


Figure 16. Schematic drawing of dilatometer.

aluminum block heavily insulated from the beaker, thus isolating the block from rapid or erratic temperature fluctuations caused by the nitrogen. To prevent nitrogen vapor from spilling over the top of the beaker and disturbing the even temperature distributions in the core, a cover plate, sealed with a Quad-ring, was used. Three holes were drilled through the lid, through the insulation and well into the aluminum core. Quartz tubes containing the test samples were inserted into these cavities. A Neoprene foam sheet was laid on top of the beaker cover with undersized holes for the quartz tubes to form a seal against the ambient air. A center hole provided the cavity for the thermocouples required to control and monitor the temperature.

Specimens of the material to be tested were machined to 13 mm x 13 mm x 51 mm long and placed in the bottom of the quartz tubes. Then small, light quartz rods with flat bakelite feet were inserted in the tubes over the specimen as indicated in Figure 16. The vertical movement of these rods, reflecting the expansion and contraction of the specimen, were measured with small linear variable differential transformers mounted at the top of the tube.

Once the apparatus was assembled and readied, a test cycle was performed to determine whether or not the cooling and heating rates would be satisfactory (<1 K/min). Further, one of the quartz rods was positioned against the bottom of a quartz tube without a sample in place. The resulting output gave a system error characteristic of the device for which a correction could subsequently be made when reducing data.

A plot of temperatures versus time for this trial run is shown in Figure 17. The device inherently cools at a faster rate than it warms, but in both instances the rates were well below 1 K/min. The lowest temperature recorded during the trial run was 160 K while the test plans were to go as low as 123 K. Therefore, the cooling portion of the cycle was continued for a longer duration to extend the lower excursion.

The conduct of the actual tests were performed with two specimens, one of each material. Two such tests were conducted. The outputs of both the thermocouples and LVDT's were sensed and recorded on paper tape at 900 second intervals.

Figures 18 and 19 indicate the results of the tests for the RL-1973, and Figures 20 and 21 for the PD-200-16 silicone resin sponges. The thermal strains, defined as the change in length divided by the original length, are plotted versus temperature. The data were collected both during the cooling and warming portion of tests so hysteresis accounts for a significant portion of the apparent scatter.

Two straight lines were drawn through the data points for each material and their slopes were calculated to give the linear (as opposed to volumetric) coefficients of thermal expansions. It is evident that the straight lines fit the test data for the PD-200-16 sponge better than for the RL-1973. The intersection of the two lines on each graph indicates the value of the glassy transition temperature. These results are summarized in Table III.

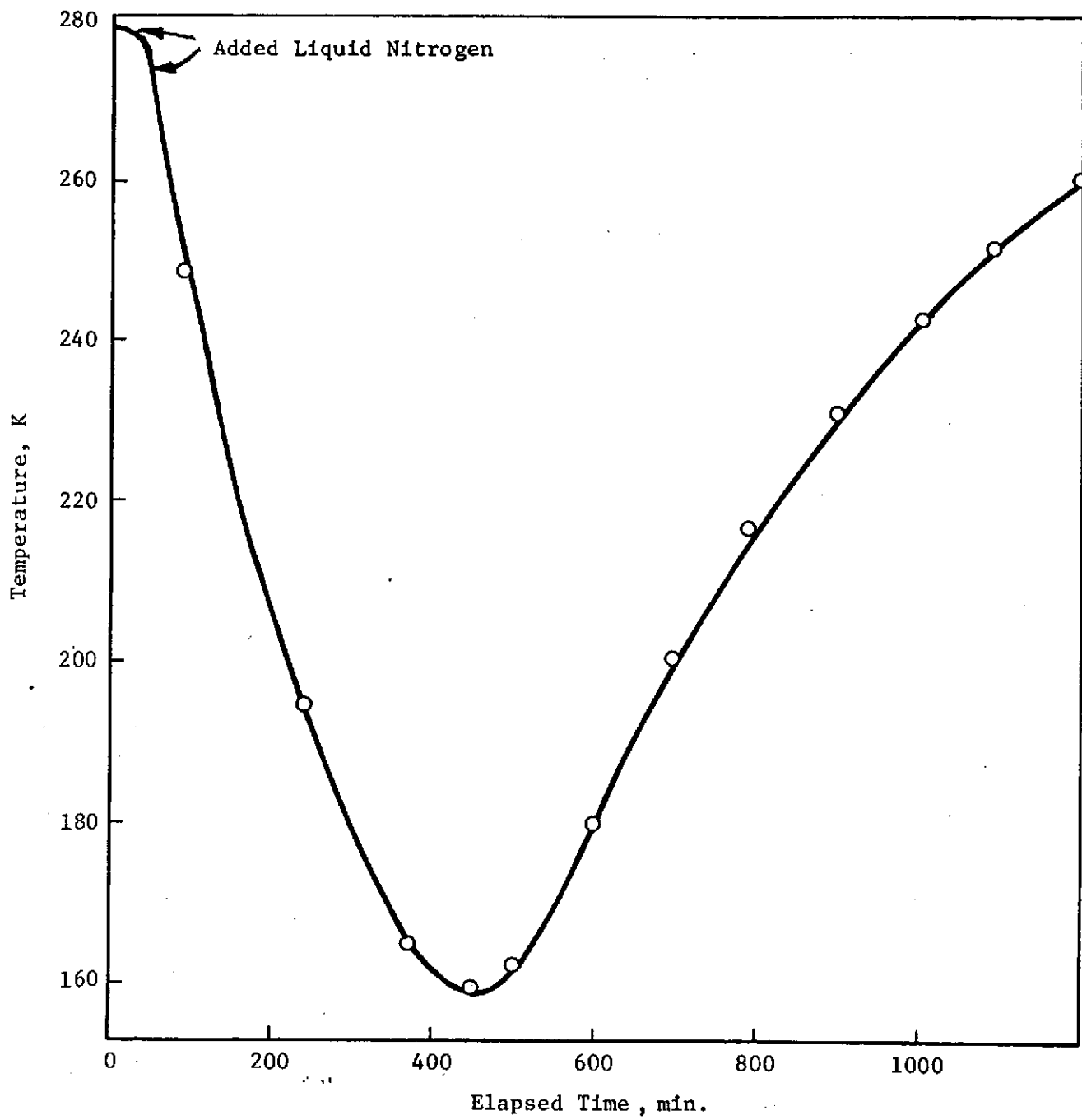


Figure 17. Curve showing the temperature measured in the dilatometer during a trial test cycle.

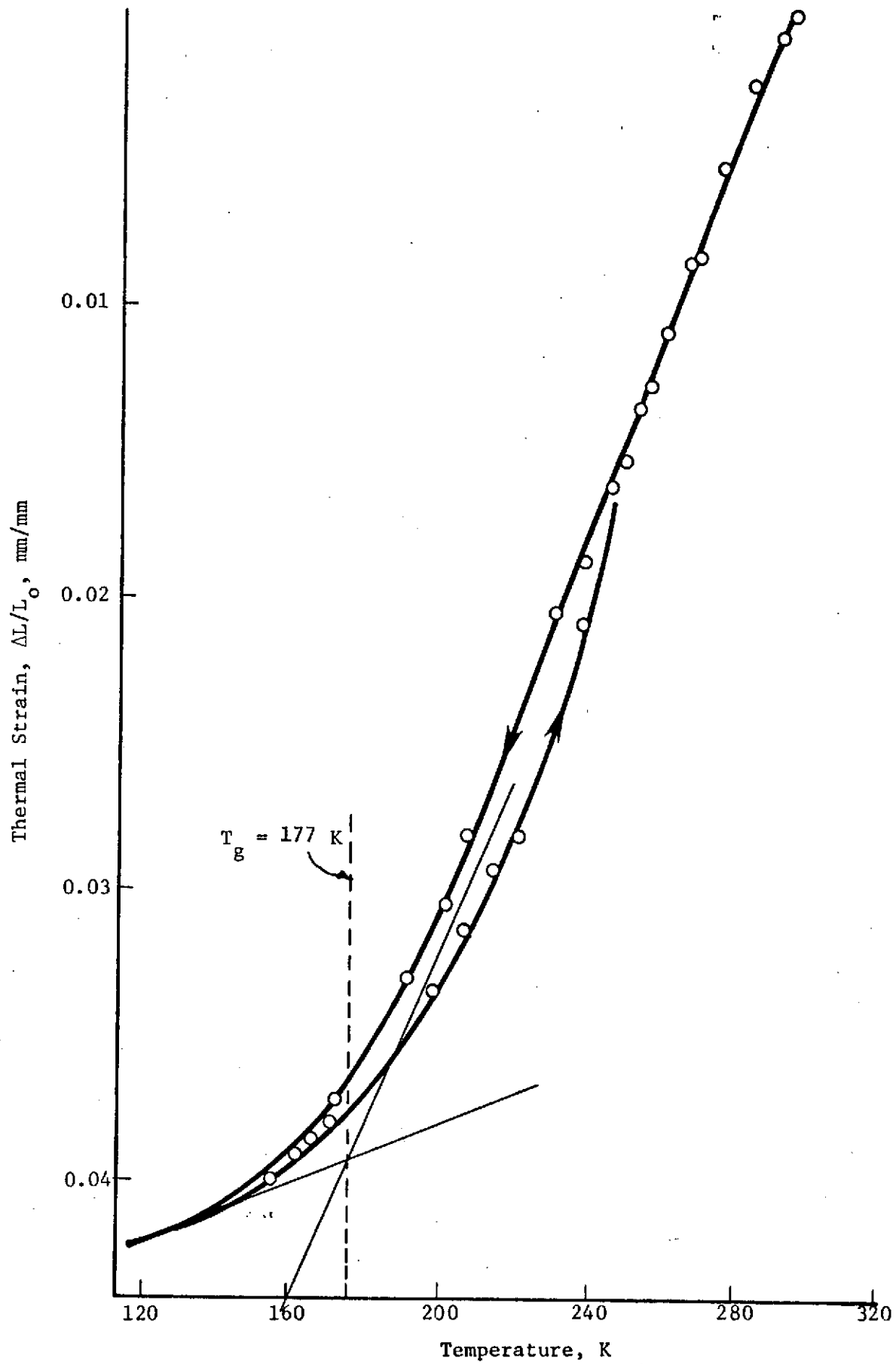


Figure 18. Curve showing the thermal strains as a function of temperature for the RL-1973, Sample 1.

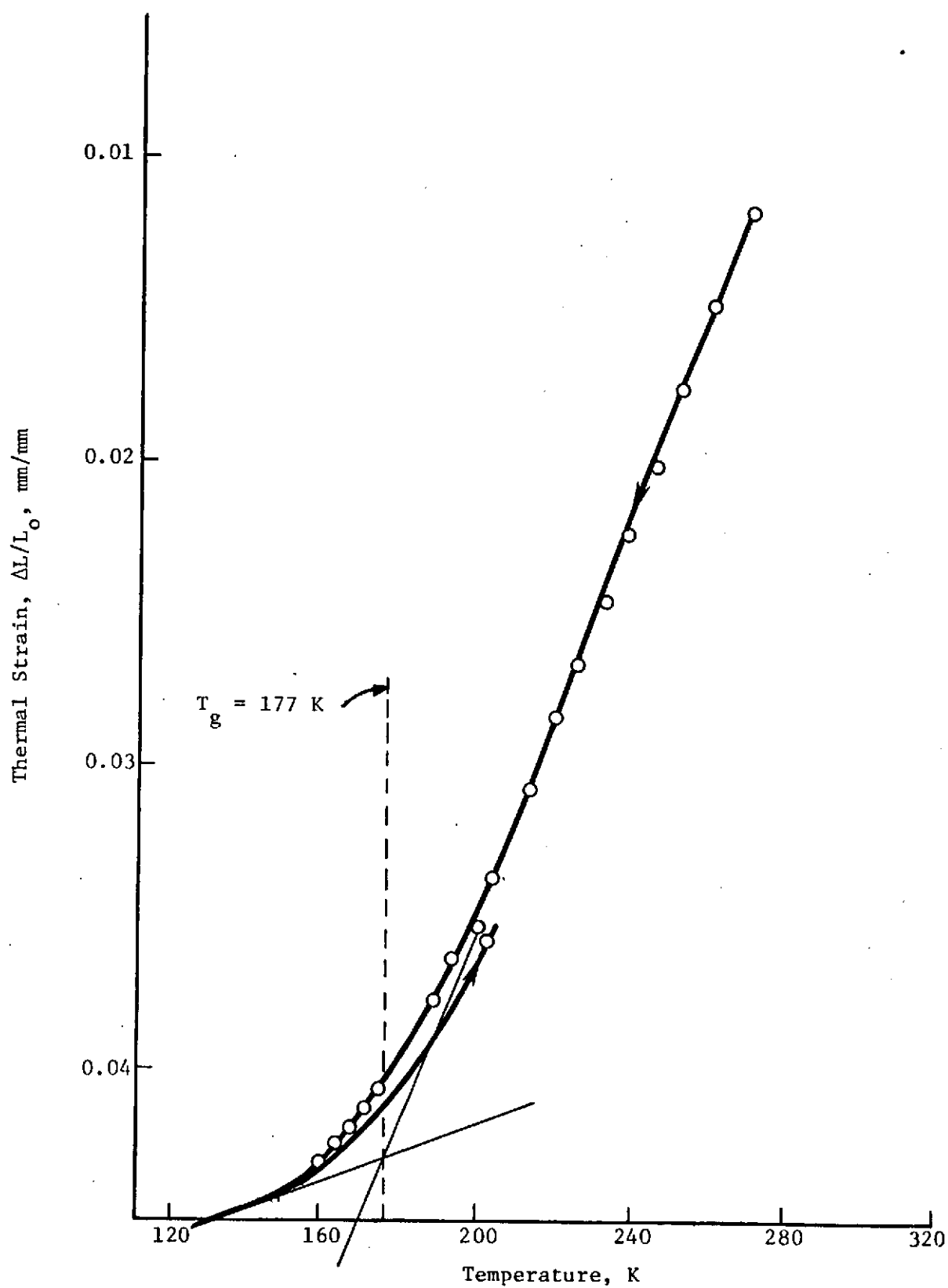


Figure 19. Curve showing the thermal strains as a function of temperature for the RL-1973, Sample 2.

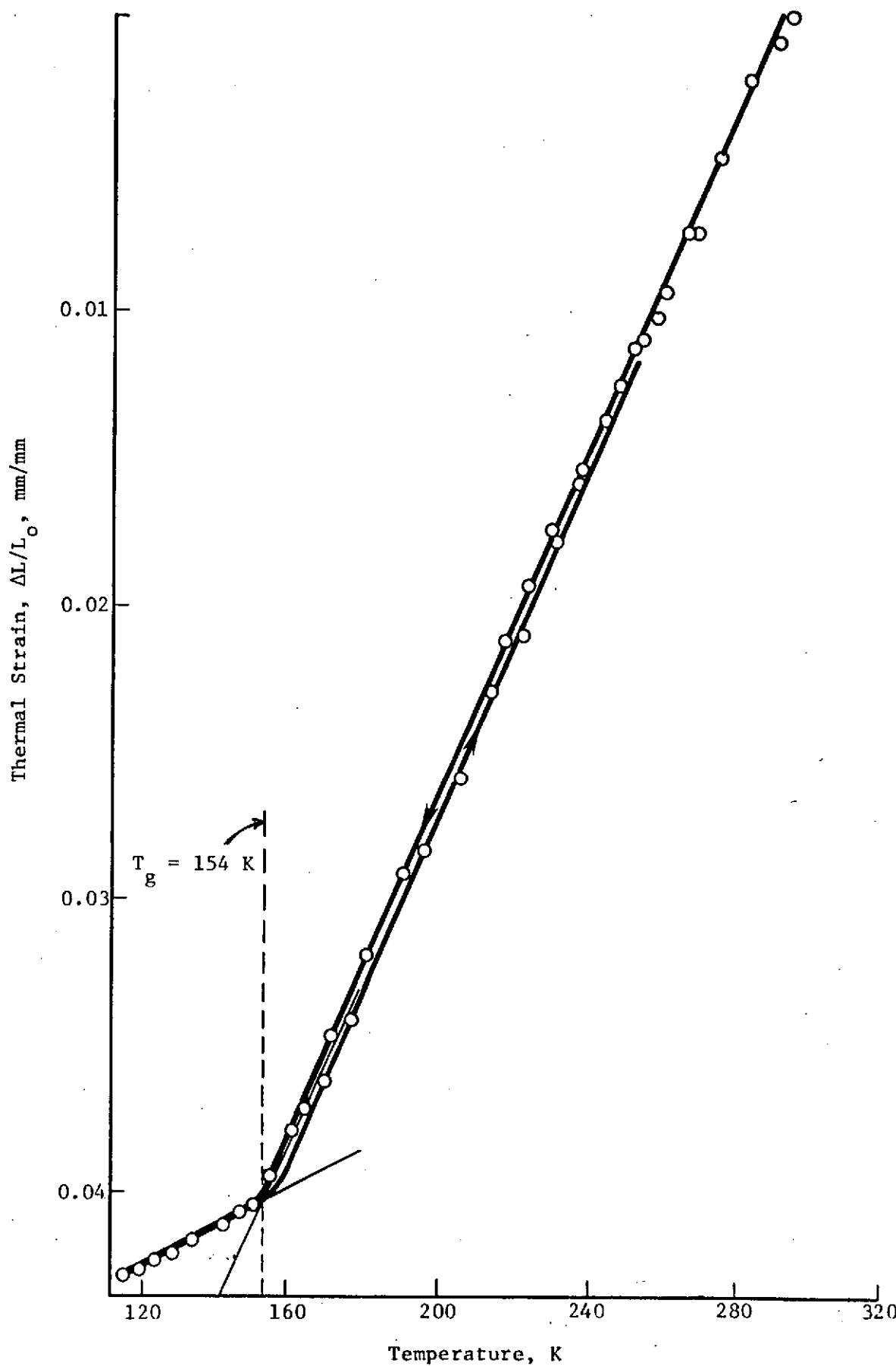


Figure 20. Curve showing the thermal strains as a function of temperature for the PD-200-16, Sample 1.

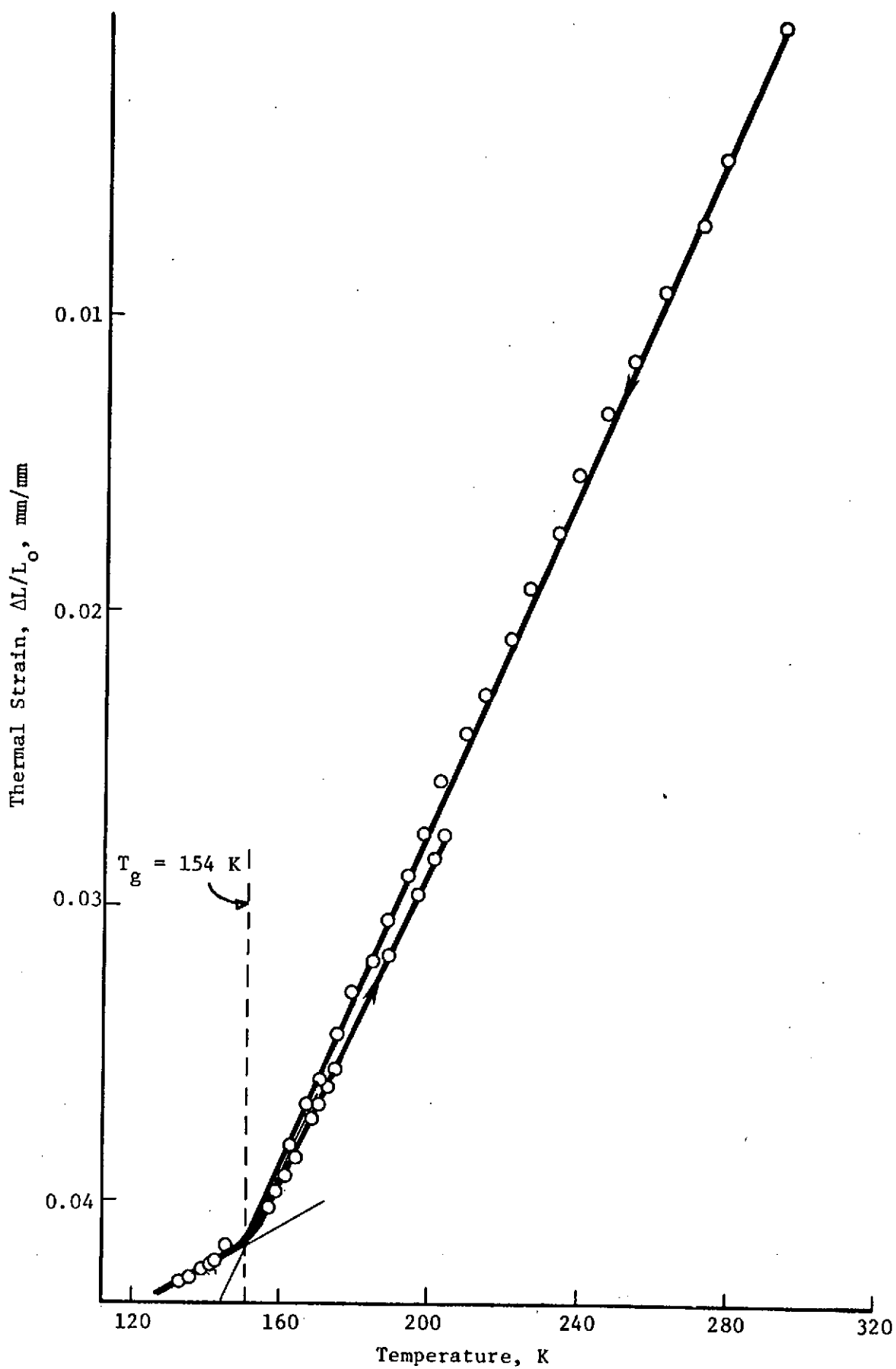


Figure 21. Curve showing the thermal strains as a function of temperature for the PD-200-16, Sample 2.

TABLE III. Measured Thermal Properties of the Silicone Resin Sponge (SRS) Materials

	<u>PD-200-16</u>	<u>RL-1973</u>
Glassy Transition Temperature, $T_g$ (K)	154	174
Average Linear Coefficient of Thermal Expansion above $T_g$ (mm/mm/K)	$28 \times 10^{-5}$	$33 \times 10^{-5}$
Average Linear Coefficient of Thermal Expansion below $T_g$ (mm/mm/K)	$6.1 \times 10^{-5}$	$4.8 \times 10^{-5}$

The experimentally determined glass transition temperatures given above are consistent with those for silicone rubbers as found in the literature (ref. 1). On the other hand, the results reflected in Figures 6 and 7 would indicate a significant amount of stiffening at temperatures well below these glassy temperatures. This characteristic, often observed for silicones, is not consistent with that experienced with other organic polymers which typically exhibit a maximum stiffness at the  $T_g$ . The reasons for this behavior have not yet been established.

One possible explanation for this behavior is that the temperature related property changes may lag, in time, the actual temperature change in the sample. Such delays have been observed by measuring volumetric changes in a material while undergoing temperature excursions. In carefully controlled tests significant volumetric shrinkage will continue well after a steady-state lower temperature has been reached. If such phenomena are also characteristic of stiffnesses and other properties (e.g. Poisson's ratio) then a ready explanation is available for the observations described above.

This hypothesis can be verified by conducting an additional series of selective stress relaxation tests utilizing a number of different

conditioning times at temperatures below  $T_g$ . The time at which the modulus ceases to change with storage time will be the recommended conditioning time.

### 3.4 Failure Data

Following the relaxation tests the specimens were strained to failure at a constant-rate strain of  $0.002\text{ s}^{-1}$ .

Failure was defined simply as the point of maximum force (See Figure 5). It was noted during the 300 K (room temperature) tests that specimen tearing or other signs of failure were always present prior to reaching maximum load. However, since the majority of the tests were performed with the specimen concealed within a conditioning chamber it was not always possible to observe and record these earlier indications of failure. In order to be consistent the point of failure was taken to be where the load attained its largest value.

Figures 22 and 23 show the maximum stresses and the corresponding strains for the PD-200-16 and RL-1973, respectively. These stresses and strains are plotted in their unreduced form; i.e., without the  $T_0/T$  correction factor.

Note should be taken of the fact that the constant displacement rate tests were interrupted at various strain levels (1, 3, 5 or 10%) to perform the relaxation tests. These strain levels are low compared to subsequent strains at failure. Therefore, it seems reasonable to assume that the failure data was not significantly influenced by the intervening relaxation.

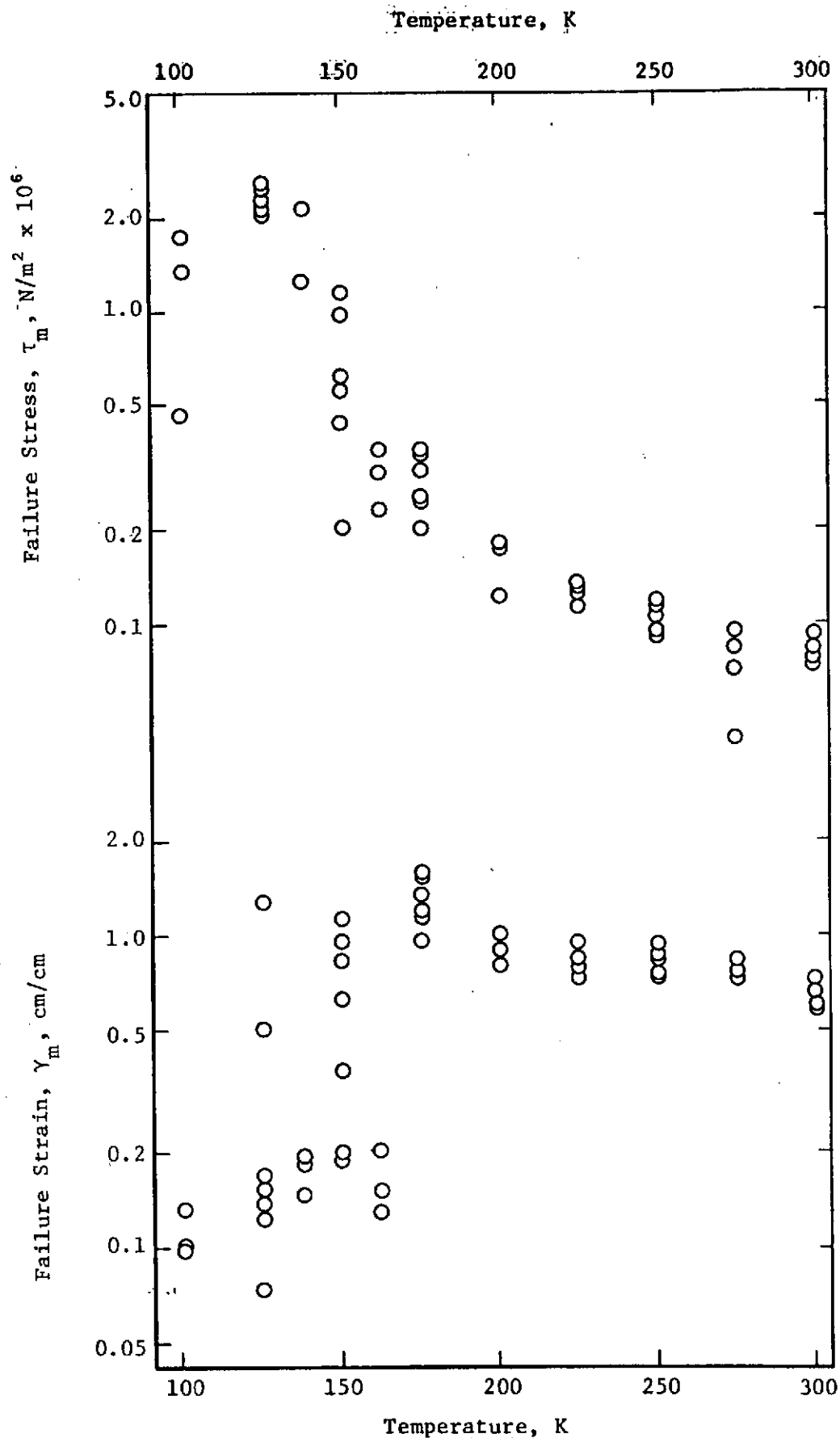


Figure 22. Failure shear stresses and corresponding strains observed for the PD-200-16 at the various test temperatures.

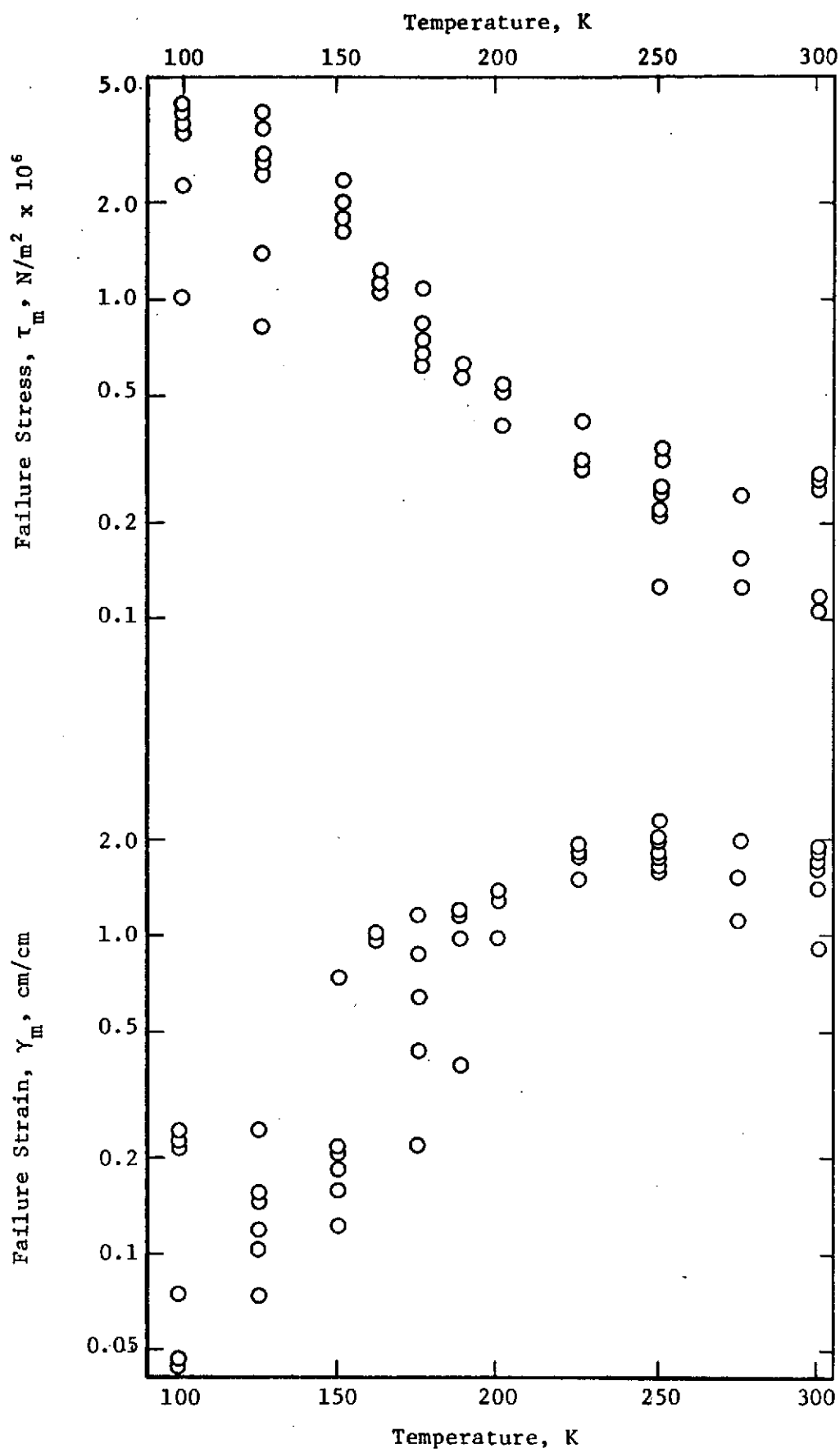


Figure 23. Failure shear stresses and corresponding strains observed for the RL-1973 at the various test temperatures.

Finally, Figures 24 and 25 show the maximum stresses plotted against the maximum strains. Such plots are often used to show failure data obtained from uniaxial tests and are referred to as failure envelopes (ref. 6). Such curves imply that failure is independent of the loading history, often a convenient but also often an invalid assumption.

The stresses used in these plots were adjusted by the factor  $T_0/T$  where  $T_0$  was arbitrarily selected to be 300 K. Therefore, the failure stresses at the lower temperatures were considerably magnified.

Several points are shown plotted with a diagonal arrow pointing upward and to the right. For one reason or another these failures were believed to be invalid and premature. For example, a specimen which failed by debonding the adhesive from the aluminum bar would be so labeled. As a result, such points were considered to give, at best, only a lower limit for the true failure stress and strain.

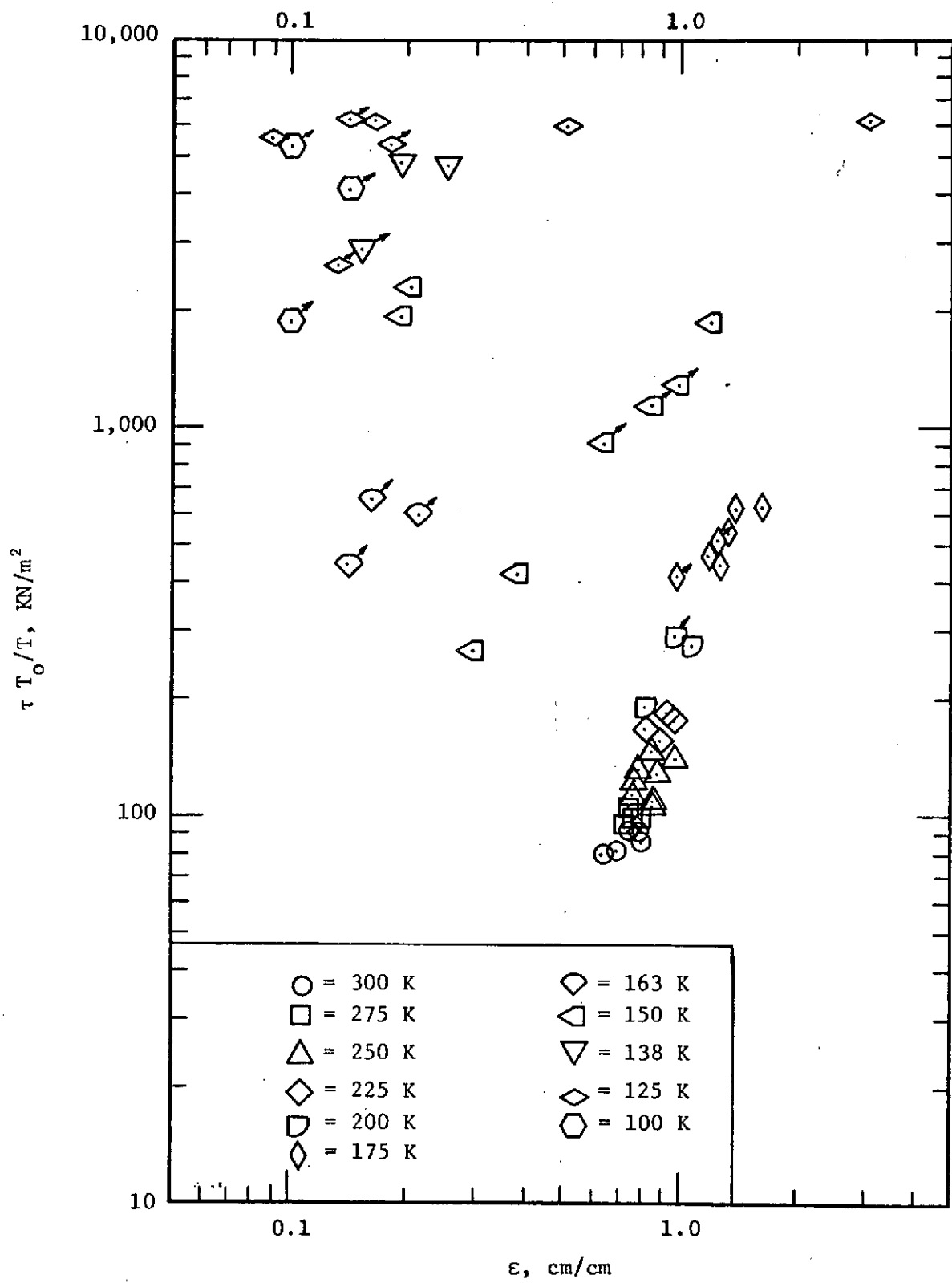


Figure 24. The stresses at maximum load plotted against the corresponding strains for the PD-200-16.

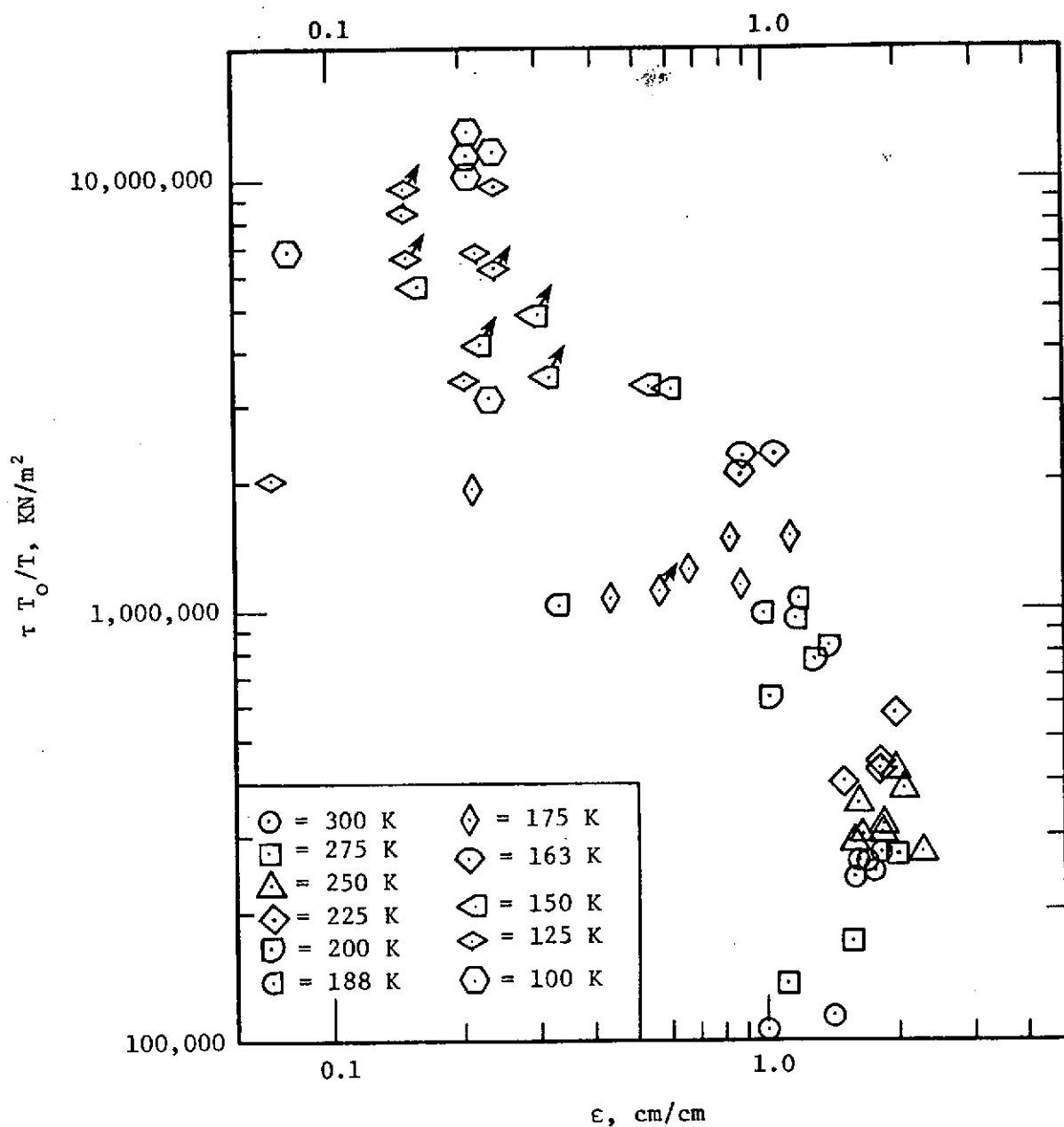


Figure 25. The stresses at maximum load plotted against the corresponding strains for the RL-1973.

## 4.0 CONCLUSIONS AND RECOMMENDATIONS

### 4.1 Conclusions

The stress relaxation response characteristics of PD-200-16 and RL-1973 silicone resin foams were measured over a temperature range of 100 to 300 K and four strain levels (1, 3, 5 and 10%). Initial tangent, secant moduli and failure properties were also determined for each material at these test conditions. The following represent the conclusions reached:

1. The two silicone foams studied, PD-200-16 and RL-1973, were both extremely compliant at room temperature (i.e., respectively less than 100 and 200 N/m<sup>2</sup>) over a range of temperatures from 300 K down to near their respective transition temperatures. Almost inevitably the PD stiffness was 100 N/m<sup>2</sup> or below and the RL was 200 N/m<sup>2</sup> or below over this range.
2. Only a slight amount of stress relaxation was observed in both materials during the 60 minute test periods except at intermediate temperatures. The slope of the log-log relaxation curve never exceeded 0.1 except in this locale.
3. The experimentally determined transition temperatures of 154 K for the PD and 177 K for the RL were consistent with those found in the literature (ref. 1) for similar chemically structured materials. It should be noted that these transitions while reflecting a change in the rate of thermal expansion did not fit the classical definition of glassy transition because the shear modulus at this temperature (and below) was in no sense "glassy" or elastic. However, the transition temperature

did indicate the onset, with cooling, of an extremely rapid increase in the stiffness.

4. The stiffness increased approximately two orders of magnitude over the range of temperatures of the tests.

5. The data were extremely scattered. This scatter can possibly be explained by an apparent change of the properties as a function of the duration of the thermal conditioning time. The possibility of this phenomenon, suggested by I. K. Spiker of NASA's Johnson Space Center led to several exploratory side tests which seemed to indicate its validity.

6. No decisive evidence was found relating the measured stiffness values to the test strain levels.

7. Both stress and strain values measured at failure may be unconservative for design purposes because of the inability to observe specimen behavior in the cryostat.

#### 4.2 Recommendations for Future Work

Figures 6 and 7 indicate that both PD-200-16 and RL-1973 experience the greatest degree of viscoelasticity at temperatures below their respective glass transition temperatures. This is contrary to that normally expected in rate dependent materials. If this represents the true characteristic of silicone rubbers such behavior would be unique. If it is not, any modelling of this behavior and consequently any analysis which incorporates this model would be suspect.

One possible reason for this behavior can be attributed to insufficient sample conditioning. If a test were run prematurely the results

produced would tend to be shifted to the shorter times (i.e., to the left) as shown in Figures 6 and 7. As the test temperature assumes lower values the conditioning times required to reach thermal equilibrium increases. It is therefore recommended that a more in-depth study of the transition zones of the two materials be undertaken, with initial consideration being devoted toward establishing the necessary pre-test conditioning time to achieve thermal equilibrium in the samples.

This can be accomplished by extending the one hour conditioning time used throughout this program and rerunning selective relaxation tests. In addition to temperature, volumetric contraction during conditioning should also be monitored. The time required for the thermal contractions to cease will establish the desired conditioning time. Stress relaxation tests at this conditioning time should verify or refute the existence of the high degree of viscoelasticity in the two materials below their  $T_g$ . These results would also be extremely beneficial to future characterizations of polymers for use at cryogenic temperatures.

## REFERENCES

1. Owen, H. T.; and Carroll, M. T.: Development of Design Allowable Data for Adhesives for Attaching Reusable Surface Insulation, Final Technical Report for Contract No. NAS9-12392, General Dynamics, Convair Aerospace Division, October 1972.
2. Telephone conversation with Dr. A. Hiltz of General Electric, Valley Forge Space Center, Box 8555, Philadelphia, Pa. 19101 and Mr. J. Owens of Raybestos-Manhattan, Garco and Oher Ave., North Charleston, S. C. 29406.
3. General Electric RTV Silicone Rubber, Technical Data Book S-35 Silicone Products Department, Waterford, N. Y.
4. A. V. Tobolsky; and R. D. Andrews: J. Chem. Phys., Vol. 11, p. 123 (1943).
5. ICRPG Solid Propellant Mechanical Behavior Manual, The Johns Hopkins University Applied Physics Laboratory, Silver Spring, Maryland, Chemical Propulsion Information Agency Publication No. 21, September 1963.
6. Smith, T. L.: Proceedings of the Royal Society, A, Vol. 282, p. 102 (1964).

STRESS RELAXATION AND MECHANICAL PROPERTIES

OF

RL-1973 AND PD-200-16

SILICONE RESIN SPONGE MATERIALS

by

D. Saylak  
J. S. Noel  
J. S. Ham  
R. McCoy

APPENDIX A

COMPUTER PROGRAM FORMAT

Mechanics and Materials Research Center  
Texas A&M University  
College Station, Texas 77843

Final Technical Report

on

Contract No. NAS1-13342

1 March 1975

National Aeronautics and Space Administration

Langley Research Center

Hampton, Virginia 23665

*Best available copy*

1 A

**PRECEDING PAGE BLANK NOT FILMED**

## APPENDIX A

This appendix contains a listing of the FORTRAN Code used to reduce the test data to the format shown in Appendix B.

LISTING OF PROGRAM USED TO REDUCE DATA

```

IMPLICIT REAL * 8 (A-H, Ø-Z)
DIMENSION STRESS(100), STRAIN(100), ET(100), ES(100)
100 CONTINUE
C      READ IN DATA
      STRANØ= 0.0
      STRESØ= 0.0
      READ(5,10) SAM1, SAM2, SAM3, SAM4, SAM5, SAM6, SAM7
10     FØRMAT(7A8)
      READ(5,20) PØINTS,STØP
20     FØRMAT(2F10.5)
      N = PØINTS
      DØ 30 I = 1,N
30     READ(5,40) STRESS(I), STRAIN(I)
40     FØRMAT (2F10.5)
C      CALIBRATE DATA
      DØ 50 I = 1,N
      STRESS(I) = STRESS(I) * 6895.
      STRAIN(I) = STRAIN(I) * 100.
      IF(STRAIN(I).EQ.0.0) GØ TØ 110
      ADD = STRESS(5) - STRESS(6)
      IF(I.GT.5) STRESS(I) = STRESS(I) + ADD
      ES(I) = STRESS(I) / STRAIN(I) * 100.
      ET(I) =(STRESS(I) - STRESØ) / (STRAIN(I) - STRANØ) * 100.
110   CONTINUE
      STRESØ = STRESS(I)
      STRANØ = STRAIN(I)
      IF(I.GT.5) STRESS(I) = STRESS(I) - ADD
50     CONTINUE
C      WRITE ØUT DATA
      WRITE(6,60) SAM1, SAM2, SAM3, SAM4, SAM5, SAM6, SAM7
60     FØRMAT('1', //, 10X, 7A8)
      WRITE(6, 70)
70     FØRMAT(//, 13X, ' STRESS ',12X ' STRAIN ',14X, ' GT MØDULUS ',
*10X,'GS MØDULUS')
      DØ 80 I = 1,N
80     WRITE(6,90) STRESS(I), STRAIN(I), ET(I), ES(I)
90     FØRMAT( 10X, F10.1, 10X, F10.4, 10X, F12.0, 10X, F12.0)
C      DRAW THE STRESS-STRAIN CURVE
      CALL CURVE(STRESS, STRAIN, SAM1, SAM2, SAM3, SAM4, SAM5, SAM6, SAM
*7, N)
      IF(STØP.EQ.0.) GØ TØ 100
      CALL LINE4
      WRITE(6,120)
120   FØRFORMAT('1')
      STØP
      END

```

(CONTINUED)

```

SUBROUTINE CURVE(STRESS, STRAIN, SAM1, SAM2, SAM3, SAM4, SAM5, SAM
*6, SAM7, N)
REAL*8 STRESS(100), STRAIN(100), SAM1, SAM2, SAM3, SAM4, SAM5,
C SAM6, SAM7
DIMENSION STRES(100), STRAN(100)
S1 = 500000.
S2 = 1000000.
S3 = 2000000.
S4 = 4000000.
E1 = 50.
E2 = 200.
S1DX=S1/10.
S2DX = S2/10.
S3DX=S3/10.
S4DX=S4/10.
E1DX=E1/10.
E2DX=E2/10.
D0 10 I = 1,N
STRES(I) = STRESS(I)
10  STRAN(I) = STRAIN(I)
    IF(STRESS(N).LE.S1) CALL AXIS1(0.0,0.0,' STRESS (N/MS)', 
C 14, 10., 90., 0.0, S1DX, 20.)
    IF(STRESS(N).LE.S1) G0 T0 20
    IF(STRESS(N).LE.S2) CALL AXIS1(0.0, 0.0, ' STRESS (N/MS)', 
C14, 10., 90., 0.0, S2DX, 20.)
    IF(STRESS(N).LE.S2) G0 T0 20
    IF(STRESS(N).LE.S3) CALL AXIS1(0.0, 0.0, ' STRESS (N/MS)', 
C 14, 10., 90., 0.0, S3DX, 20.)
    IF(STRESS(N).LE.S3) G0 T0 20
    CALL AXIS1(0.0, 0.0, ' STRESS (N/MS)', 
C 14, 10., 90., 0.0, S4DX, 20.)
20  C0NTINUE
    IF(STRAIN(N).LE.E1) CALL AXIS1(0.0,0.0, 'STRAIN (PERCENT)',-16,
C10., 0.0, 0.0, E1DX, 20.)
    IF (STRAIN(N).LE.E1) G0 T0 40
    CALL AXIS1( 0.0, 0.0, 'STRAIN (PERCENT)',-16, 10., 0.0, 0.0,E2DX,
C20.)
40  C0NTINUE
    IF(STRESS(N).GT.S1) G0 T0 30
    IF(STRAIN(N).GT.E1) G0 T0 35
    CALL LINE1(E1, 0.0, S1, 0.0,E1DX,S1DX)
    G0 T0 75
35  CALL LINE1(E2, 0.0, S1, 0.0,E2DX,S1DX)
    G0 T0 75
30  IF(STRESS(N).GT.S2) G0 T0 50
    IF(STRAIN(N).GT.E1) G0 T0 55
    CALL LINE1(E1, 0.0, S2, 0.0, E1DX,S2DX)
    G0 T0 75
55  CALL LINE1(E2, 0.0, S2, 0.0, E2DX,S2DX)
    G0 T0 75
50  IF (STRESS(N).GT.S3) G0 T0 60
    IF(STRAIN(N).GT.E1) G0 T0 65
    CALL LINE1(E1, 0.0, S3, 0.0, E1DX,S3DX)
    G0 T0 75

```

(CONTINUED)

```
65    CALL LINE1(E2, 0.0, S3, 0.0, E2DX,S3DX)
      G $\emptyset$  T $\emptyset$  75
60    IF(STRAIN(N).GT.E1) G $\emptyset$  T $\emptyset$  70
      CALL LINE1(E1, 0.0, S4, 0.0, E1DX,S4DX)
      G $\emptyset$  T $\emptyset$  75
70    CALL LINE1(E2, 0.0, S4, 0.0, E2DX,S4DX)
75    C $\emptyset$ NTINUE
      CALL SYMB $\emptyset$ L(1., 10.,.2, SAM1, 0.0, 8)
      CALL SYMB $\emptyset$ L(2.4,10.,.2, SAM2, 0.0, 8)
      CALL SYMB $\emptyset$ L(3.7,10.,.2, SAM3, 0.0, 8)
      CALL SYMB $\emptyset$ L(4.95, 10., .2, SAM4, 0.0, 8)
      CALL SYMB $\emptyset$ L(6.35, 10., .2, SAM5, 0.0, 8)
      CALL SYMB $\emptyset$ L(7.75,10.,.2,SAM6,0.0,8)
      CALL SYMB $\emptyset$ L(9.15,10.,.2,SAM7,0.0,8)
      CALL LINE2(STRAN, STRES, N, 2,1,1)
      CALL LINE3(15.)
      RETURN
      END
```

(END)

STRESS RELAXATION AND MECHANICAL PROPERTIES  
OF  
RL-1973 AND PD-200-16  
SILICONE RESIN SPONGE MATERIALS

by

D. Saylak  
J. S. Noel  
J. S. Ham  
R. McCoy

APPENDIX B

COMPUTER PRINTOUT

Mechanics and Materials Research Center  
Texas A&M University  
College Station, Texas 77843

Final Technical Report

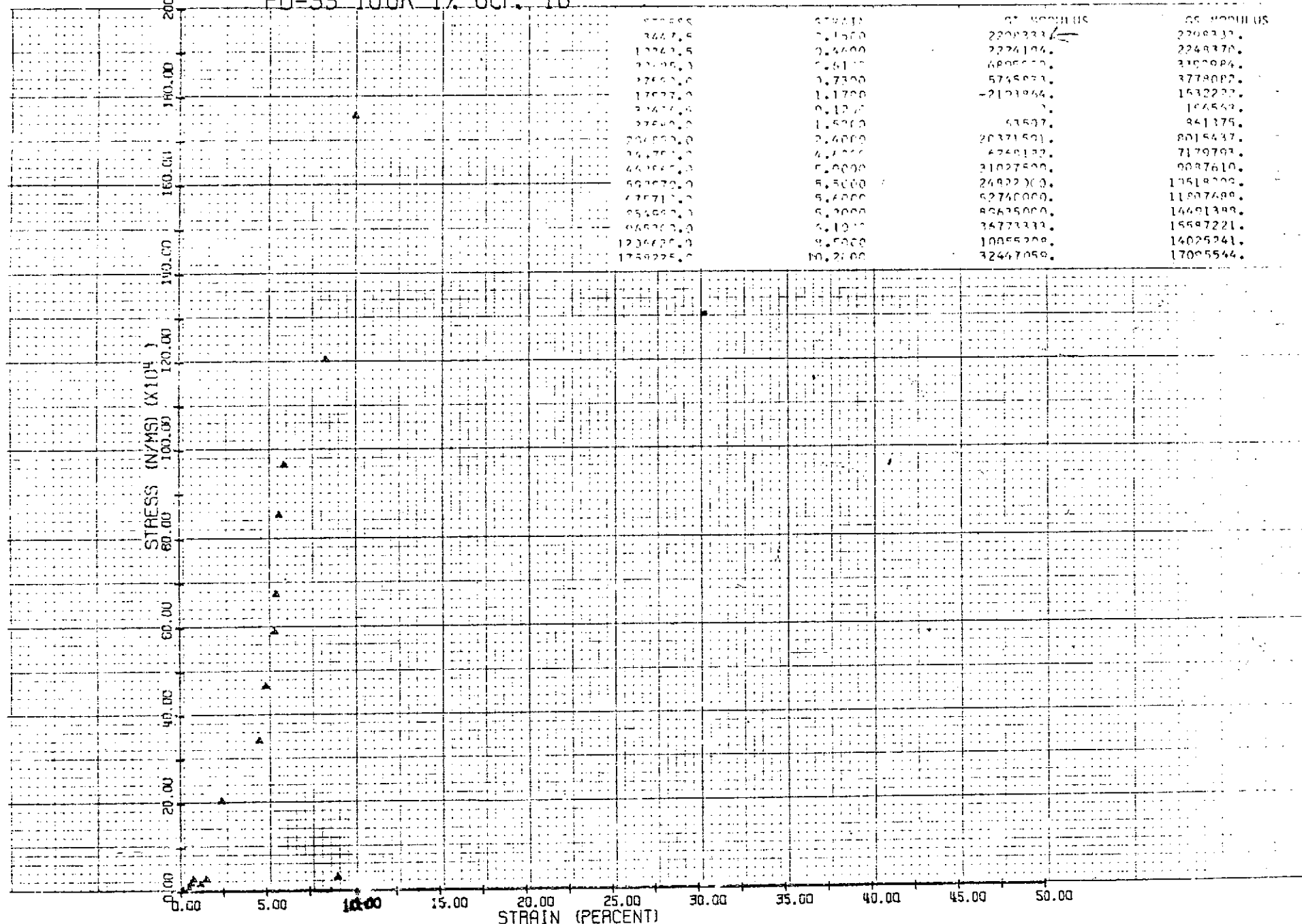
on

Contract No. NAS1-13342

1 March 1975

National Aeronautics and Space Administration  
Langley Research Center  
Hampton, Virginia 23665

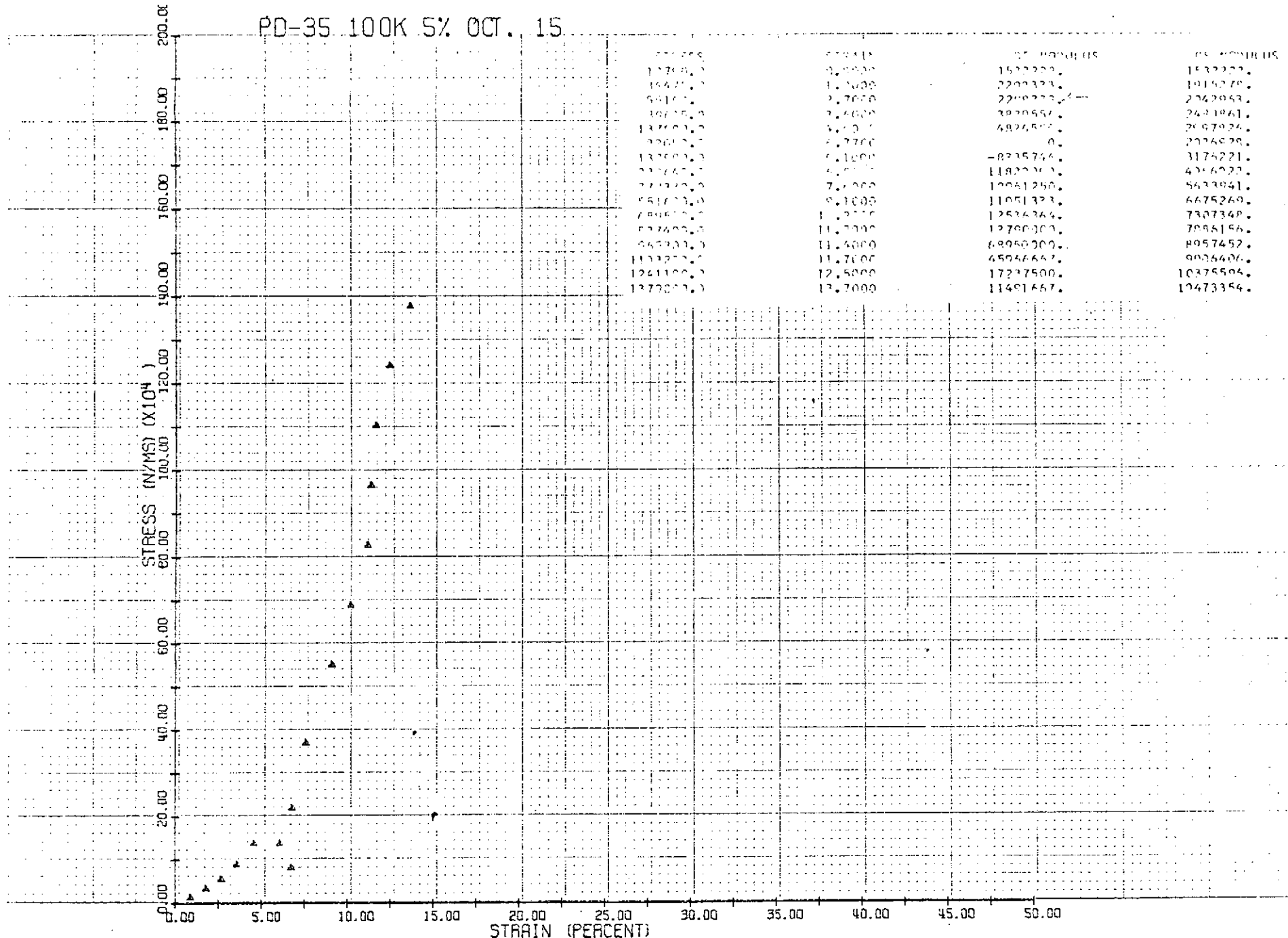
PD-33 100K 1% OCT. 16



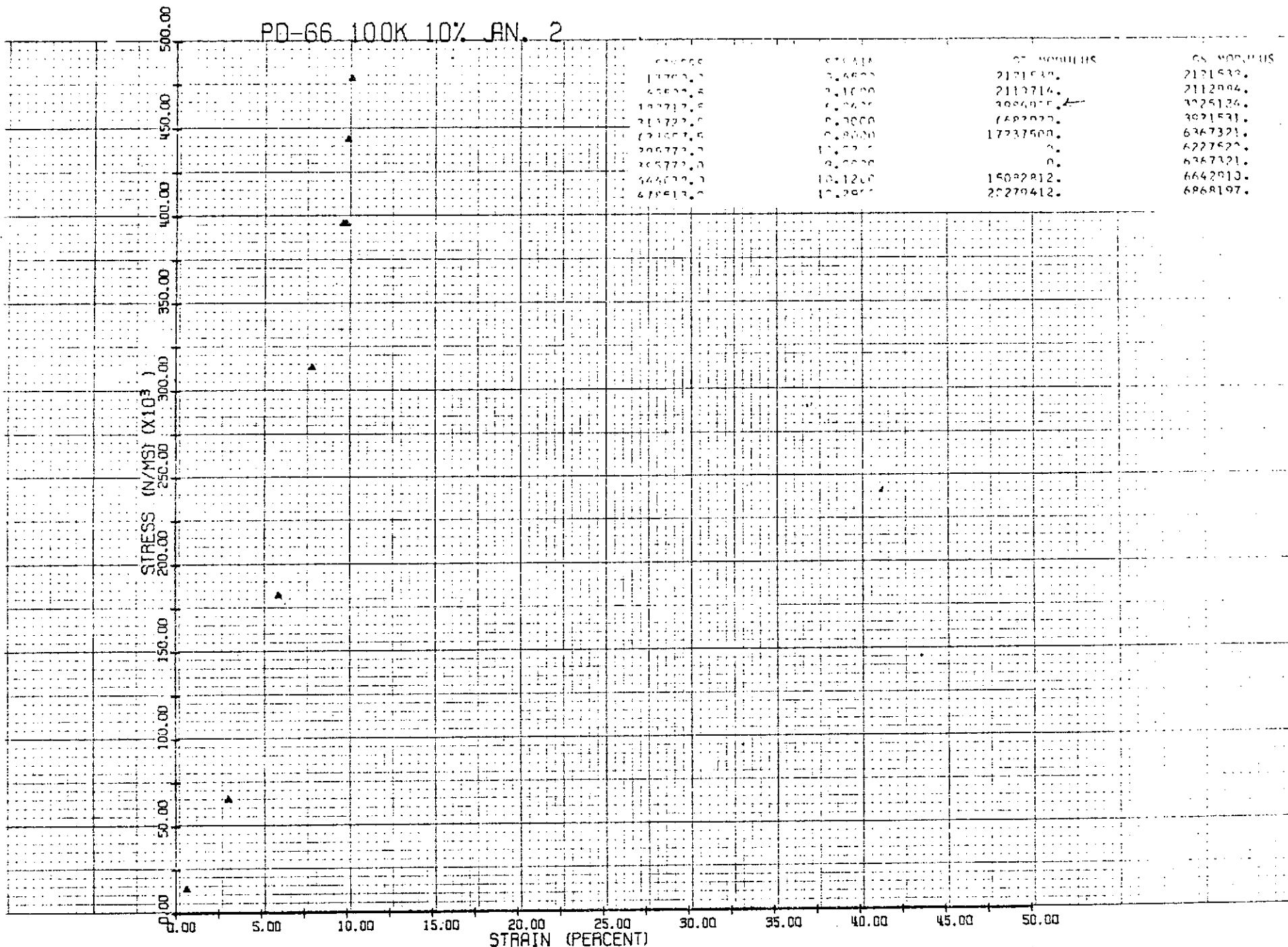
KoE KEUFFEL & ESSER CO.

PRINTED IN U.S.A.

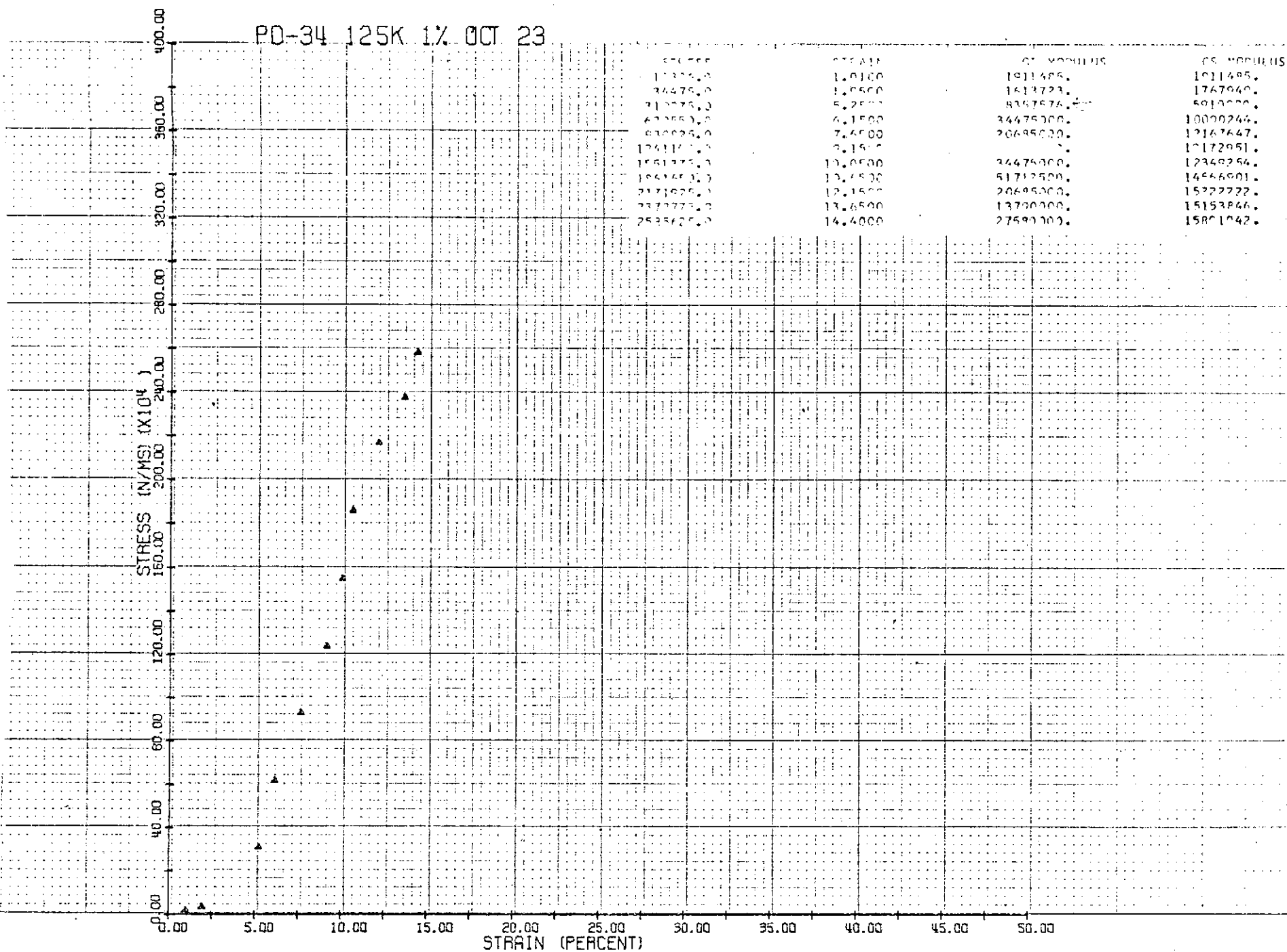
PD-35. 100K 5% OCT. 15.



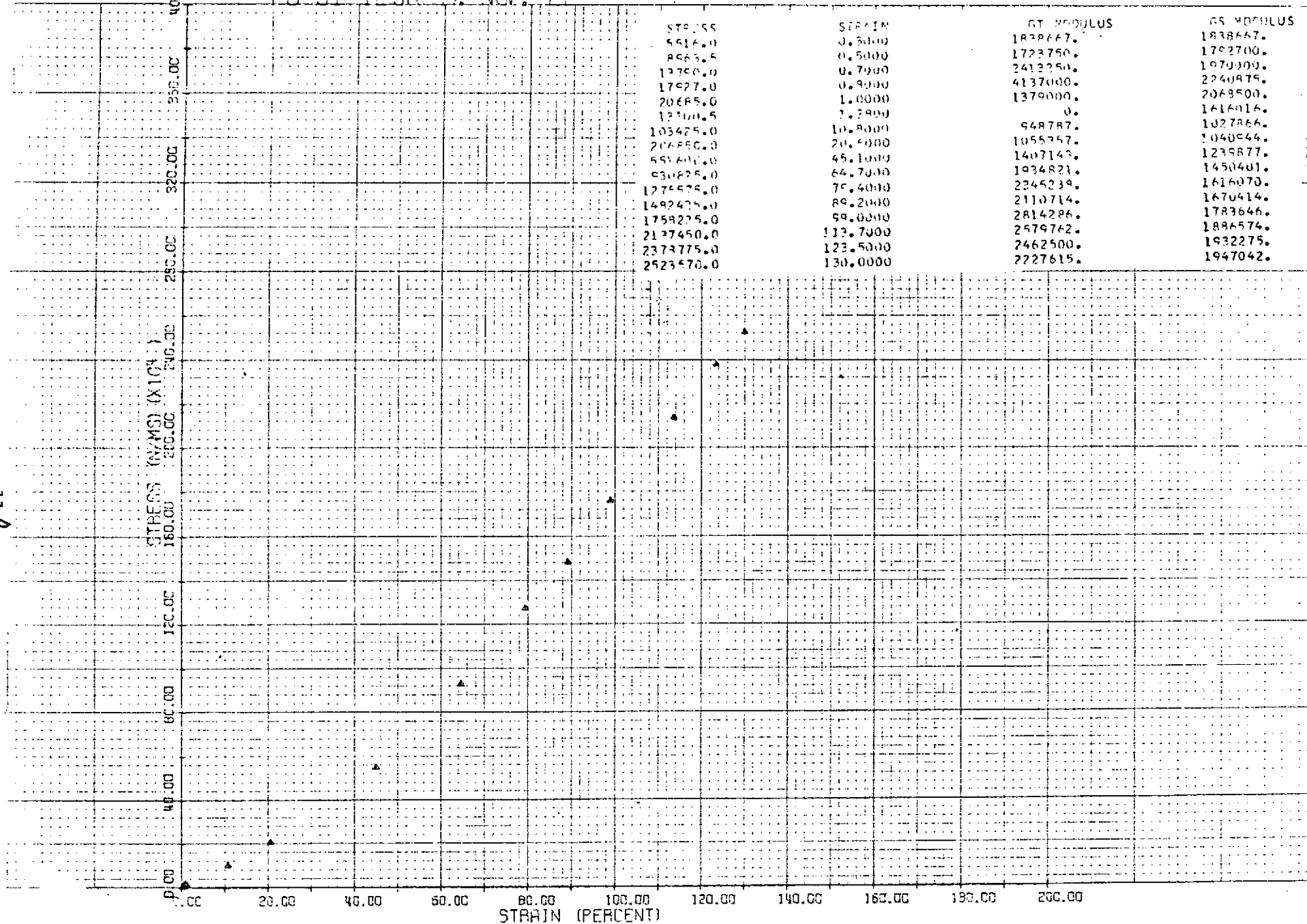
PD-66 100K 10% JAN. 2



PD-34 125K 1% OCT. 23

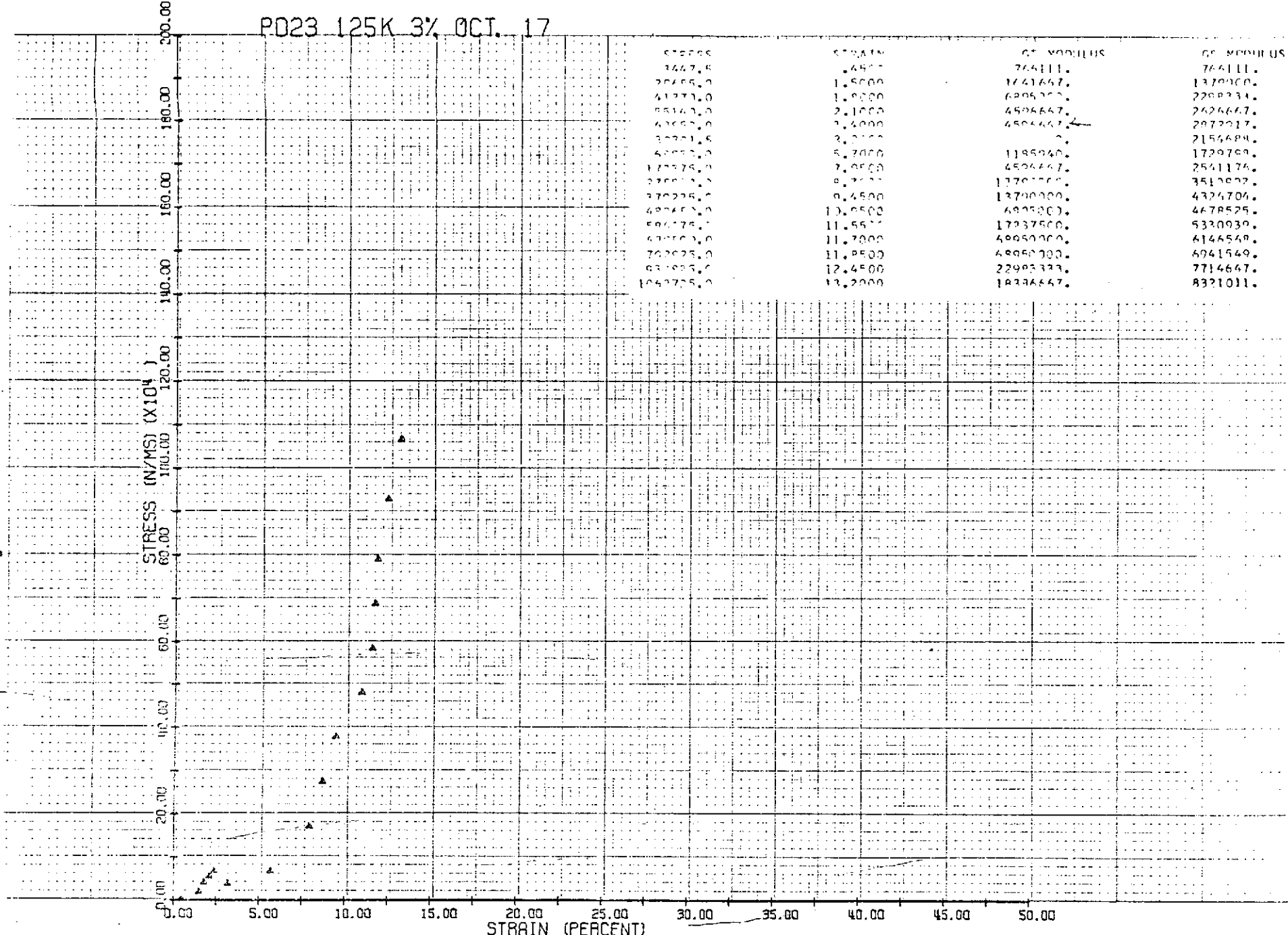


## PC-51 125k 1% NOV. 22



P023 125K 3% OCT. 17

STRESS	STRAIN	GR. MODULUS
30.00	0.0000	764111.
34.47	0.4500	1441667.
38.85	1.0000	6205700.
43.23	1.9200	2208231.
47.60	2.1000	2426647.
52.00	2.4000	2872217.
56.37	2.7000	2156484.
60.75	3.0000	1729769.
65.12	3.2000	2541174.
69.49	3.4000	3512622.
73.87	3.6000	4324704.
78.24	3.8000	4678525.
82.61	4.0000	5320930.
86.98	4.2000	6146548.
91.35	4.5000	6941549.
95.72	4.8500	7714647.
100.00	5.2000	8321011.



12

PU-52 125K 37 Nov. 20

400.

STRESS (N/MSI) ( $\times 10^4$ )

400.

360.00

320.00

280.00

240.00

200.00

160.00

120.00

80.00

40.00

0.00

0.00

5.00

10.00

15.00

20.00

25.00

30.00

35.00

40.00

45.00

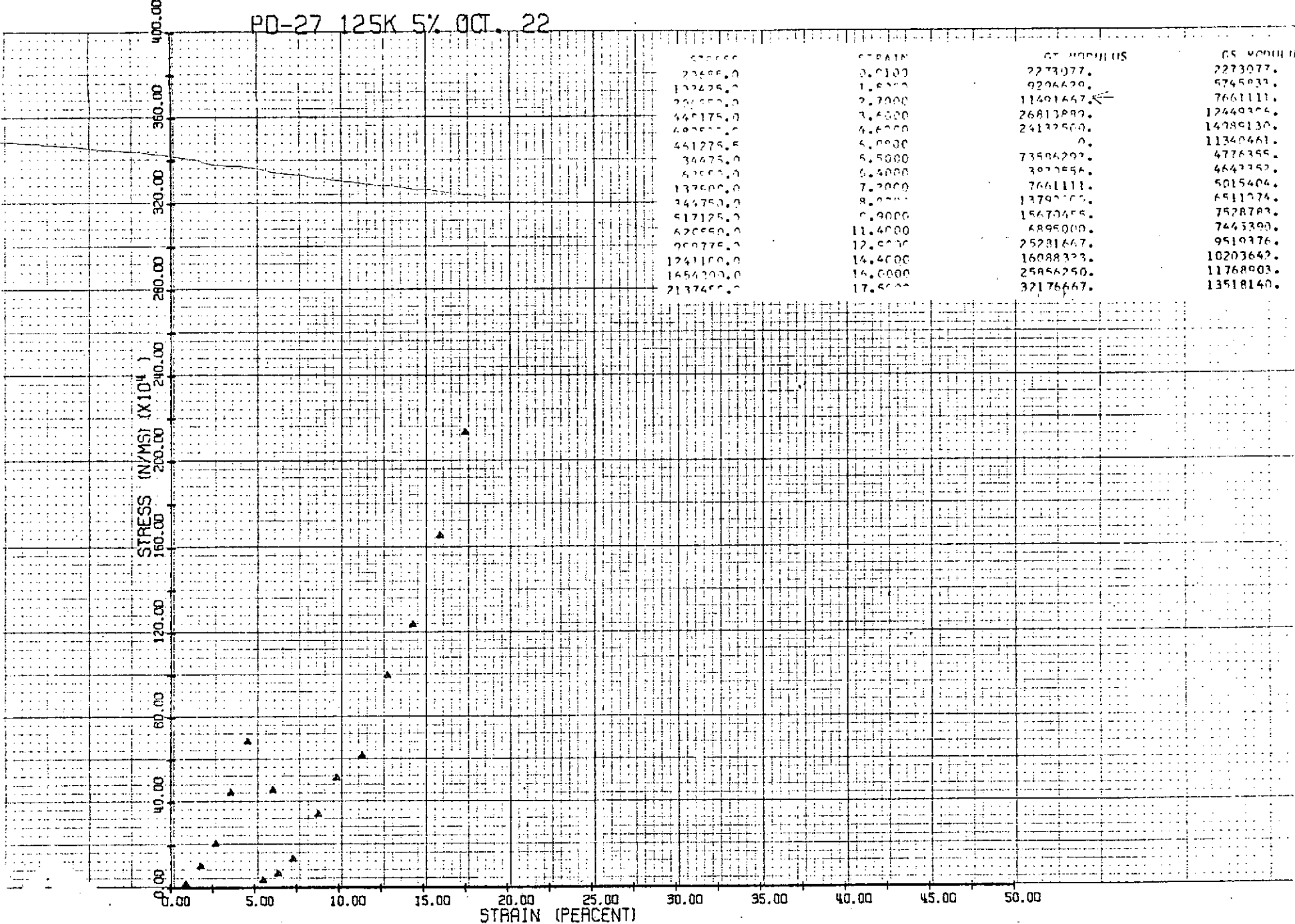
50.00

STRAIN (PERCENT)

STRESS	STRAIN	G. MODULUS	G. MODULUS
200.0	0.3200	626010.	626010.
14470.0	1.9010	1677500.	1677500.
32000.0	1.4700	2251420.	2251420.
58854.0	1.0600	2457670.	2457670.
67571.0	2.4500	2790280.	2790280.
57332.0	2.4600	0.	2543240.
112425.0	4.1970	2710820.	2547414.
214881.0	1.7400	5275790.	3710050.
271225.0	8.0000	8704640.	4955781.
505575.0	2.4710	14071420.	6371778.
961875.0	10.0400	19761000.	8035740.
1137475.0	12.4100	17261000.	9306205.
1587425.0	16.2700	17580280.	10436045.
1630275.0	15.2500	21107143.	11117345.
1751220.0	16.9200	4221420.	12514670.
2299147.0	17.0700	47175316.	12841746.
36475.0	0.4500	12075142.	11401667.
34475.0	5.7500	4444063.	6095000.
620450.0	6.7500	22083333.	10470185.
646750.0	9.2500	18386667.	11900545.
1137175.	0.1200	22981333.	12832361.

1357

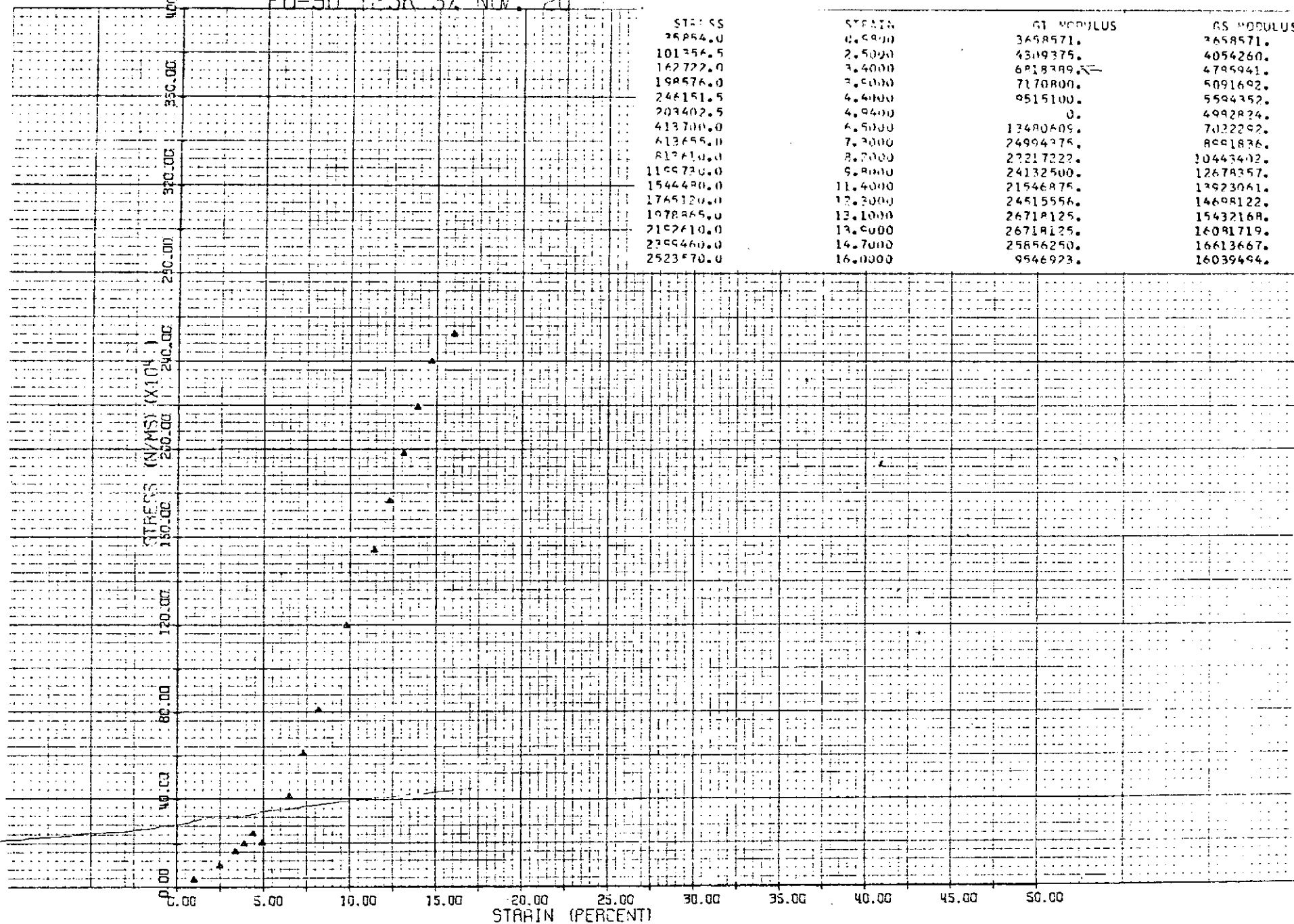
PD-27 125K 5% OCT. 22



KEUFFEL & ESSER CO.

PRINTED IN U.S.A.

PD-50 125K 5% Nov. 20



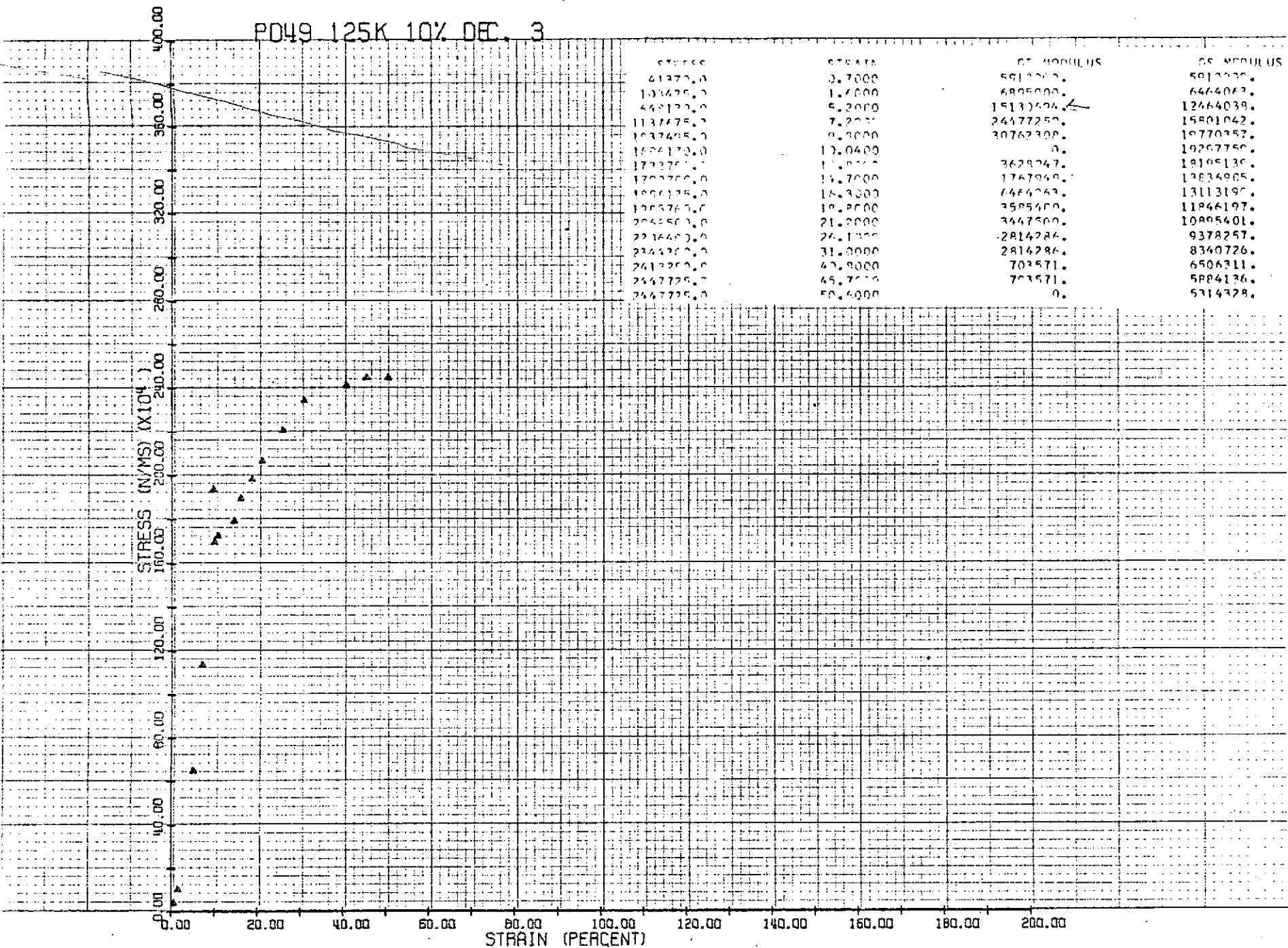
15 A

15

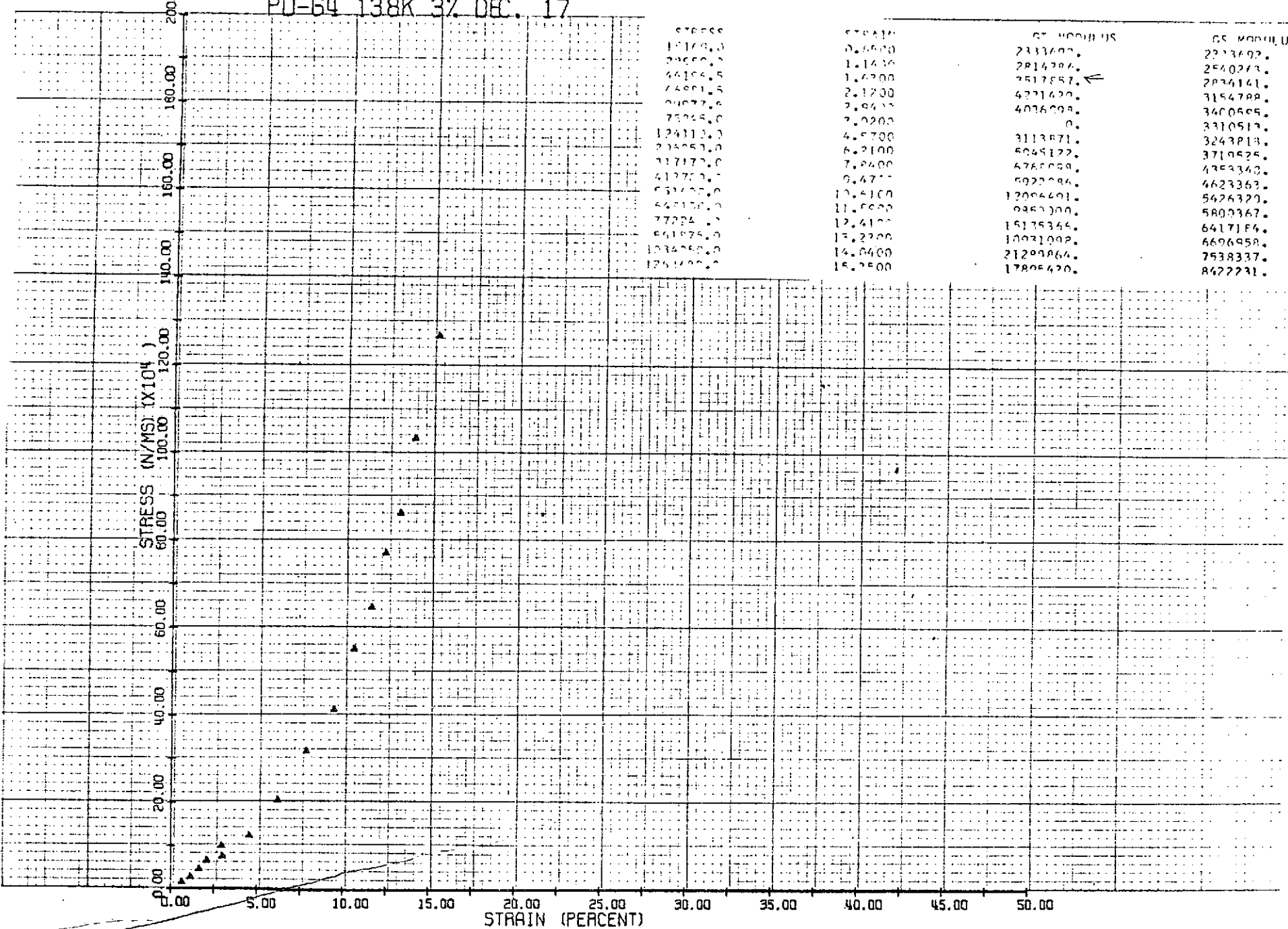
K-E KEUFFEL & ESSER CO.

PRINTED IN U.S.A.

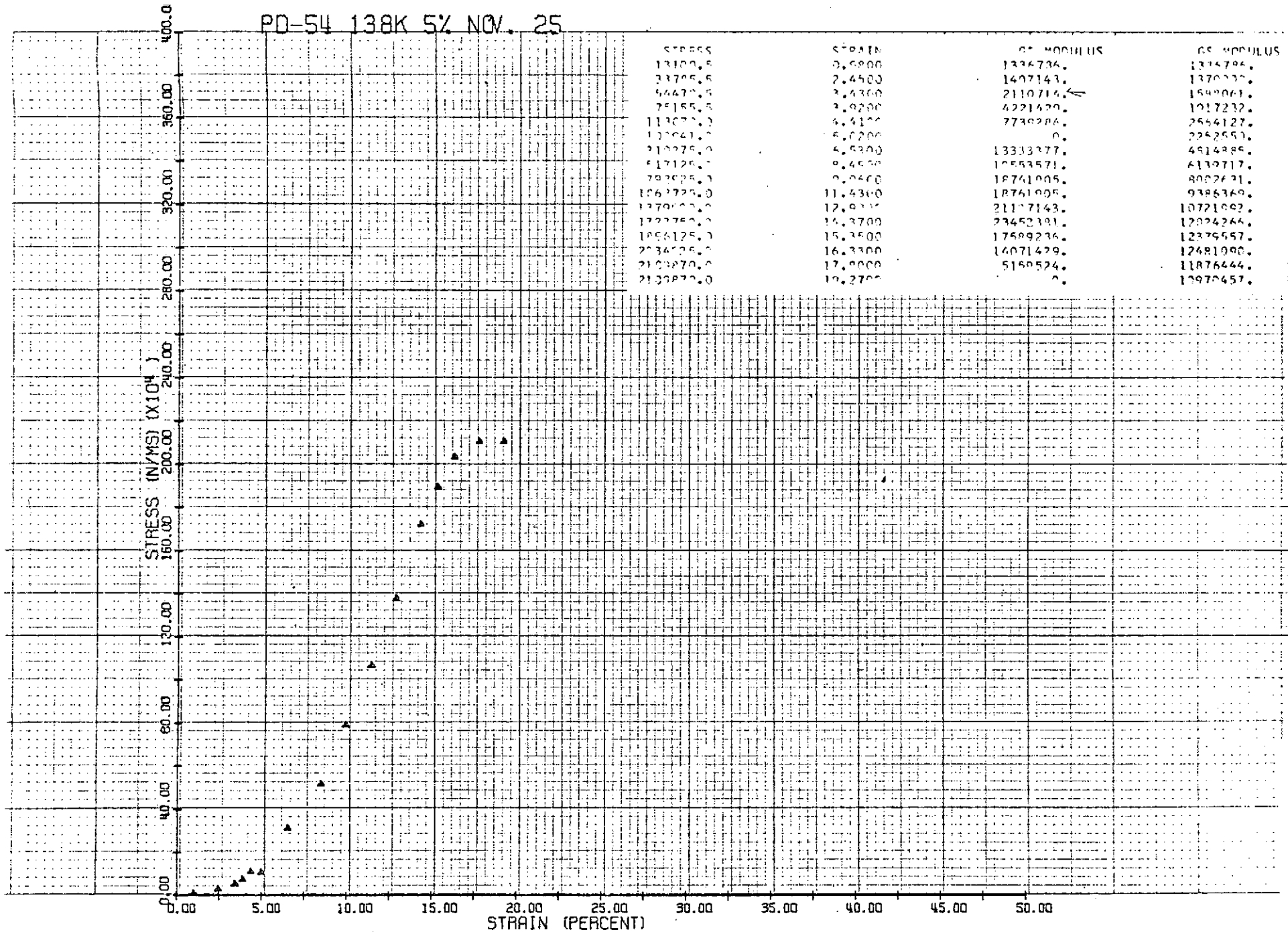
PD49 125K 10% DEC. 3



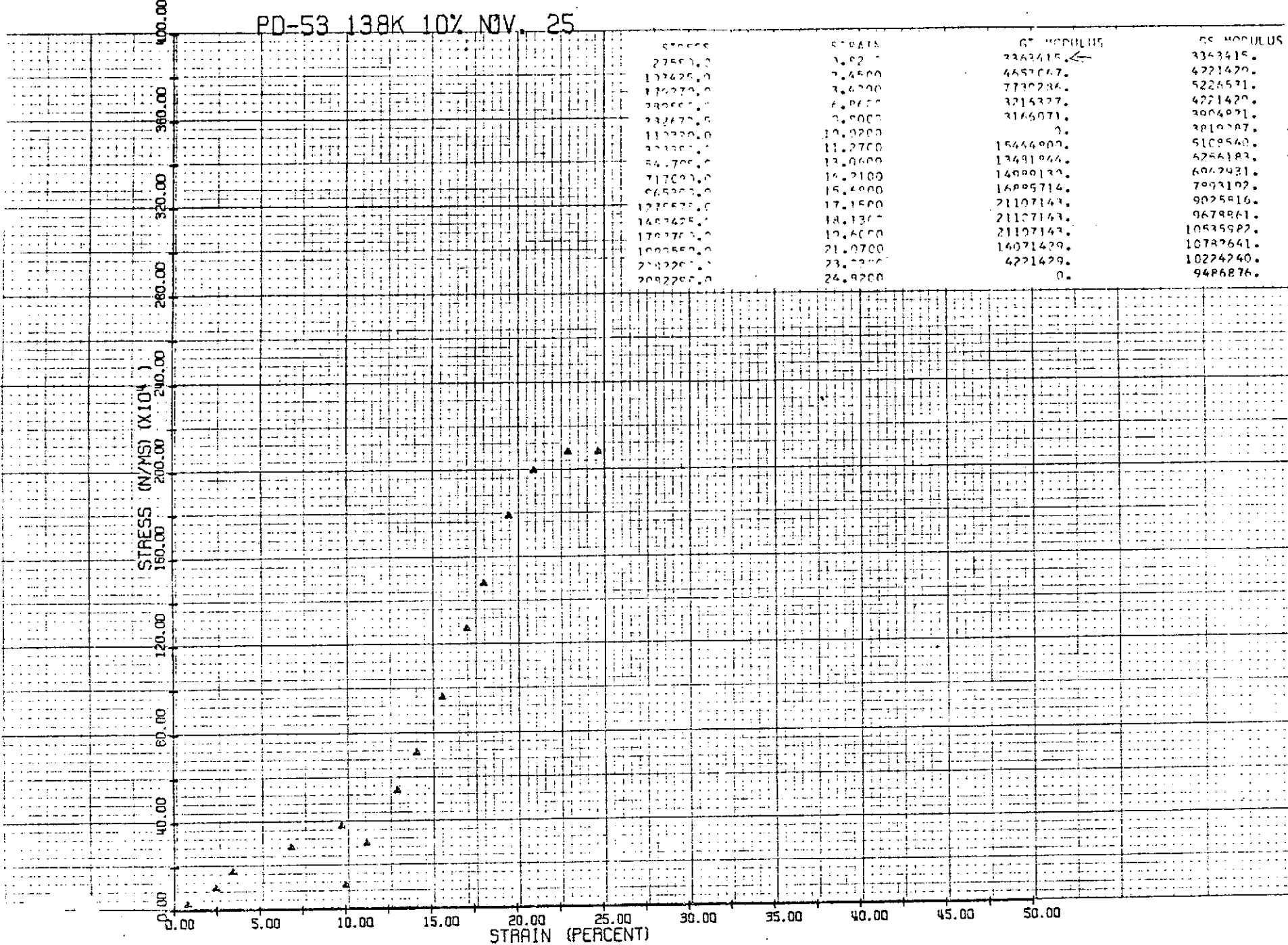
PU-64 138K 3% DEC. 17



PD-54 13.8K 5% NOV. 25



PD-53 138K 10% NOV. 25

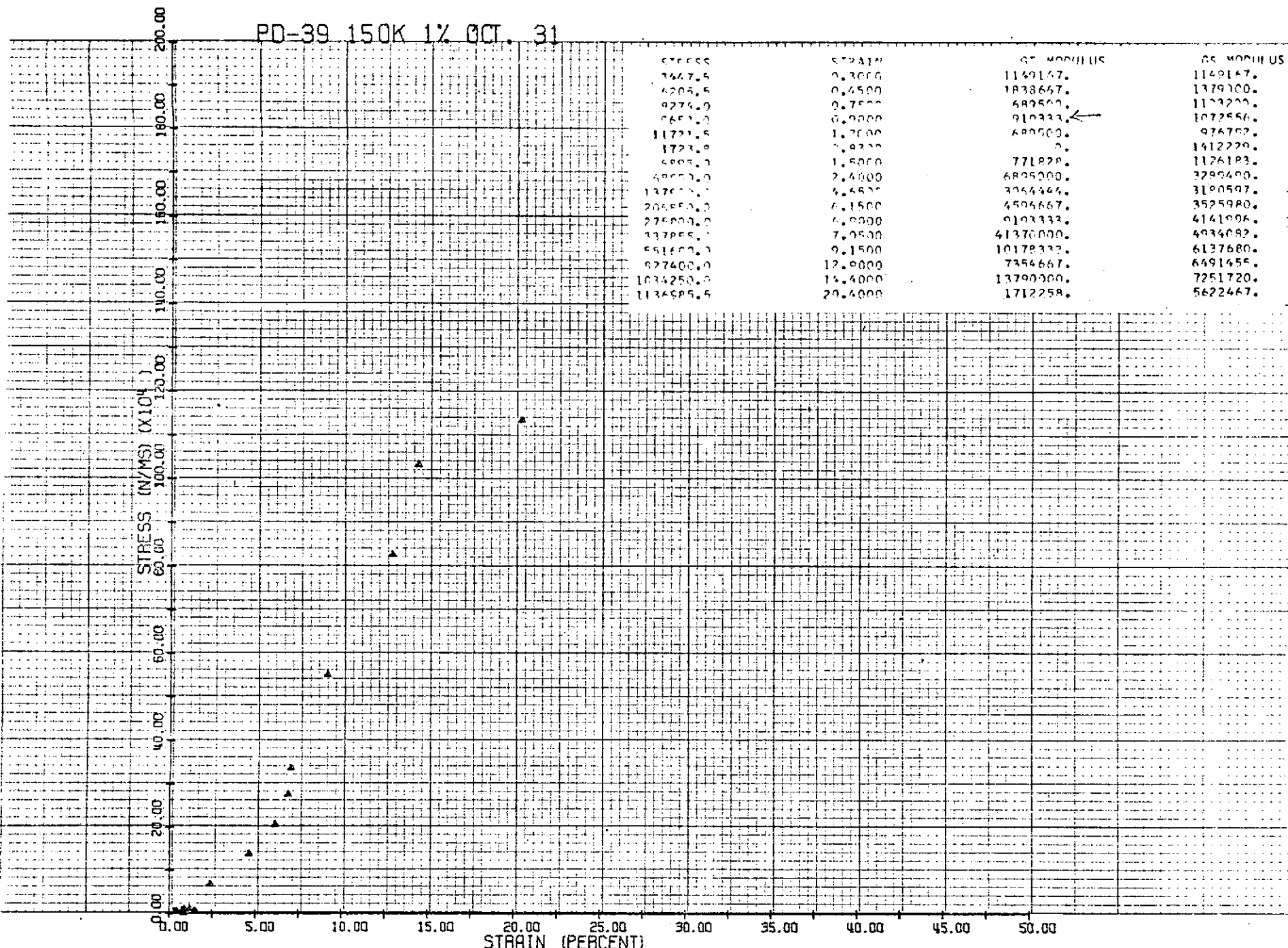


K.E

KEUFFEL & ESSER CO.

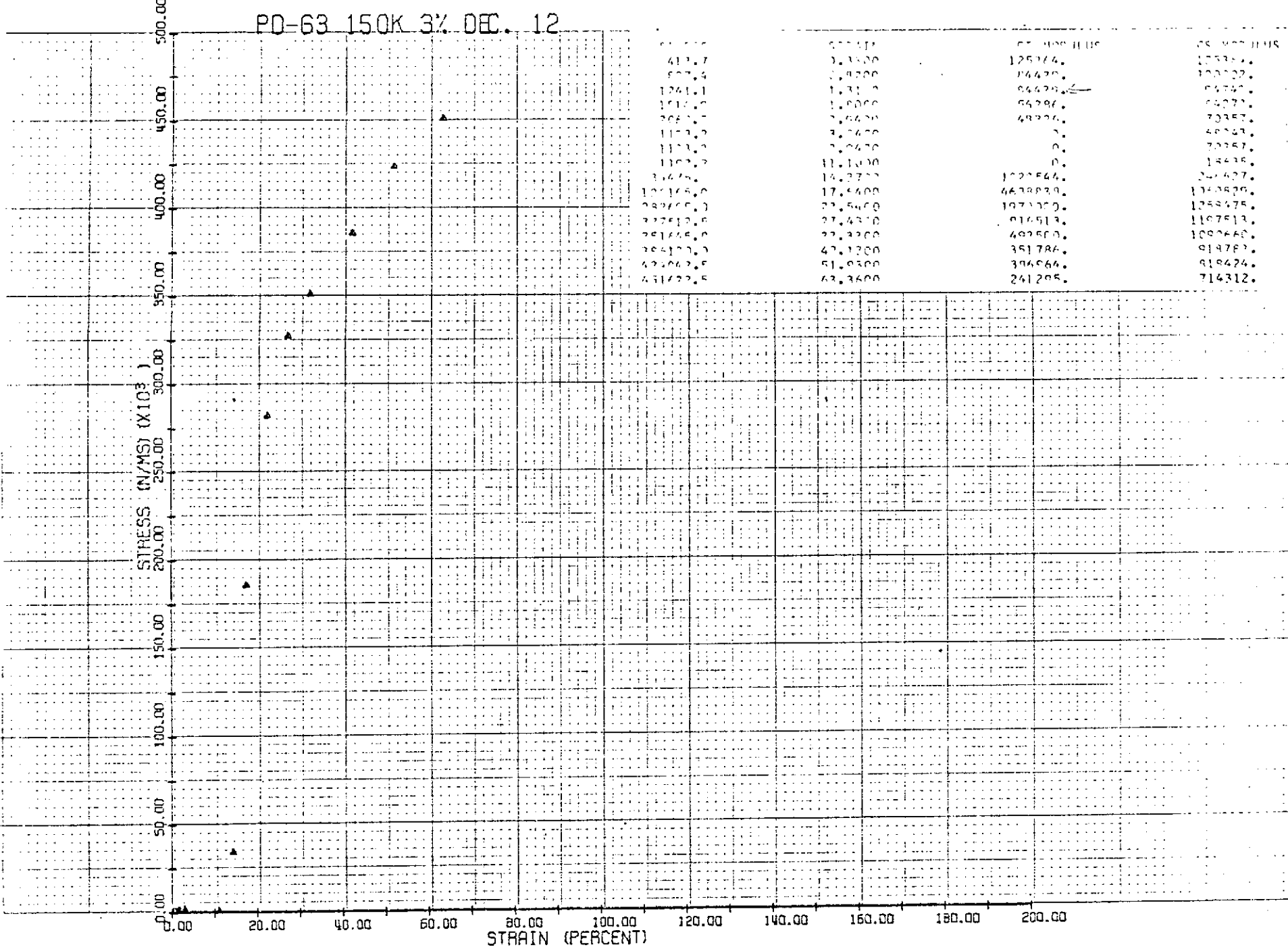
PRINTED IN U.S.A.

PD-39 150K 1% OCT. 31

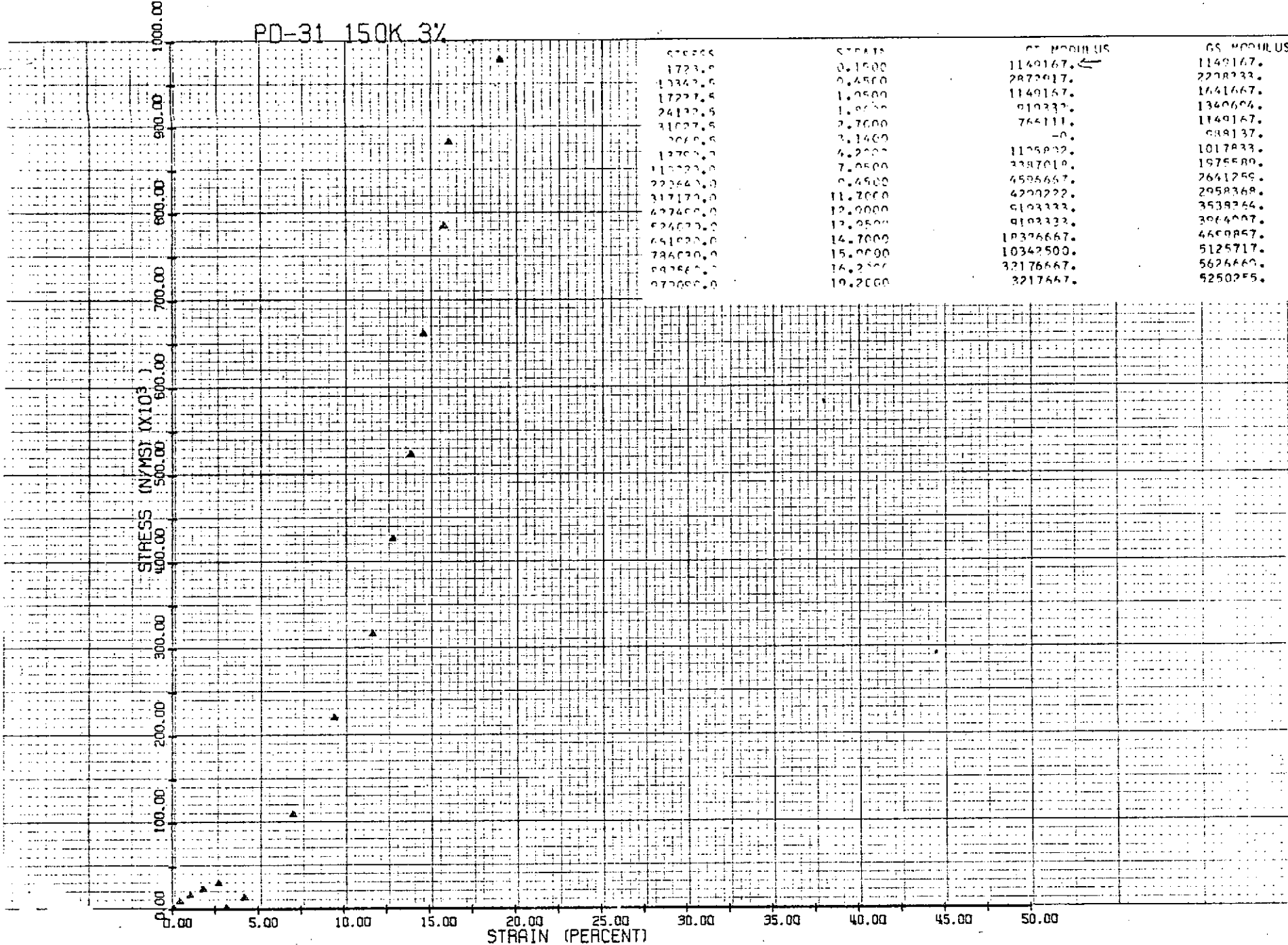


20 ft

PQ-63 150K 3% DEC. 12



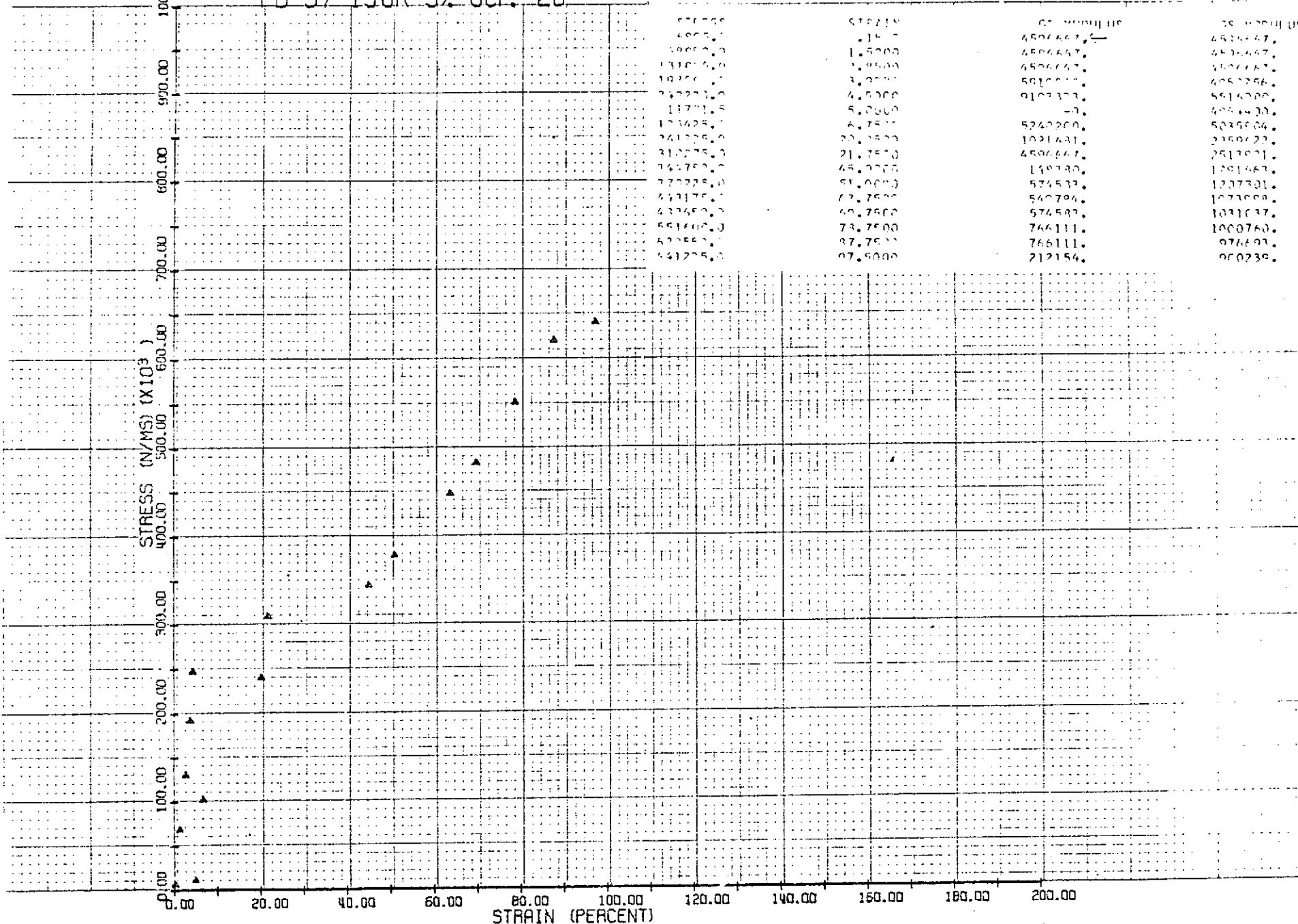
PD-31 150K 3%



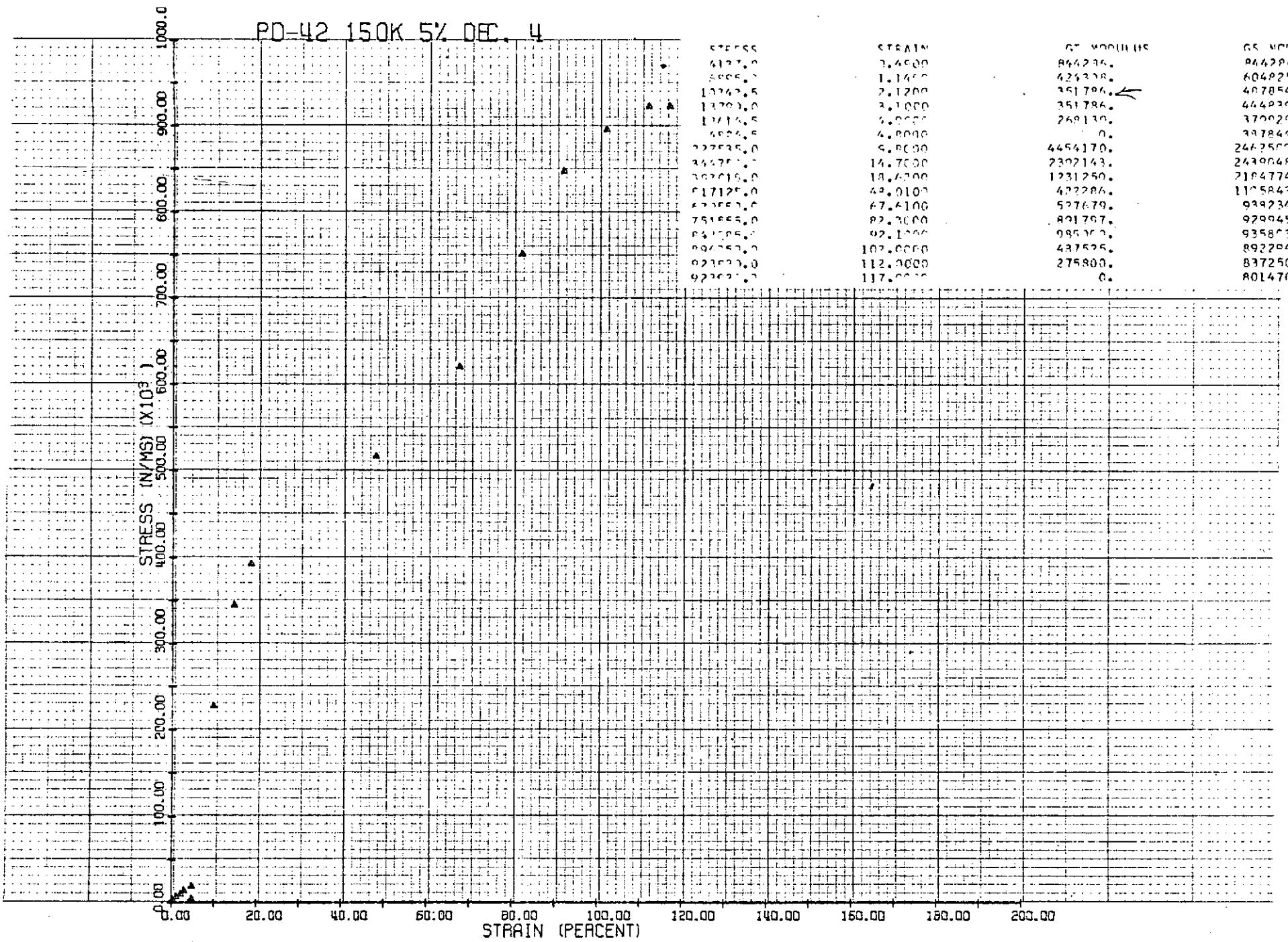
KEUFFEL & ESSER CO.

PRINTED IN U.S.A.

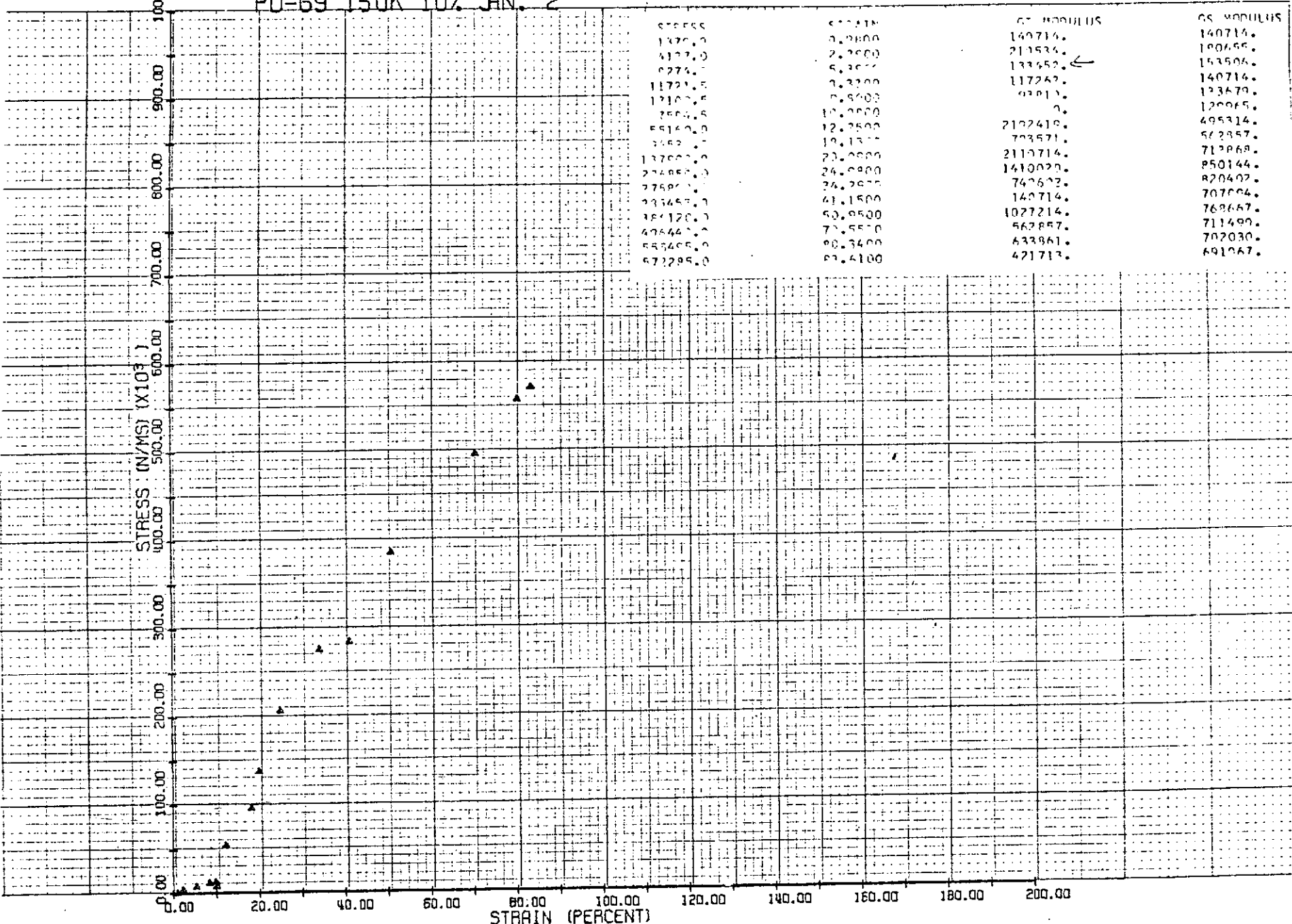
PD-37 150K 5% OCT. 28



PD-42 150K 5% DEC. 4



## PD-69 150K 10% FN. 2



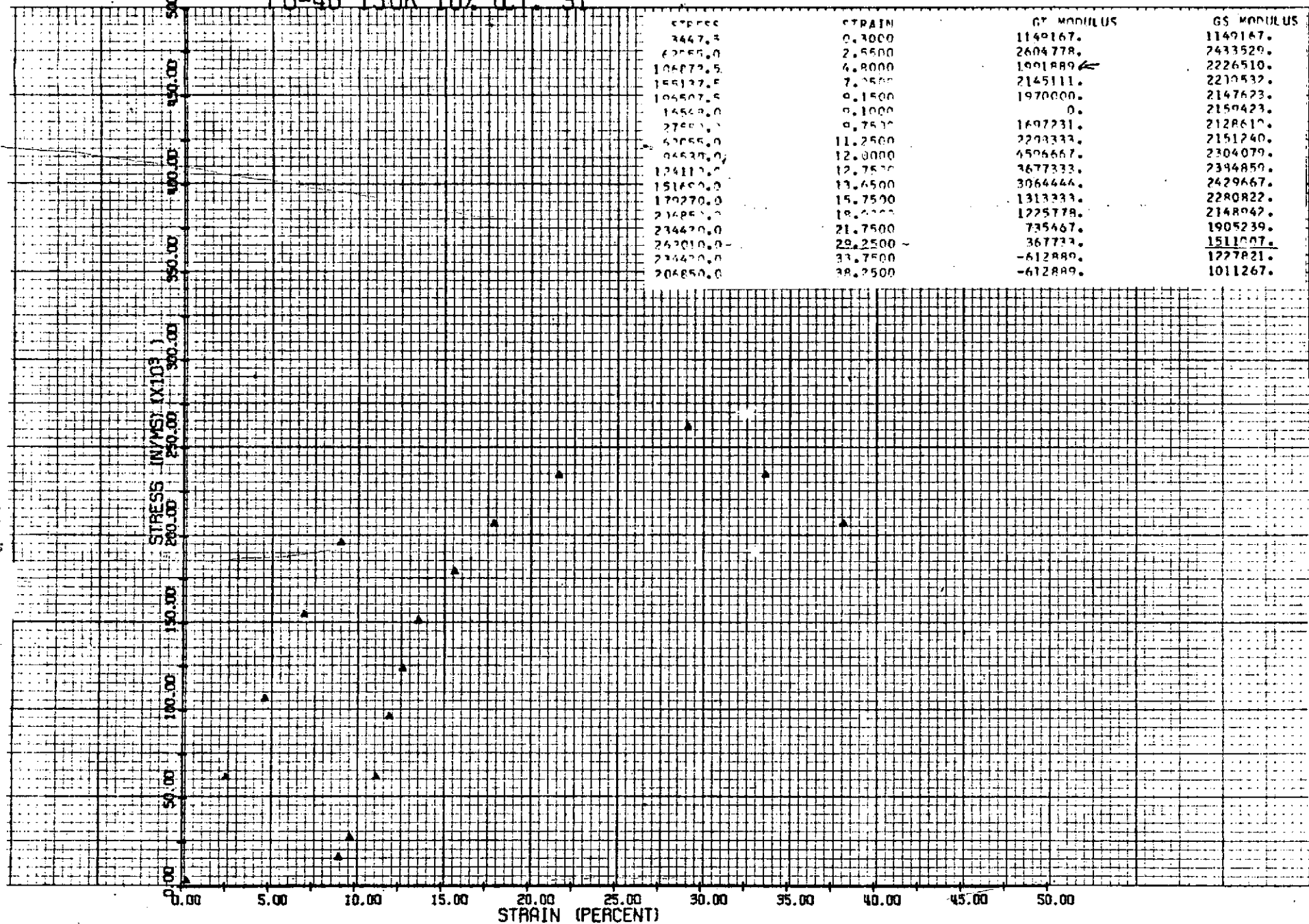
1

K-E KEUFFEL &amp; ESSER CO.

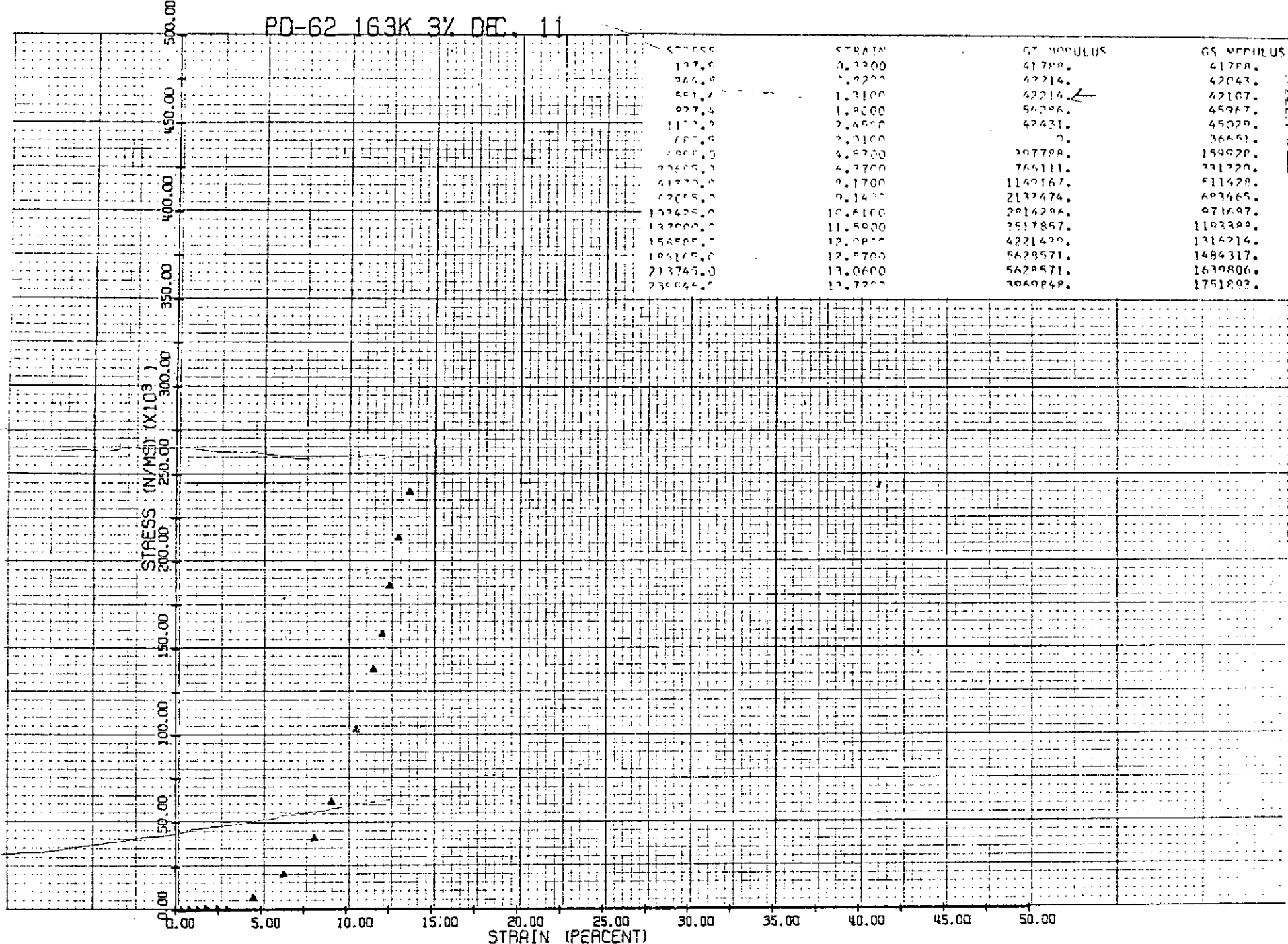
PRINTED IN U.S.A.

K-E KEI

## PO-46 150K 10% CT. 31

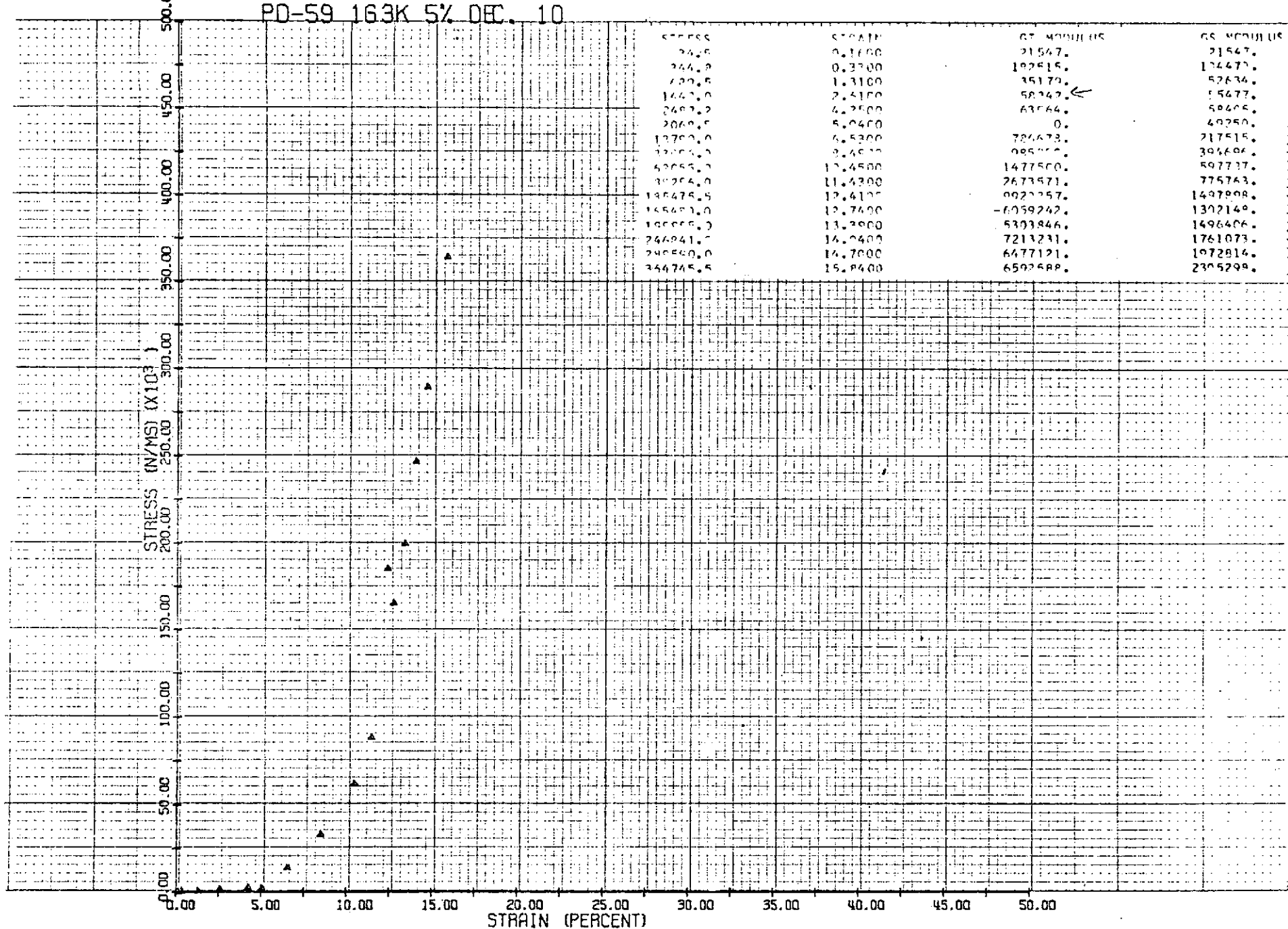


PD-62 163K 3% DEC. 11

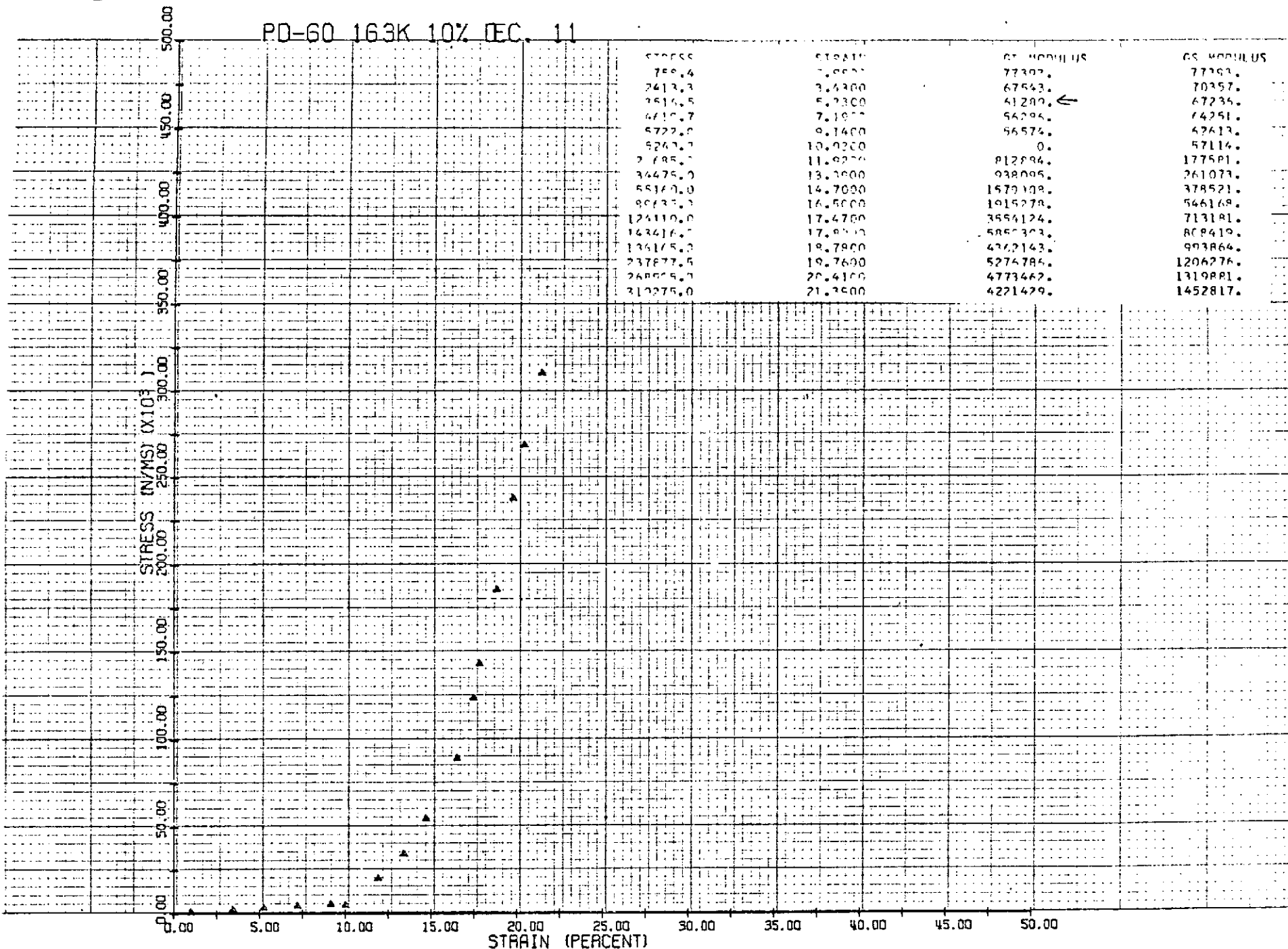


27A

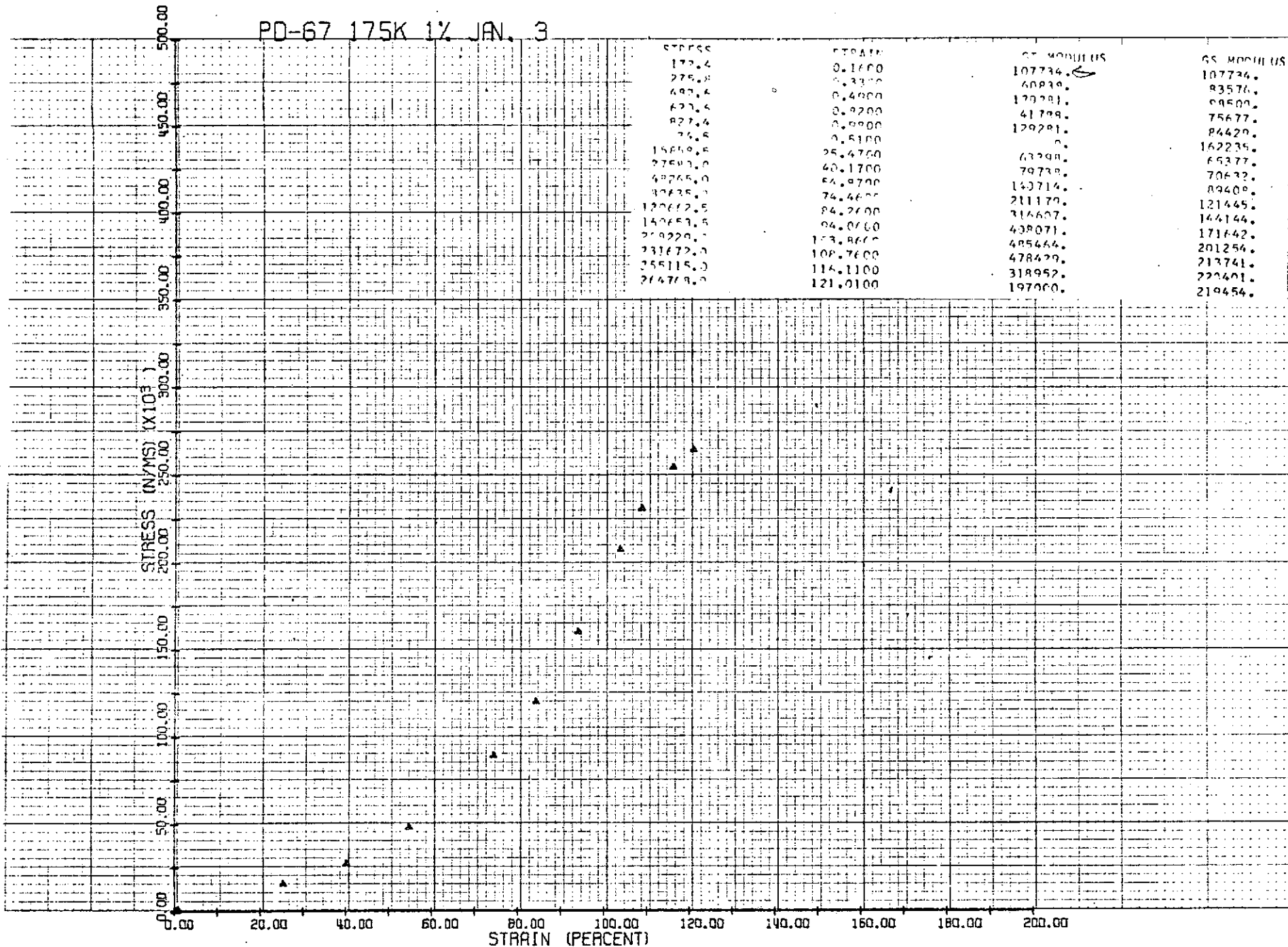
PD-59 163K 5% DEC. 10



## PD-60 163K 10% DEC. 11

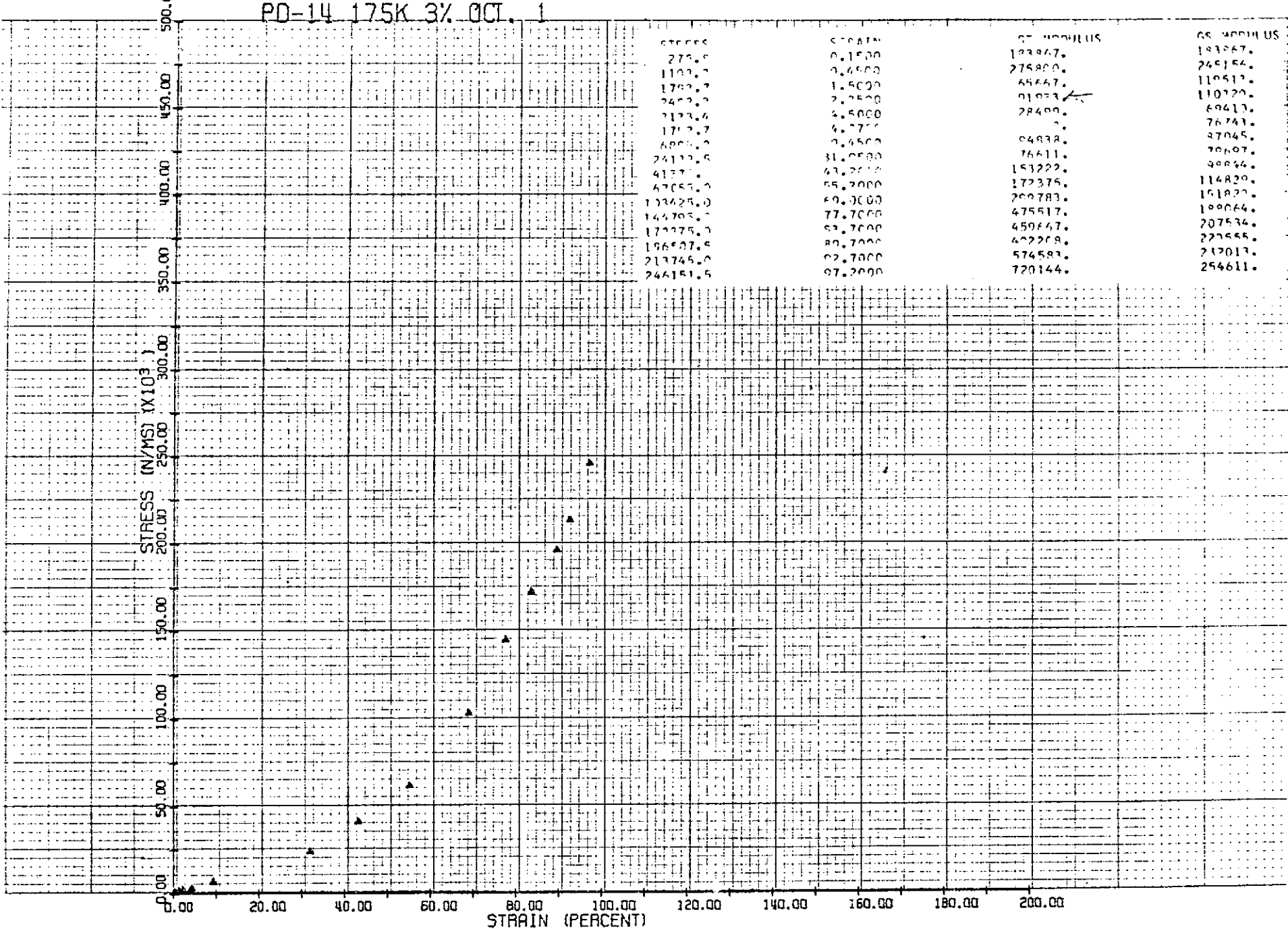


PD-67 175K 1 $\frac{1}{2}$  JAN. 3



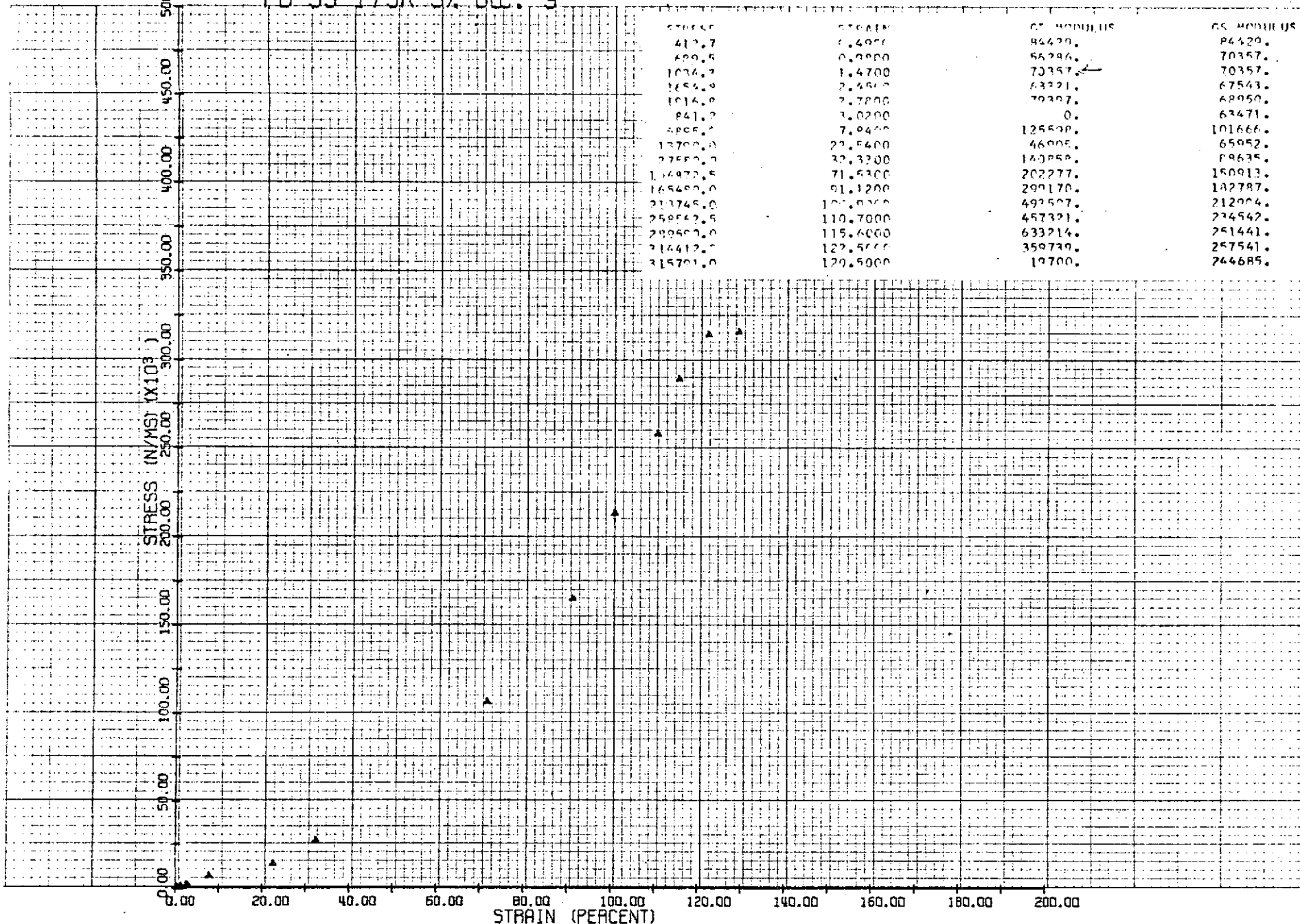
30 A

PD-14 175K 3% OCT. 1

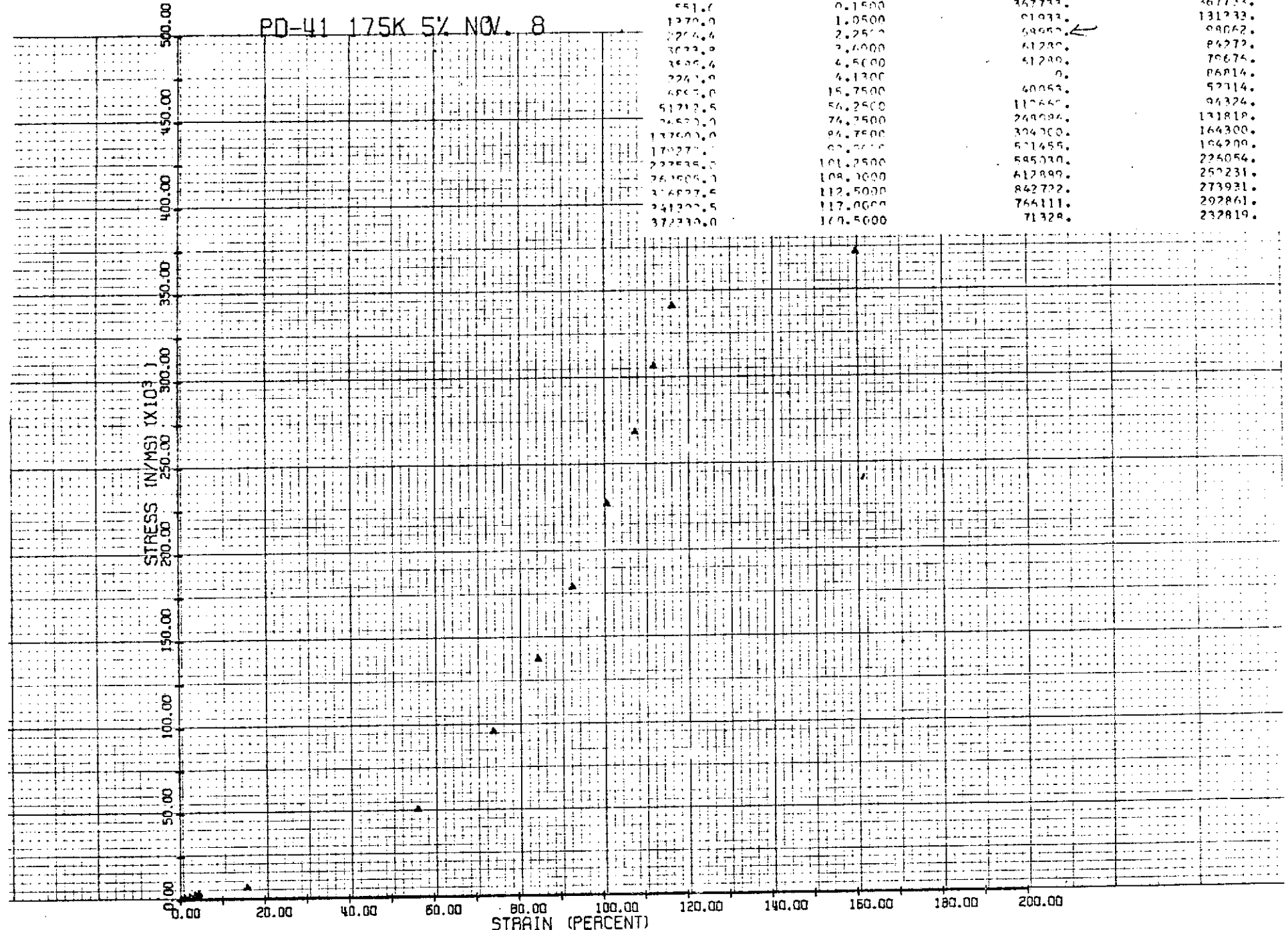


GR. YARDIN US  
143267.  
249154.  
110512.  
110720.  
69413.  
76741.  
27045.  
76607.  
90644.  
114820.  
161821.  
100644.  
207534.  
227555.  
212013.  
254611.

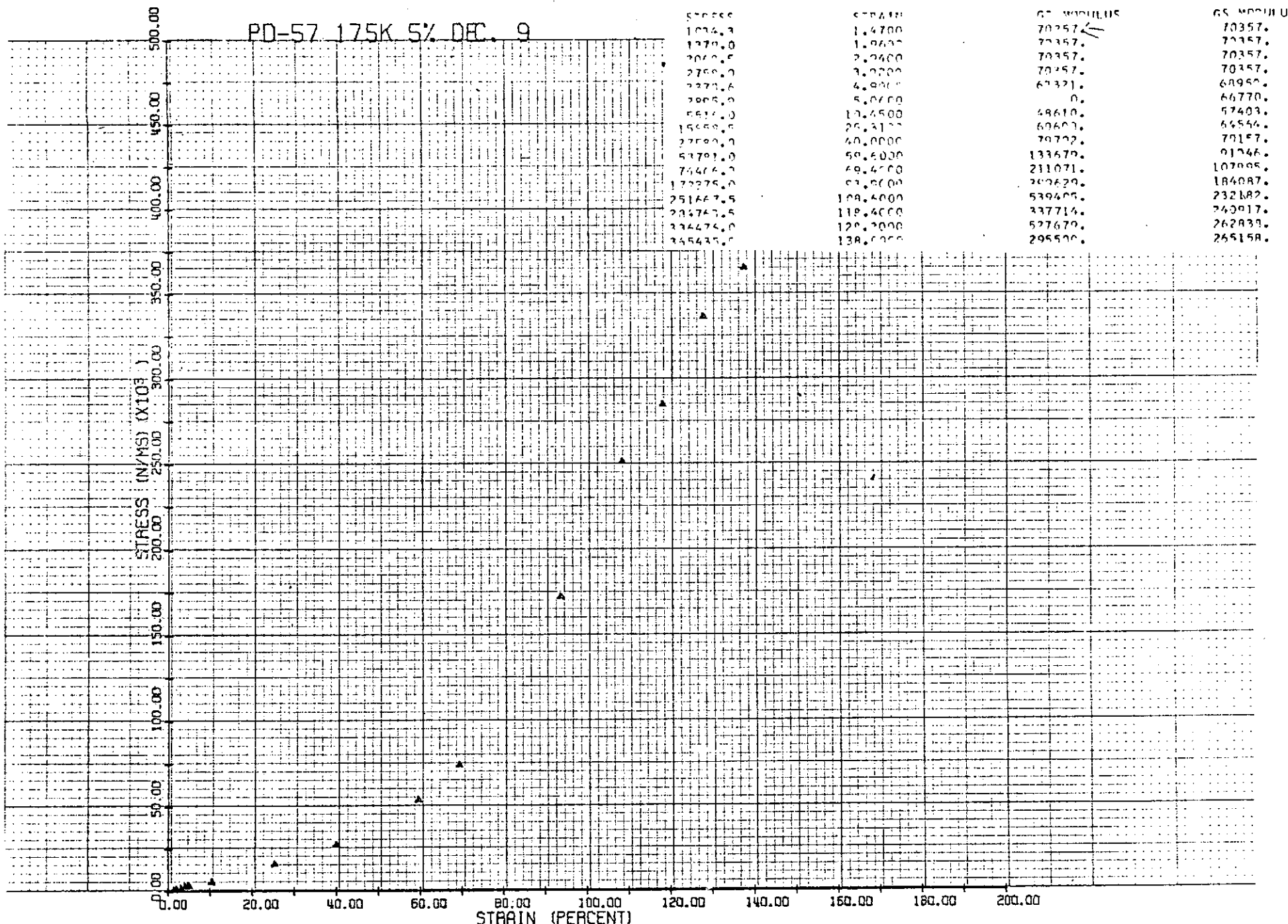
PD-55 175K 3% DEC. 9



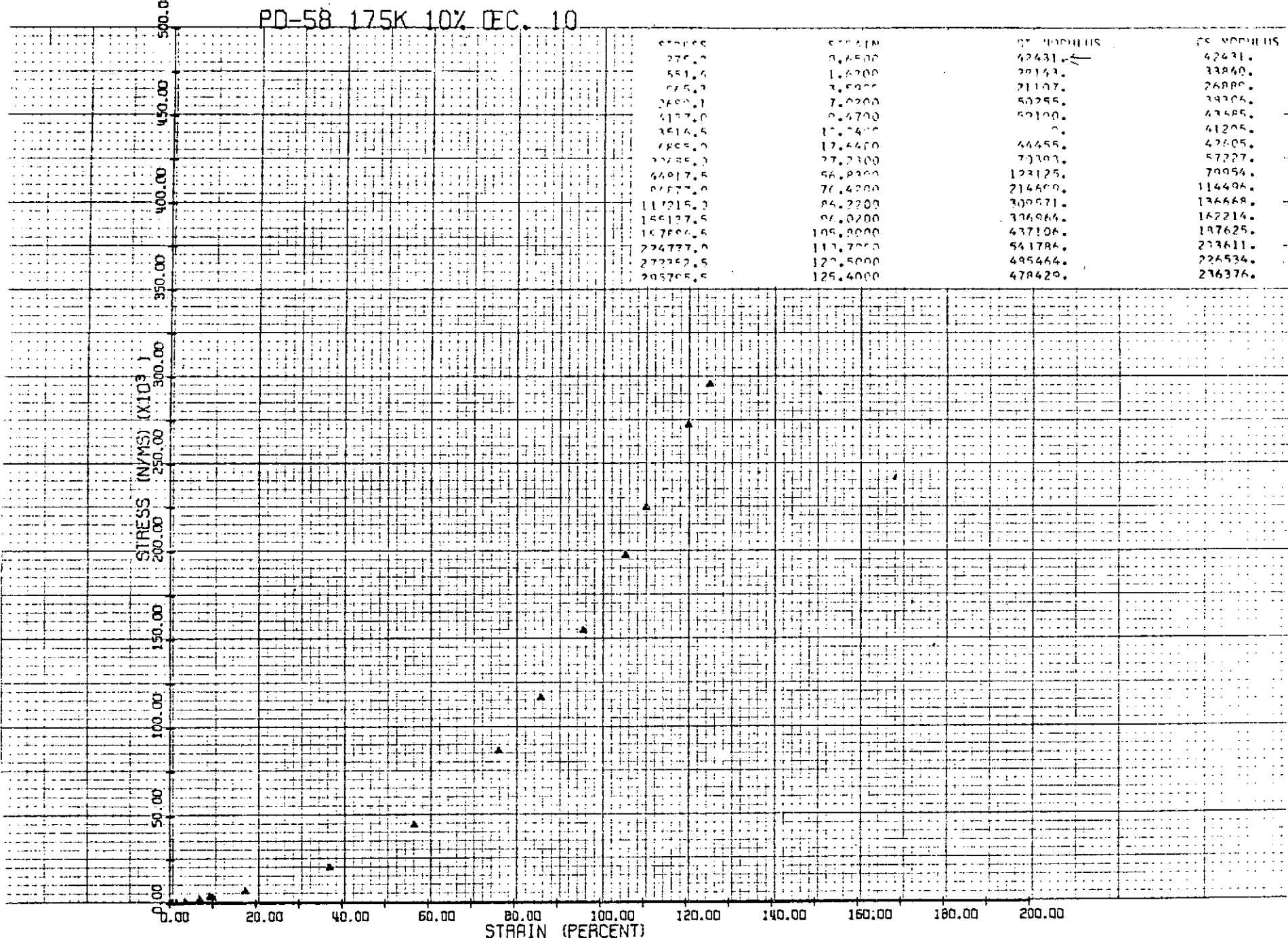
PD-41 175K 5% NOV. 8



STRESS	STRAIN	TEST NUMBER	TEST NUMBER
0.1500	0.1500	367733.	367733.
1.0500	1.0500	01933.	131233.
2.2500	2.2500	09062.	09062.
3.4000	3.4000	61280.	86272.
4.5000	4.5000	41280.	70674.
4.1300	4.1300	0.	86814.
15.7500	15.7500	60053.	92714.
56.2500	56.2500	112650.	94324.
76.2500	76.2500	249084.	131818.
96.7500	96.7500	304700.	164300.
67.0000	67.0000	571455.	164200.
101.7500	101.7500	545730.	225054.
108.0000	108.0000	612899.	251231.
112.5000	112.5000	862722.	273931.
117.0000	117.0000	766111.	292861.
170.5000	170.5000	713284.	232819.

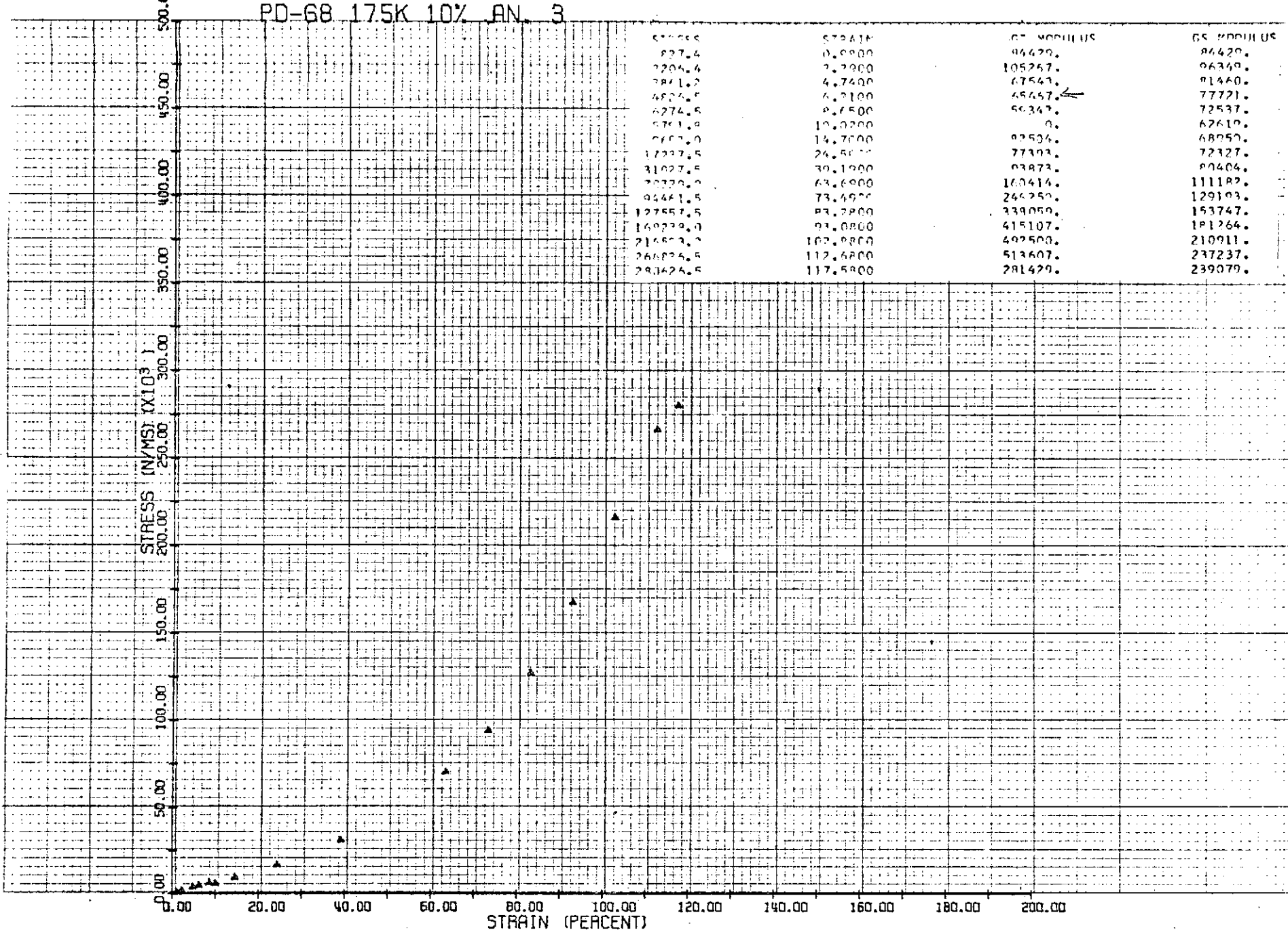


PD-58 175K 10% DEC. 10

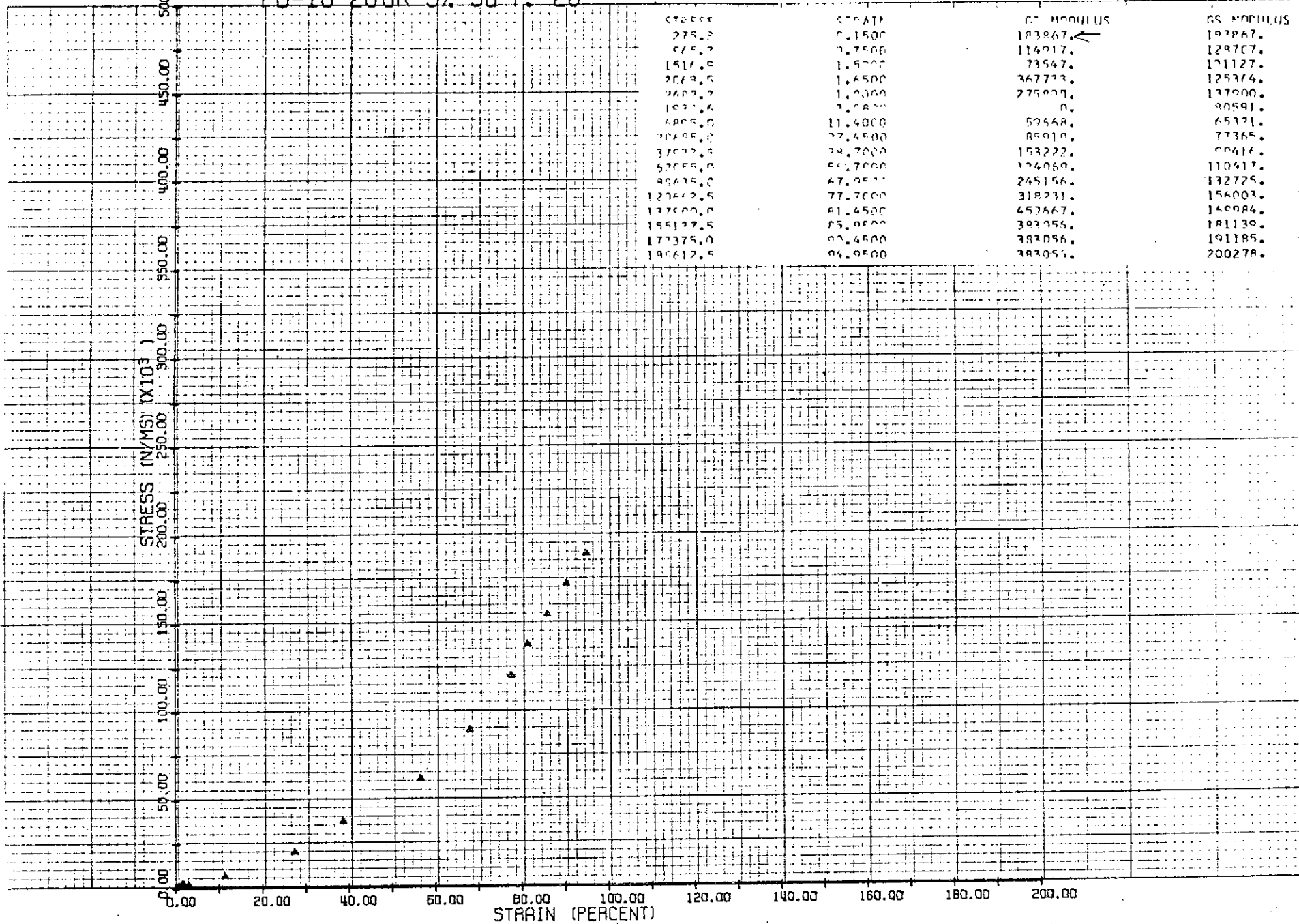


C1

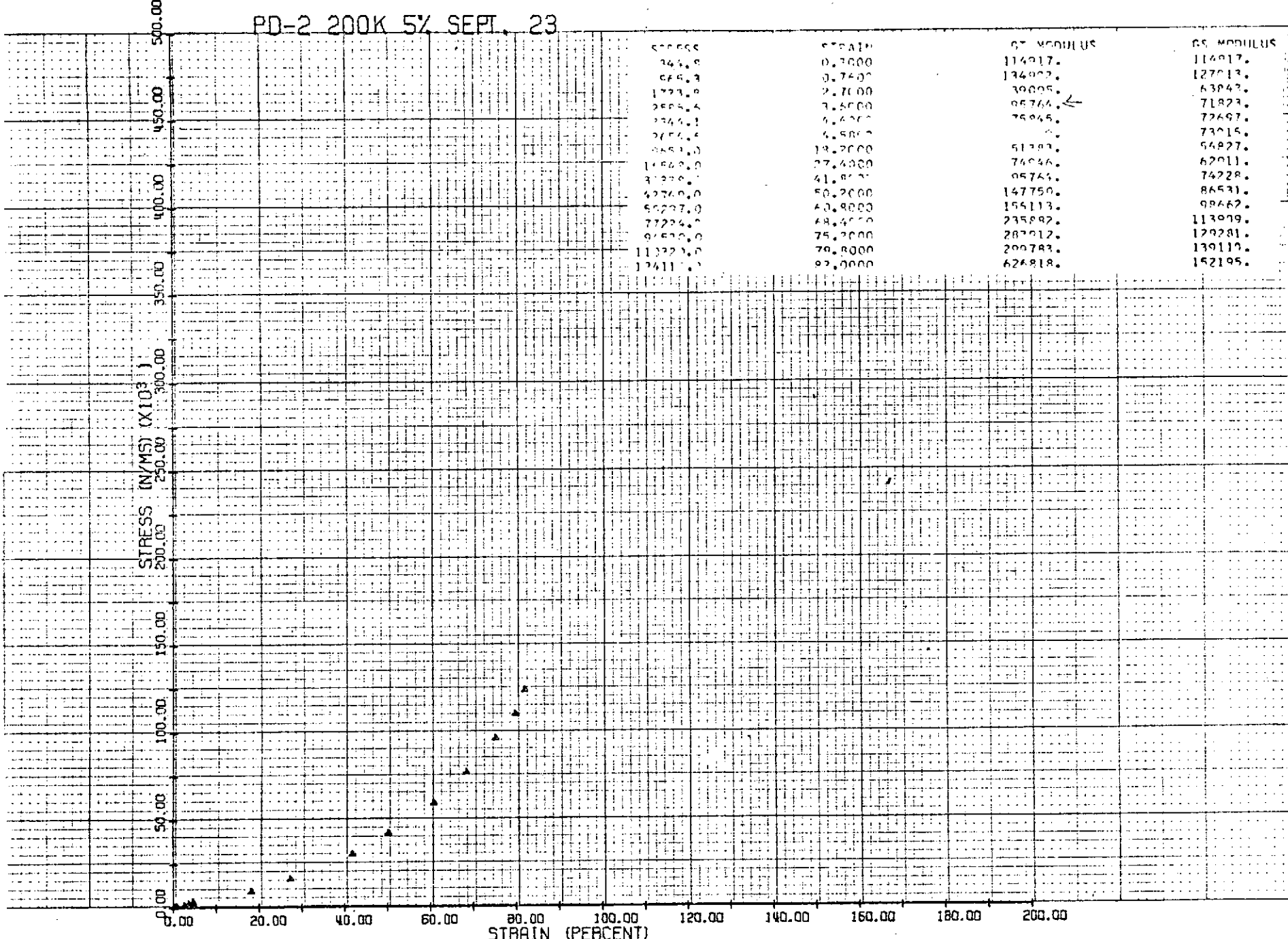
## PD-68 17.5K 10% AN 3



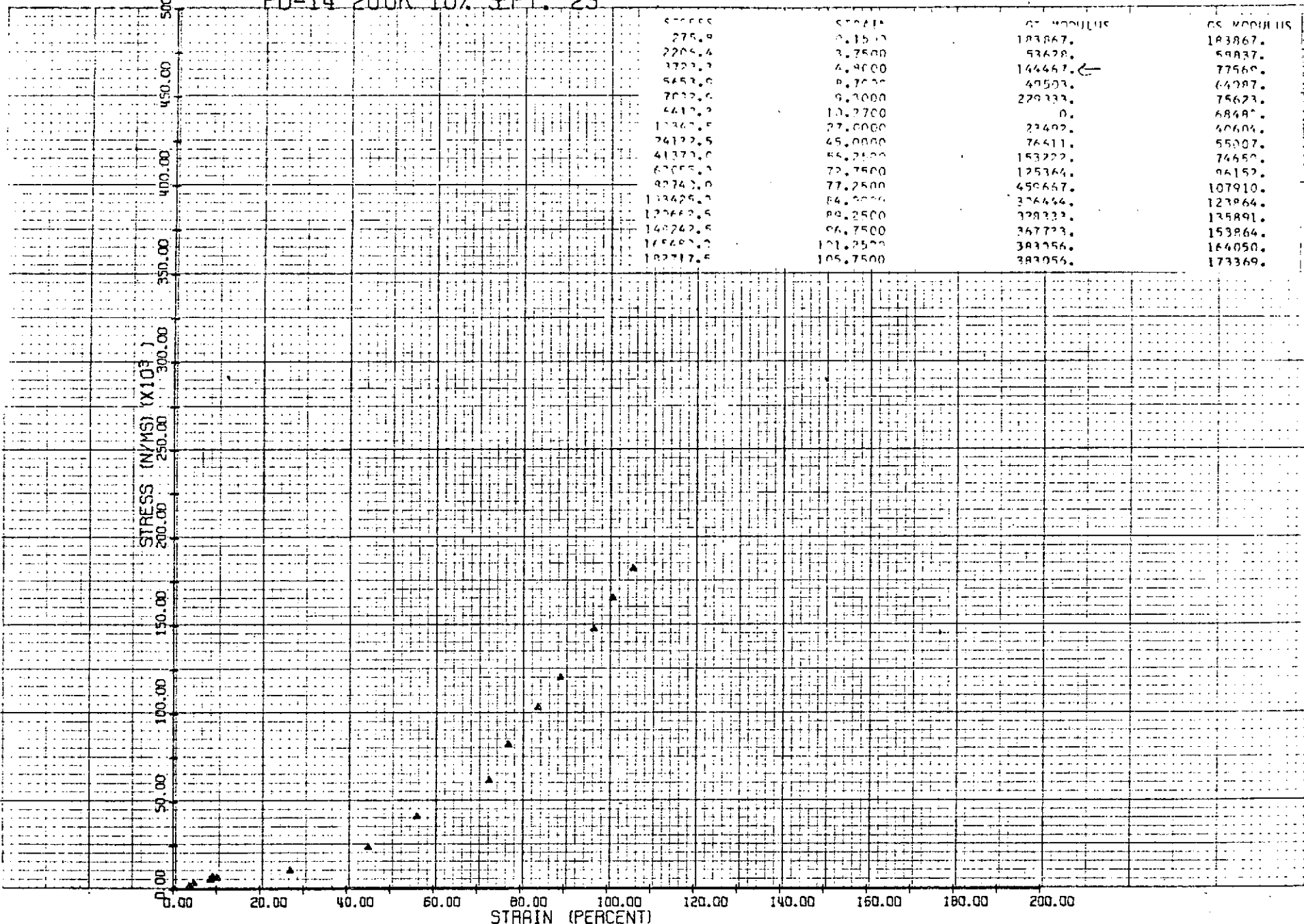
PO-10 200K 3% SEPT. 26



PD-2 200K 5% SEPT. 23

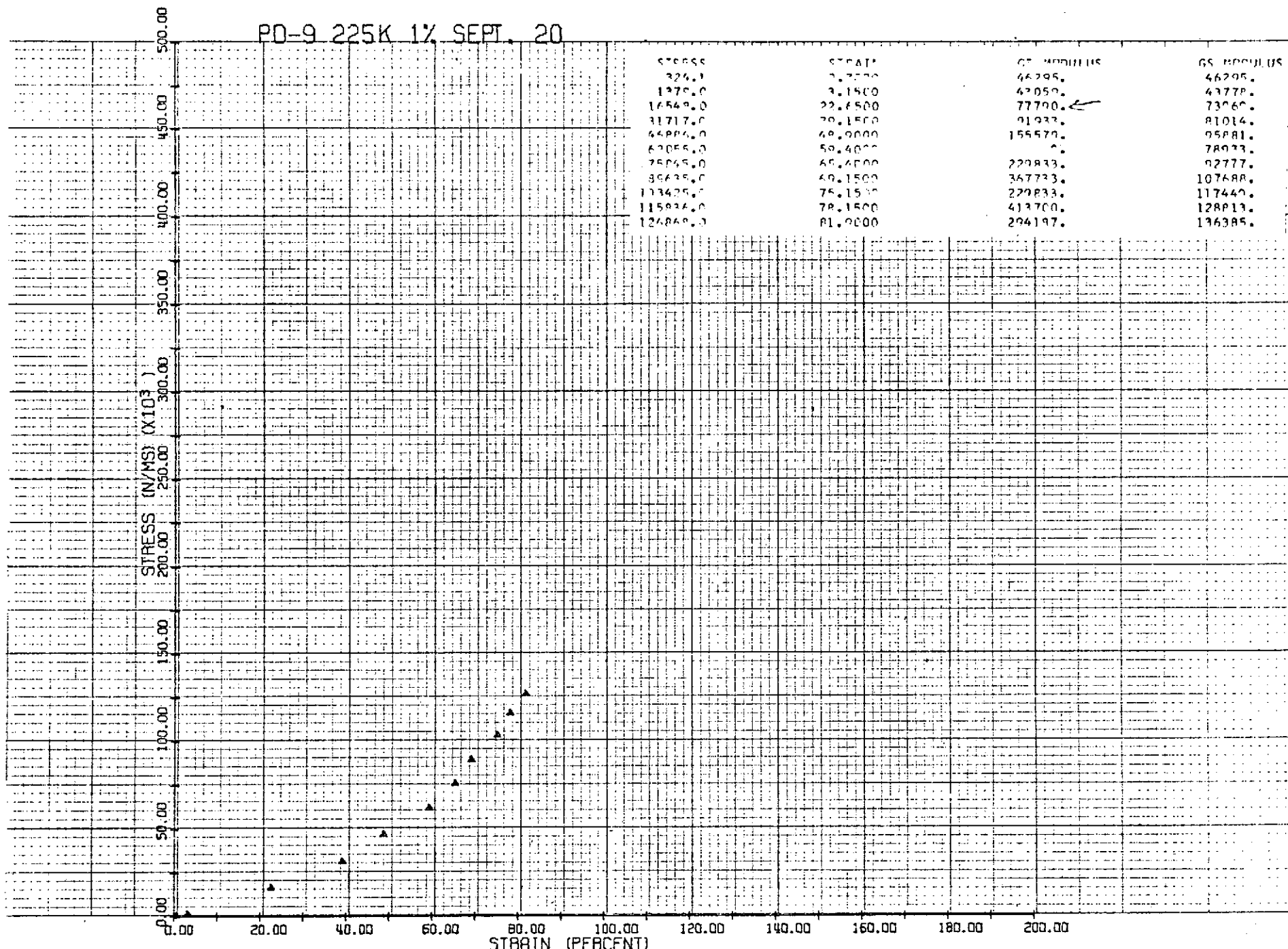


PD-14 200K 10% SEPT. 23

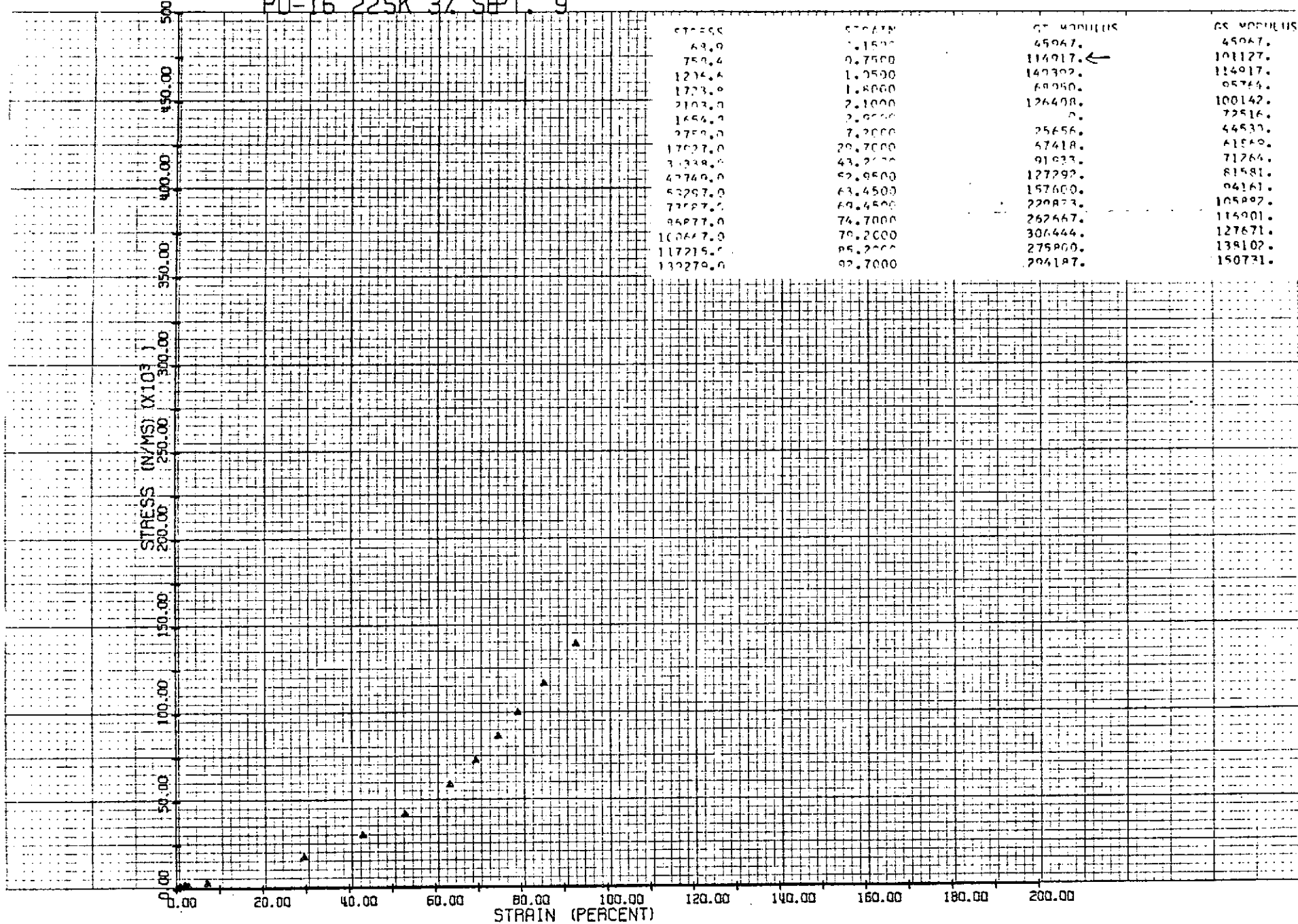


C-2

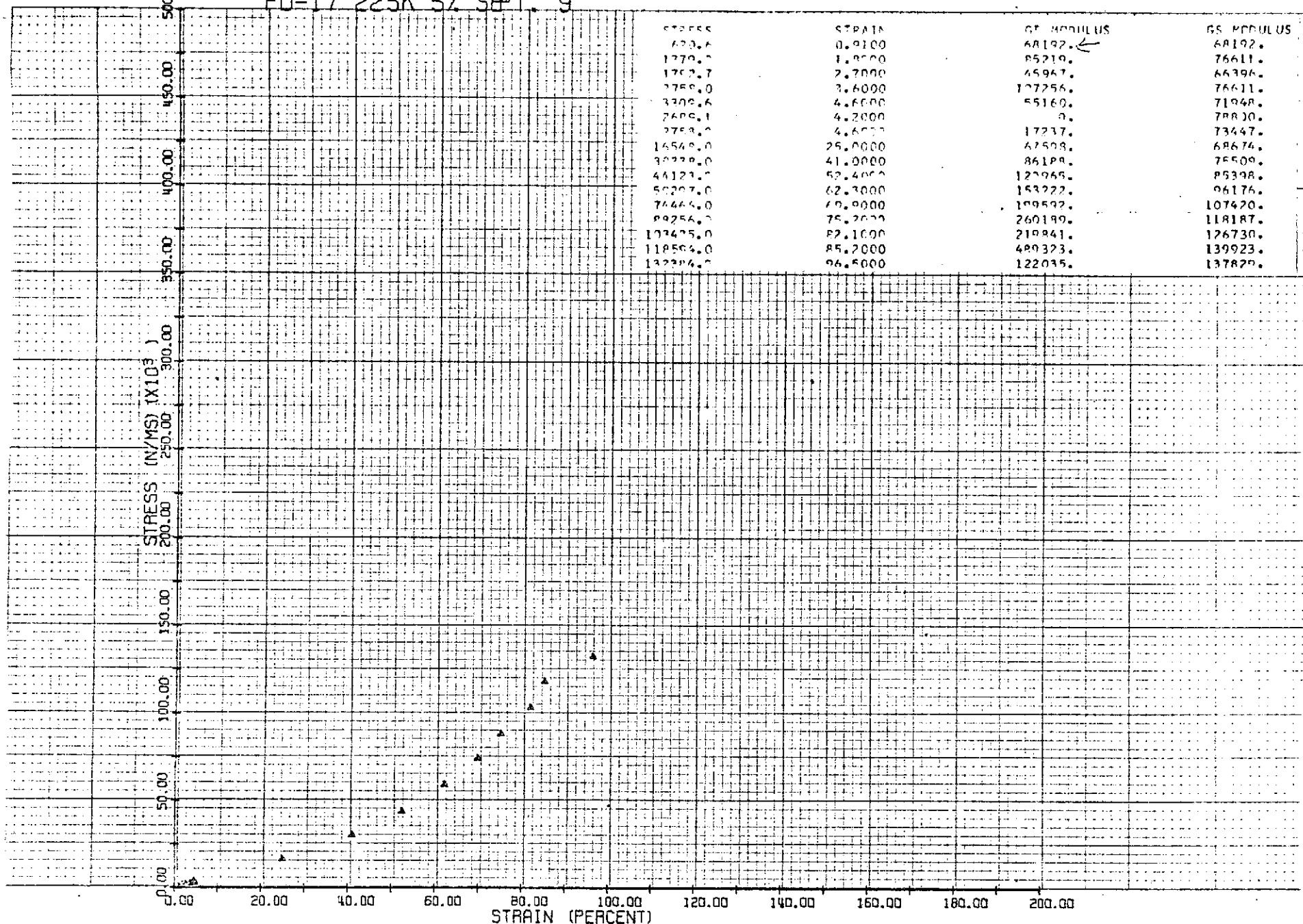
40



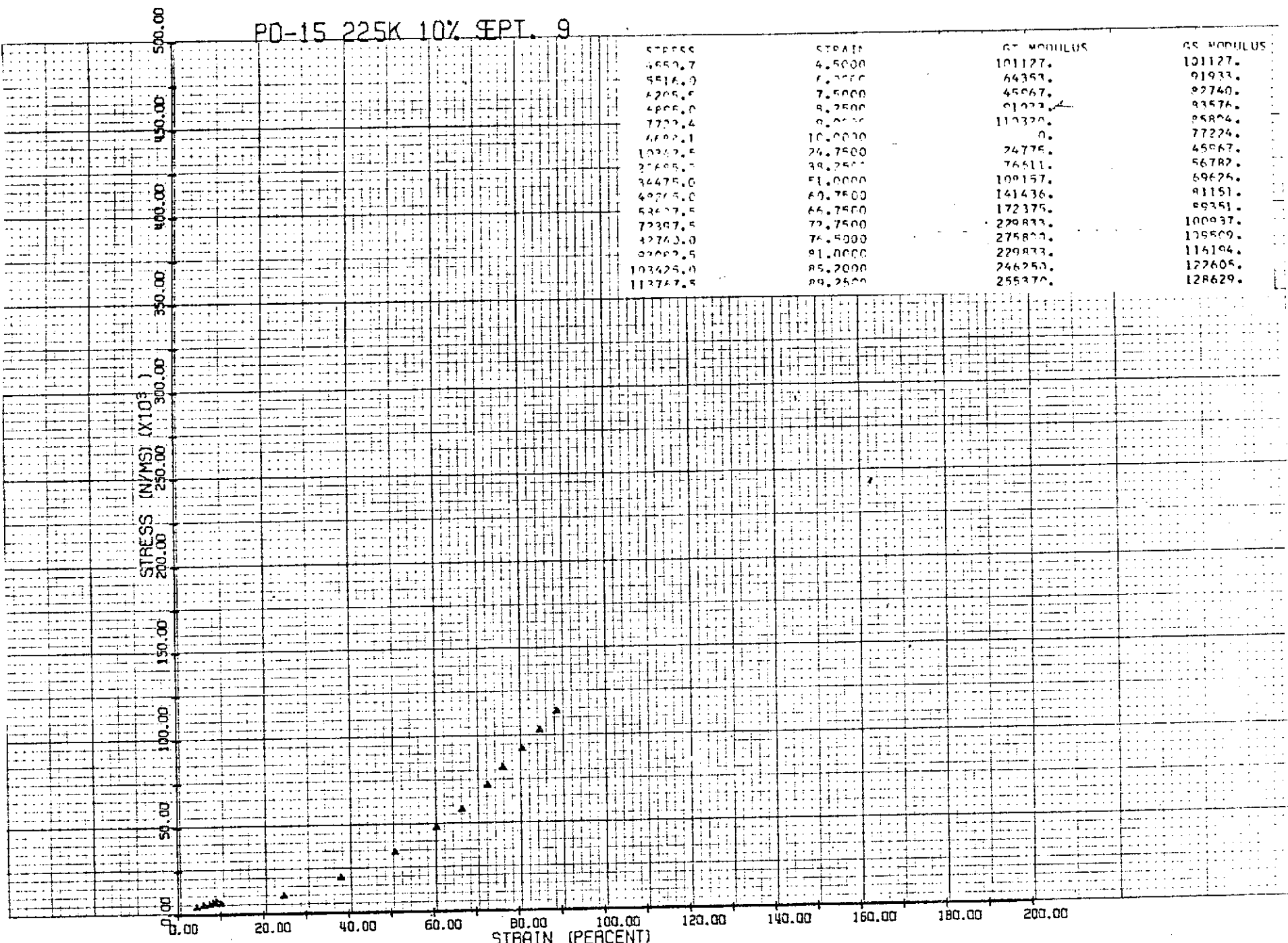
PO-16 225K 3% SEPT. 9



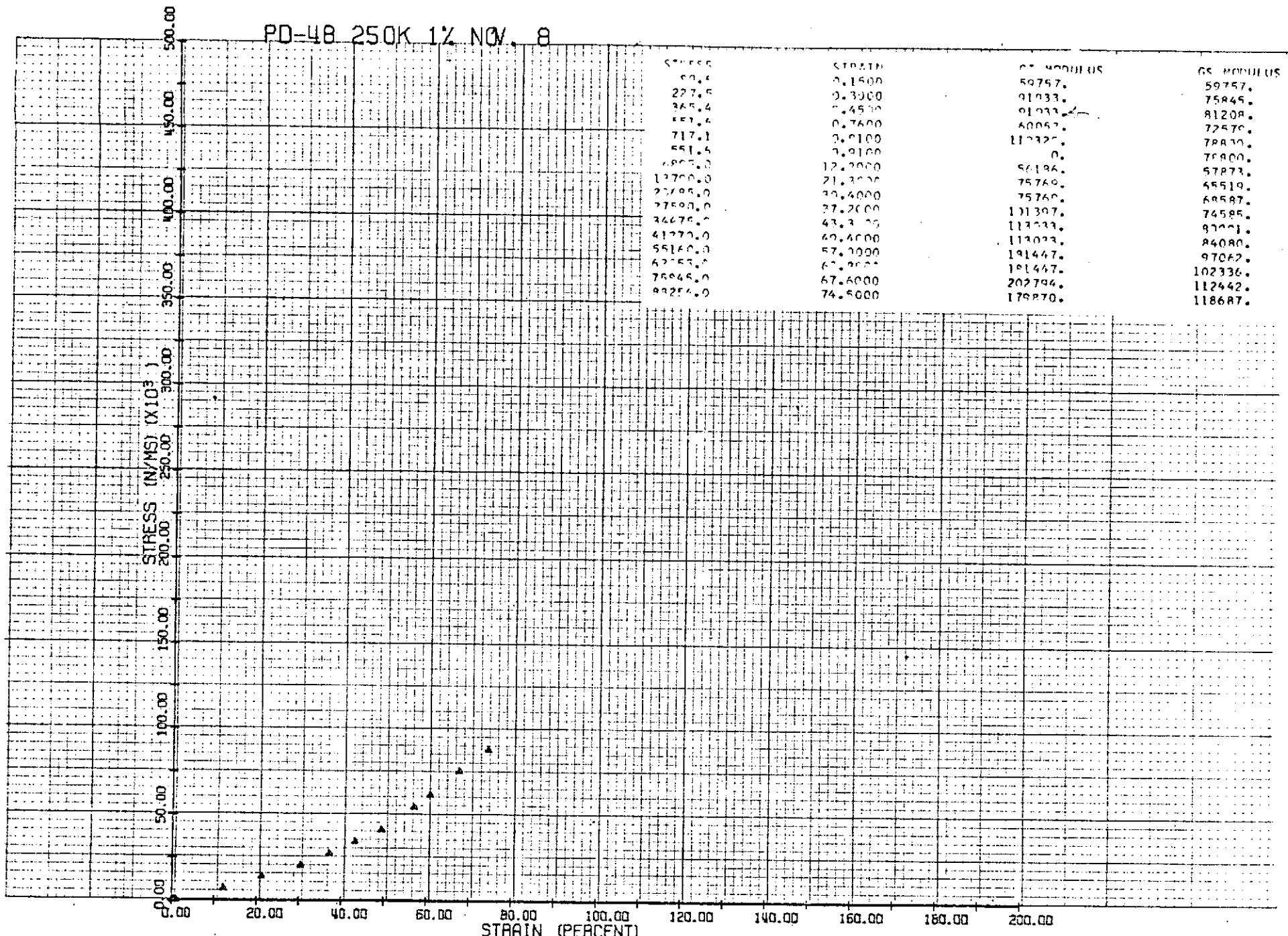
PD-17 225K 5% SPT 9



PD-15 225K 10% SEPT. 9

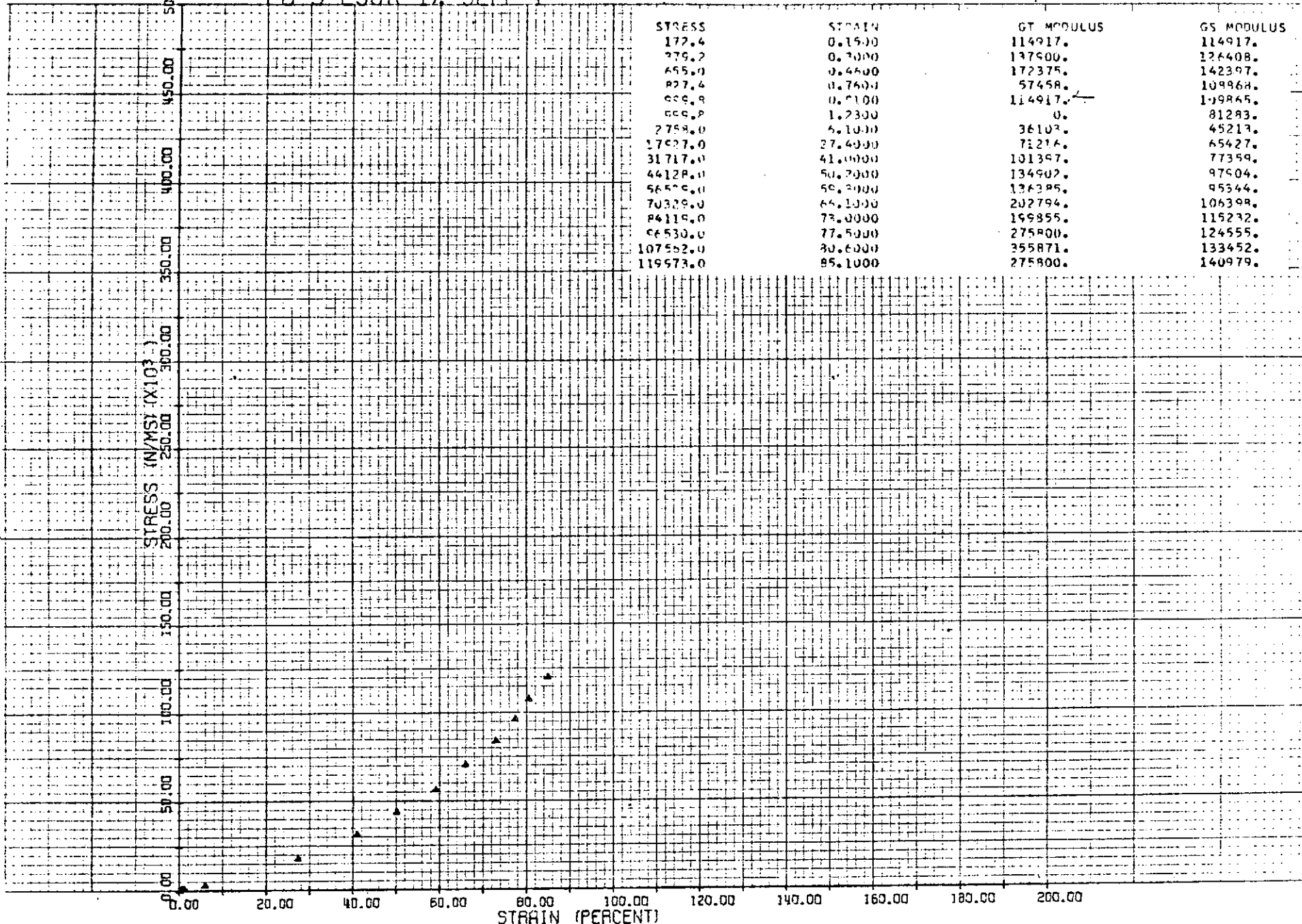


43 A

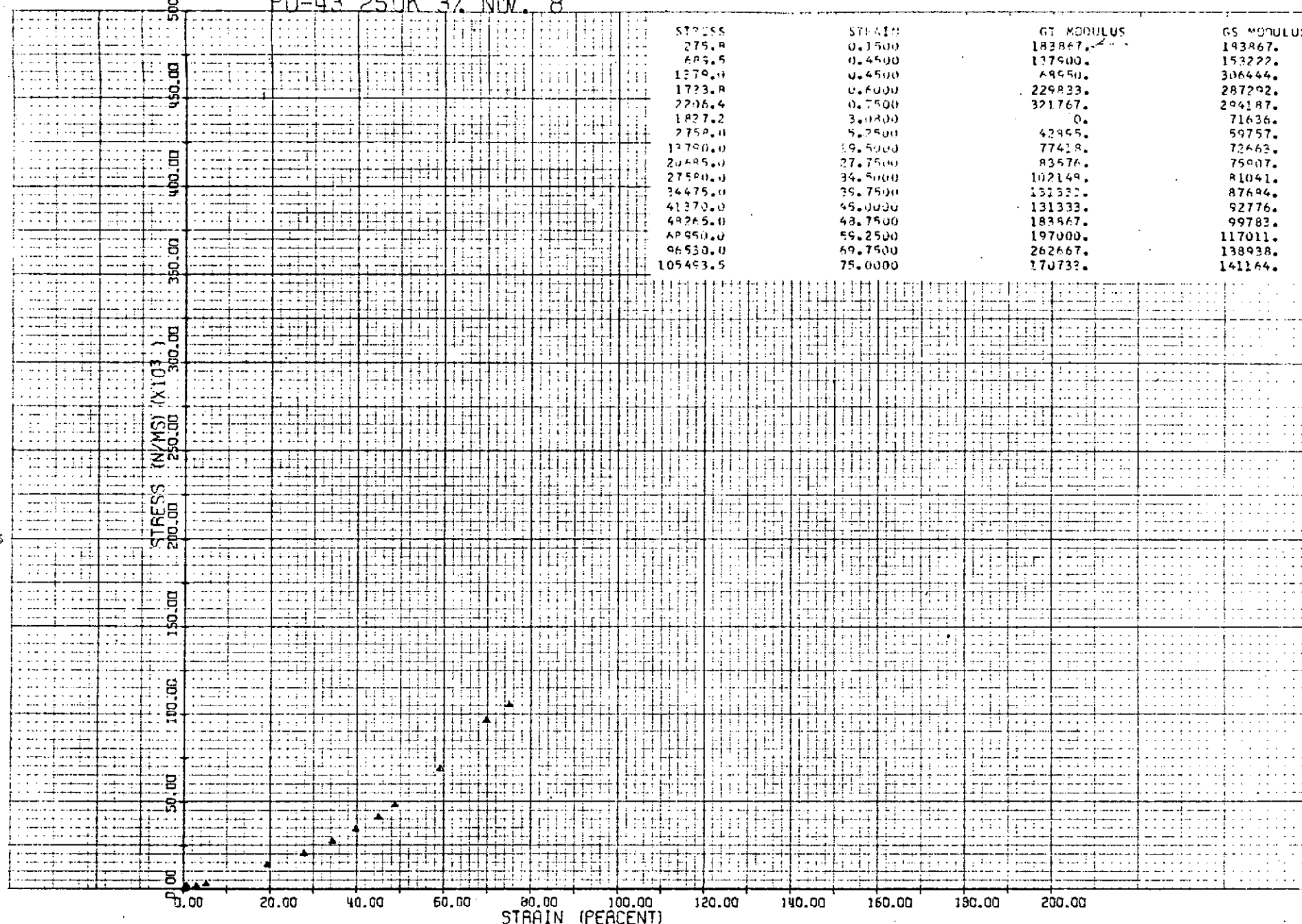


44 A

PD-3 250K 1% SEPT 4



PD-43 250K 3% Nov. 8



46

50.00

PD-6 250K 3% AUG 28

474

STRESS (KN/MSI) ( $\times 10^3$ )

500.00

450.00

400.00

350.00

300.00

250.00

200.00

150.00

100.00

50.00

0.00

-50.00

-100.00

-150.00

-200.00

-250.00

-300.00

-350.00

-400.00

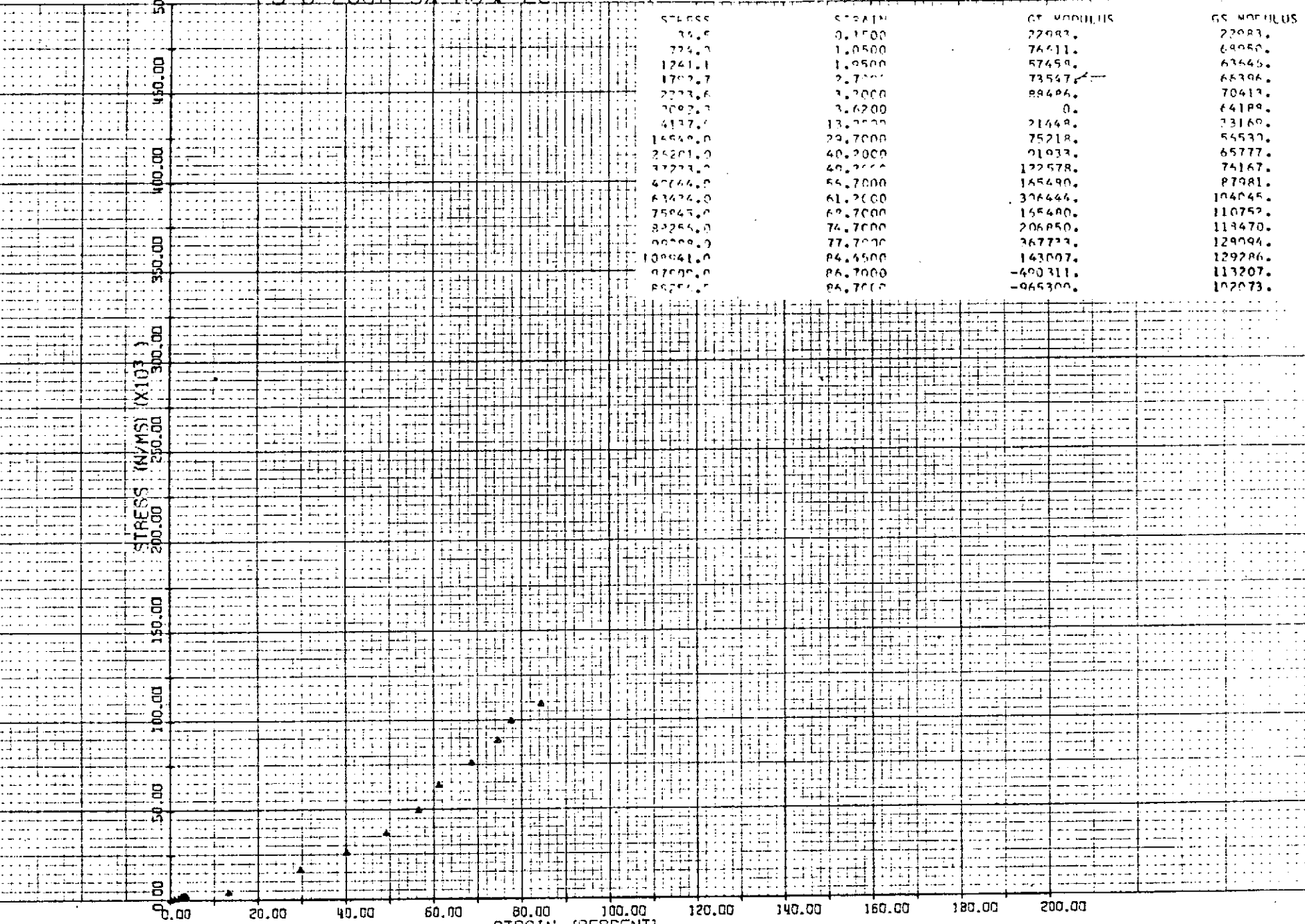
-450.00

-500.00

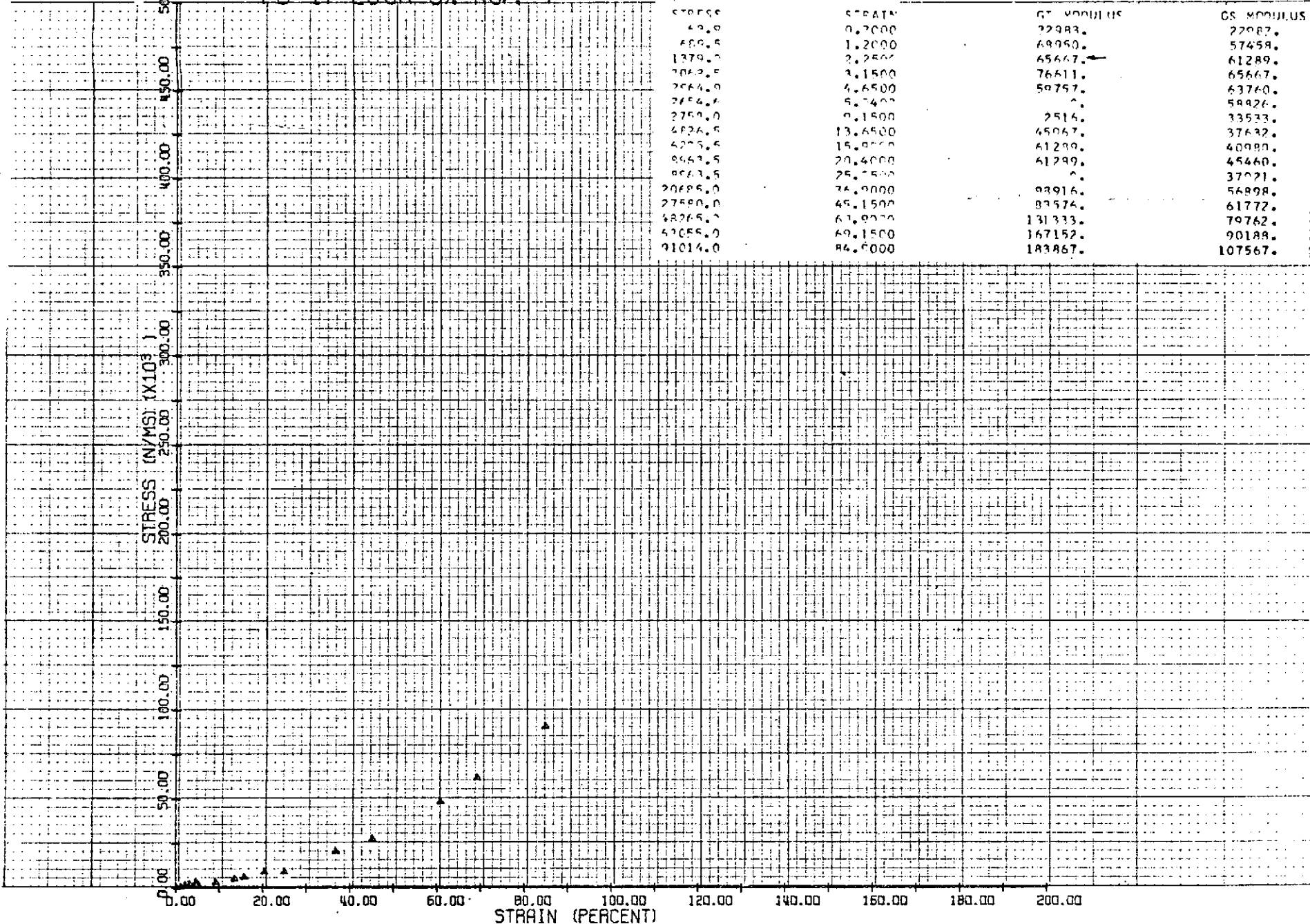
0.00 20.00 40.00 60.00 80.00 100.00 120.00 140.00 160.00 180.00 200.00

STRAIN (PERCENT)

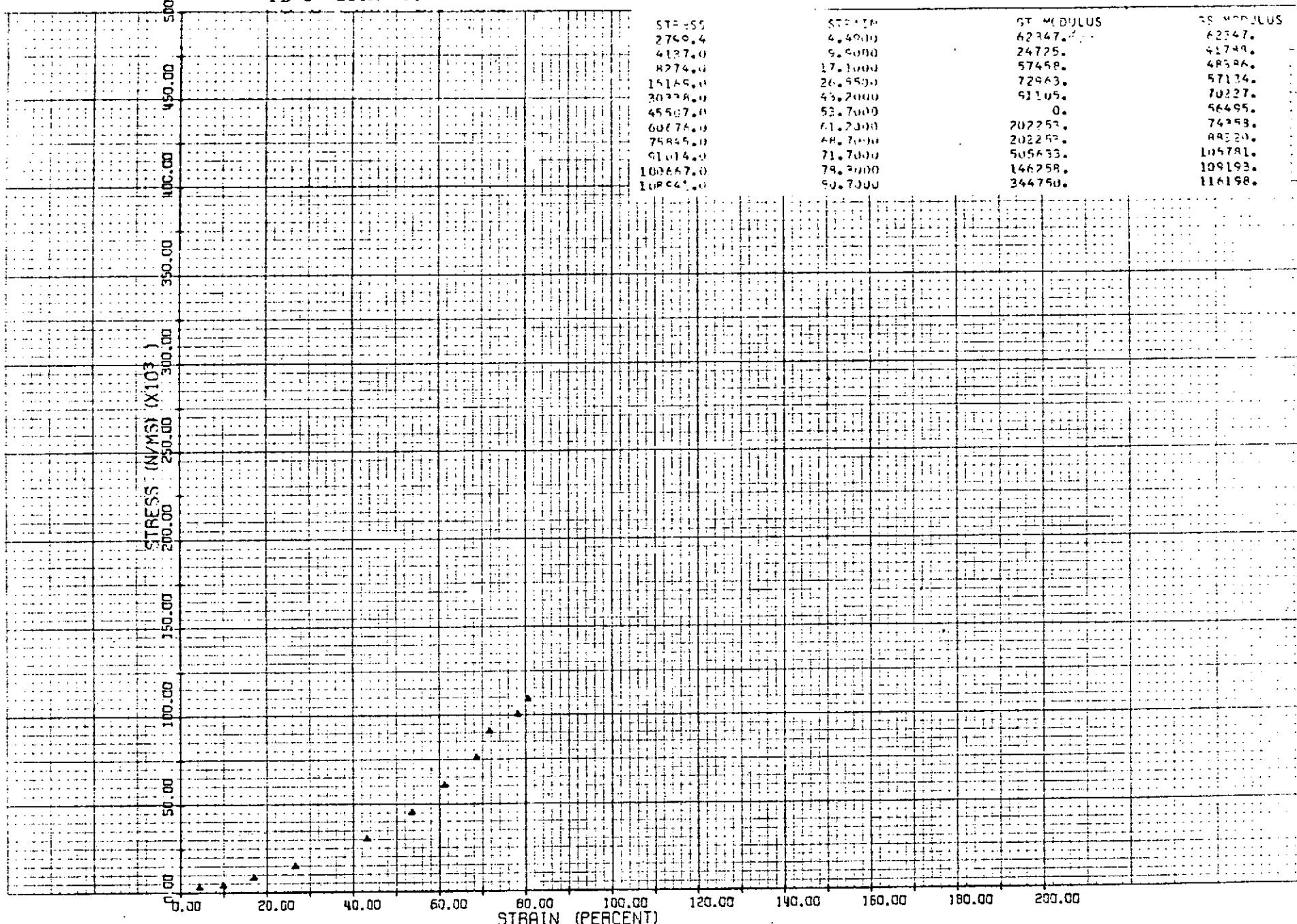
STRESS	STRAIN	GT MODULUS	GS MODULUS
-50.0	0.1700	22083.	22083.
725.0	1.0500	74411.	69050.
1261.0	1.9500	57459.	61245.
1797.0	2.7500	73547.	68398.
2333.0	3.2000	88494.	70413.
2869.0	3.6200	0.	64189.
4137.0	13.2200	21449.	73160.
15640.0	29.7000	75218.	54537.
25201.0	40.2000	91933.	65777.
37277.0	49.2000	122578.	74167.
47744.0	55.7000	145490.	87981.
61474.0	61.2000	376644.	104045.
75947.0	67.7000	155480.	110752.
83285.0	74.7000	206850.	113470.
90709.0	77.7000	267773.	124094.
100061.0	84.5000	143007.	129296.
97000.0	86.7000	-490311.	113207.
89274.0	86.7000	-965300.	102073.



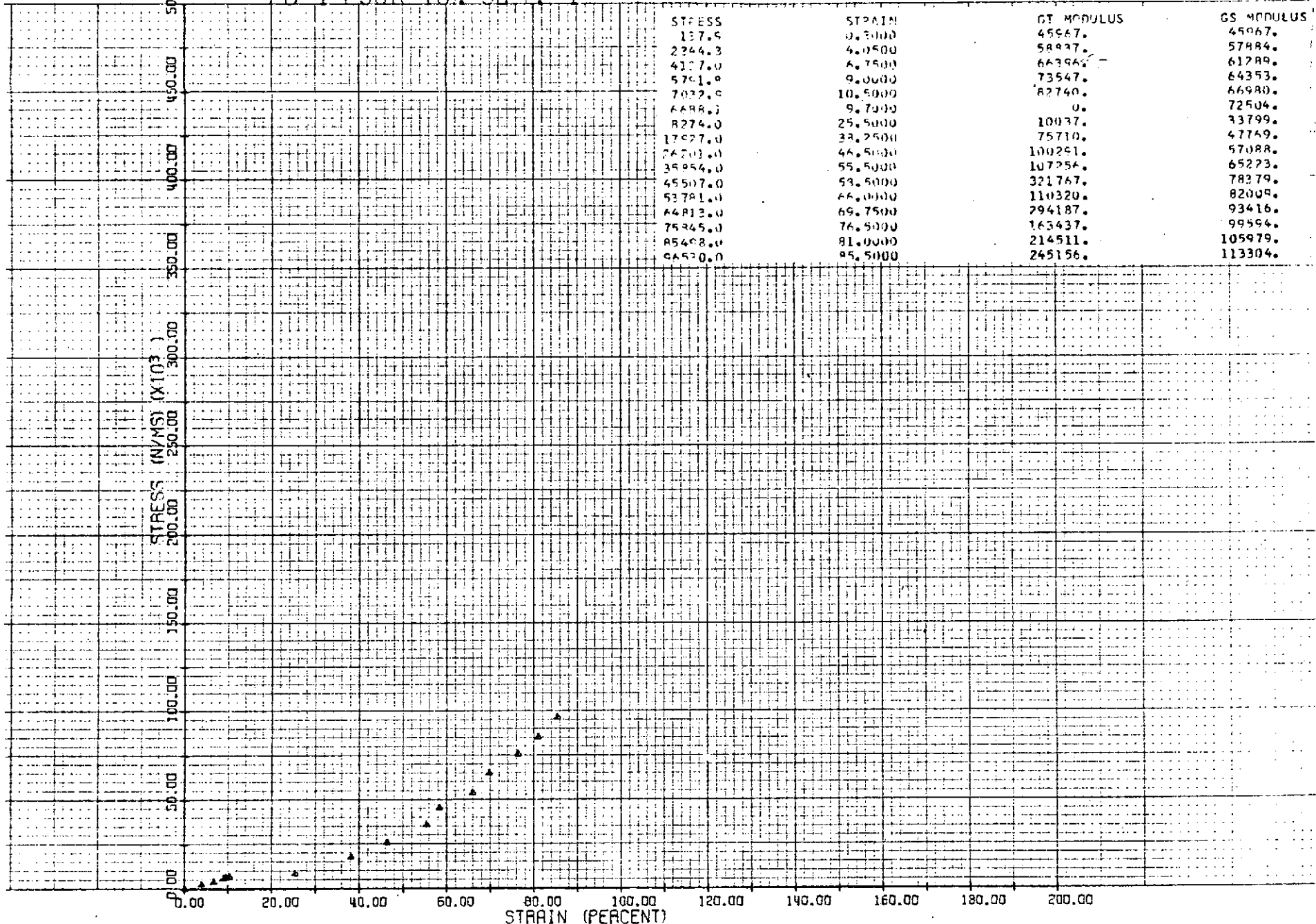
PD-47 250K 5% NOV. 7



PD-5 250K 5% AUG. 27

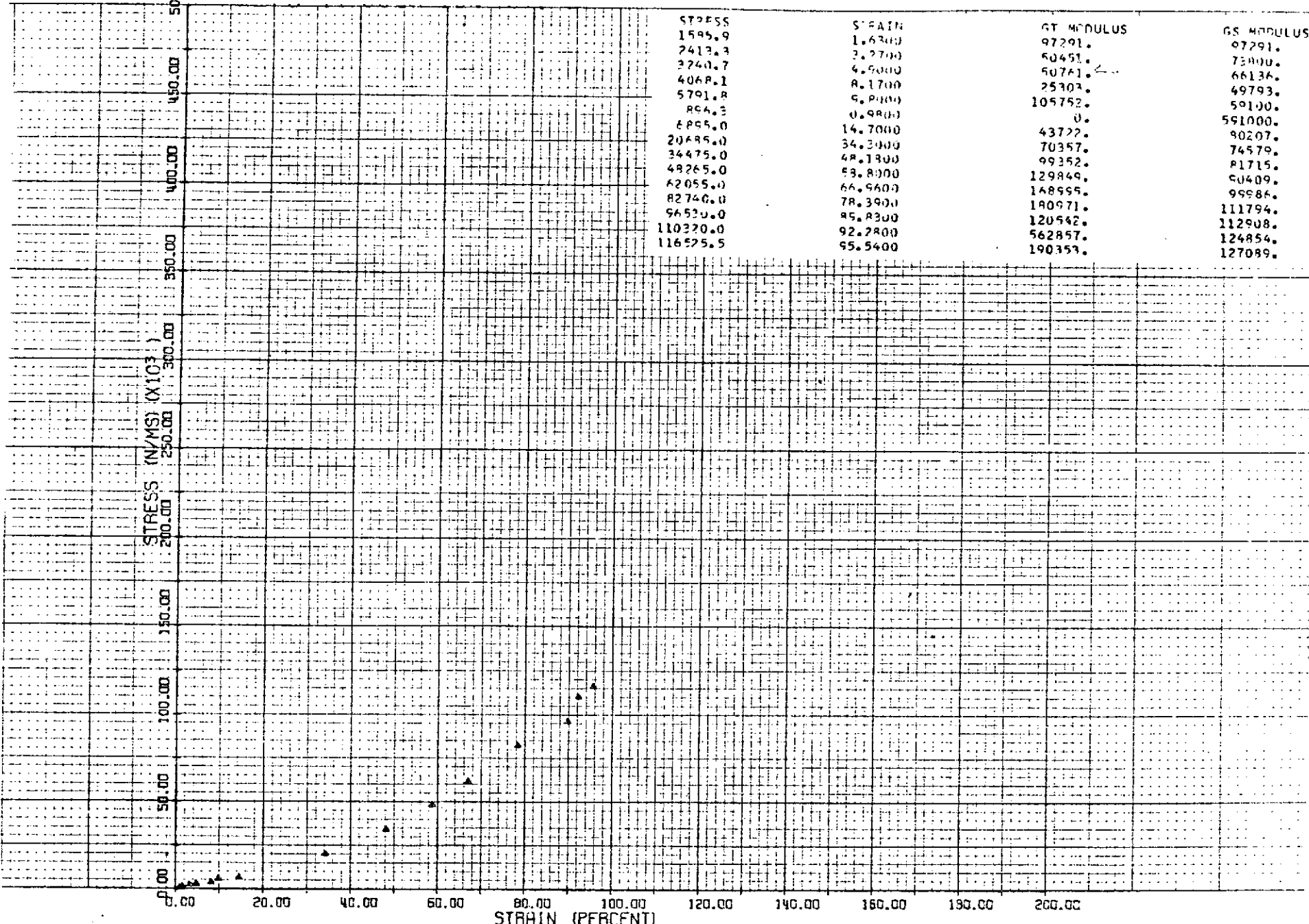


FD-4 250K 10% SEPT. 4

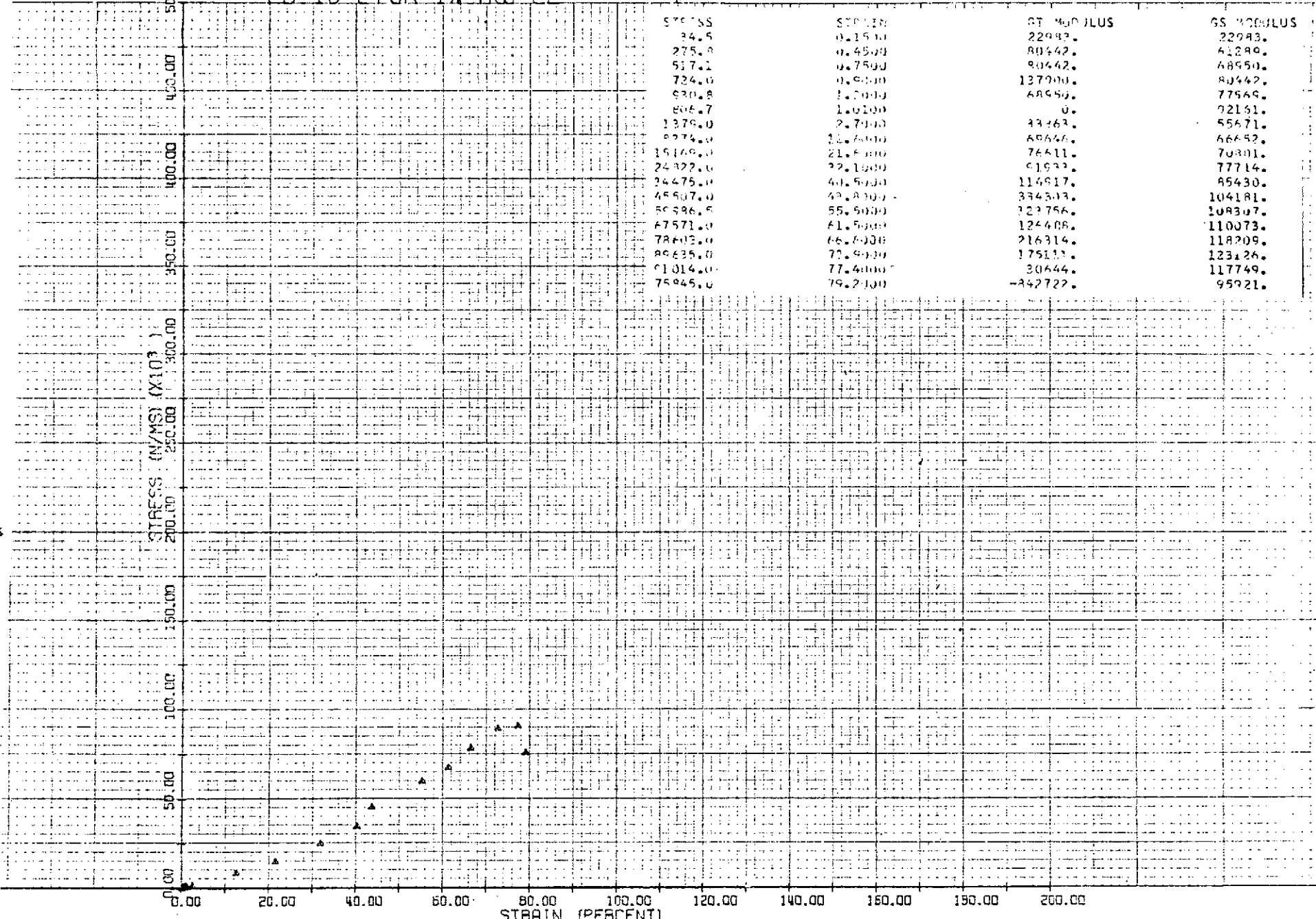


50 A

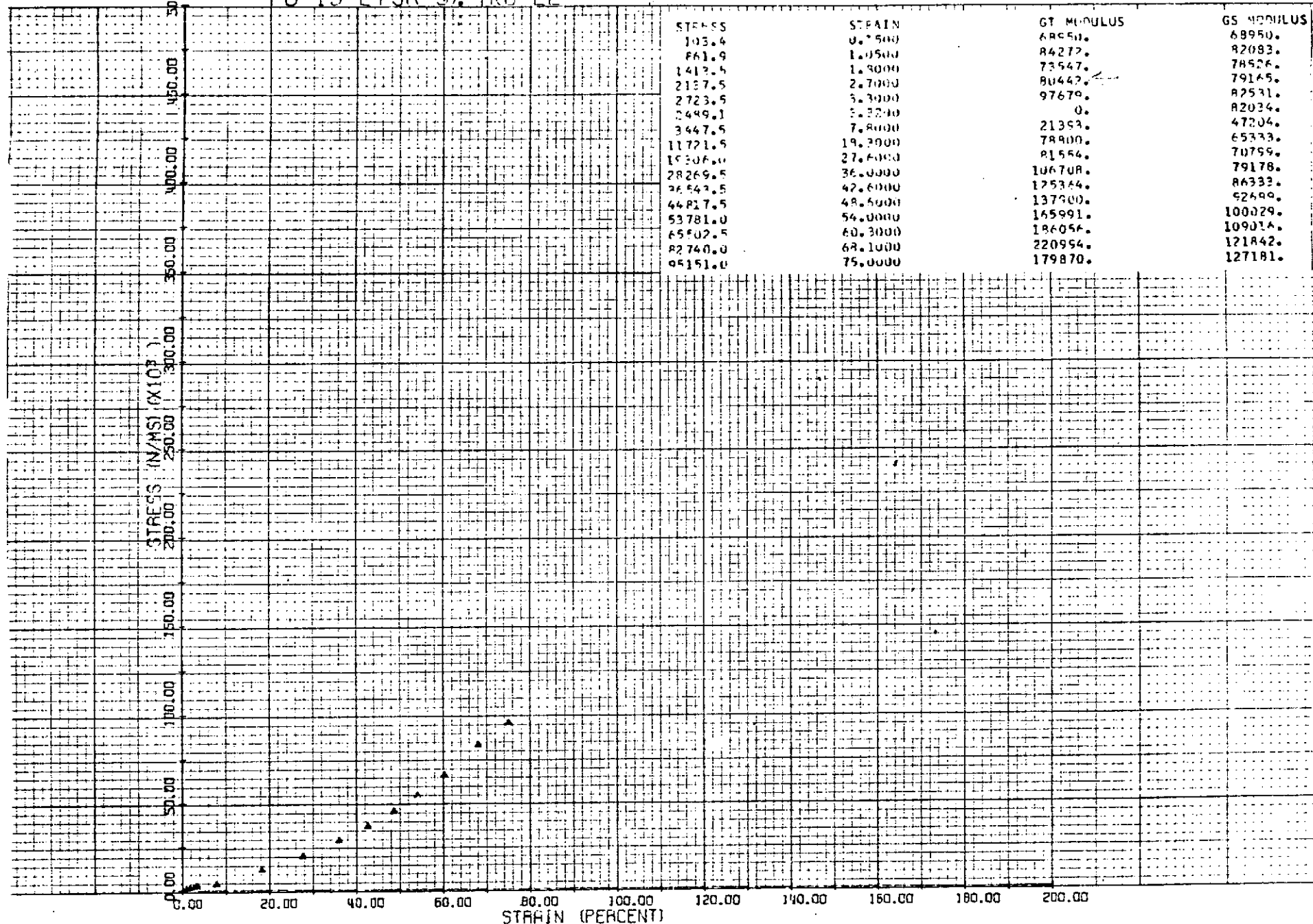
PD-44 250K 10% NOV. 6



PD-18 275K 1% AUG 22



## PD-13 275K 3% ALC 22



## PD-19 275K 5% ALG 22

500.00

STRESS (N/MS) (X10<sup>3</sup>)

500.00

450.00

400.00

350.00

300.00

250.00

200.00

150.00

100.00

50.00

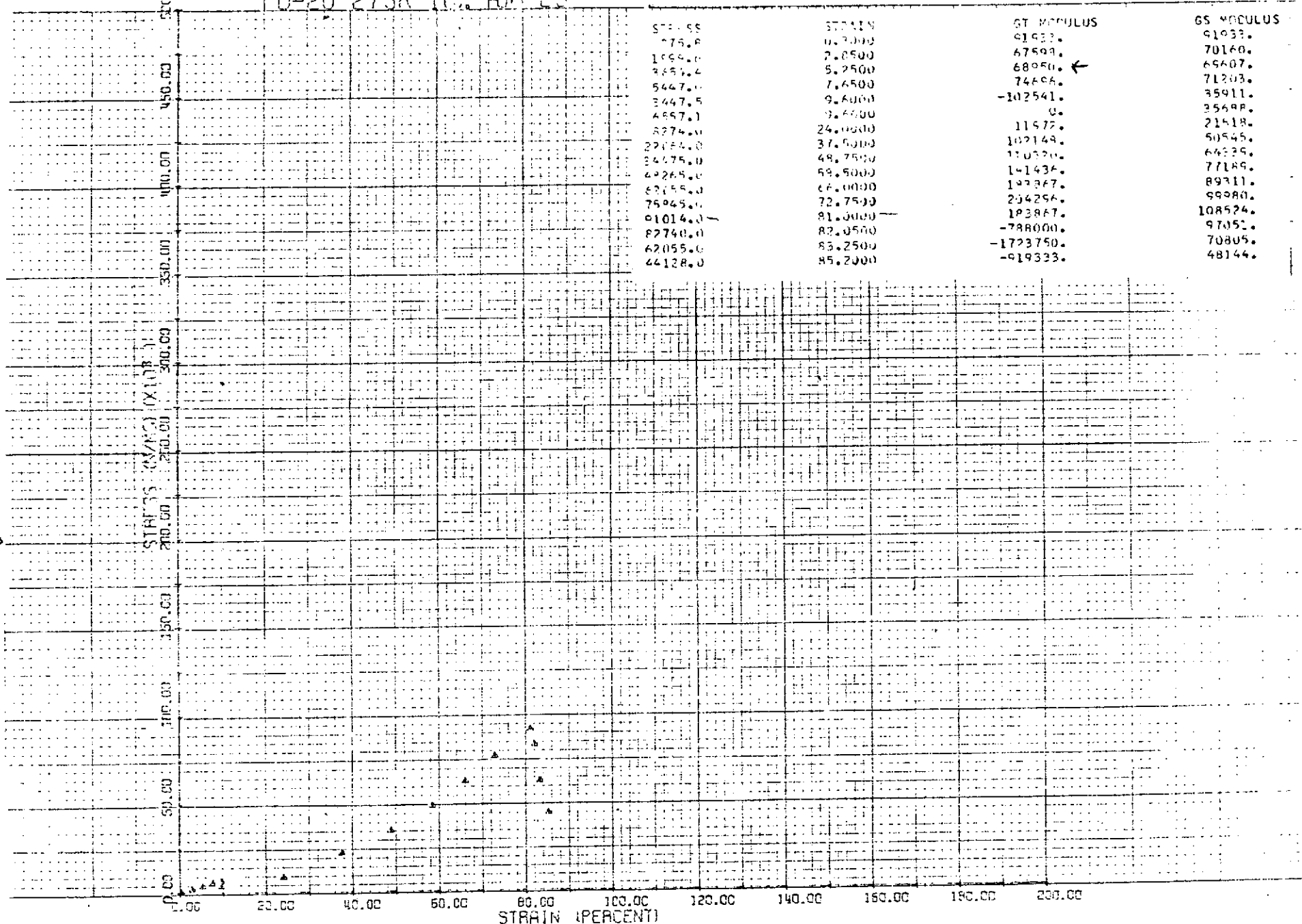
0.00

STRESS	STRAIN	GT MODULUS	GS MODULUS
34.5	0.1500	22981.	22983.
1034.3	1.5200	72976.	61043.
1861.7	2.1000	142655.	88450.
2456.4	3.6000	52842.	73738.
3516.5	4.9000	66298.	71764.
3292.3	4.6100	0.	76279.
4137.0	7.6000	24805.	54067.
9652.0	14.3000	82323.	48371.
14558.0	22.9000	82118.	73123.
24932.0	31.3000	97341.	79700.
34475.0	41.0000	99515.	84398.
46896.0	50.0000	134902.	93646.
59297.0	57.5000	170414.	103341.
68550.0	62.2000	205383.	111052.
78603.0	66.6000	219386.	118209.
86877.0	71.0000	188045.	122537.

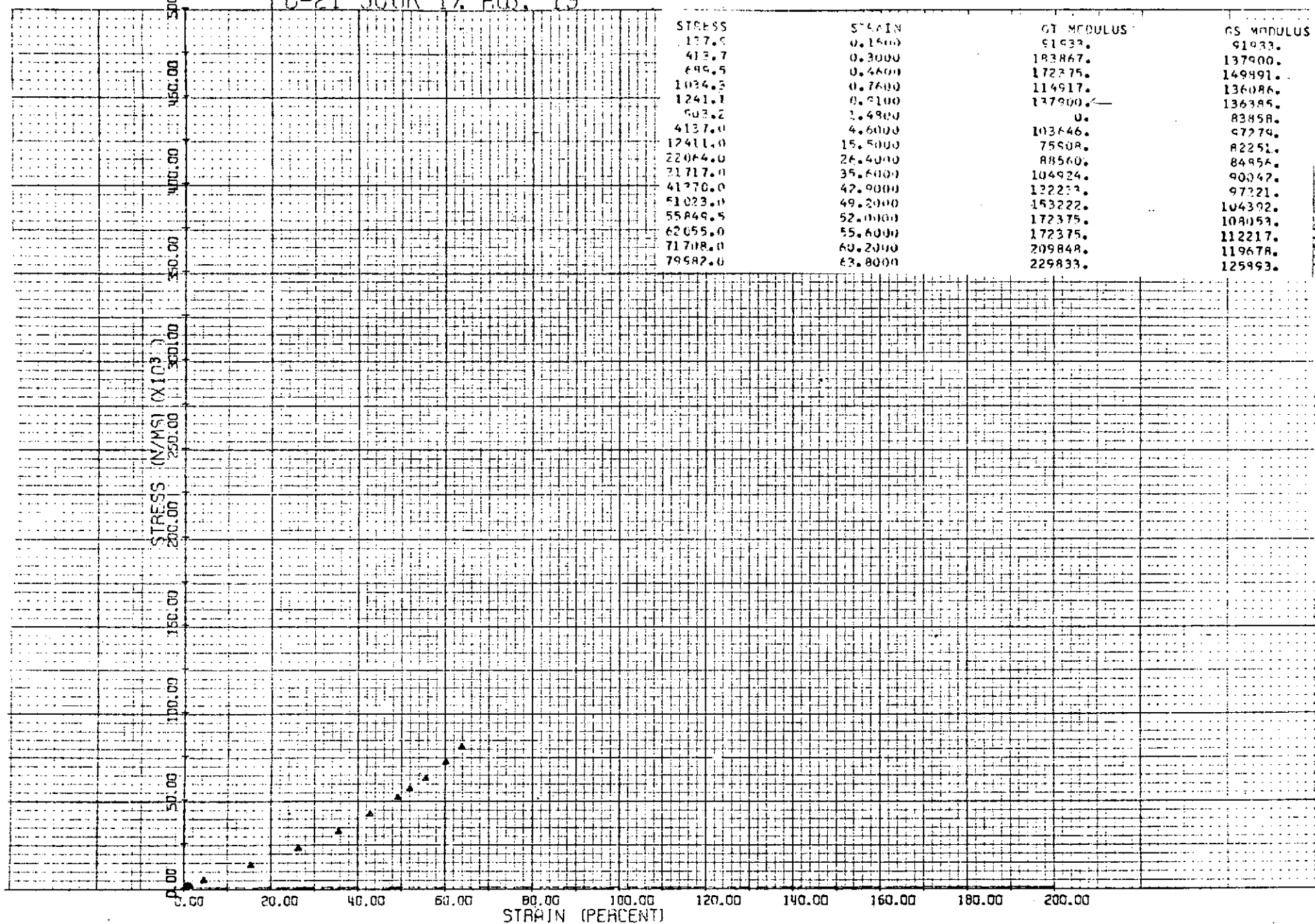
0.00 20.00 40.00 60.00 80.00 100.00 120.00 140.00 160.00 180.00 200.00

STRAIN (PERCENT)

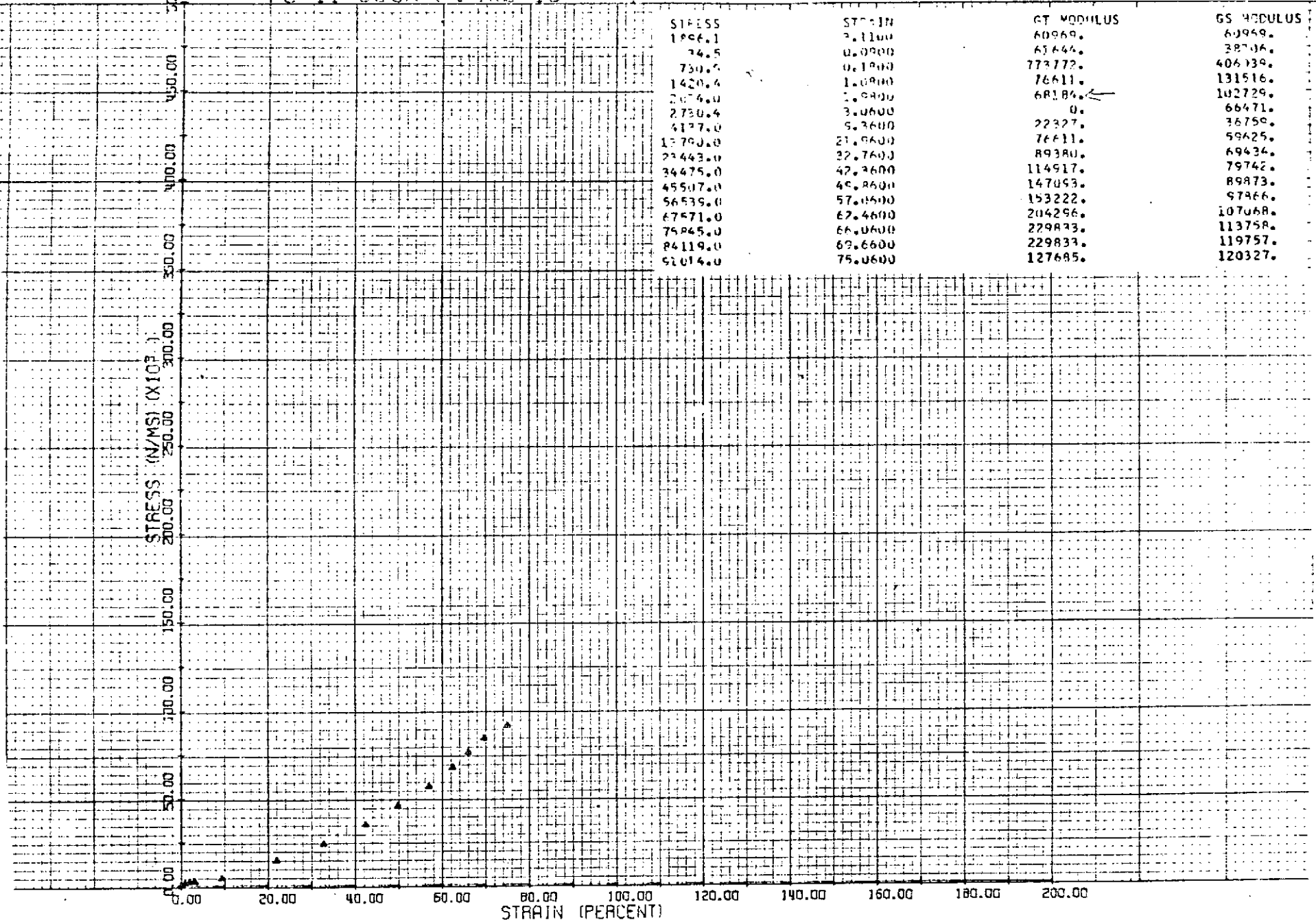
PD-20 275K 10% AUG 23



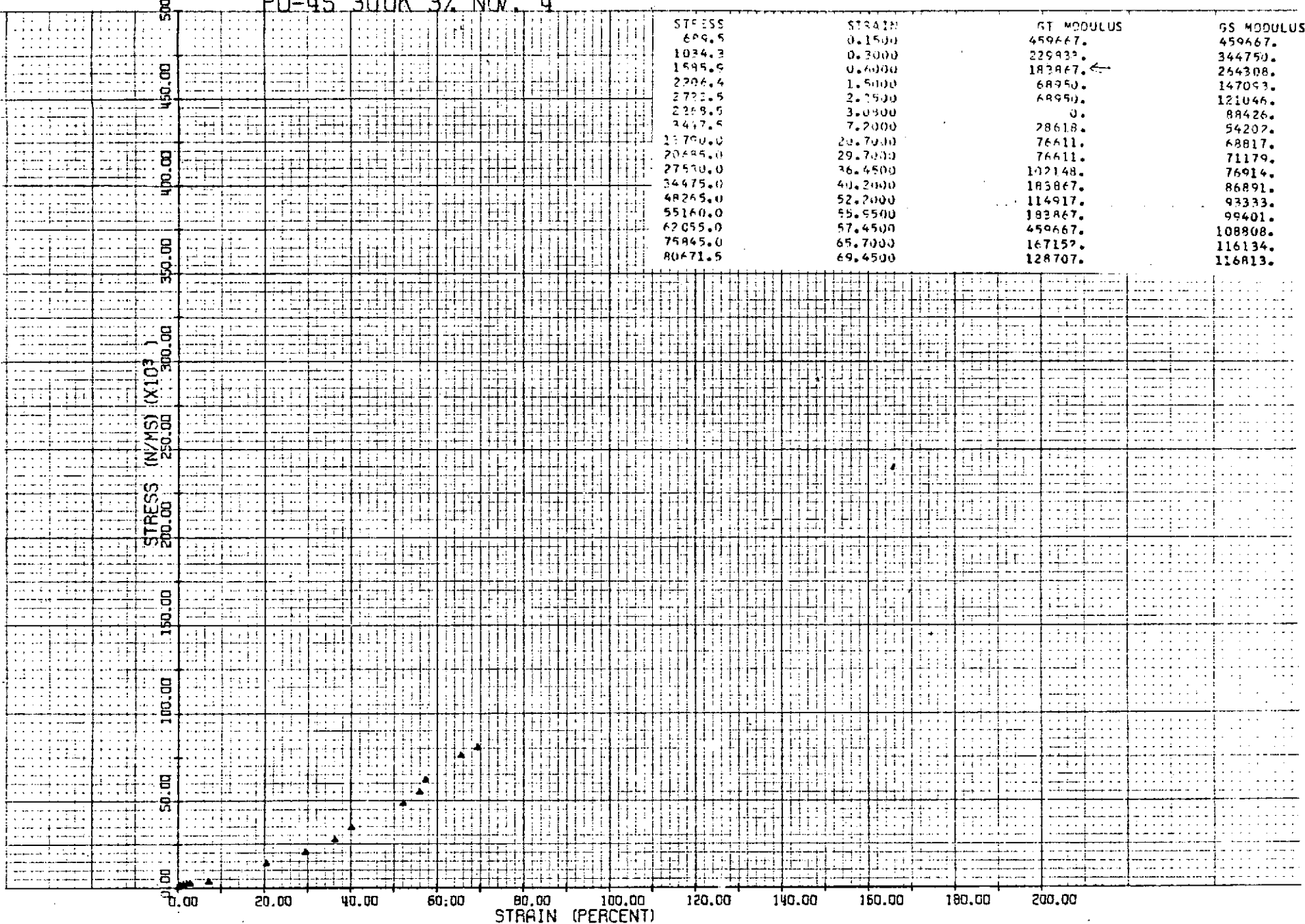
## PD-21 300K 1% FIG. 19



PO-11 300K 3% AUG 15



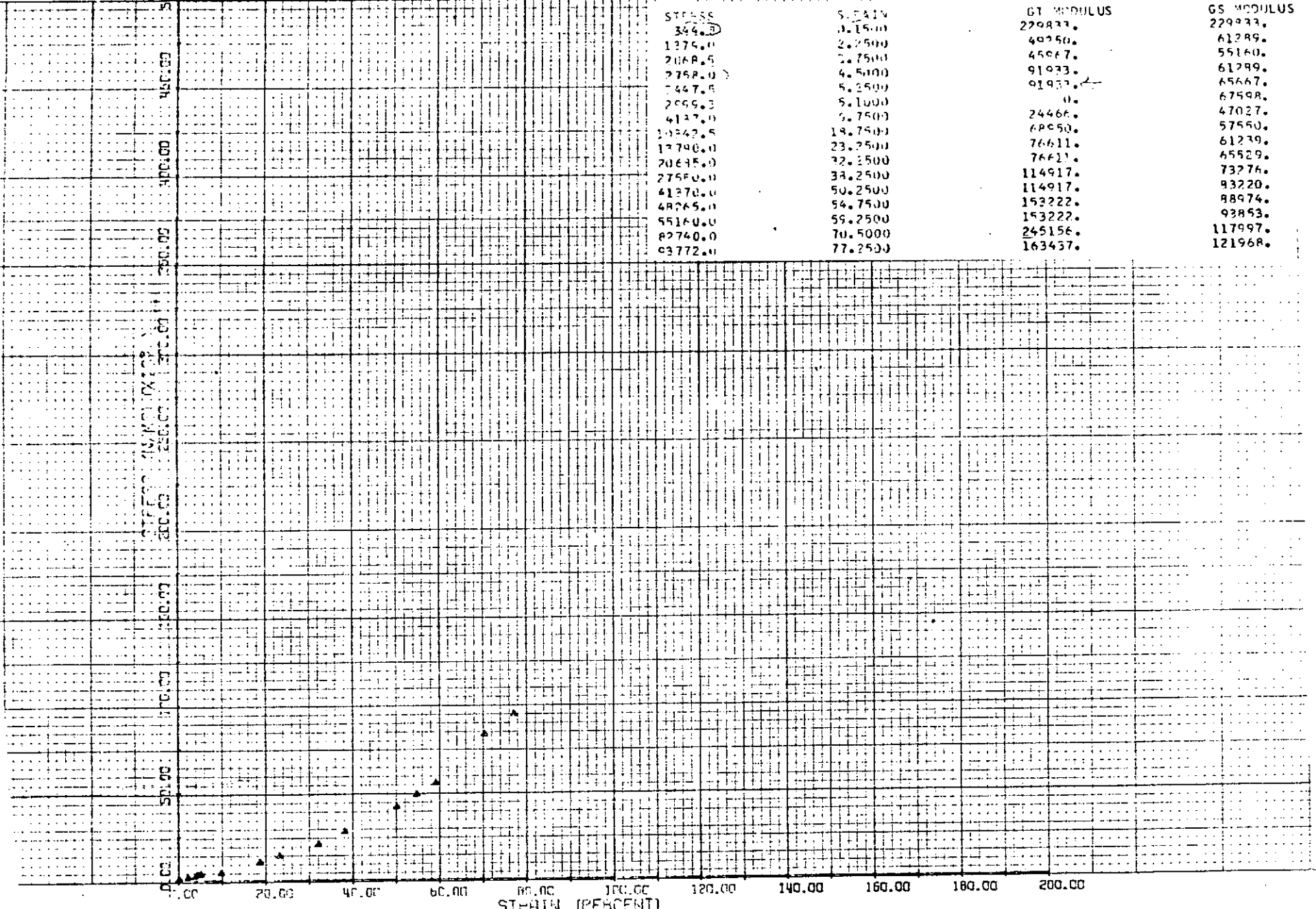
PO-45 300K 3% NOV. 4



PD-38 300K 5% OCT. 27

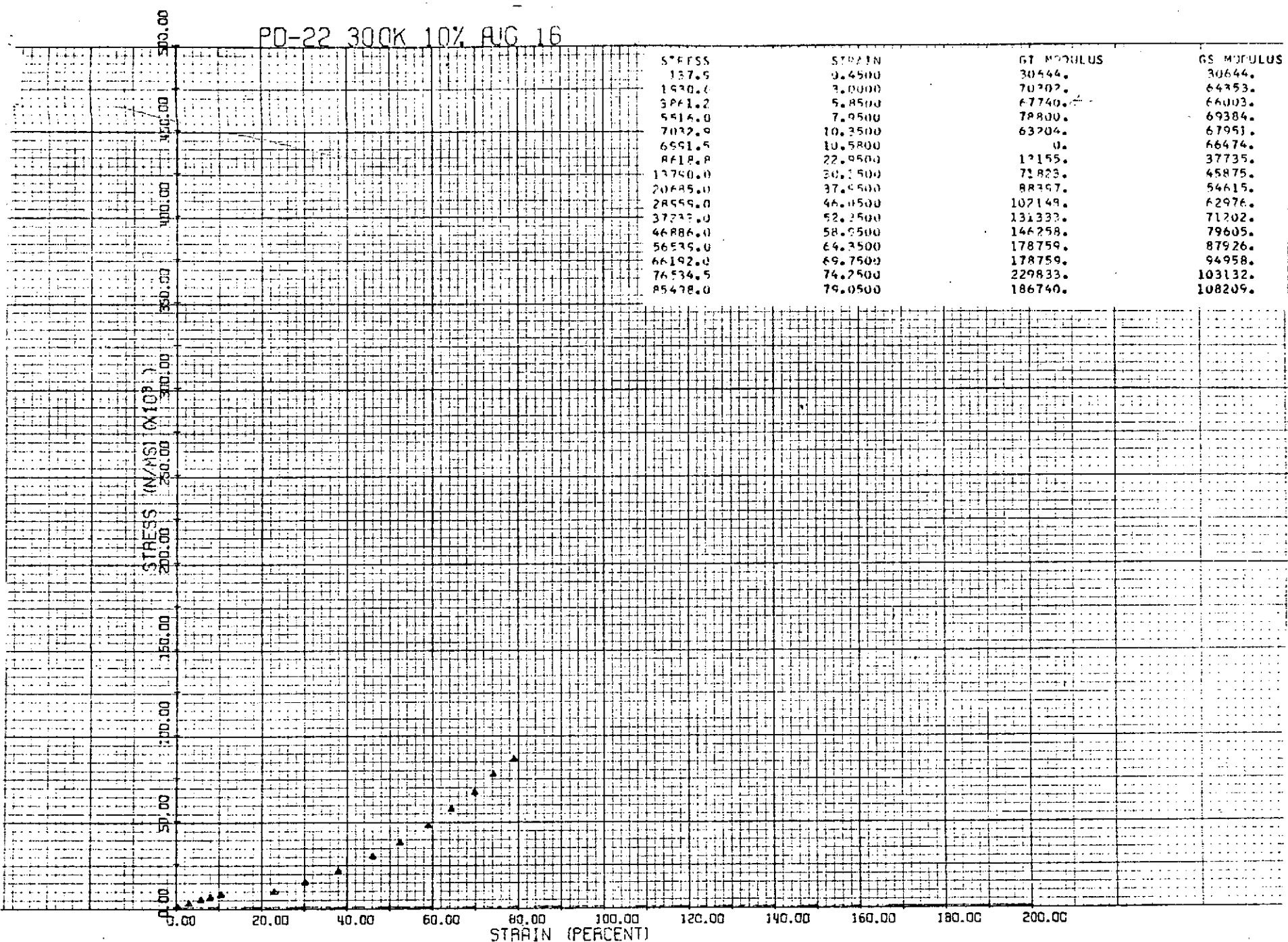
500.00

STRESS	STRAIN	G1 MODULUS	G2 MODULUS
344.0	0.1500	220877.	229933.
1274.0	0.27500	40250.	61289.
2068.0	0.47500	45667.	55160.
2758.0	0.51000	91933.	61299.
3447.0	0.52500	91933.	65667.
2066.0	0.10000	0.	67598.
4137.0	0.7500	24466.	47027.
14342.0	18.7500	68450.	57560.
13740.0	23.2500	76611.	61239.
20635.0	32.2500	76611.	65529.
27584.0	38.2500	114917.	73276.
41370.0	50.2500	114917.	93220.
48265.0	54.7500	153222.	88974.
55160.0	59.2500	153222.	93853.
82740.0	70.5000	245156.	117997.
93772.0	77.2500	163437.	121968.



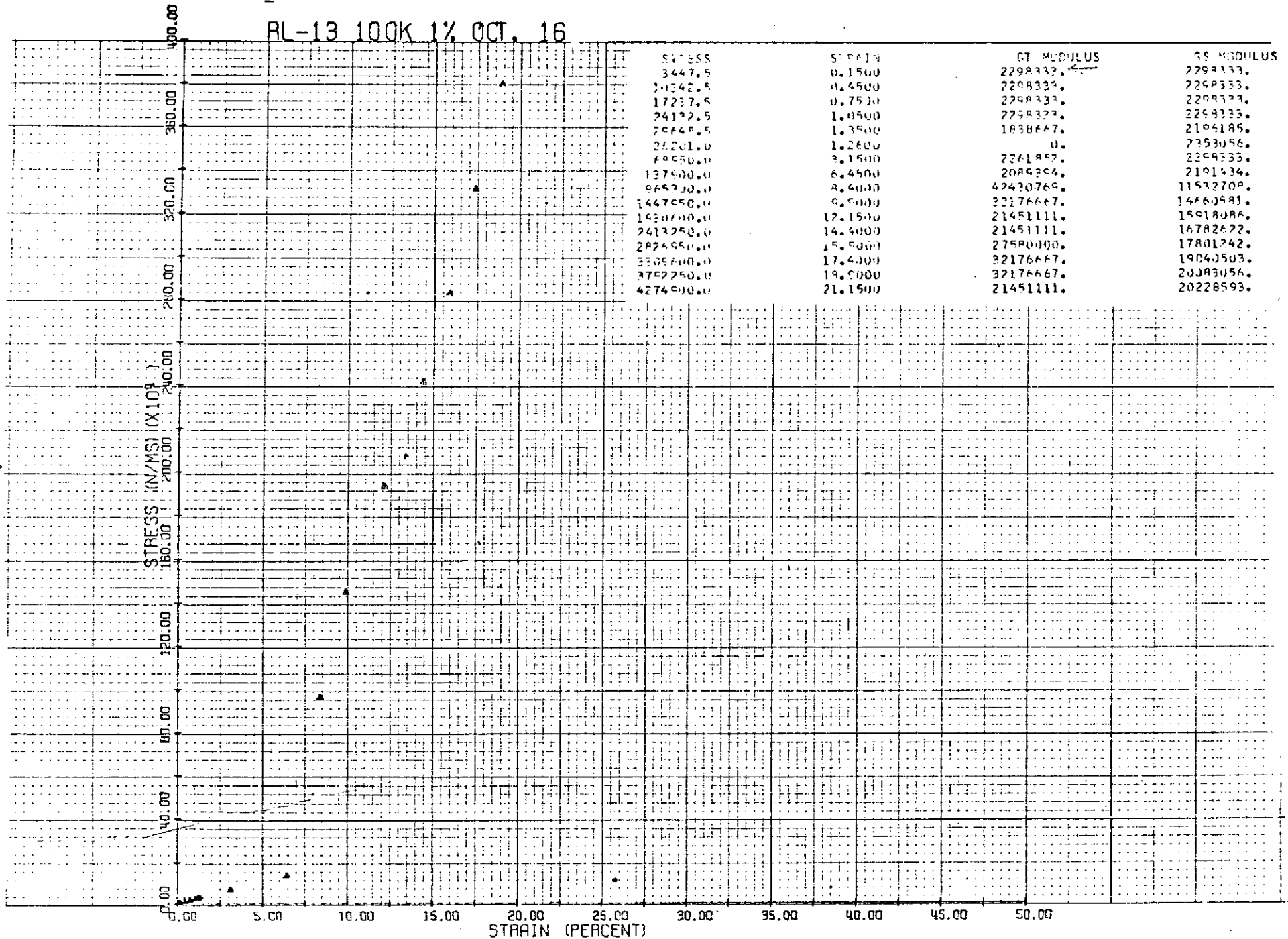
59 A

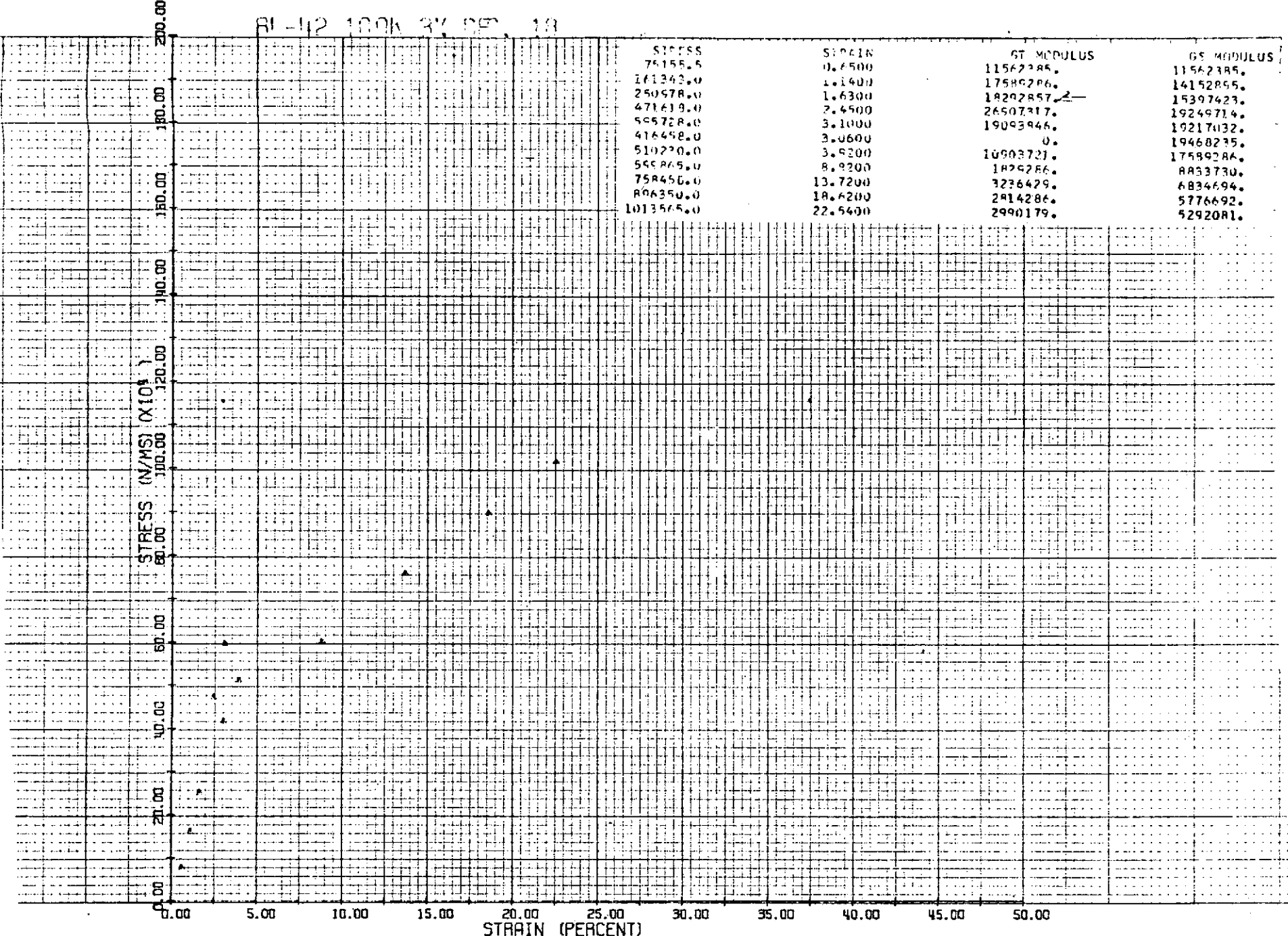
PO-22 300K 10% AUG 16



609

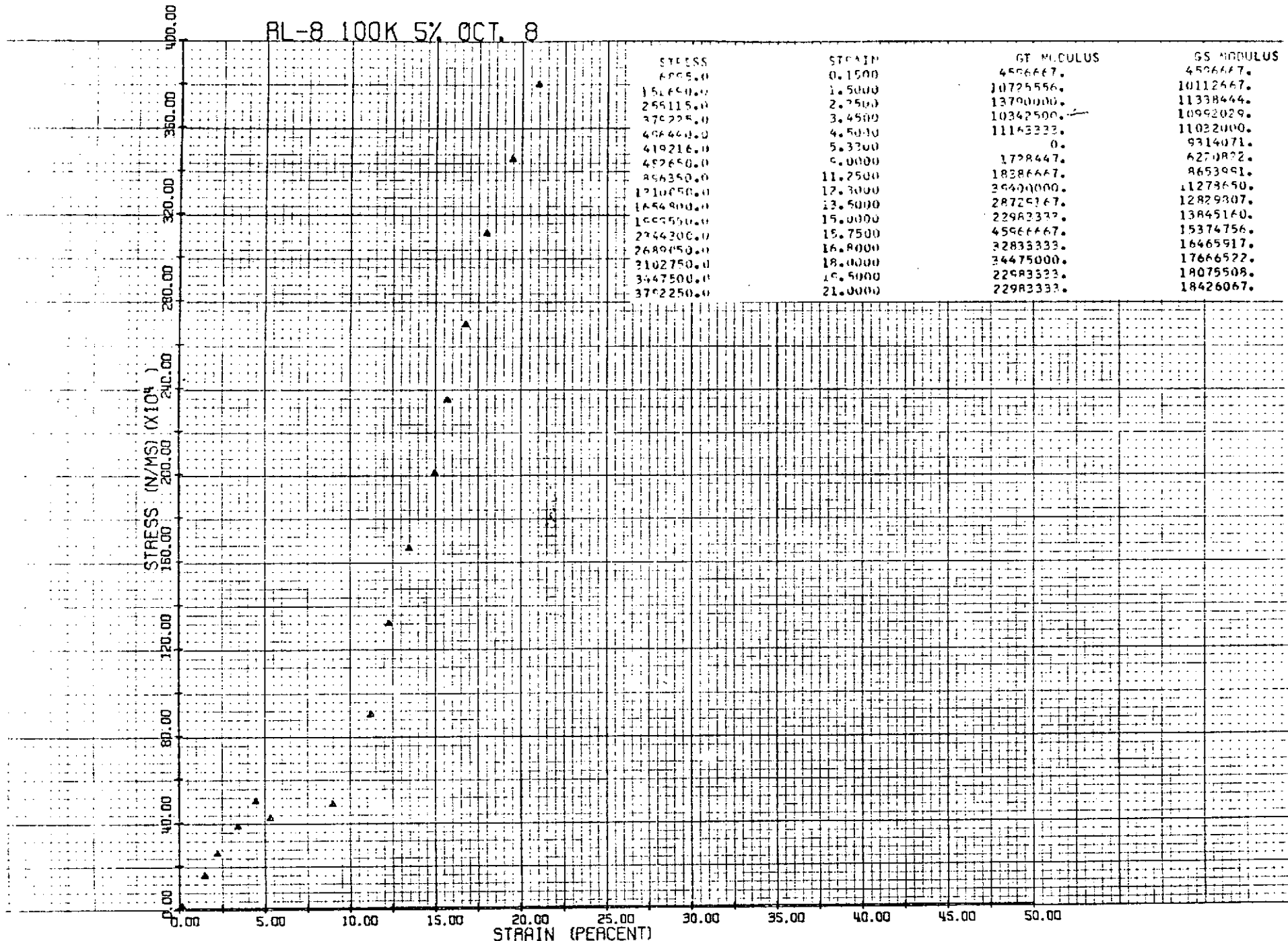
## RL-13 100K 1% OCT. 16



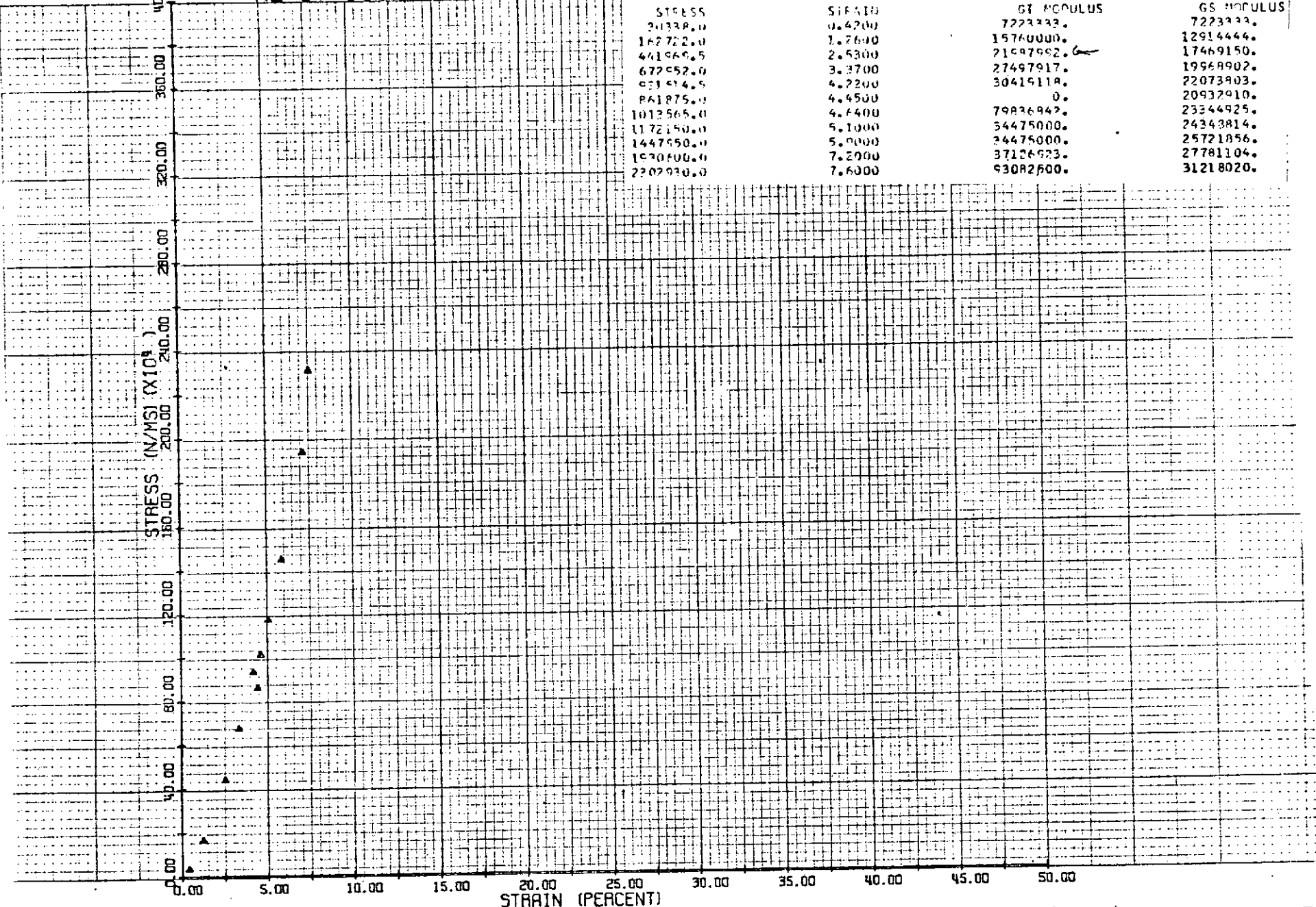


62 //

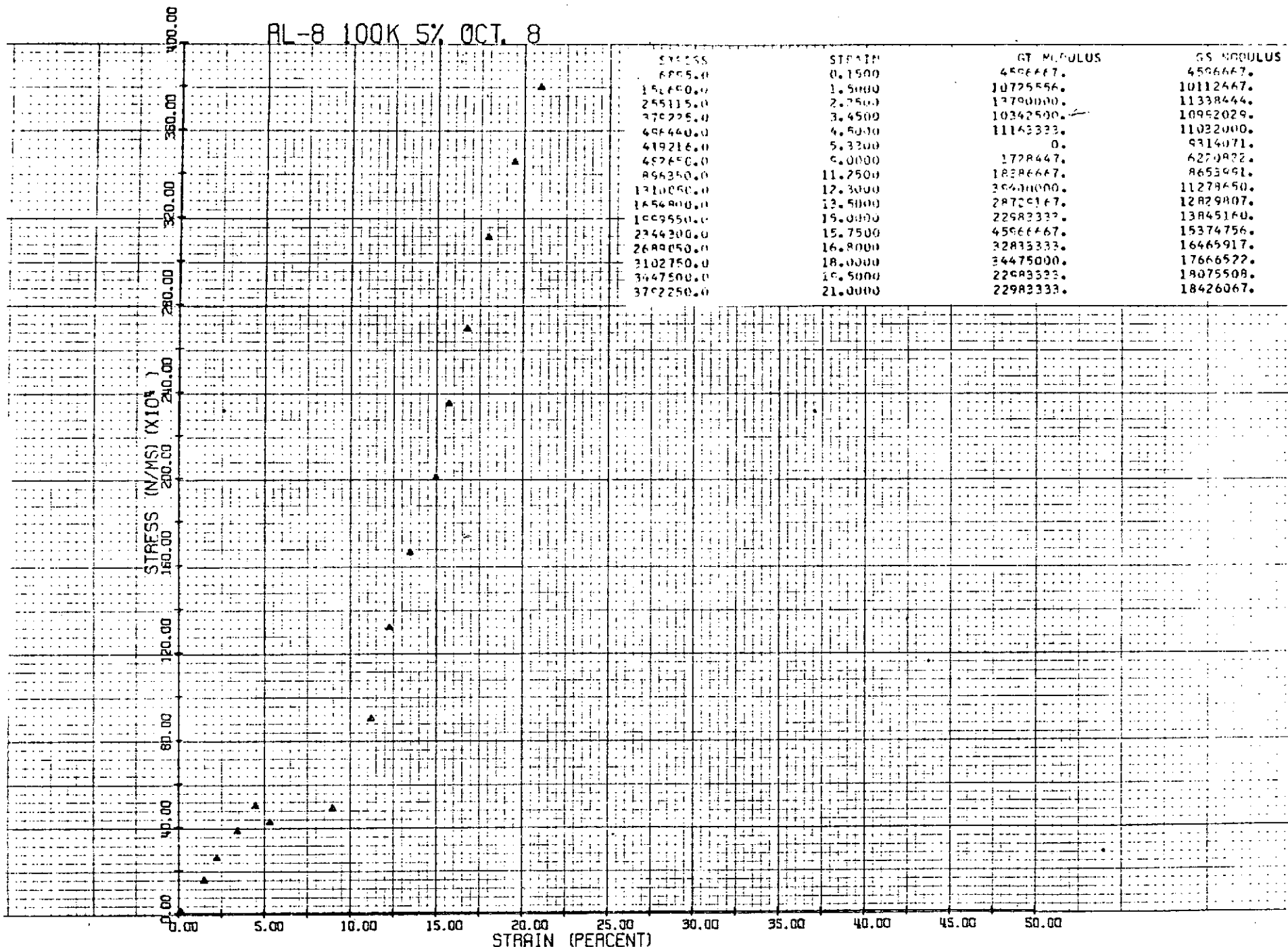
## RL-8 100K 5% OCT. 8



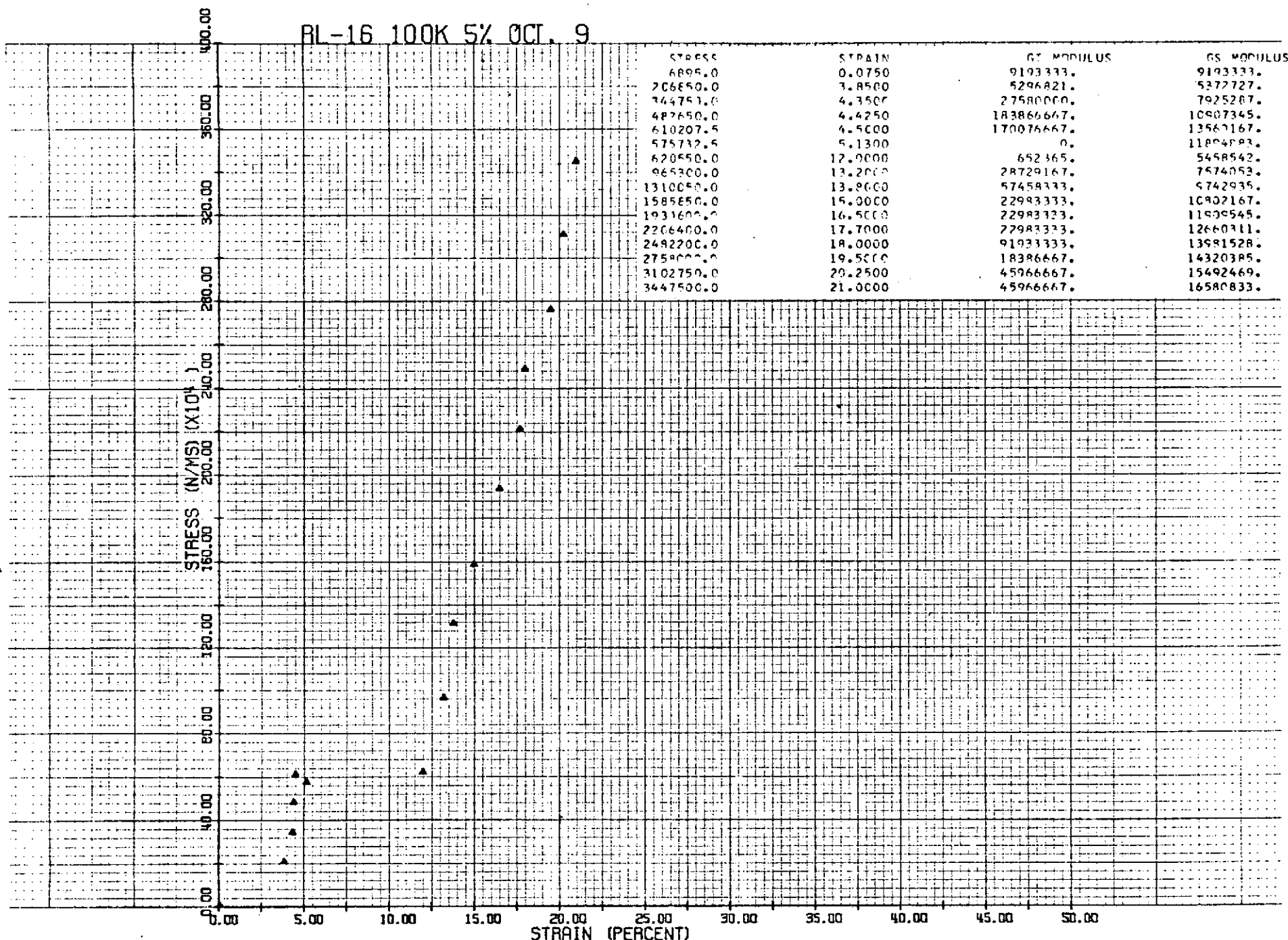
RL-67 100K 5% DEC. 4



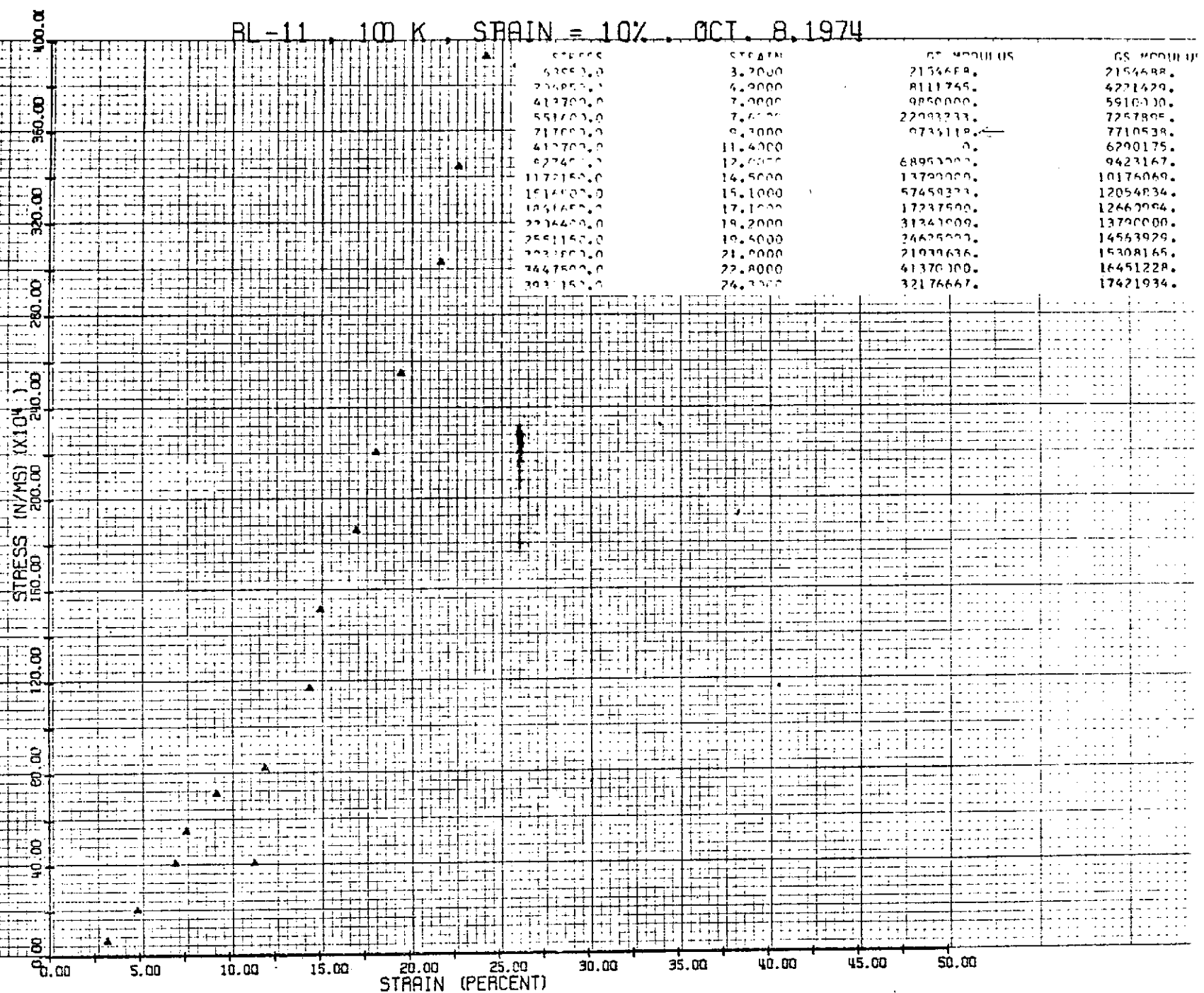
RL-8 100K 5% OCT. 8



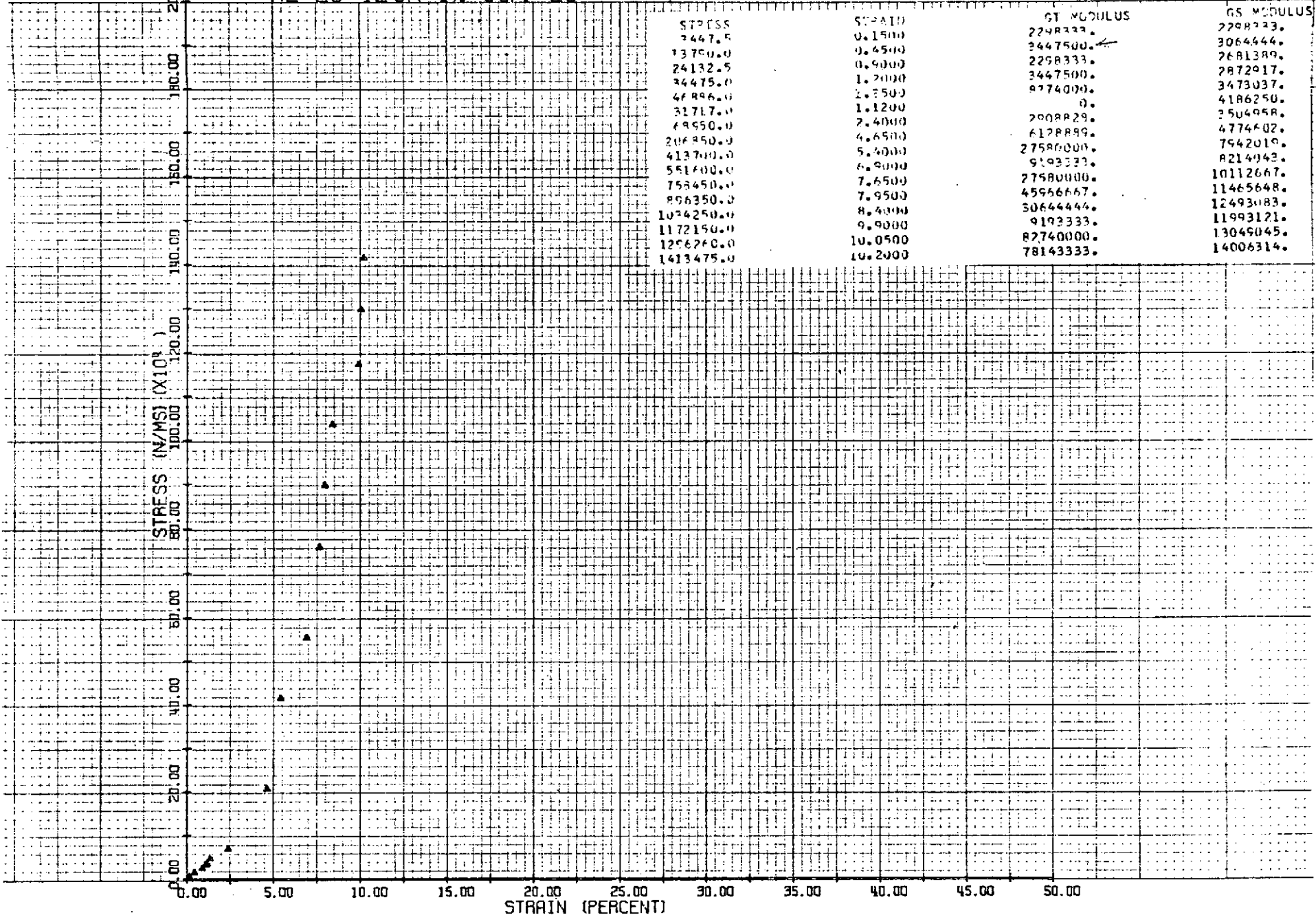
## RL-16 100K 5% OCT. 9



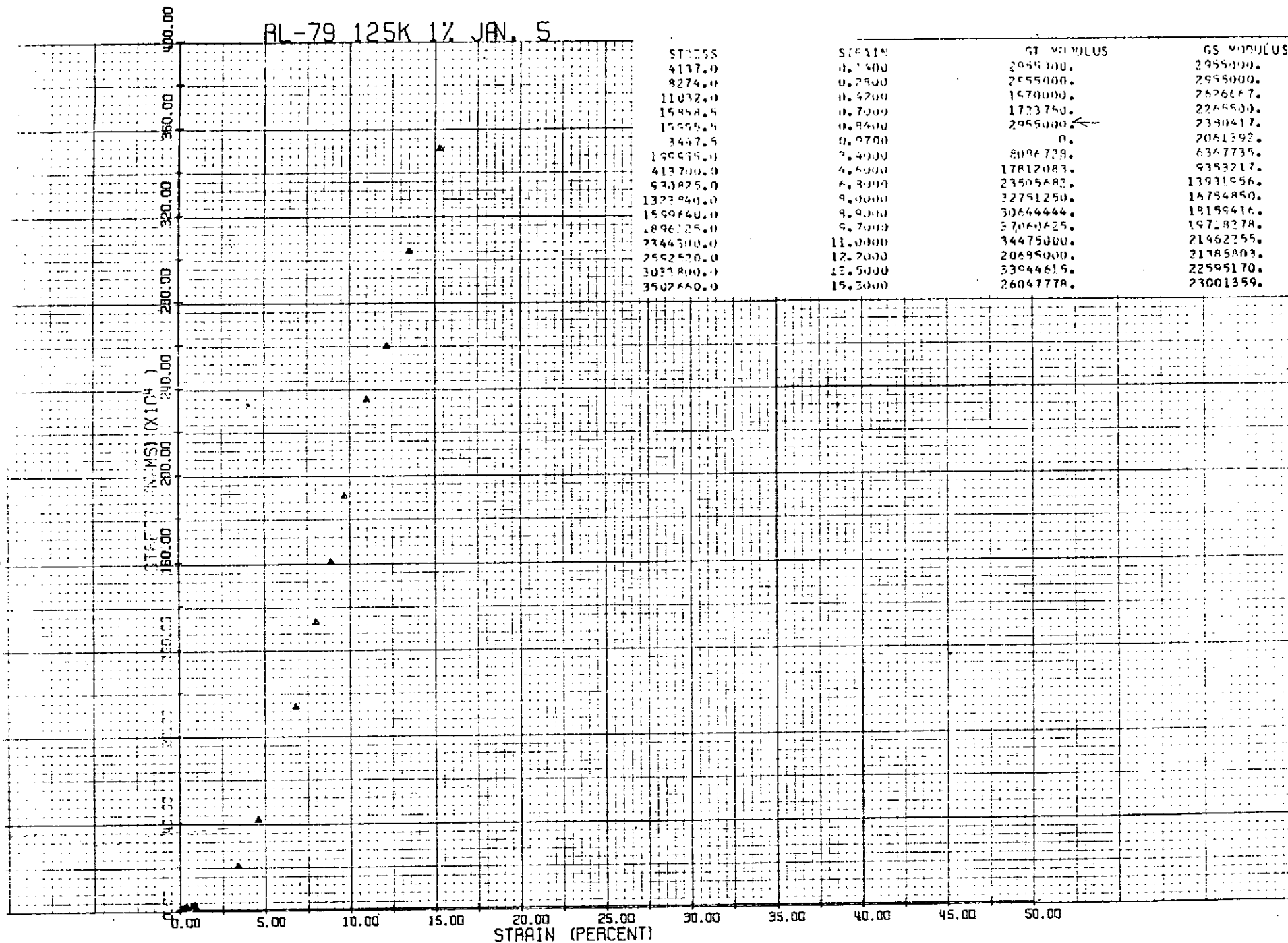
BL-11, 100 K., STRAIN = 10% OCT. 8, 1974



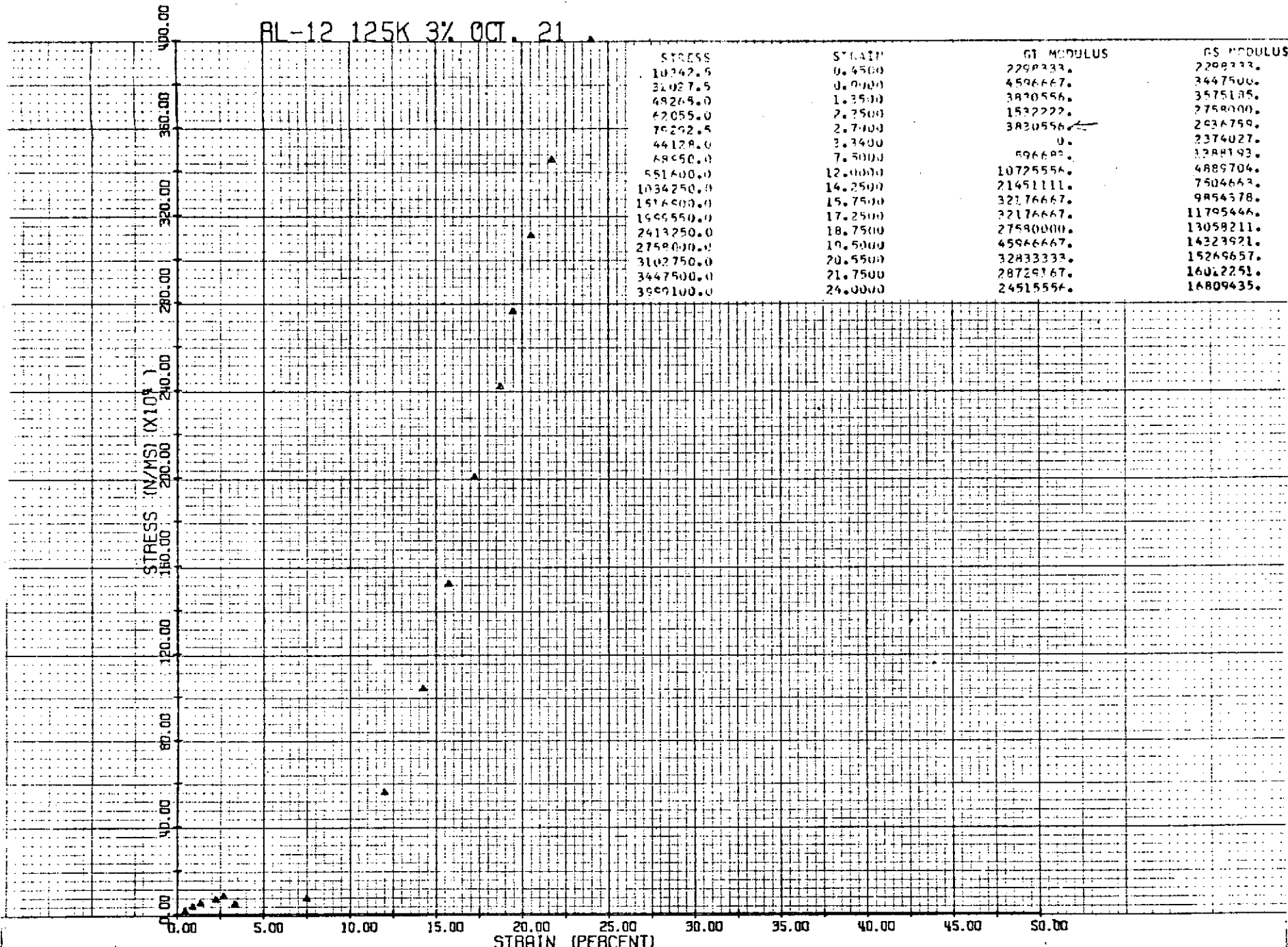
RL-26 125K 1% OCT. 23



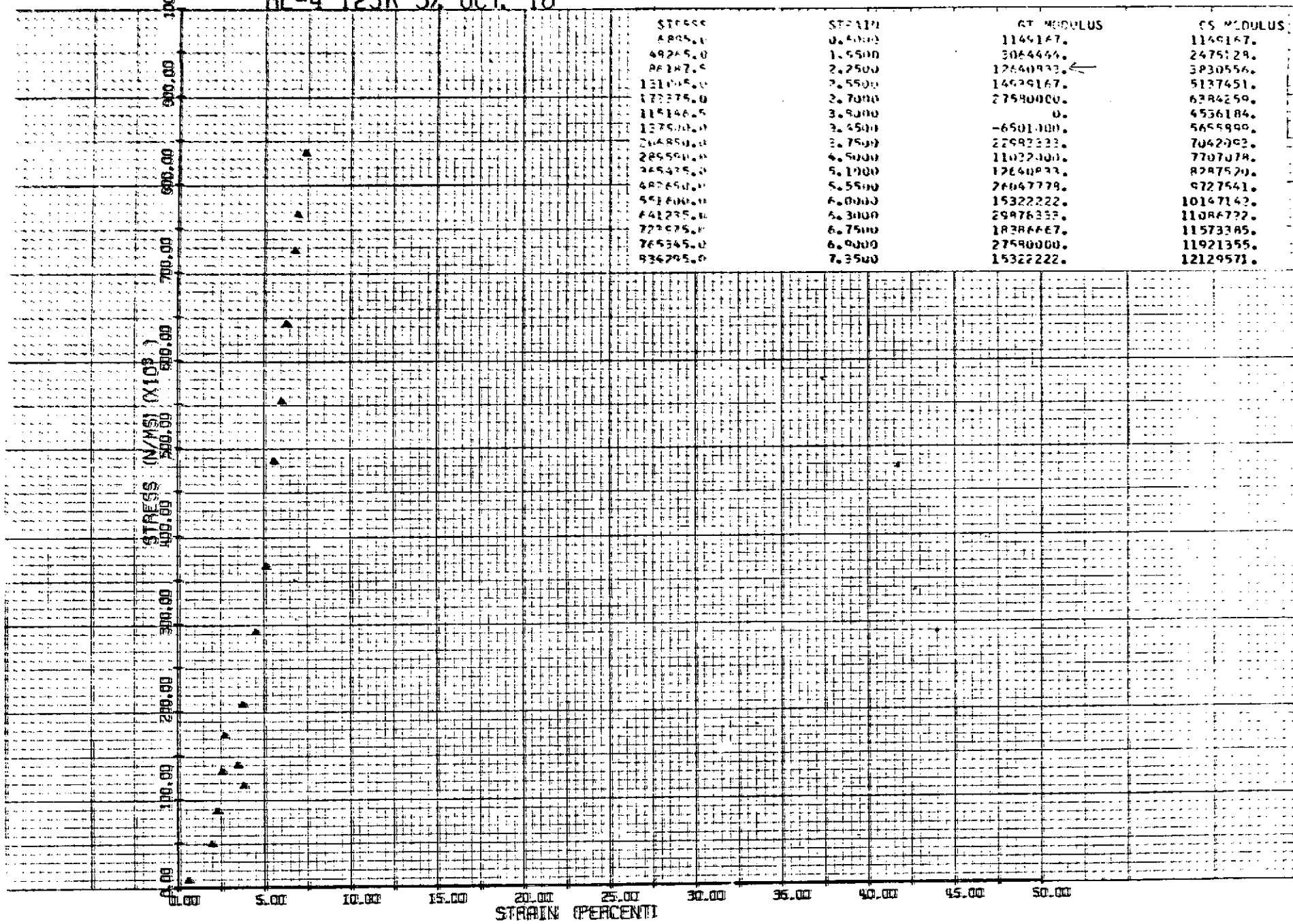
RL-79 125K 1% JAN. 5



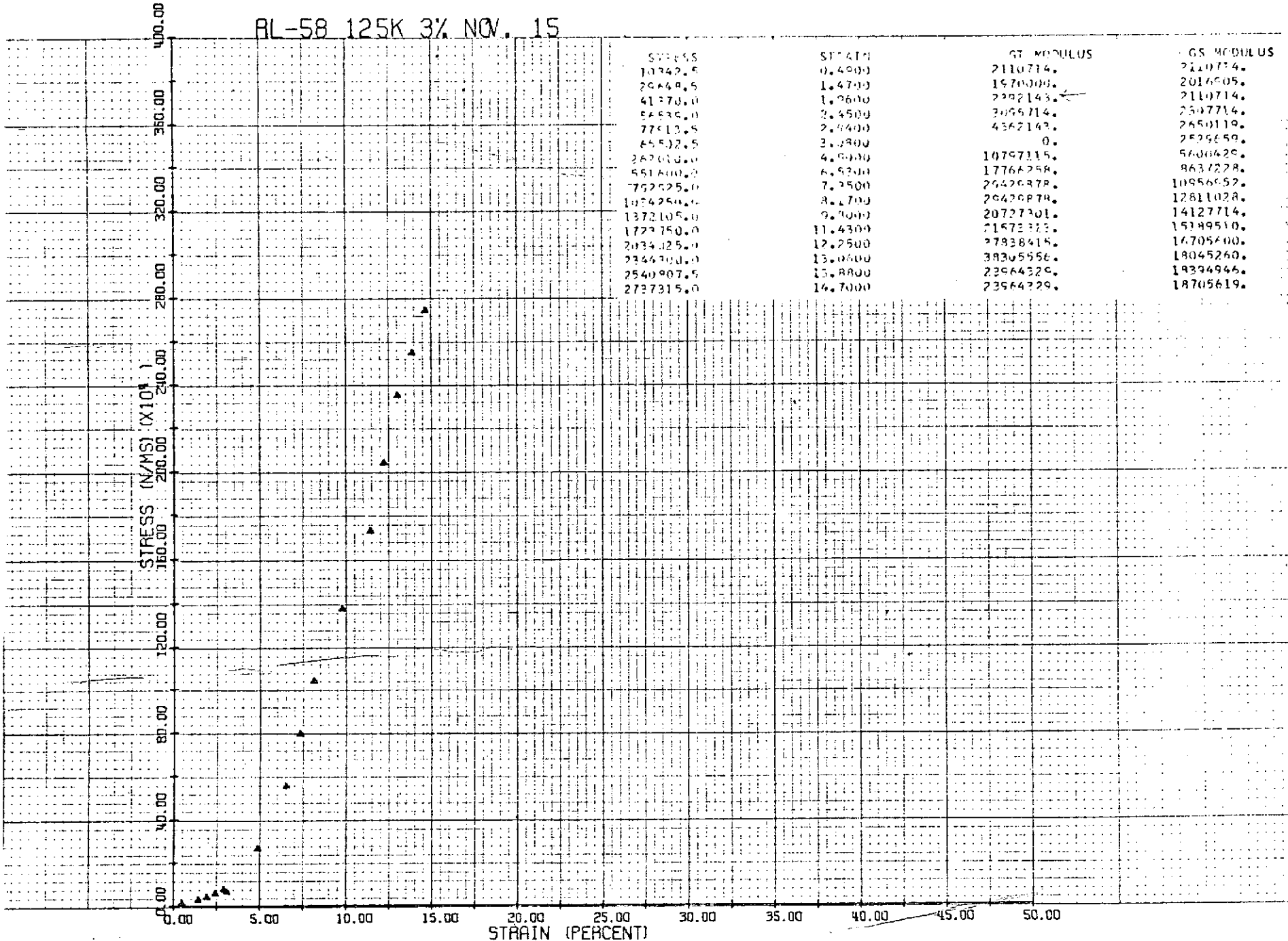
RL-12 125K 3% OCT. 21



BL-4 125K 3% OCT. 18



AL-58 125K 3% NOV. 15



RL-38 125K 5% OCT. 12

100.00  
90.00  
80.00  
70.00  
60.00  
50.00  
40.00  
30.00  
20.00  
10.00  
0.00

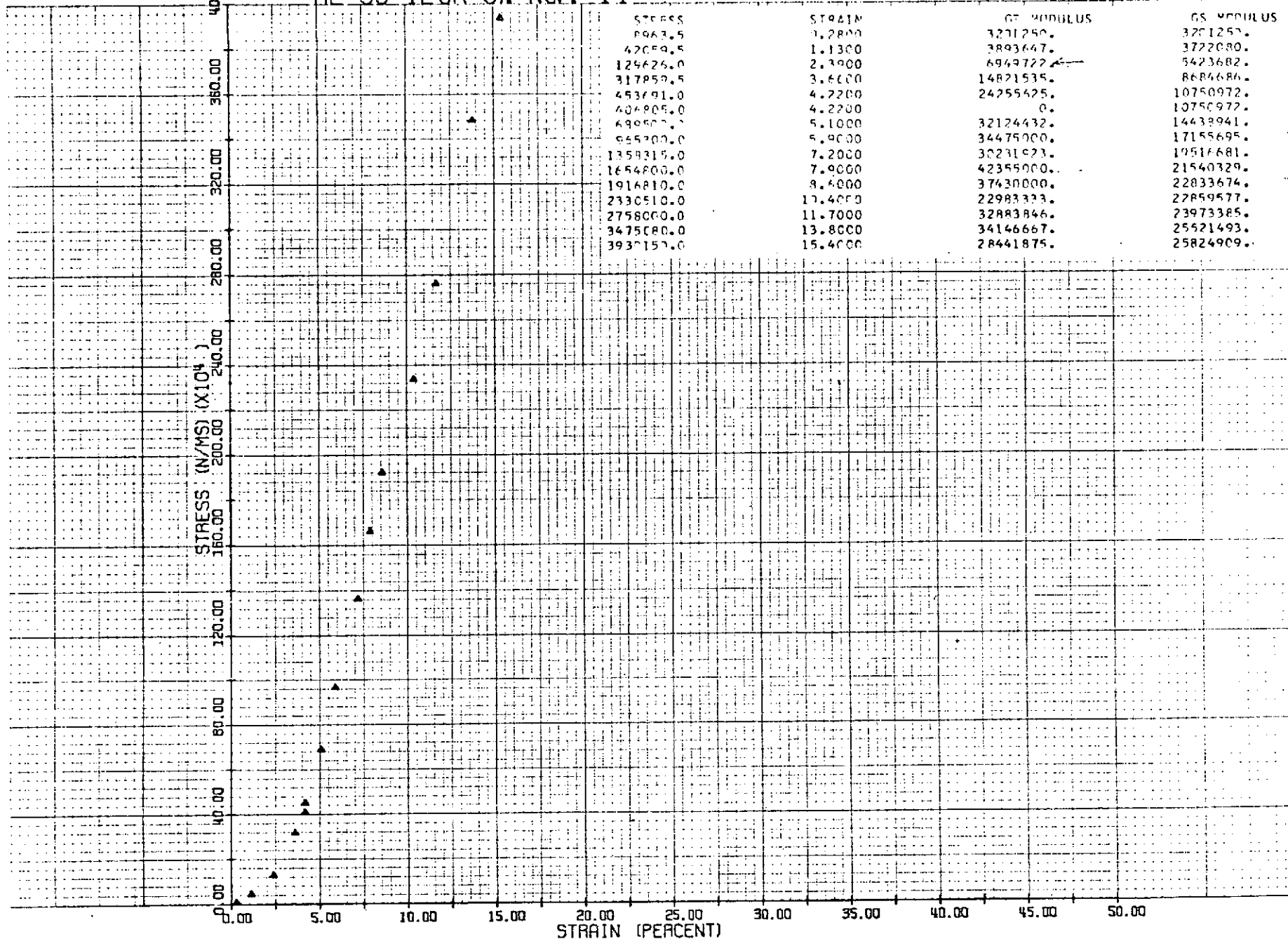
STRESS (N/MS<sup>2</sup> X10<sup>4</sup>)  
100.00 150.00 200.00 250.00 300.00

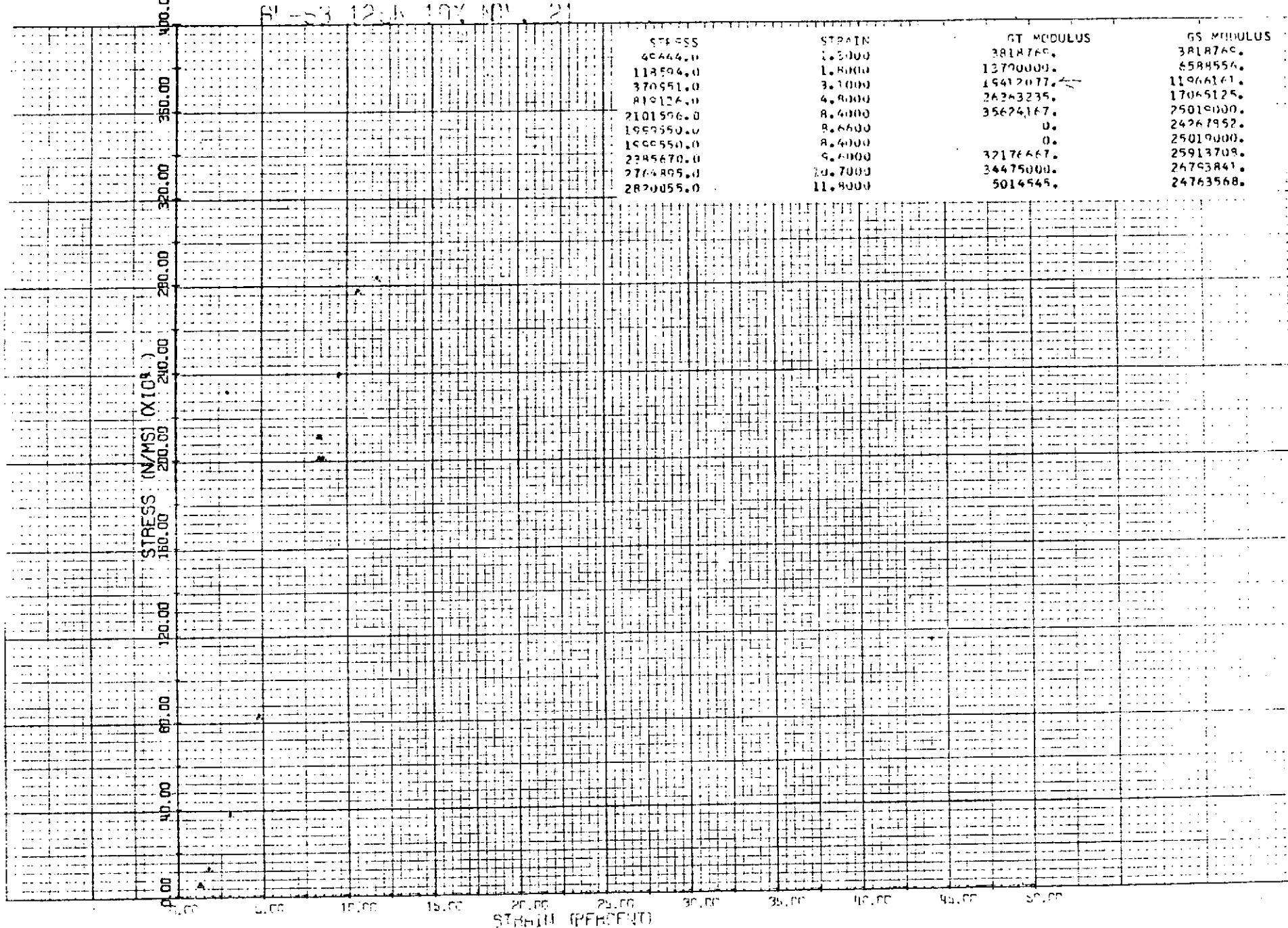
STRESS	STRAIN	GT MODULUS	GS MODULUS
15760.0	0.9100	1515385.	1515385.
20485.0	1.9000	774715.	1144167.
34475.0	2.7000	1532222.	1276852.
49255.0	3.6000	1532222.	1340494.
75845.0	4.6000	2758000.	1648804.
50233.5	5.3500	0.	1296496.
48650.0	6.0000	572815.	1038038.
275800.0	12.2000	7472581.	2449765.
551600.0	14.0000	7257995.	3606547.
967350.0	17.8000	23943332.	5267780.
1172150.0	19.0000	18384667.	6307482.
1447750.0	20.5000	18384667.	7187617.
1722750.0	21.7000	34475000.	8212495.
1930600.0	22.0000	29550000.	8891416.
2206400.0	23.3000	25072727.	9661955.
2514675.0	24.3000	25856250.	10461673.

0.00 5.00 10.00 15.00 20.00 25.00 30.00 35.00 40.00 45.00 50.00

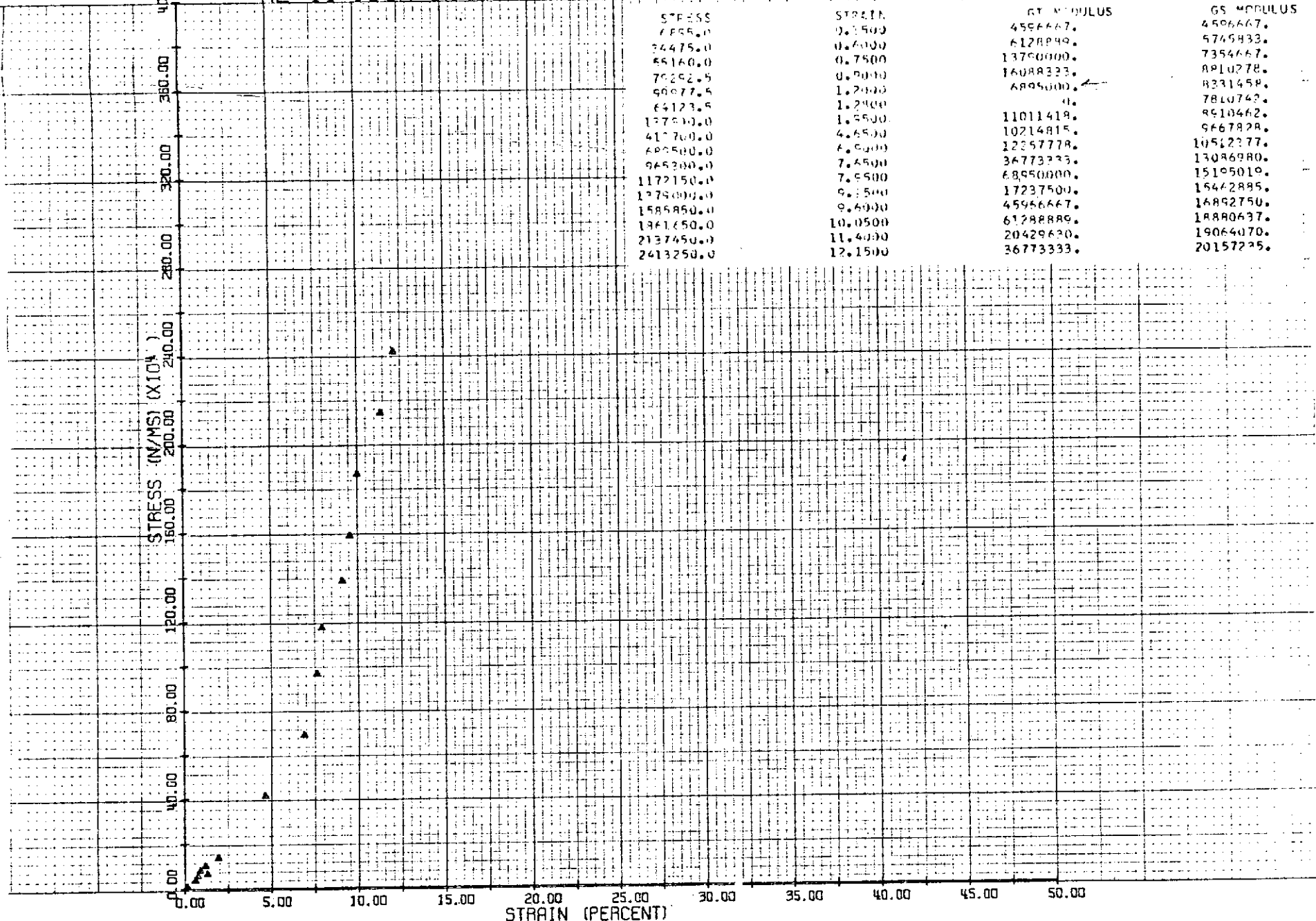
STRAIN (PERCENT)

RL-59 125K 5% NOV. 14

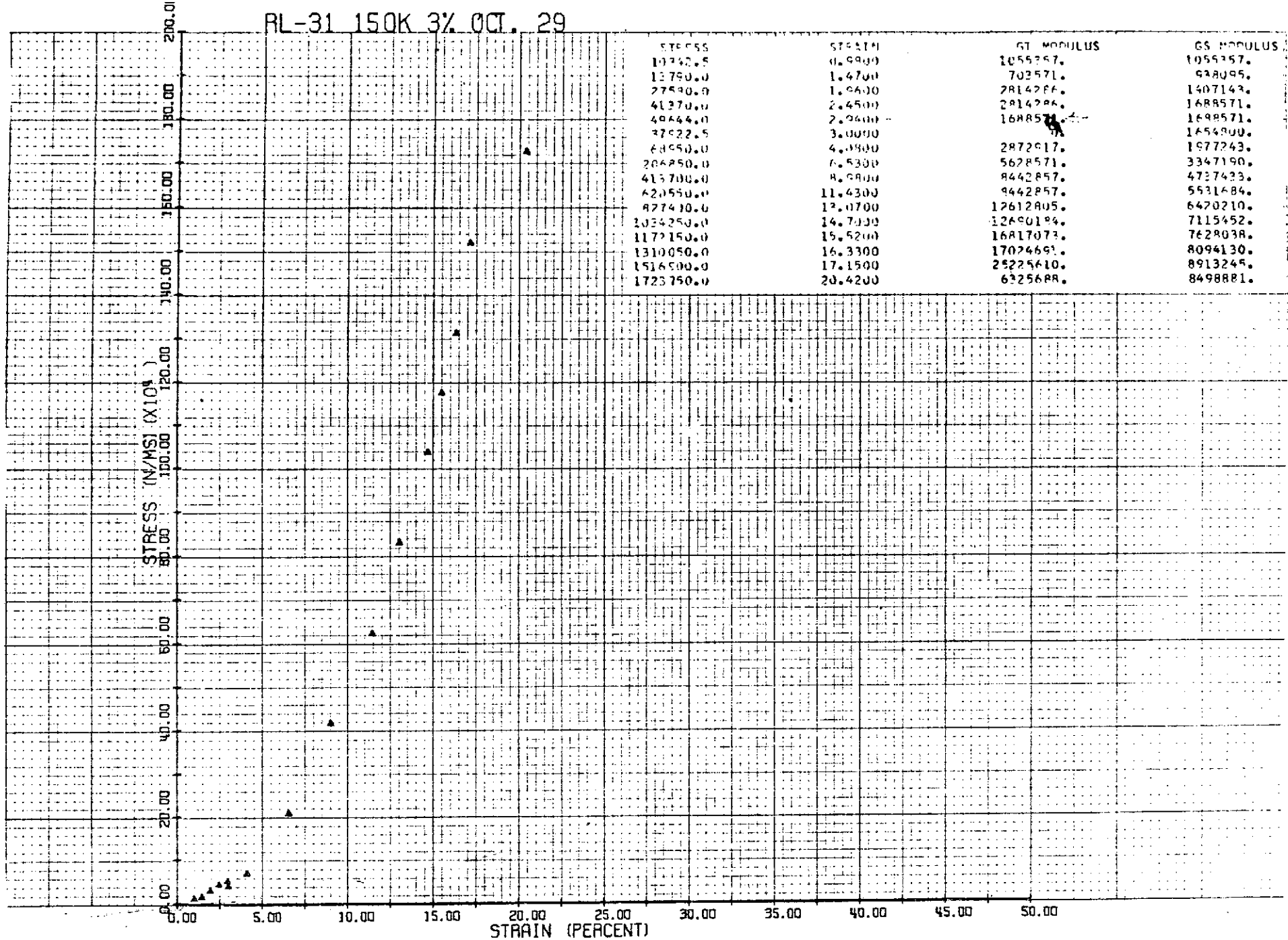




RL-44 150K 1% OCT. 29

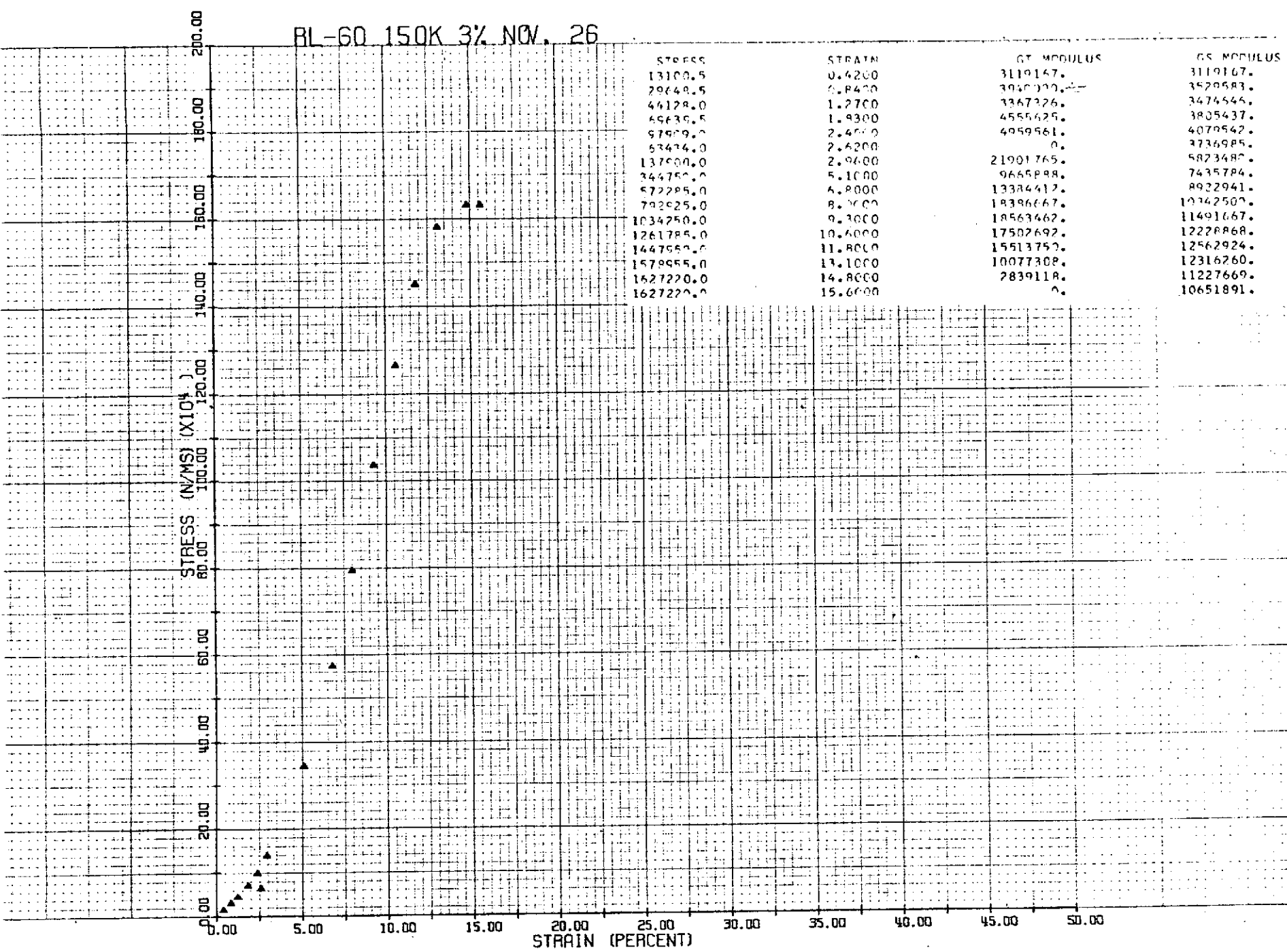


RL-31 150K 3% OCT. 29

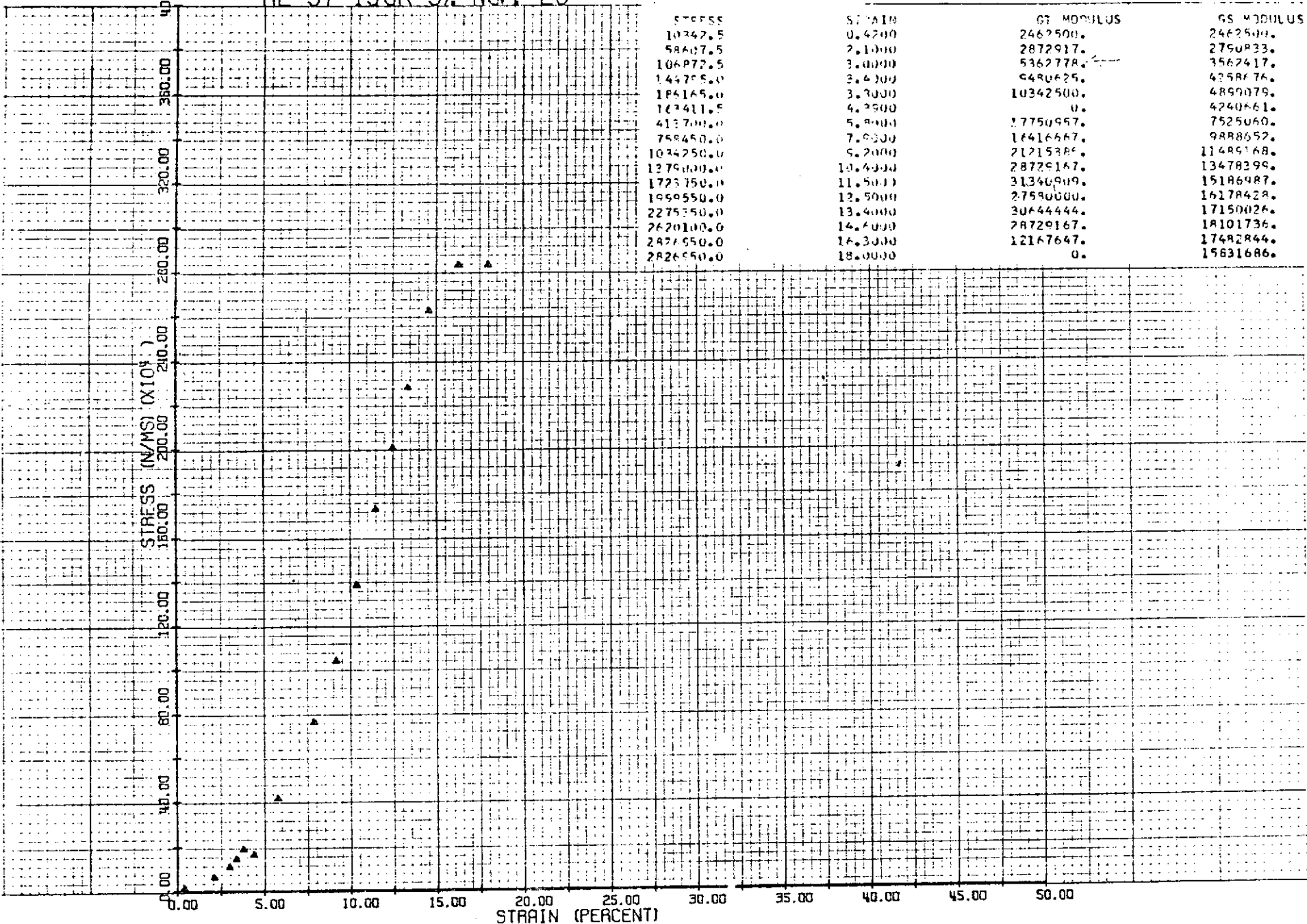


77A

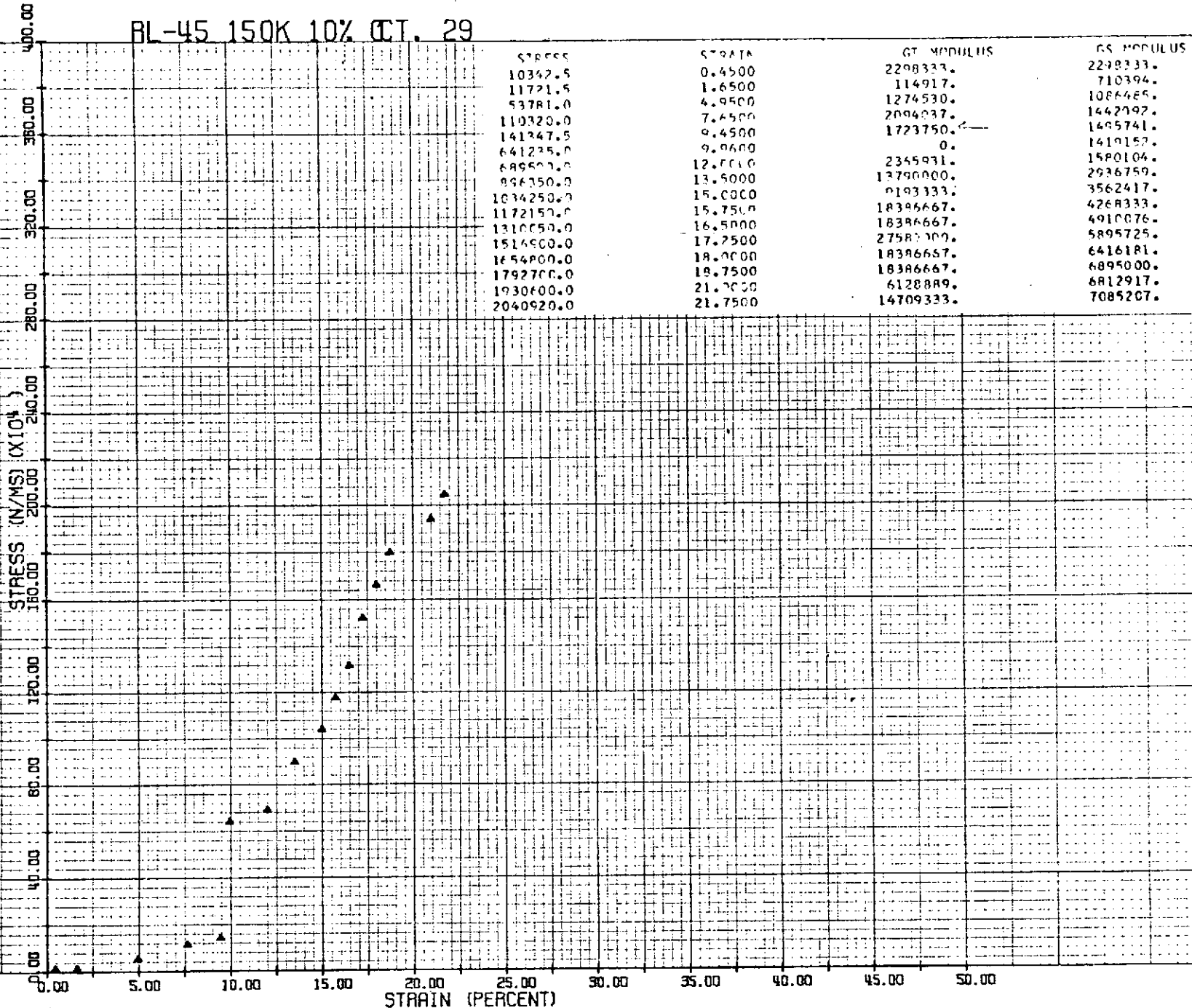
BL-60 150K 3% NOV. 26



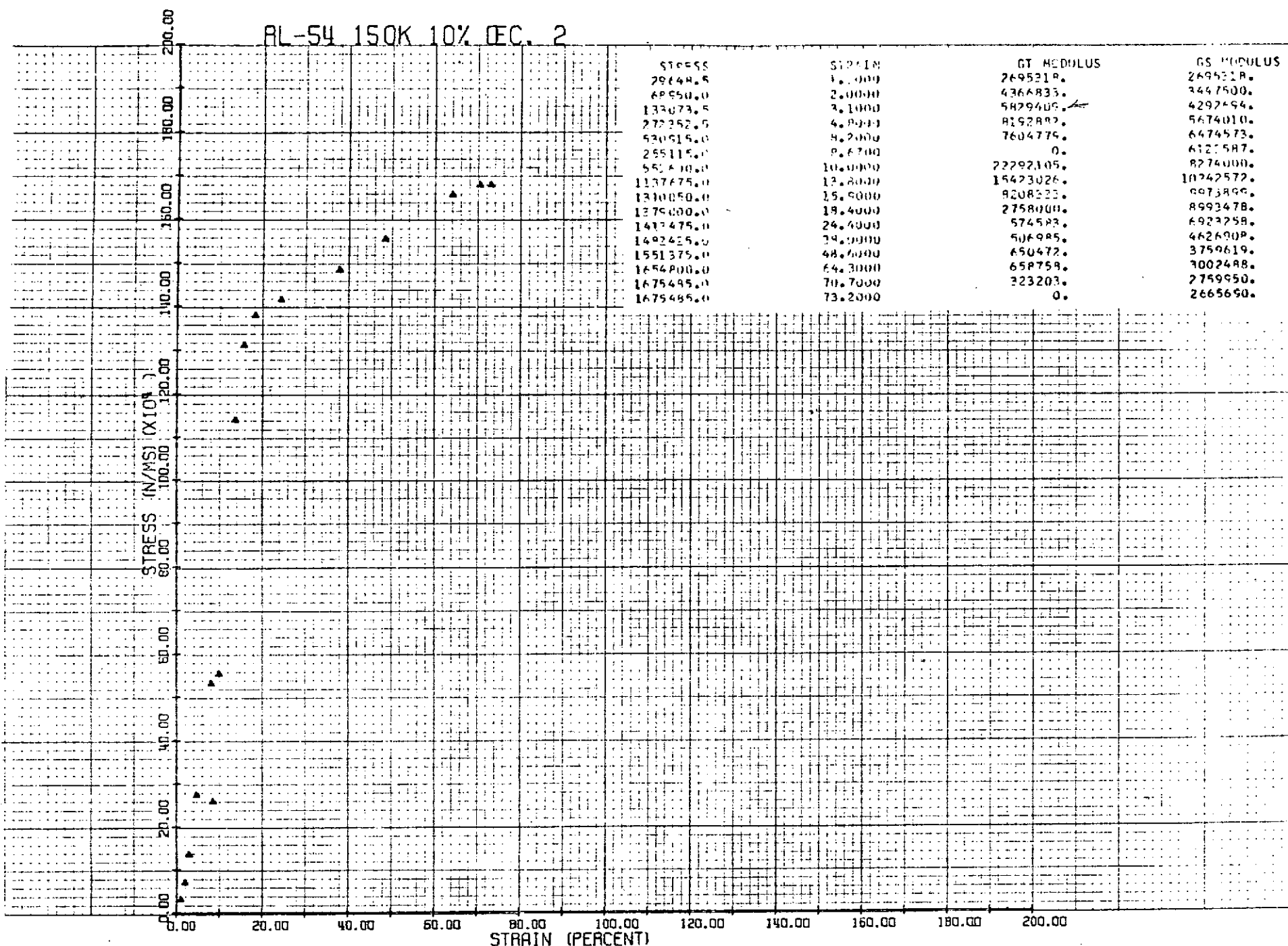
## RL-57 150K 5% NOV. 26



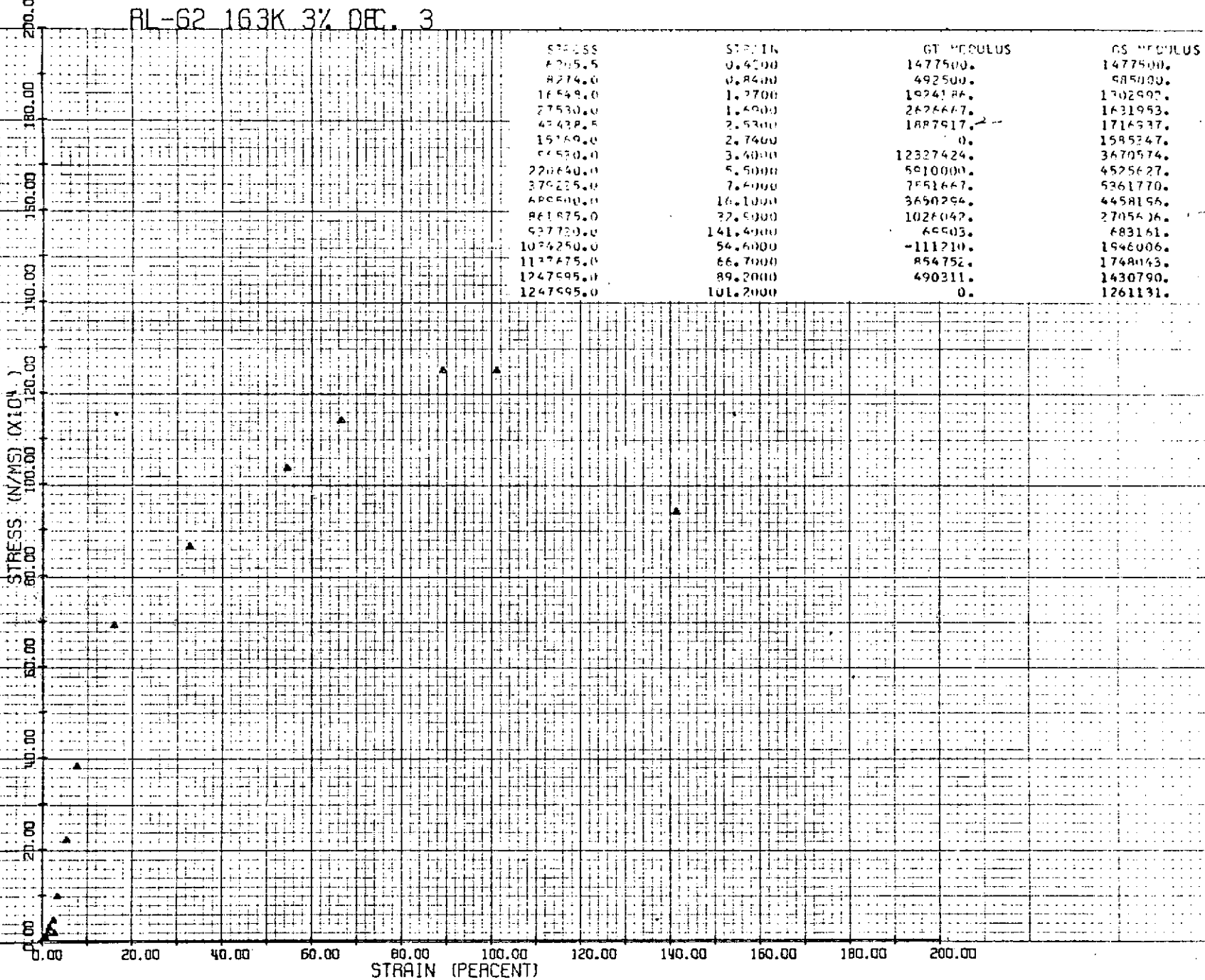
## RL-45 150K 10% CT. 29



## AL-54 150K 10% DEC. 2



RL-62 163K 3% DEC. 3



BL-55 163K 5% DEC. 2

200.0

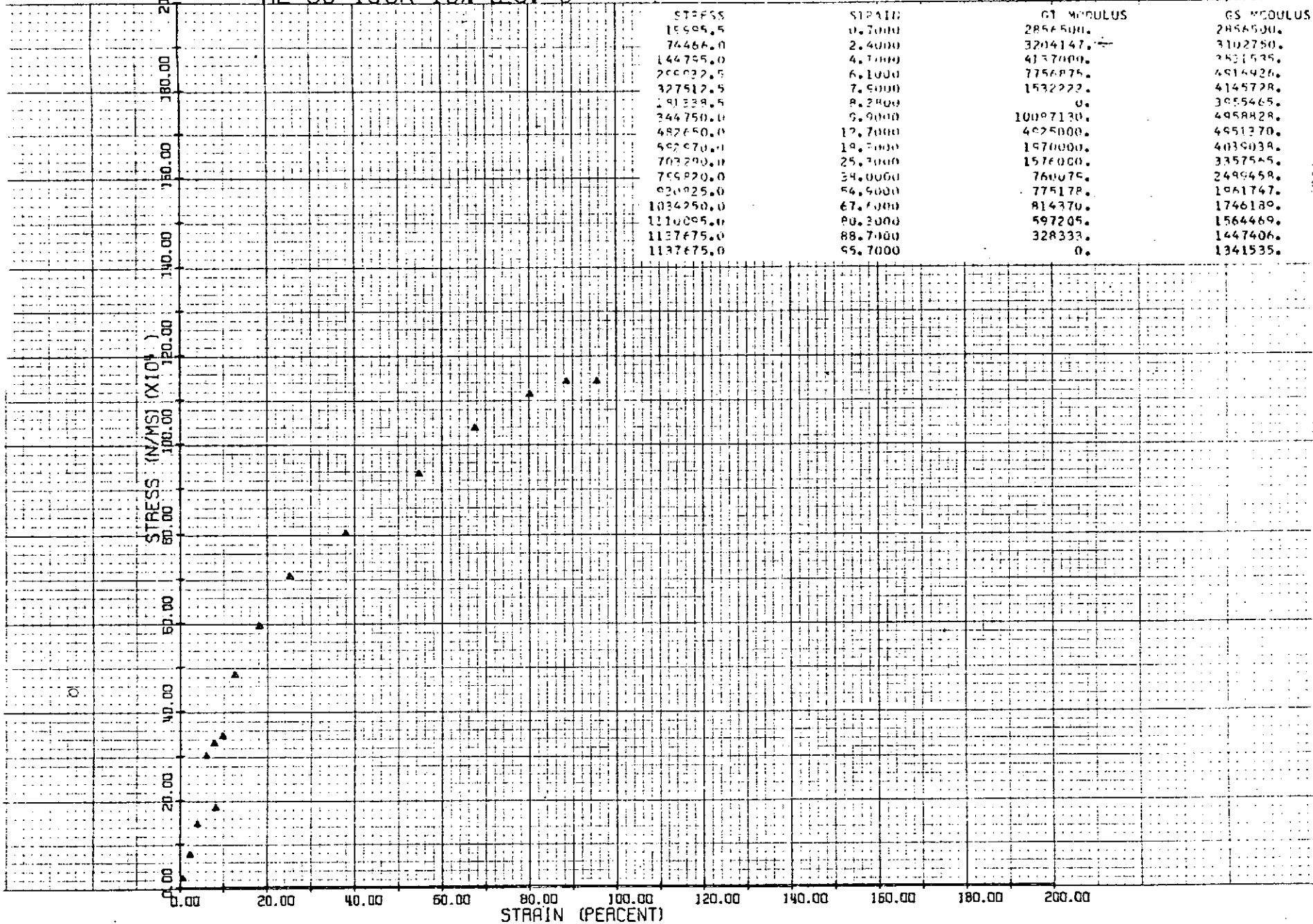
STRESS	STRAIN	GT. MODULUS	GS. MODULUS
13790.0	0.7500	1879667.	1839567.
64817.5	2.1000	2298333.	2124167.
68950.0	3.1500	2298333.	2188889.
99825.0	4.2000	1970000.	213467.
112078.0	5.1000	2604778.	2217216.
103425.0	6.6000	0.	1713303.
310275.0	19.4500	1745570.	1714027.
482650.0	20.8500	7182292.	2361165.
655025.0	32.8500	1436458.	2023373.
722975.0	41.8500	766111.	1752994.
877400.0	55.2500	766111.	1512291.
630825.0	68.8500	766111.	1345981.
665300.0	83.3500	255370.	1183914.
599775.0	91.3500	383056.	1105011.
1069725.0	102.4500	621171.	1052590.

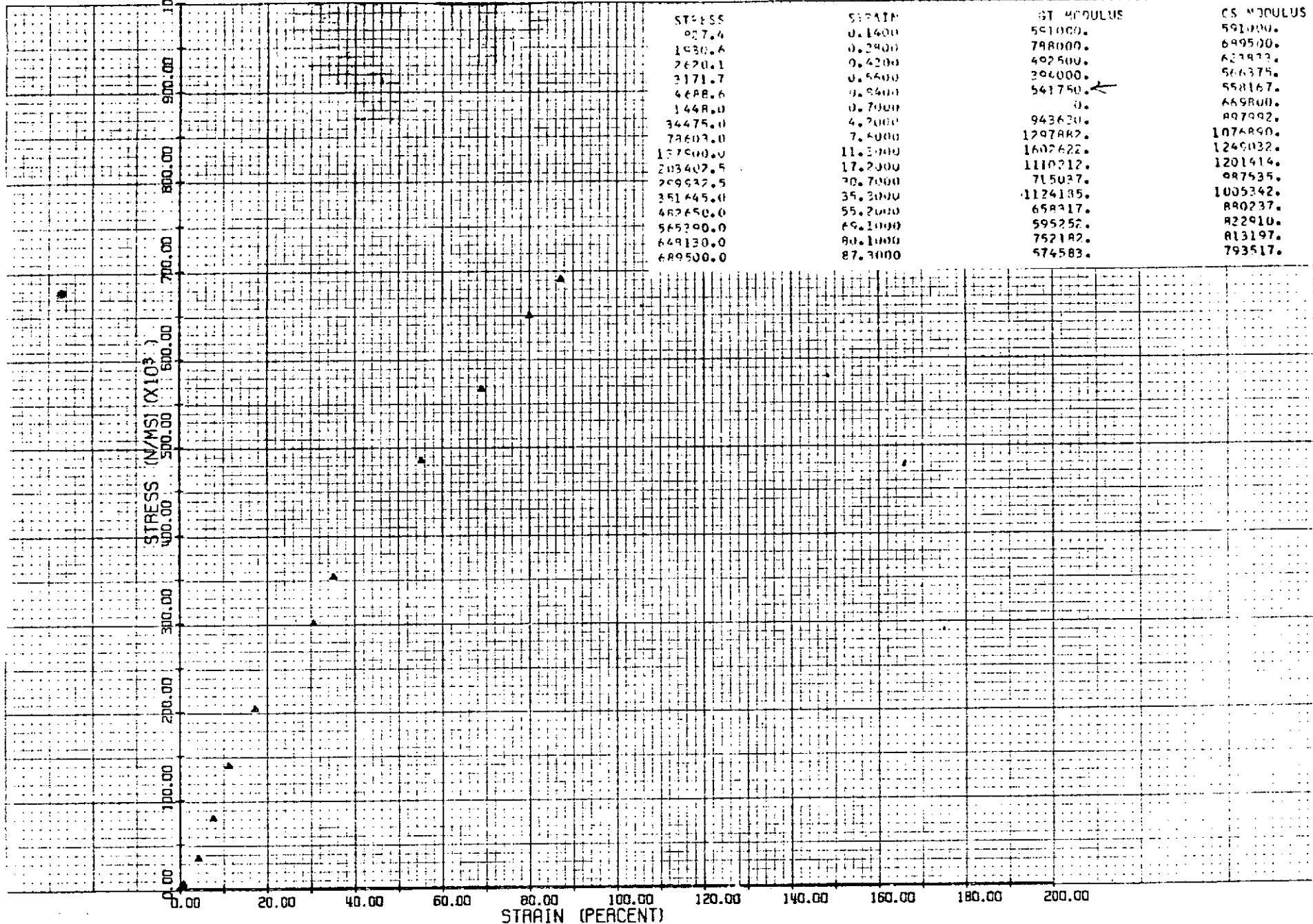
200.0  
180.0  
160.0  
140.0  
120.0  
100.0  
80.0  
60.0  
40.0  
20.0  
0.0

STRESS (N/mm<sup>2</sup>) STRAIN (%)

STRAIN (PERCENT)

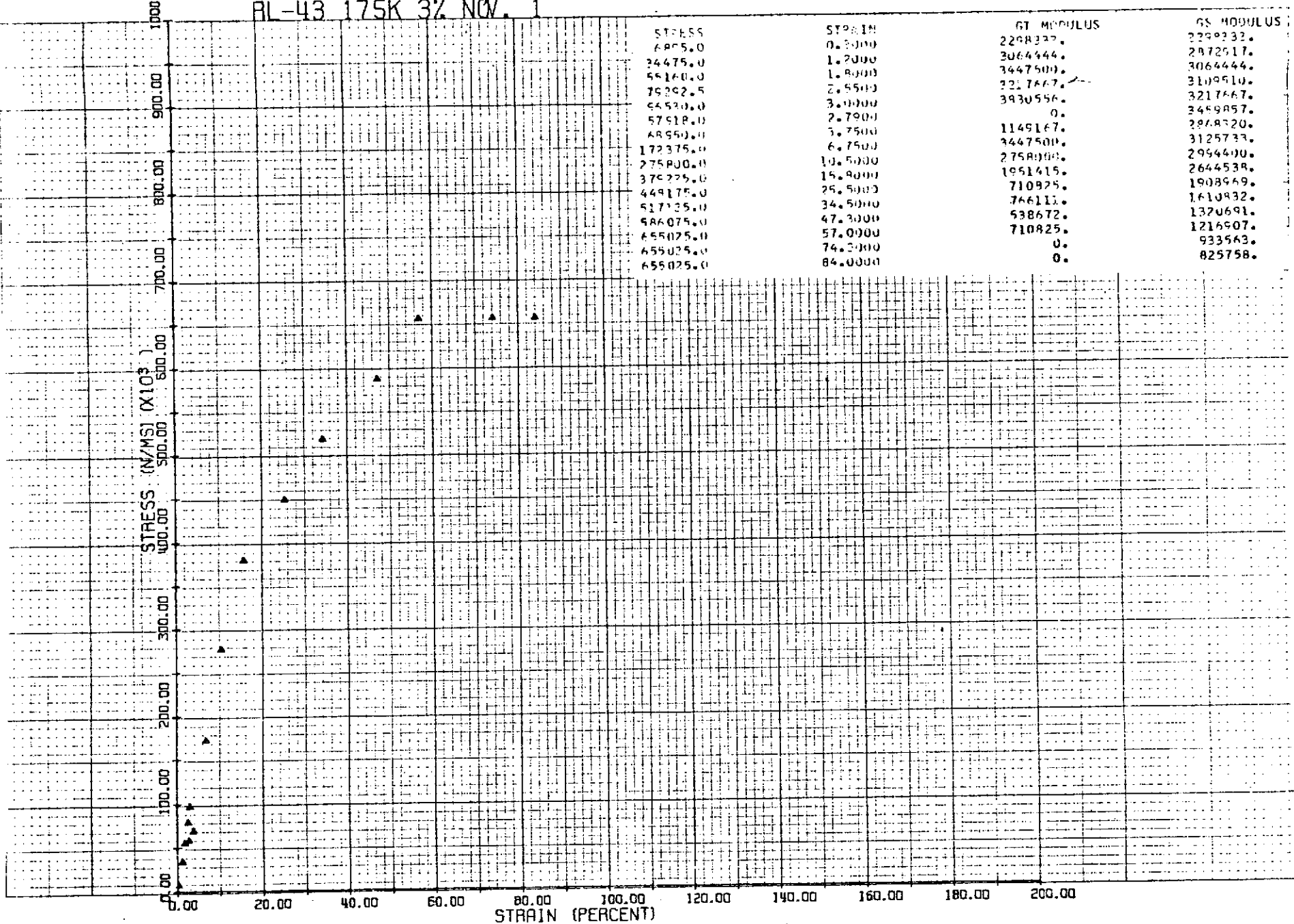
## RL-63 16.3K 10% DEC. 3





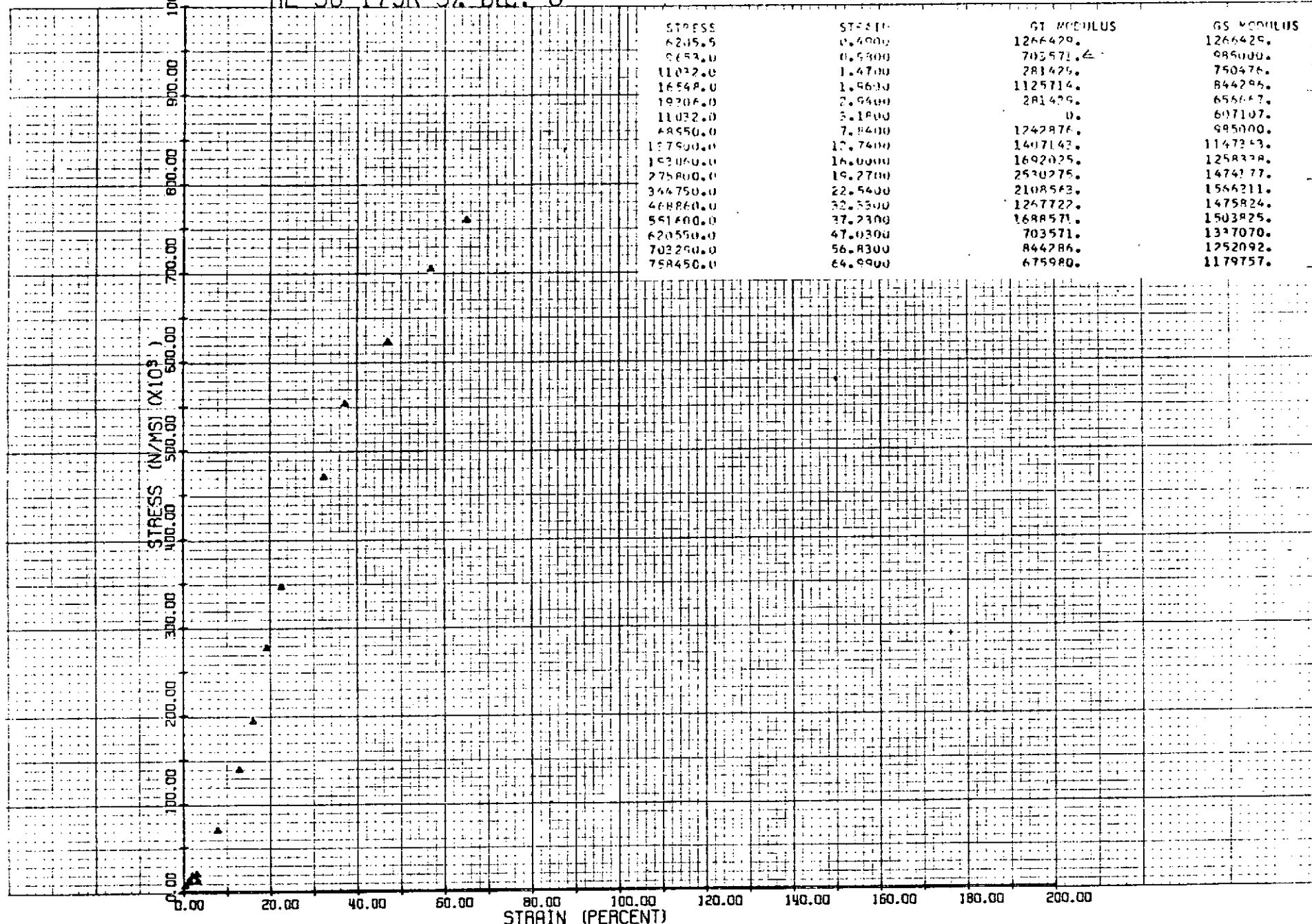
BL-43 175K 3% NOV. 1

2



## AL-36 175K 3% DEC. 6

1000.f



47

## AL-7 175K 5% AUG. 30

1000.0

1000.0

STRESS (N/mm<sup>2</sup>) (X10<sup>3</sup>)

400.00

300.00

200.00

100.00

0.00

0.00

5.00

10.00

15.00

20.00

25.00

30.00

35.00

40.00

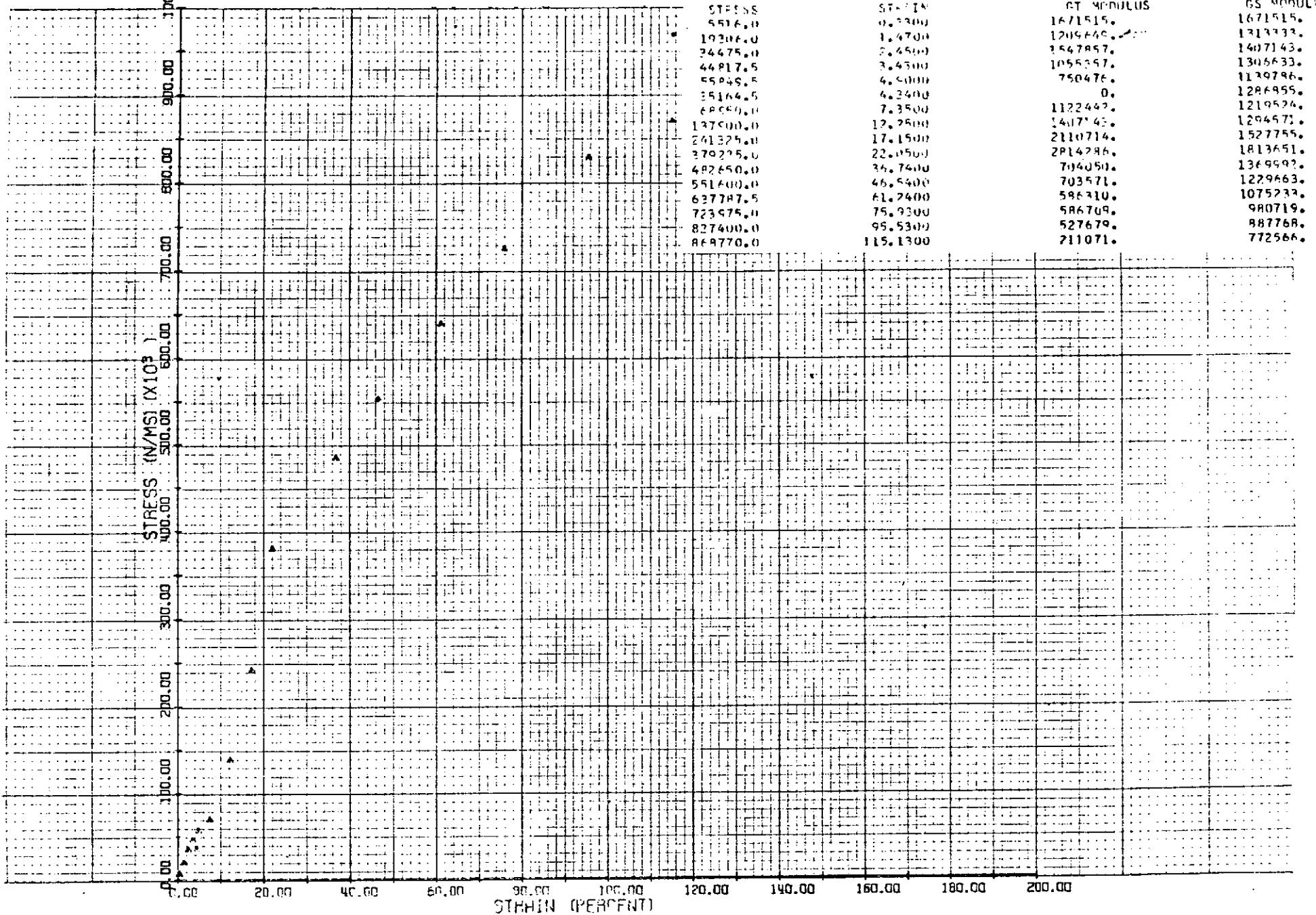
45.00

50.00

STRAIN (PERCENT)

STRESS	STRAIN	G MODULUS	G MODULUS
13790.0	0.1500	6193333.	6193333.
68550.0	1.5000	4105526.	4596667.
103425.0	2.2500	4506667.	4596667.
127600.0	2.7000	4596667.	4596667.
161742.0	4.5000	1562067.	3585400.
64461.5	4.2200	0.	3734792.
103475.0	4.6500	1422778.	3440535.
159585.0	6.7500	3064444.	3340244.
206850.0	7.5000	6435332.	3645753.
262010.0	8.2500	7254467.	3986564.
320560.0	9.1500	7661111.	4347995.
413710.0	13.5000	1902049.	5559843.
402650.0	22.5000	7661111.	2442362.
551600.0	23.0000	656667.	1874186.
620550.0	42.5000	656667.	1580302.

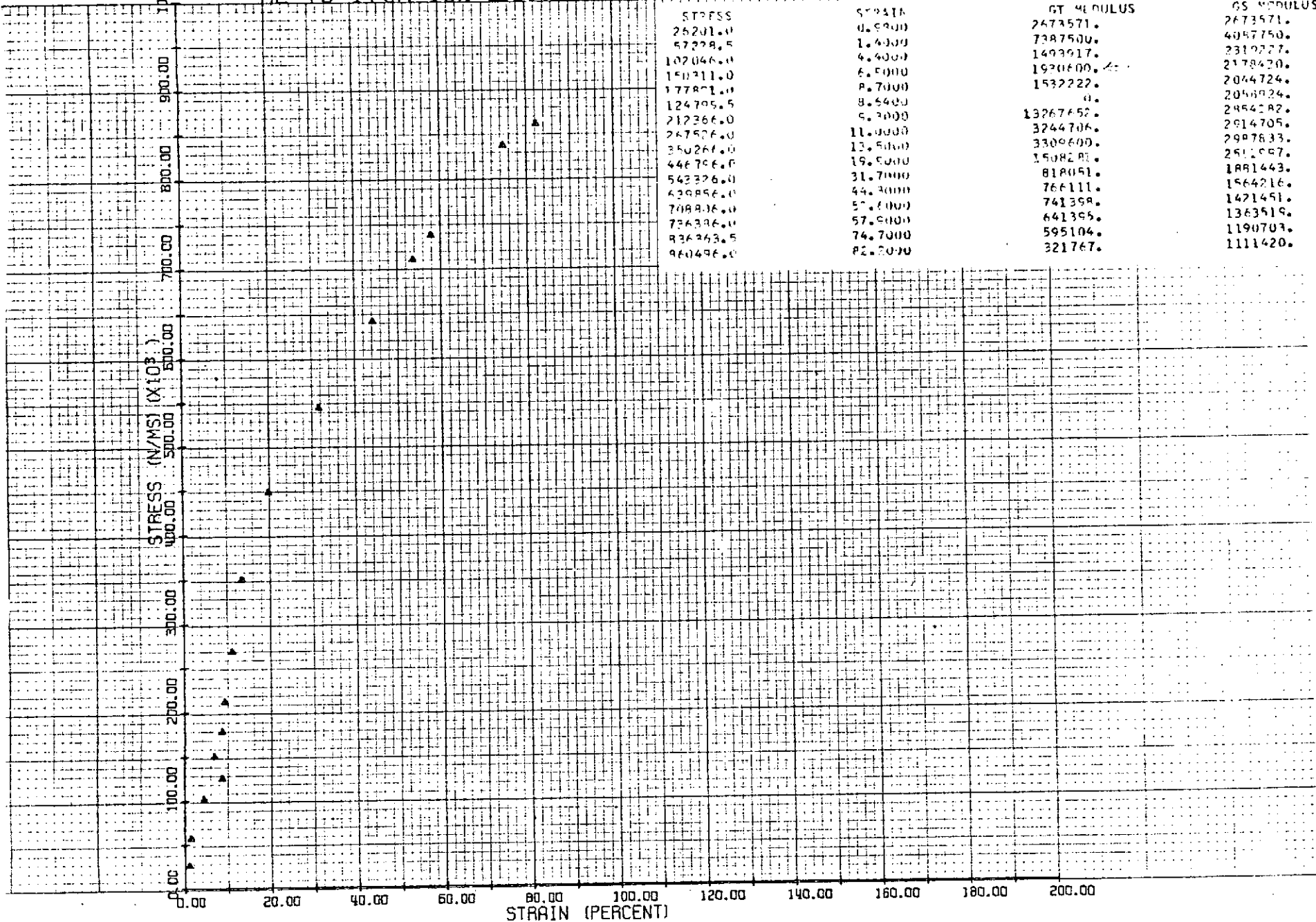
## RL-66 175K 5% DEC. 5



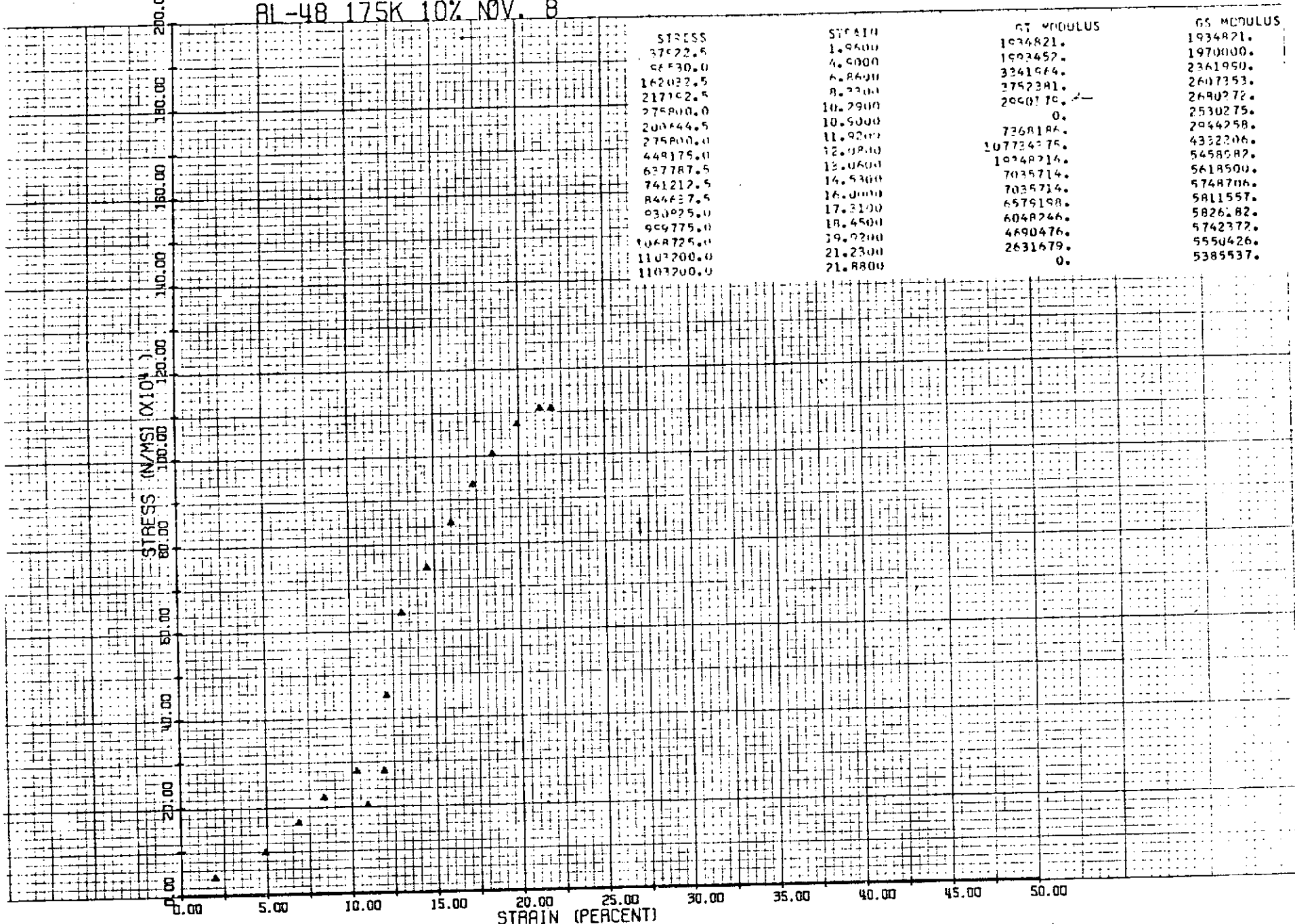
A 68

406

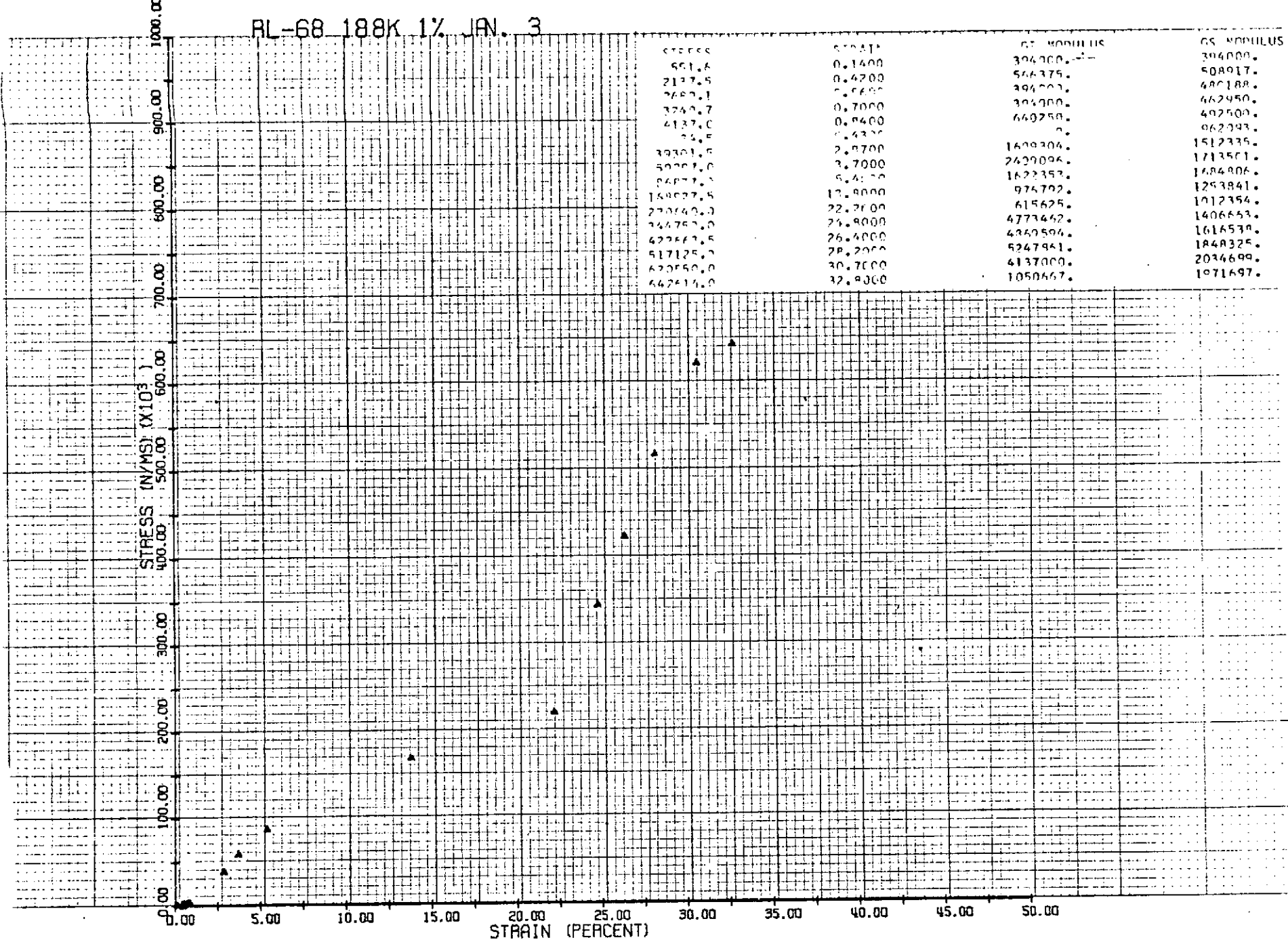
## BL-70 175K 10% DEC. 16



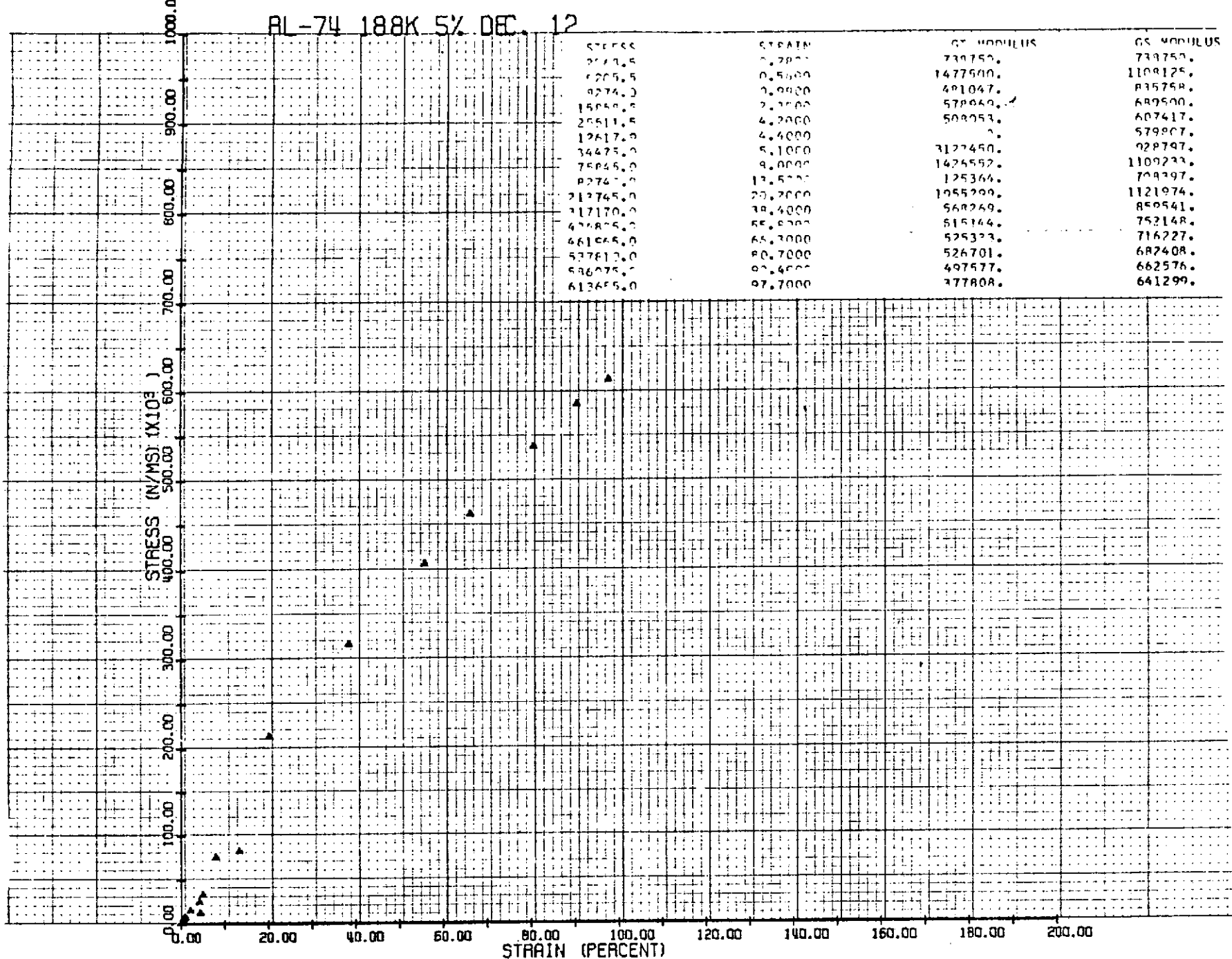
AL-48 175K 10% NOV. 8



## RL-68 188K 1% AN. 3

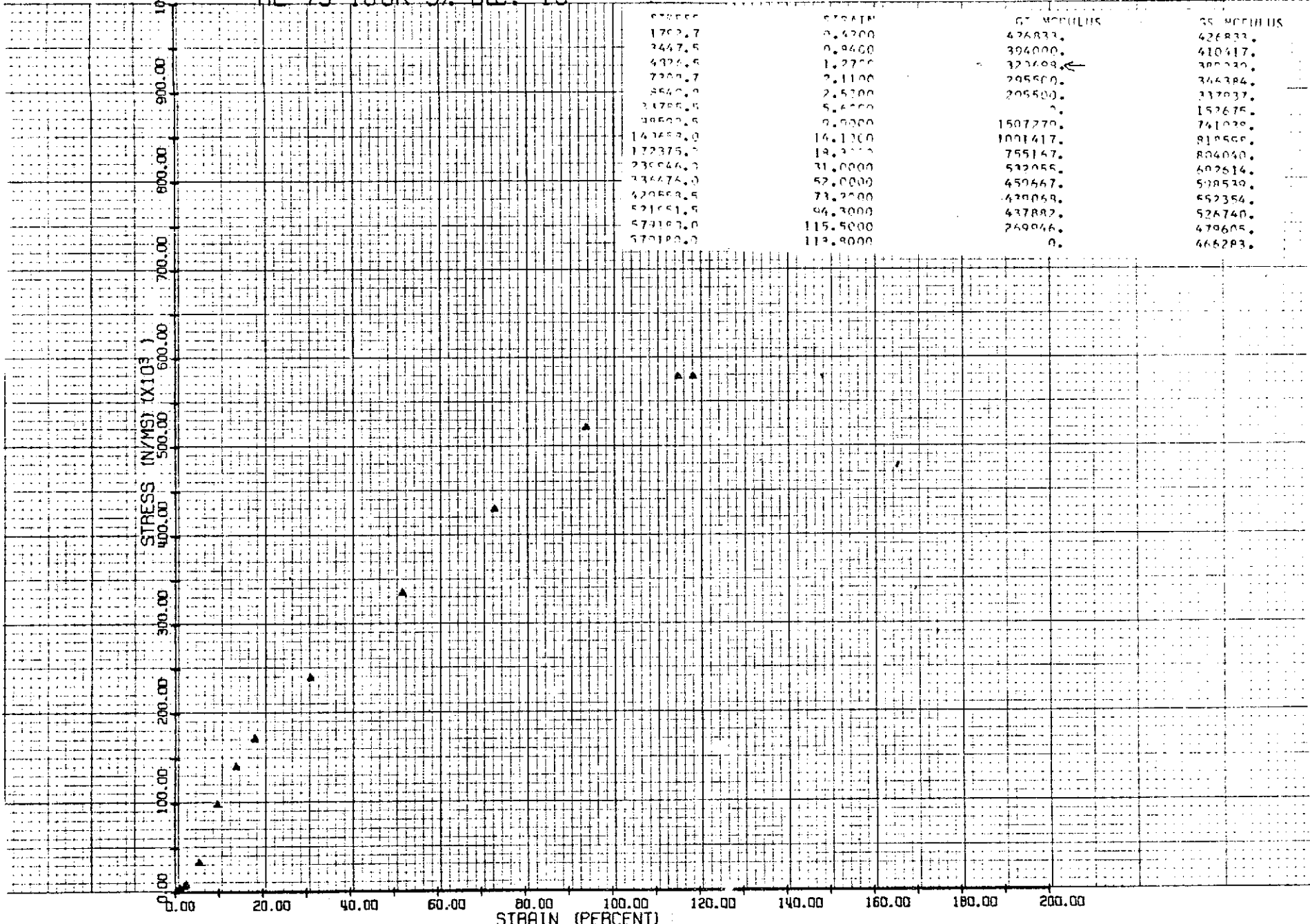


RL-74 188K 5% DEC. 12

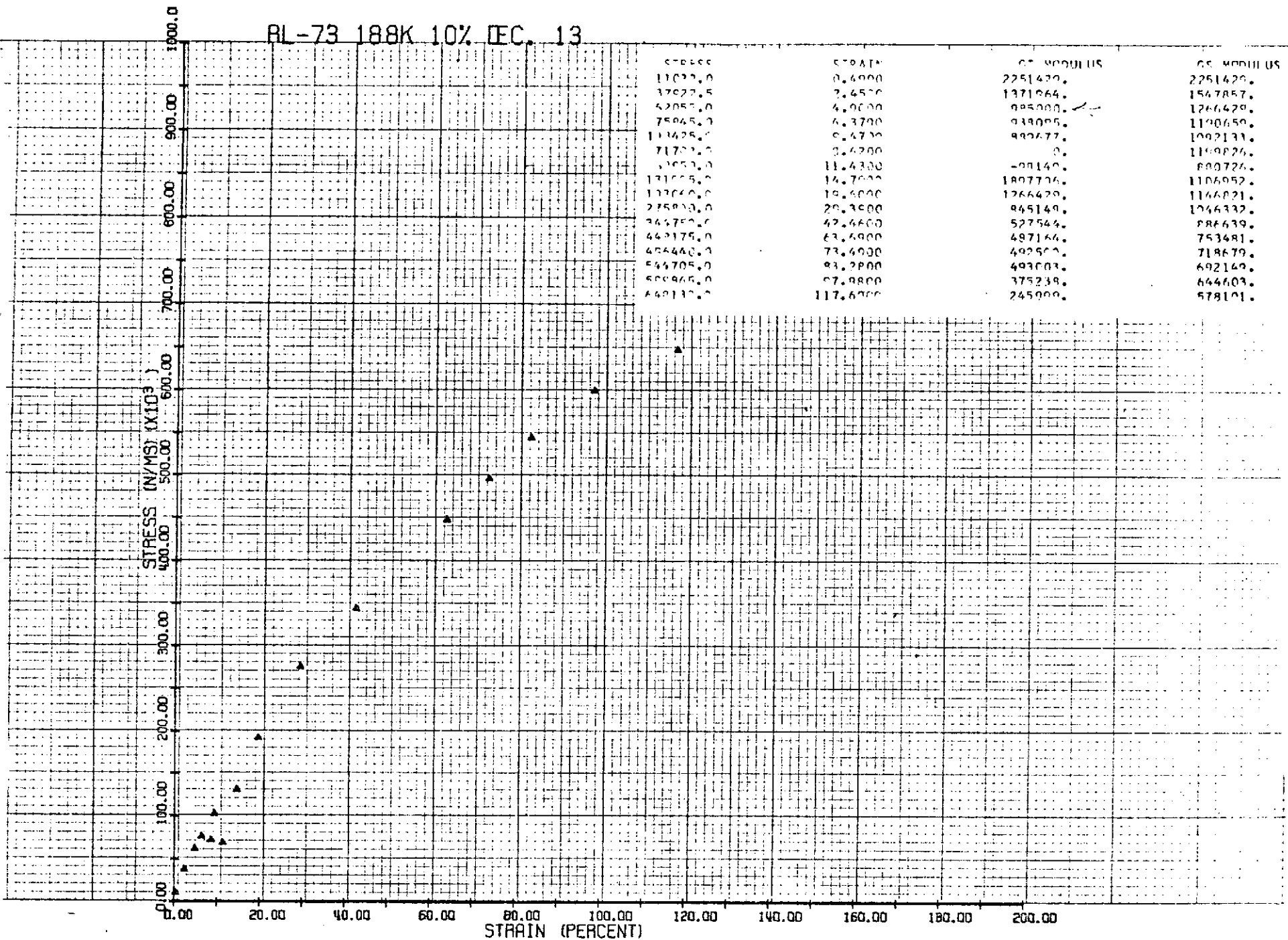


STRAIN	ST. MODULUS	G. MODULUS
0.0000	730750.	730750.
10.0000	1477000.	1109125.
20.0000	491067.	835750.
30.0000	570000.	689500.
40.0000	503053.	607417.
50.0000	^.	579907.
60.0000	3127450.	929747.
70.0000	1425552.	1109233.
80.0000	125364.	709397.
90.0000	1055200.	1121974.
100.0000	568260.	850541.
110.0000	515144.	752148.
120.0000	525323.	716227.
130.0000	526701.	687408.
140.0000	497577.	662576.
150.0000	377808.	641299.

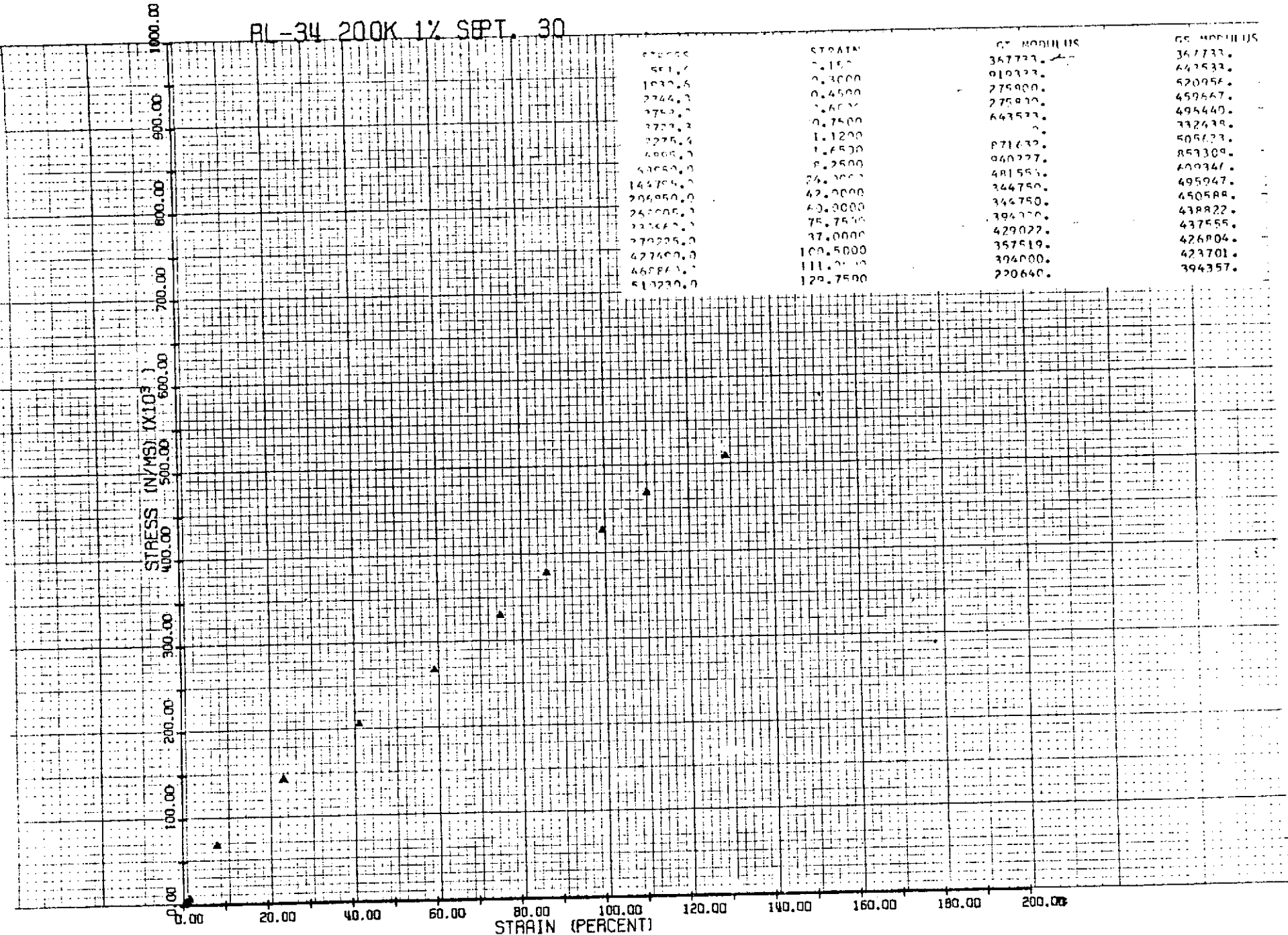
BL-75 188K 3% DEC. 13



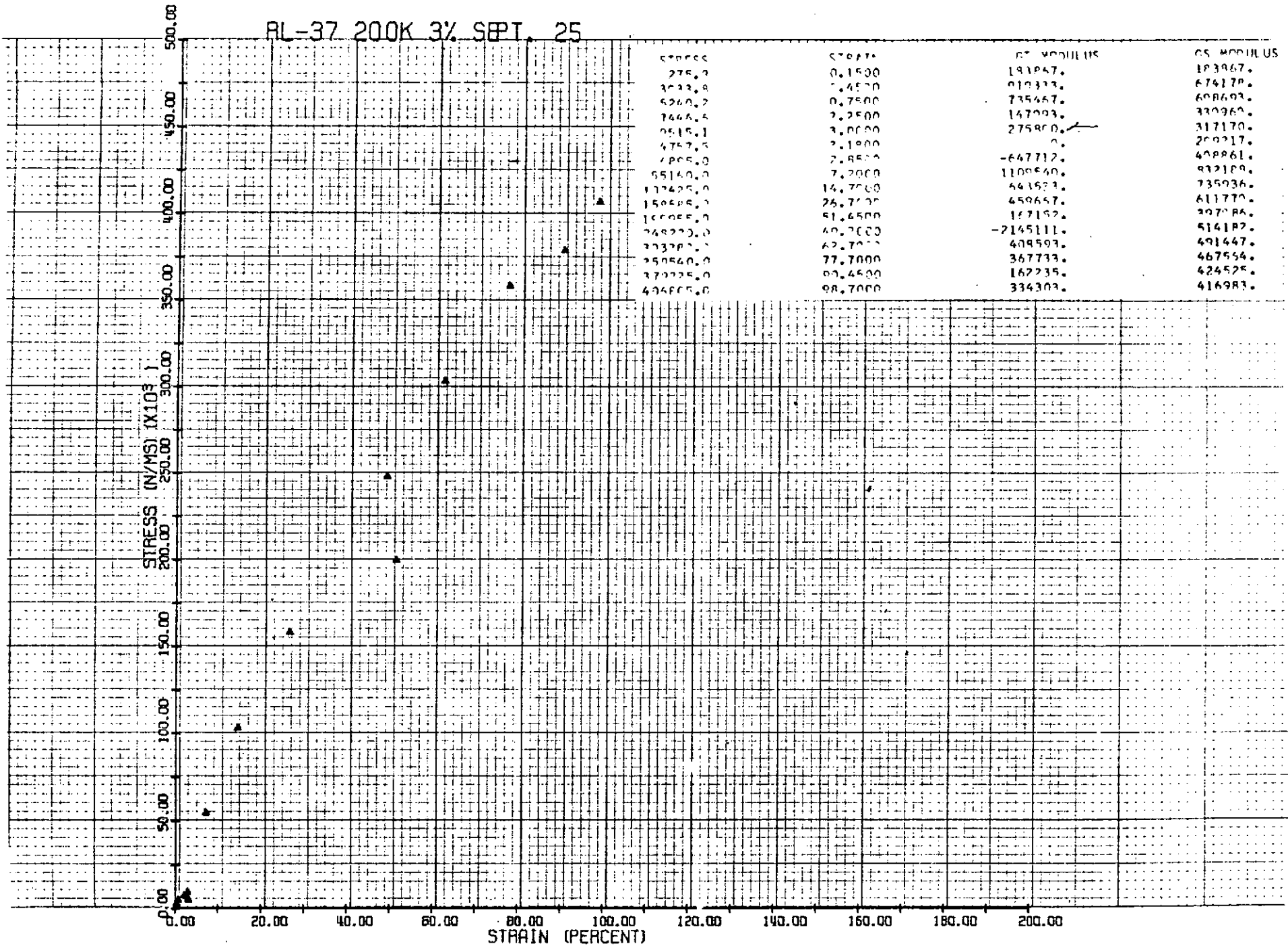
RL-73 188K 10% DEC. 13



BL-34 200K 1% SEPT. 30

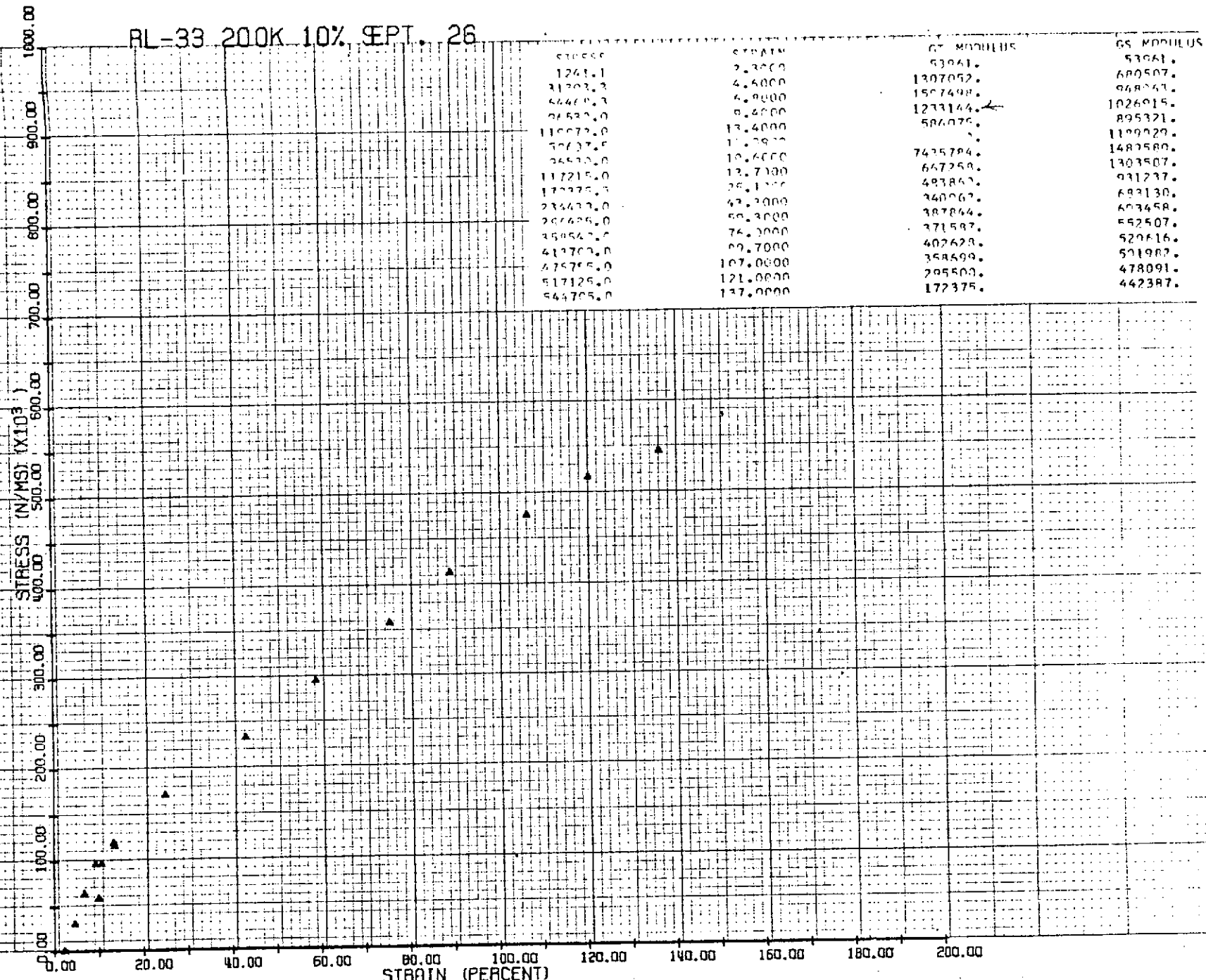


RL-37 200K 3% SEPT. 25

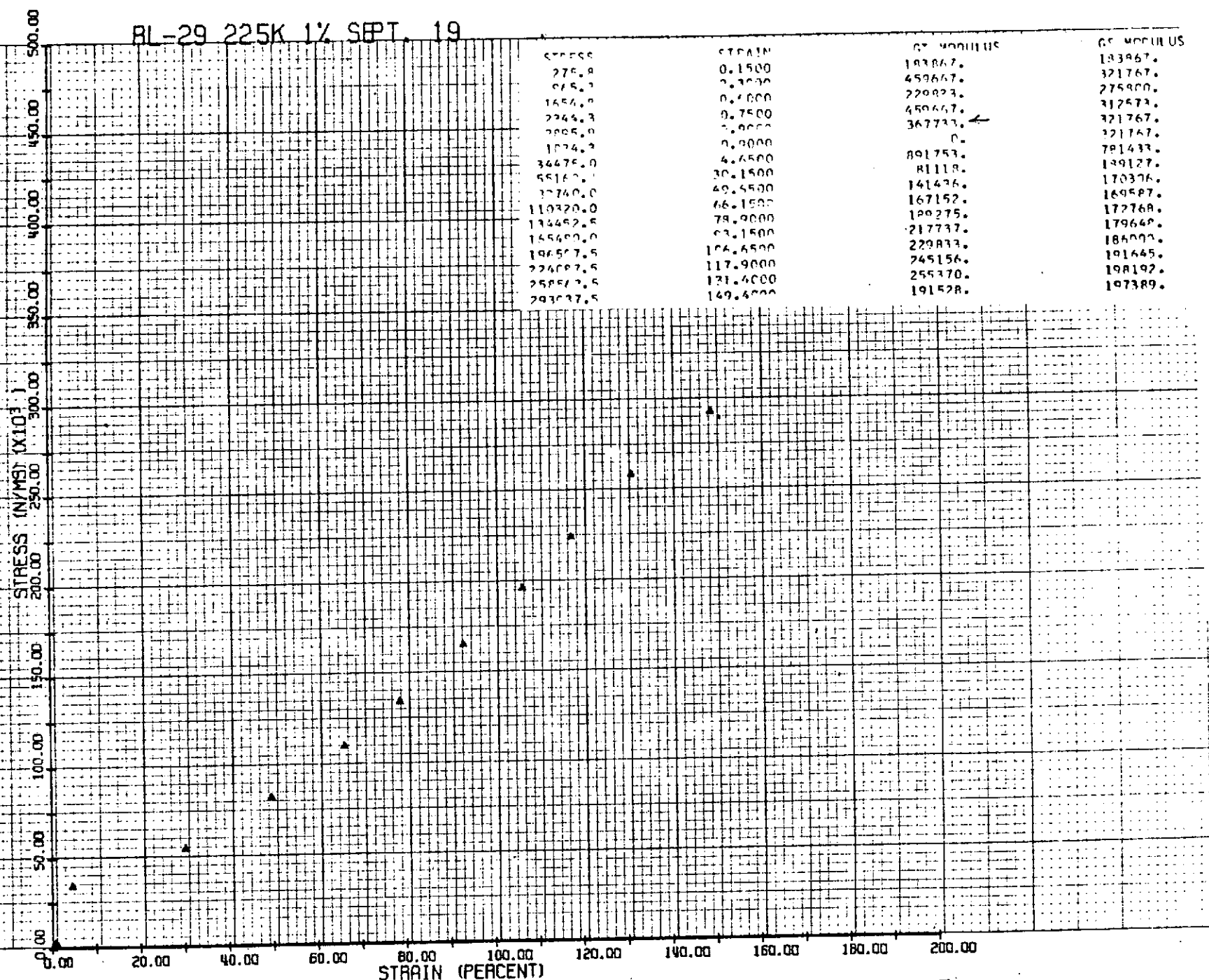


476

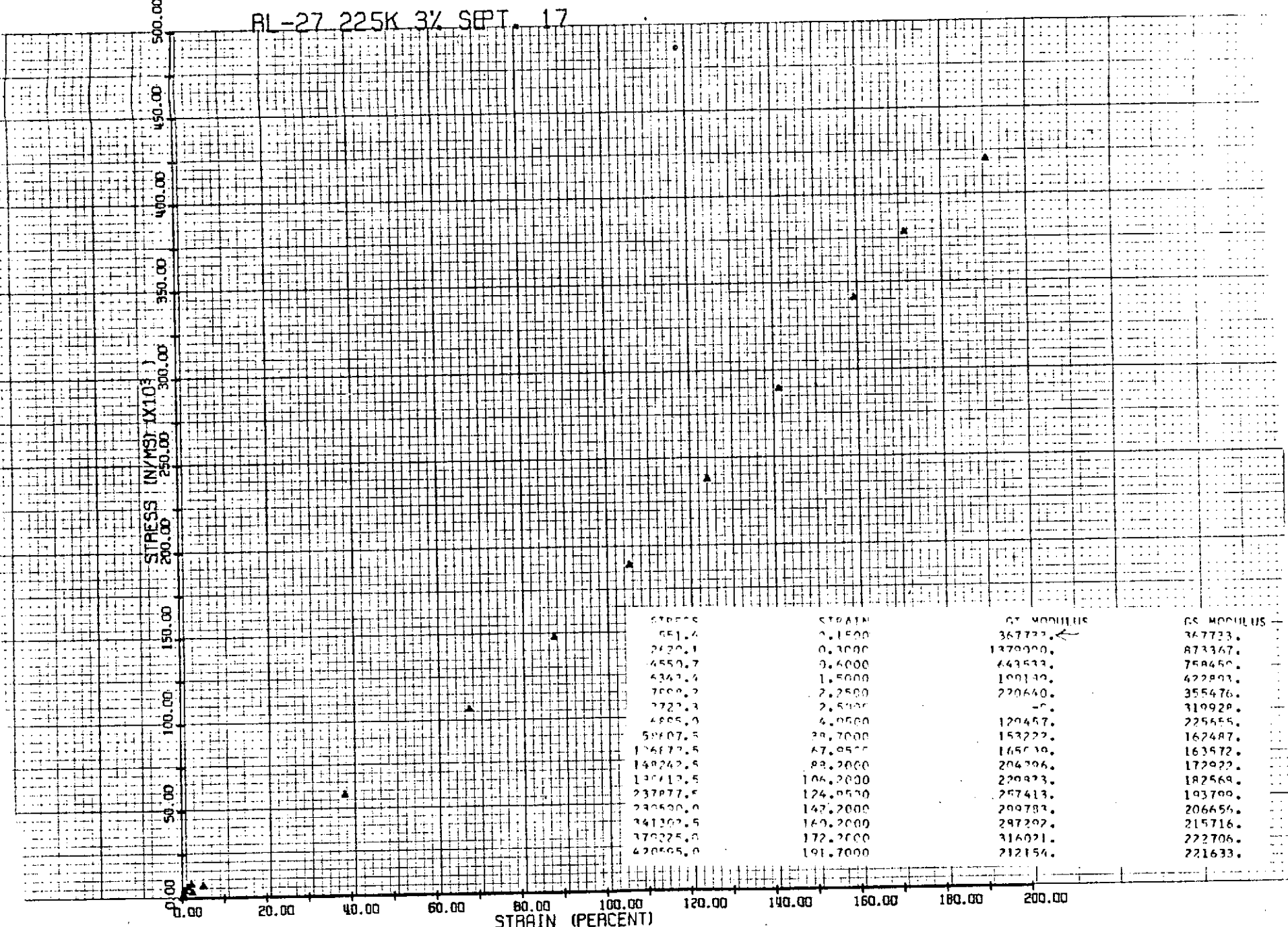
RL-33 200K 10% SEPT. 26



BL-29 225K 1% SEPT. 19



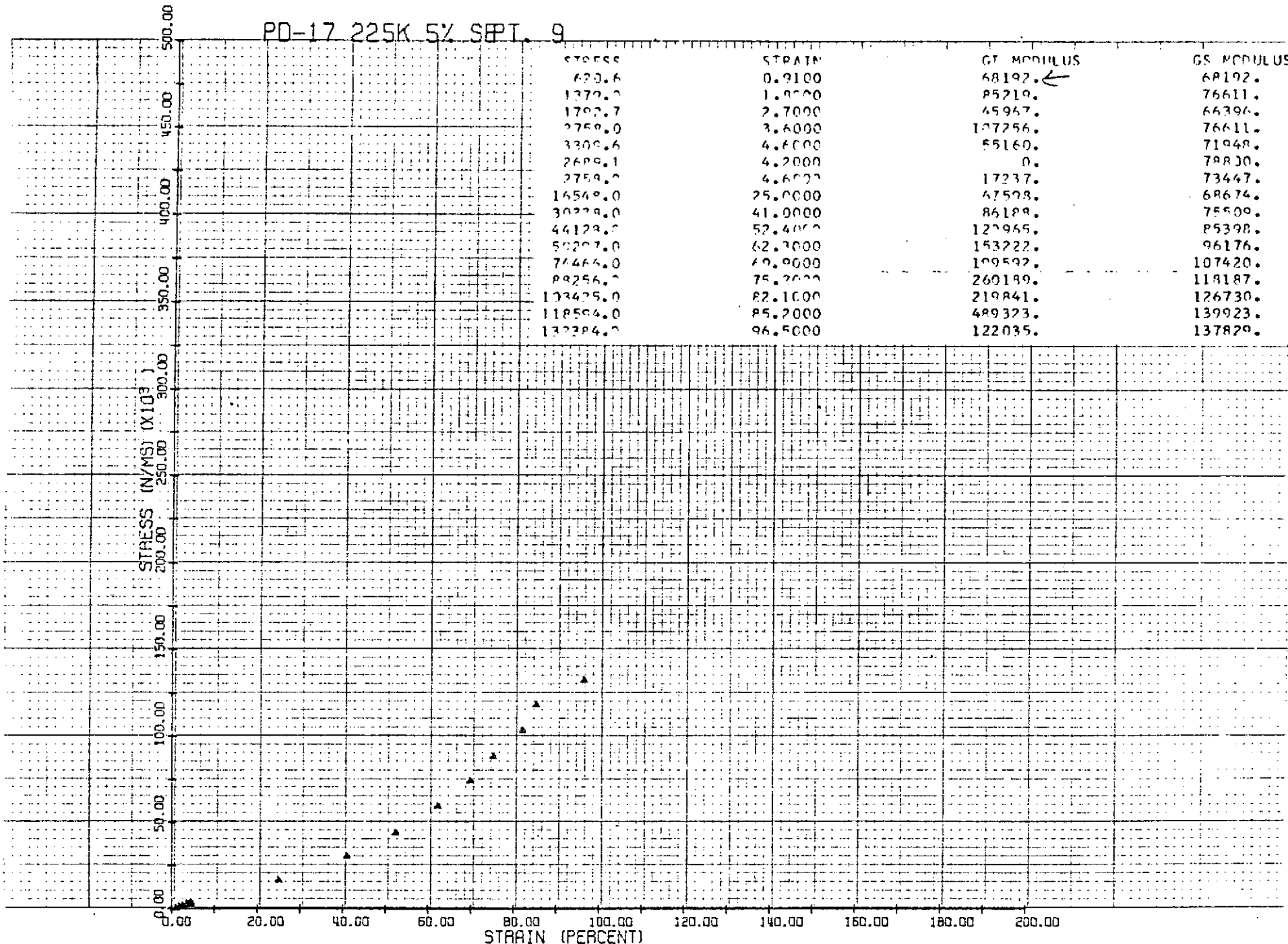
RL-27 225K 3% SEPT. 17



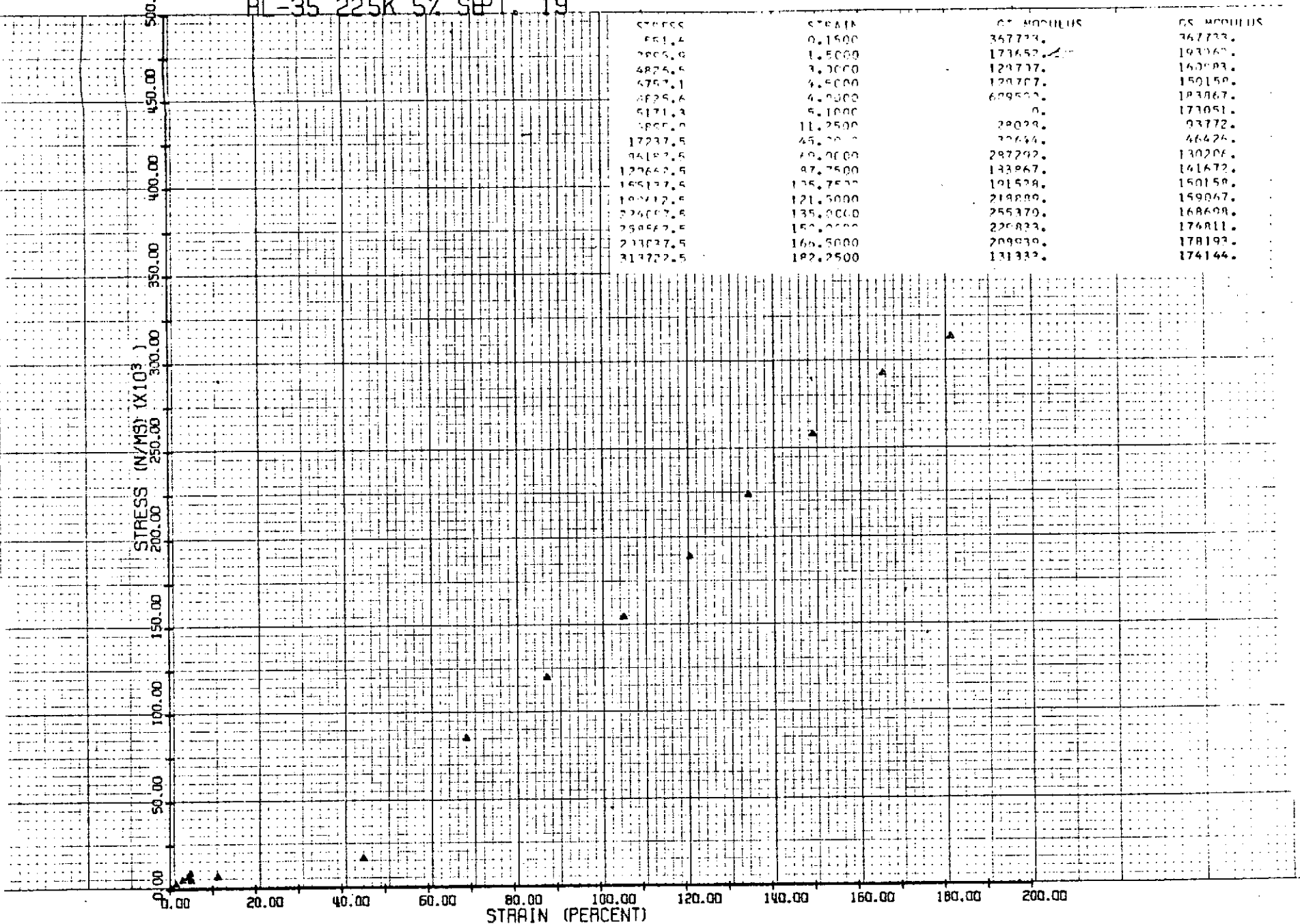
K-E KEUFFEL & ESSER CO.

PRINTED IN U.S.A.

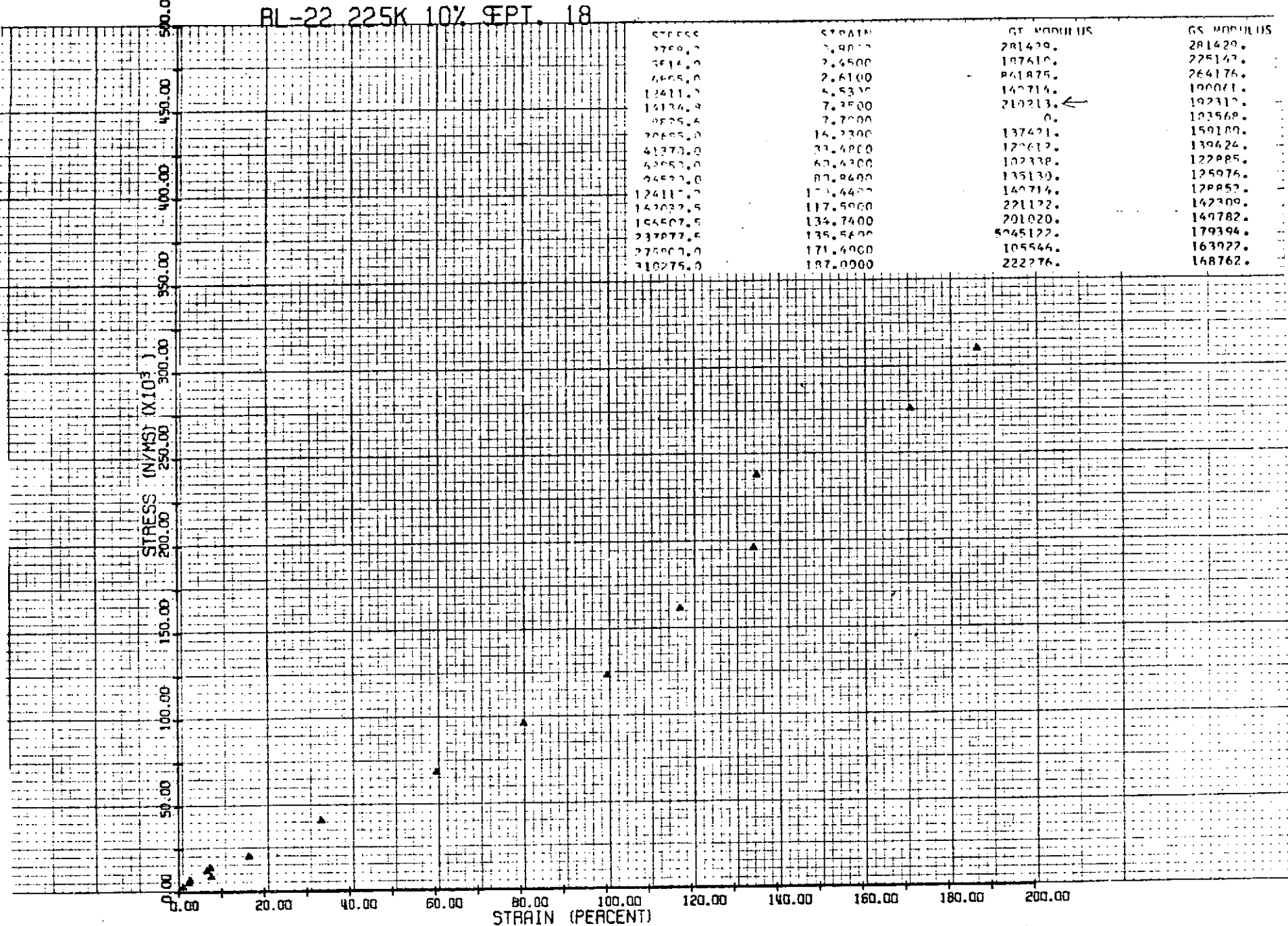
PD-17 225K 5% SEPT. 9

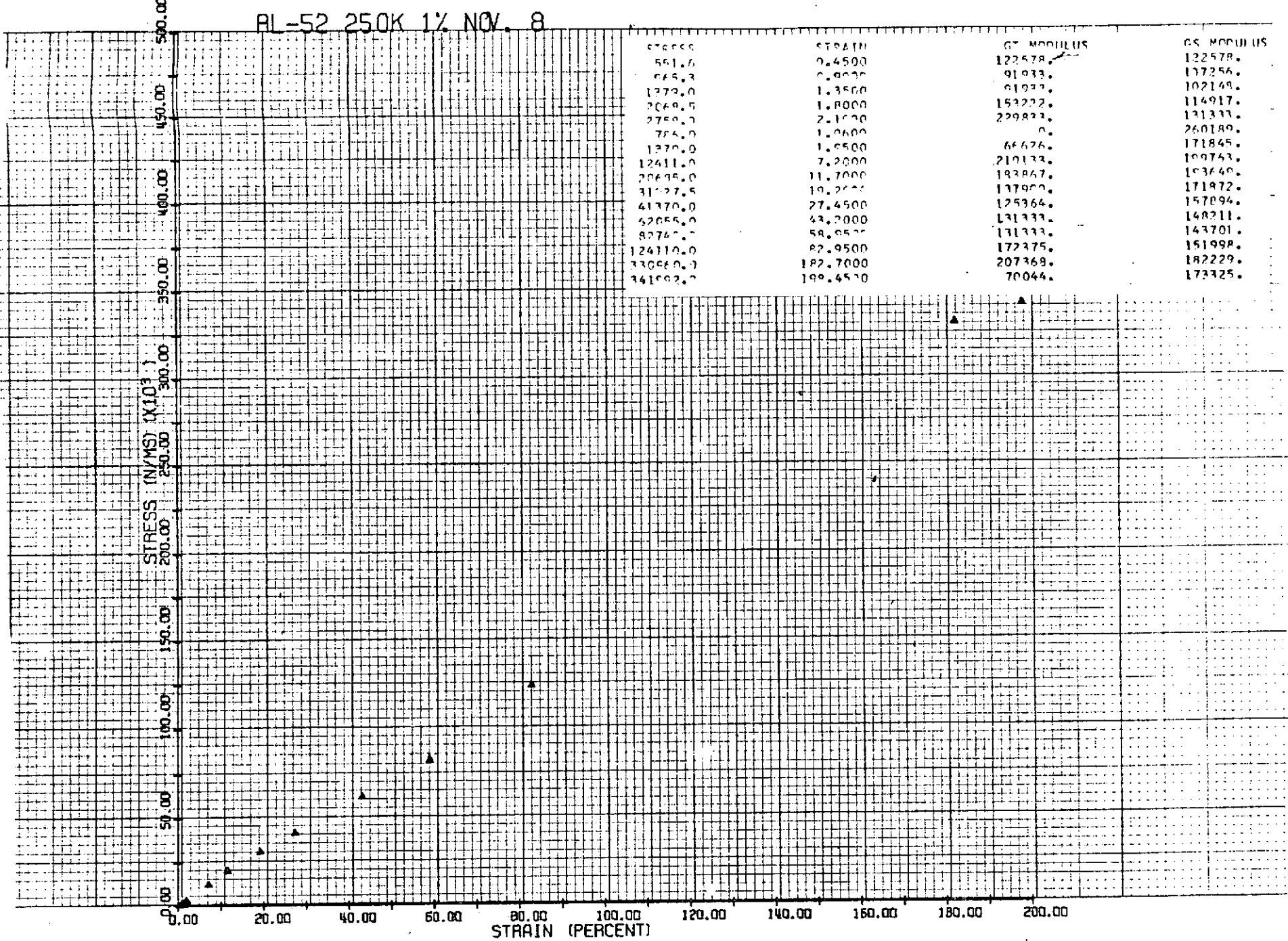


PL-35 225K 5% SEPT. 19



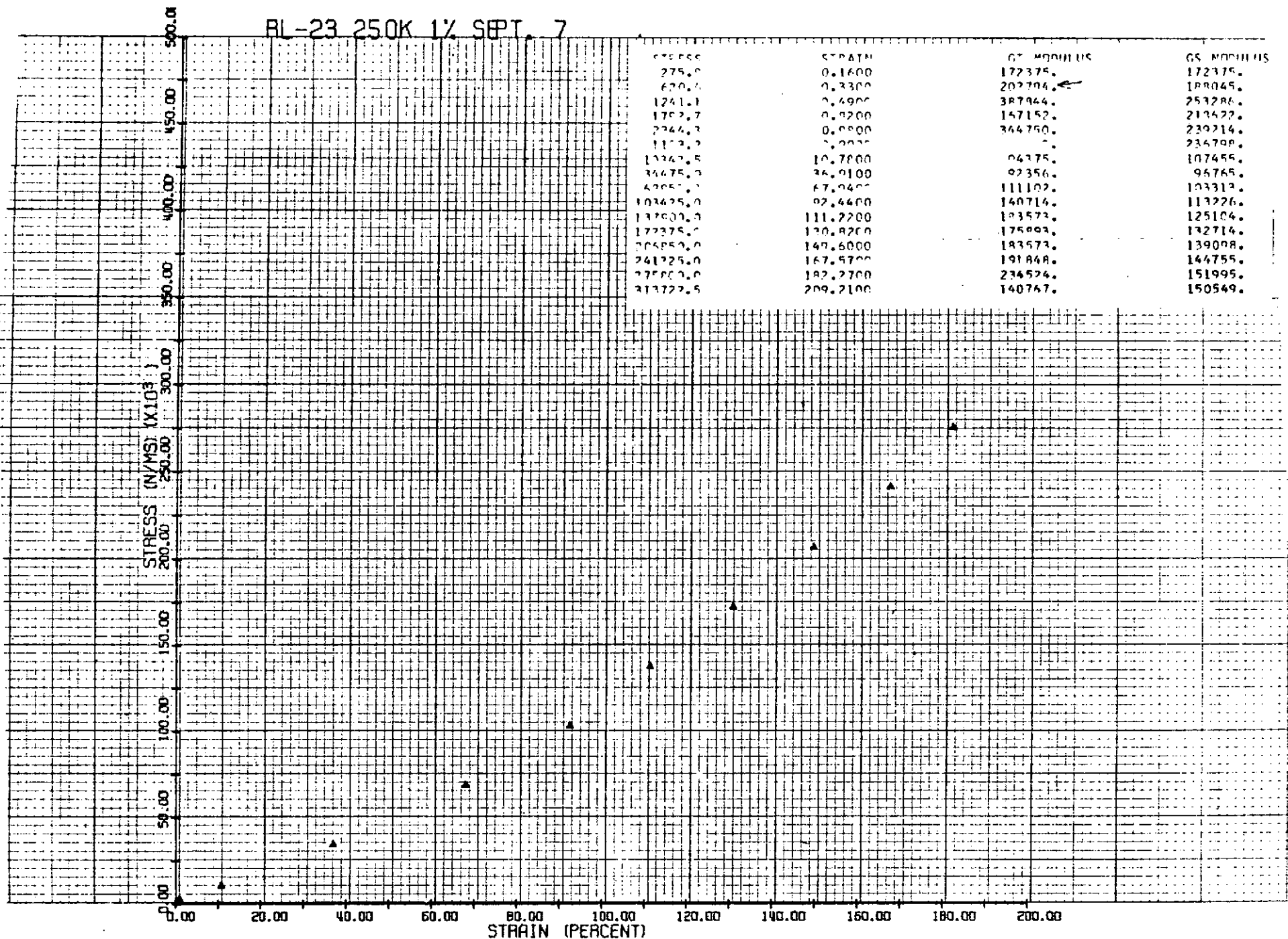
RL-22 225K 10% SEPT. 18



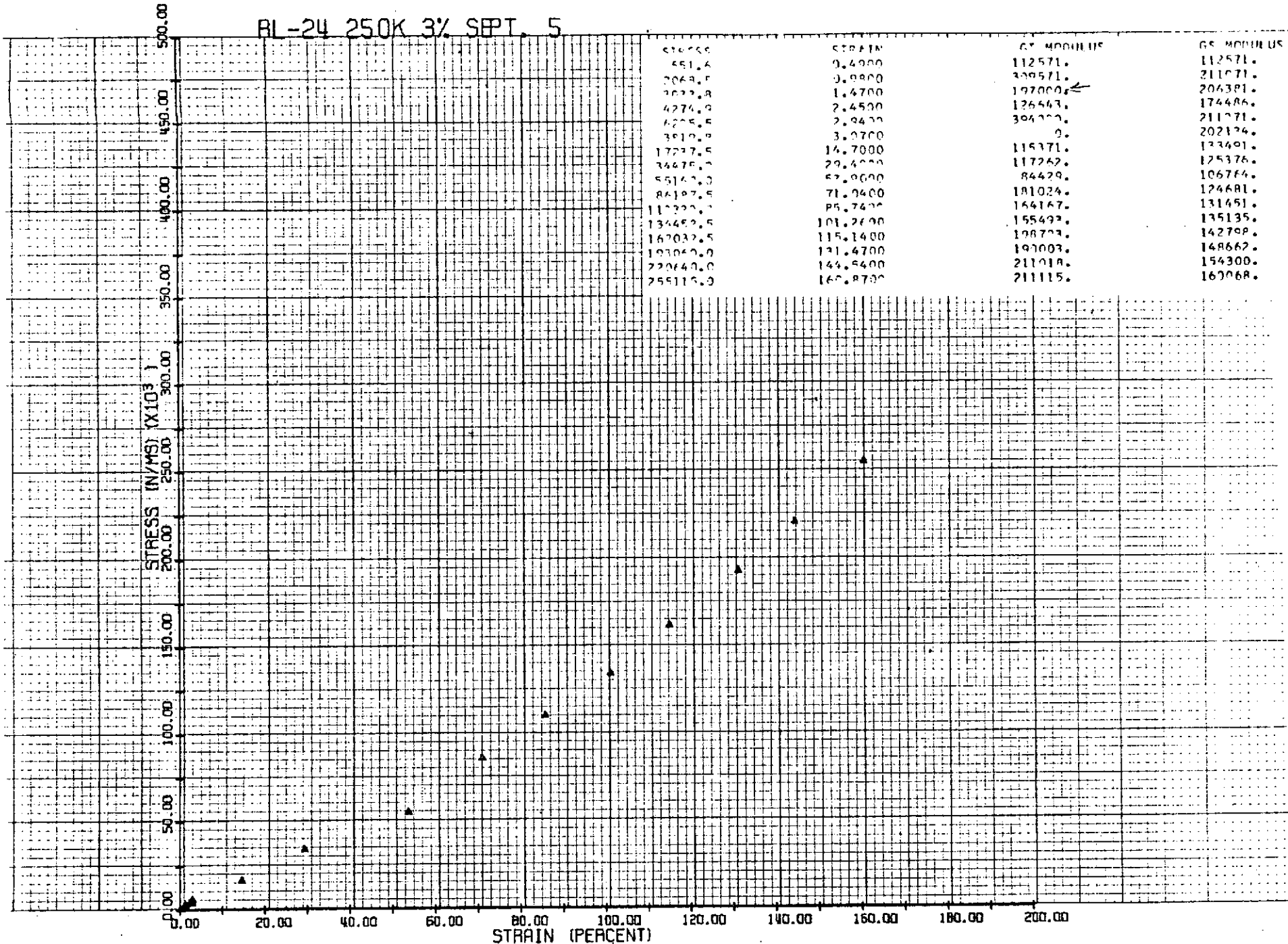


104 A

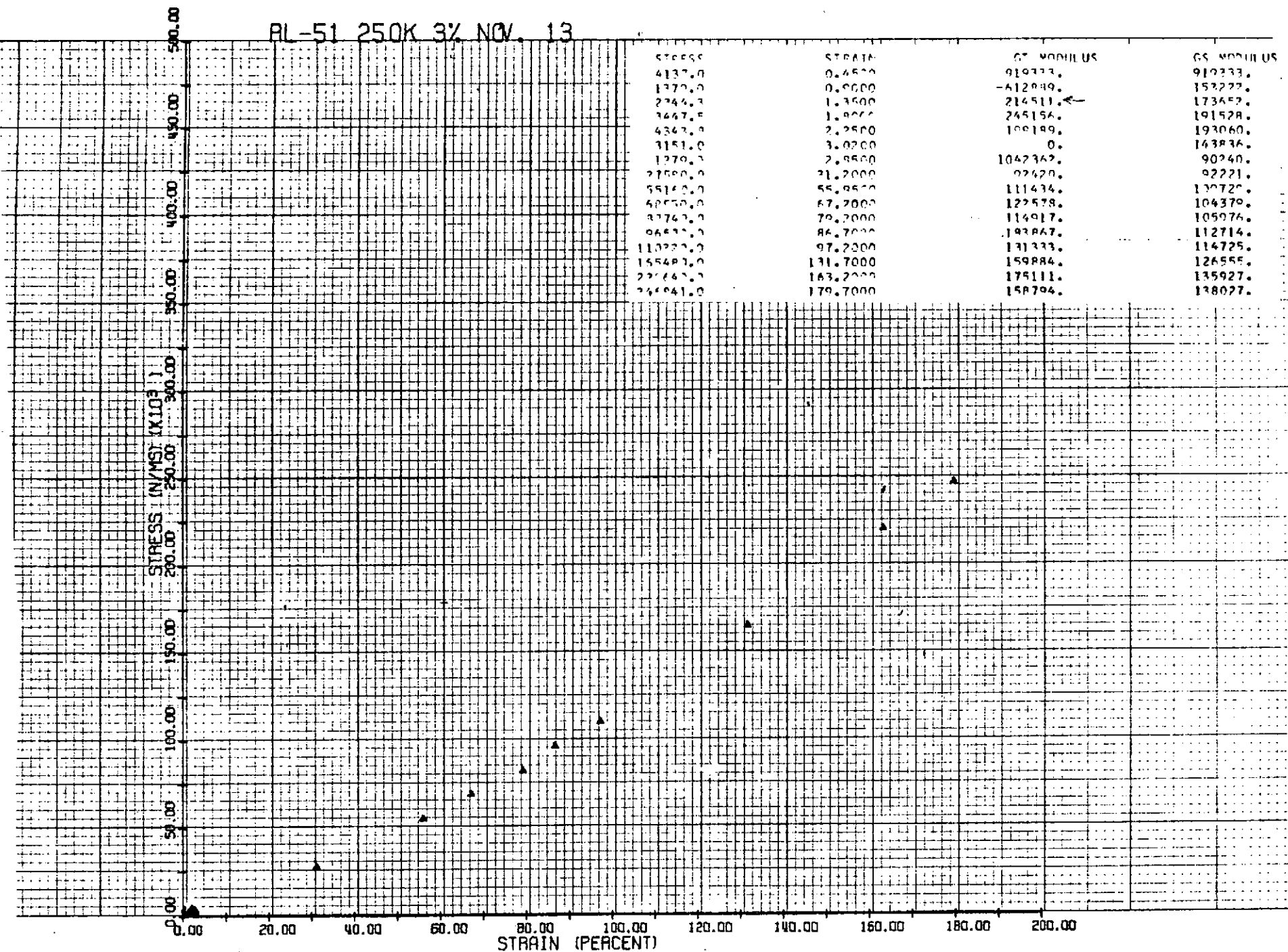
BL-23 250K 1% SEPT. 7



RL-24 25.0K 3% SEPT. 5



PL-51 250K 3% NOV. 13



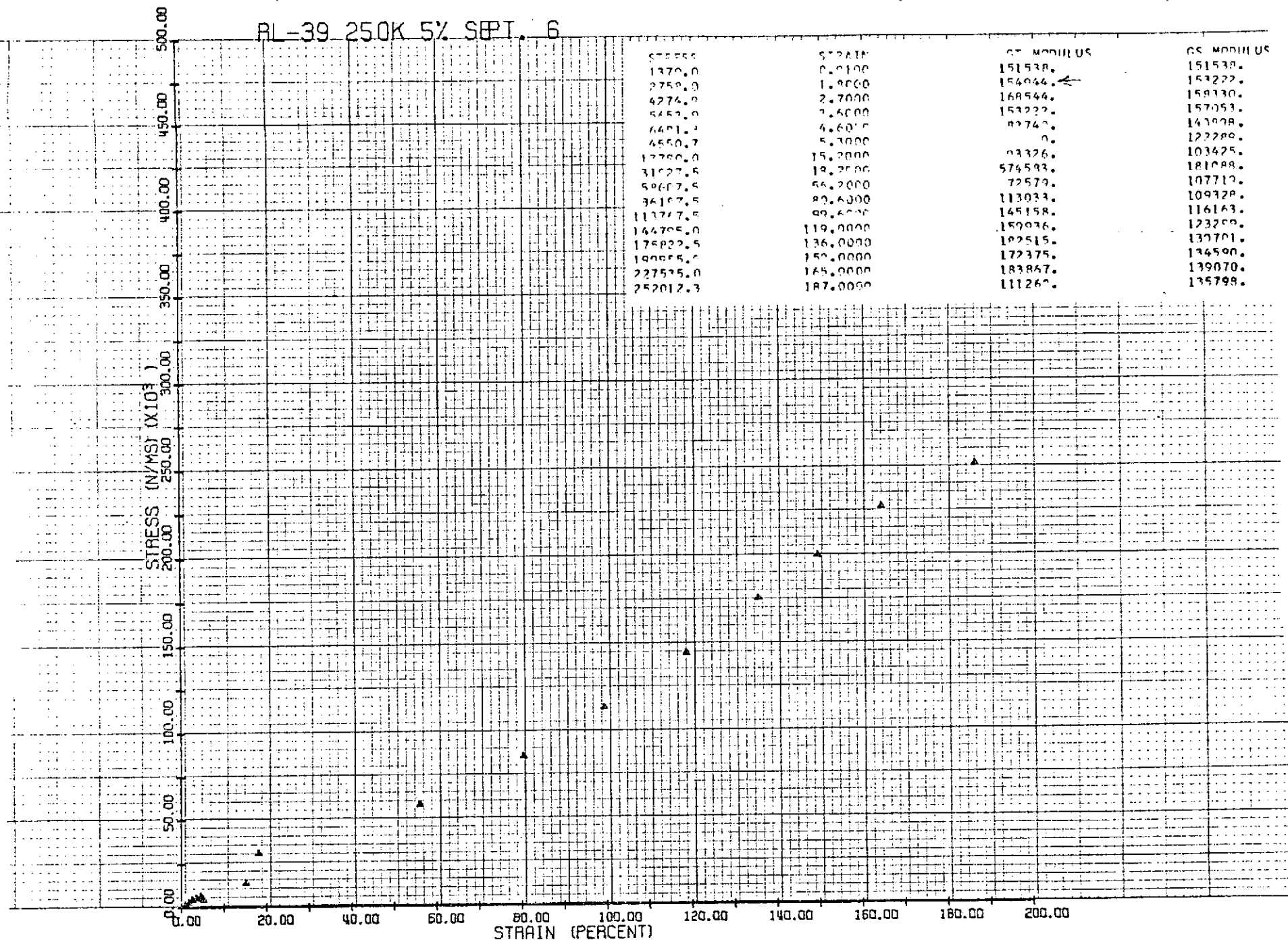
107 A



K-E KEUFFEL & ESSER CO.

PRINTED IN U.S.A.

108

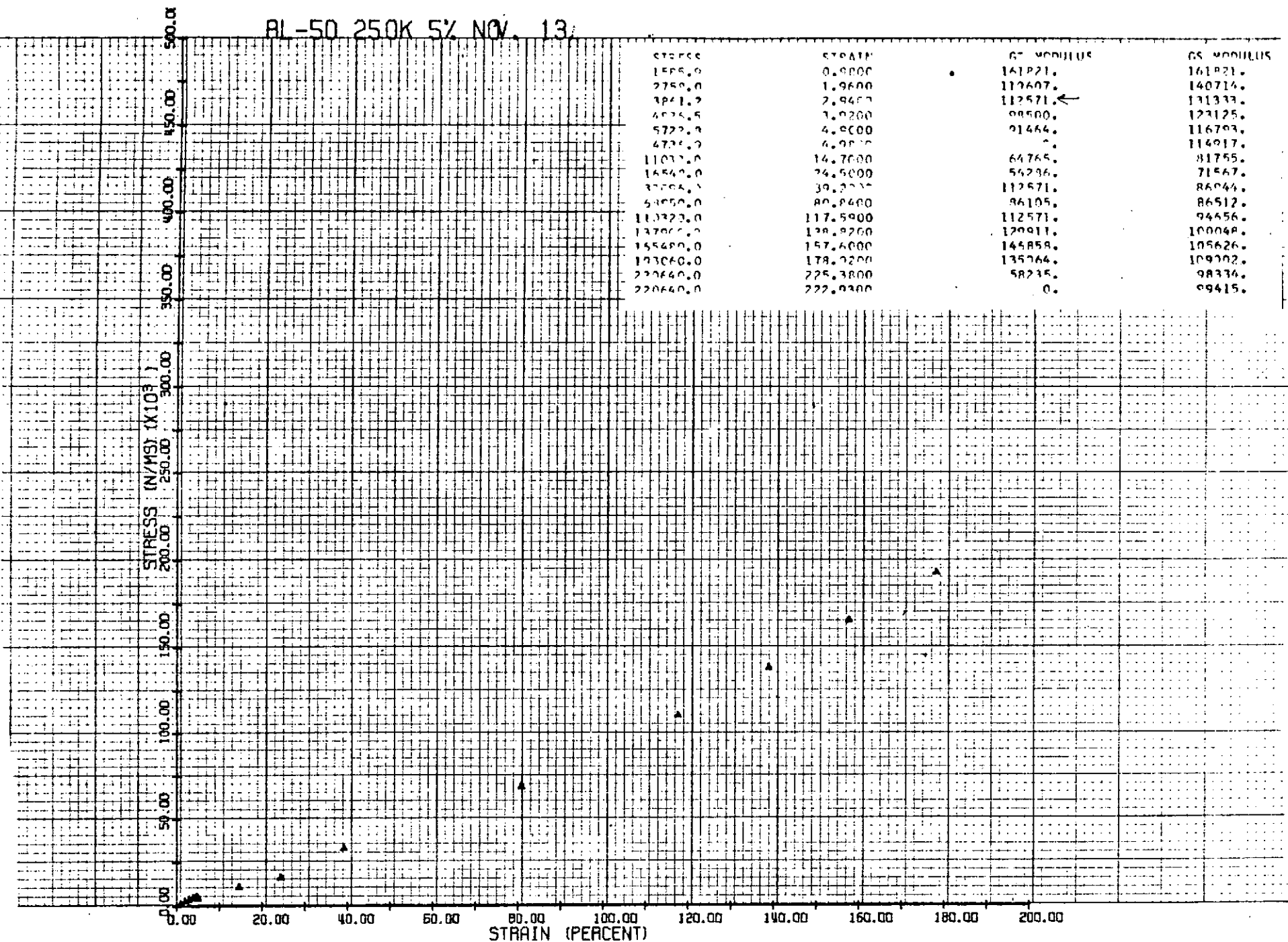


K+E

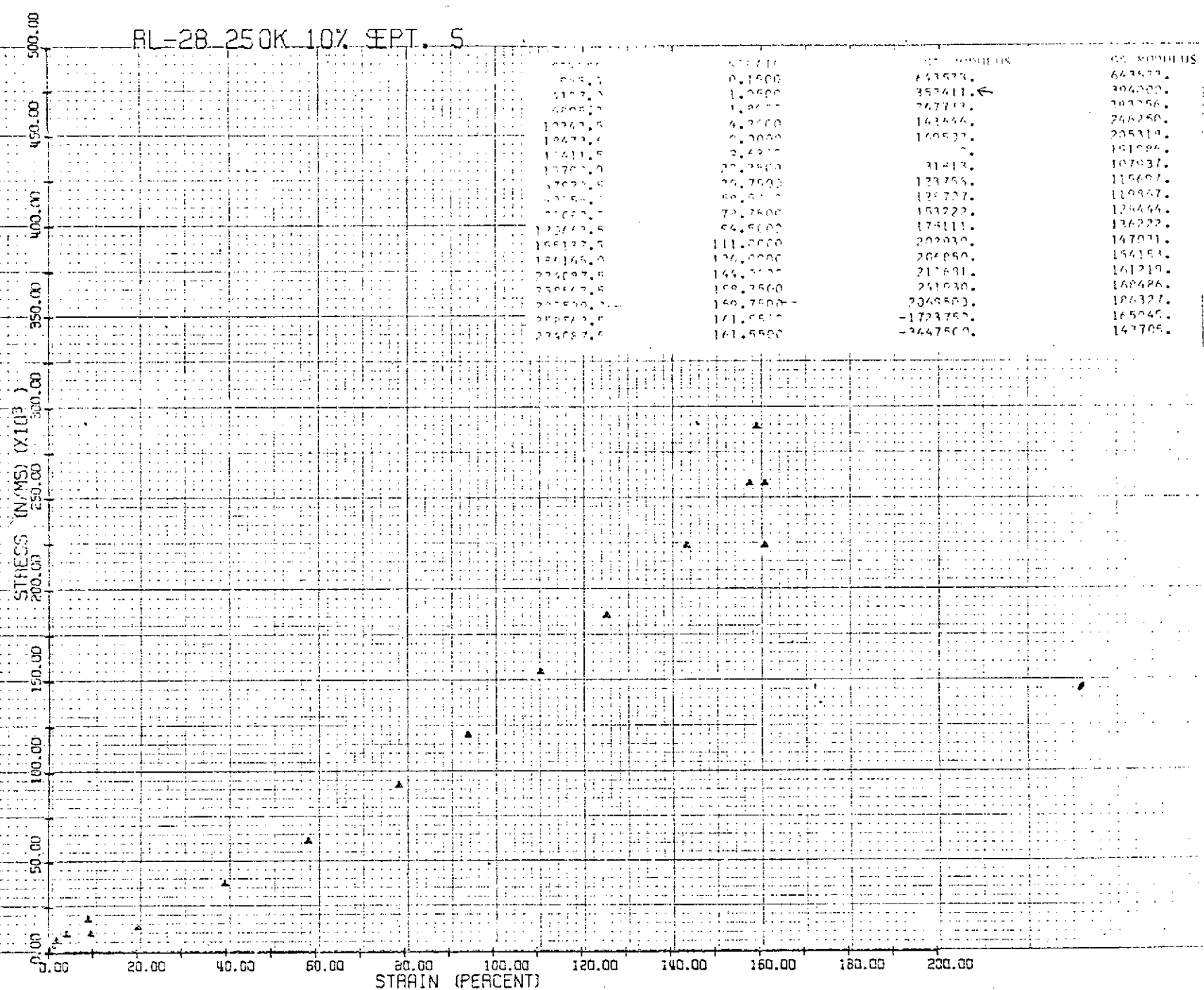
KEUFFEL &amp; ESSER CO.

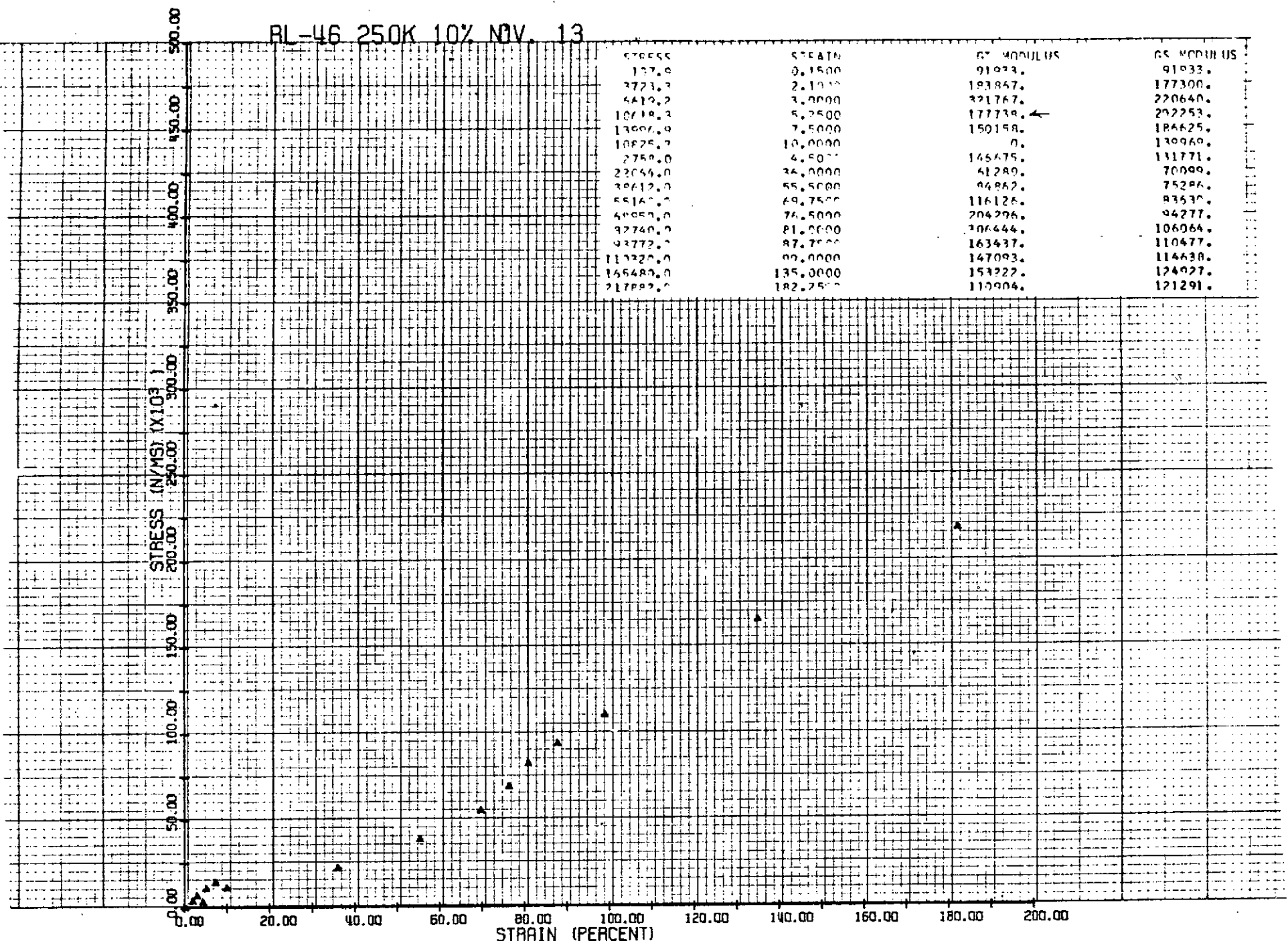
PRINTED IN U.S.A.

## RL-50 250K 5% Nov. 13



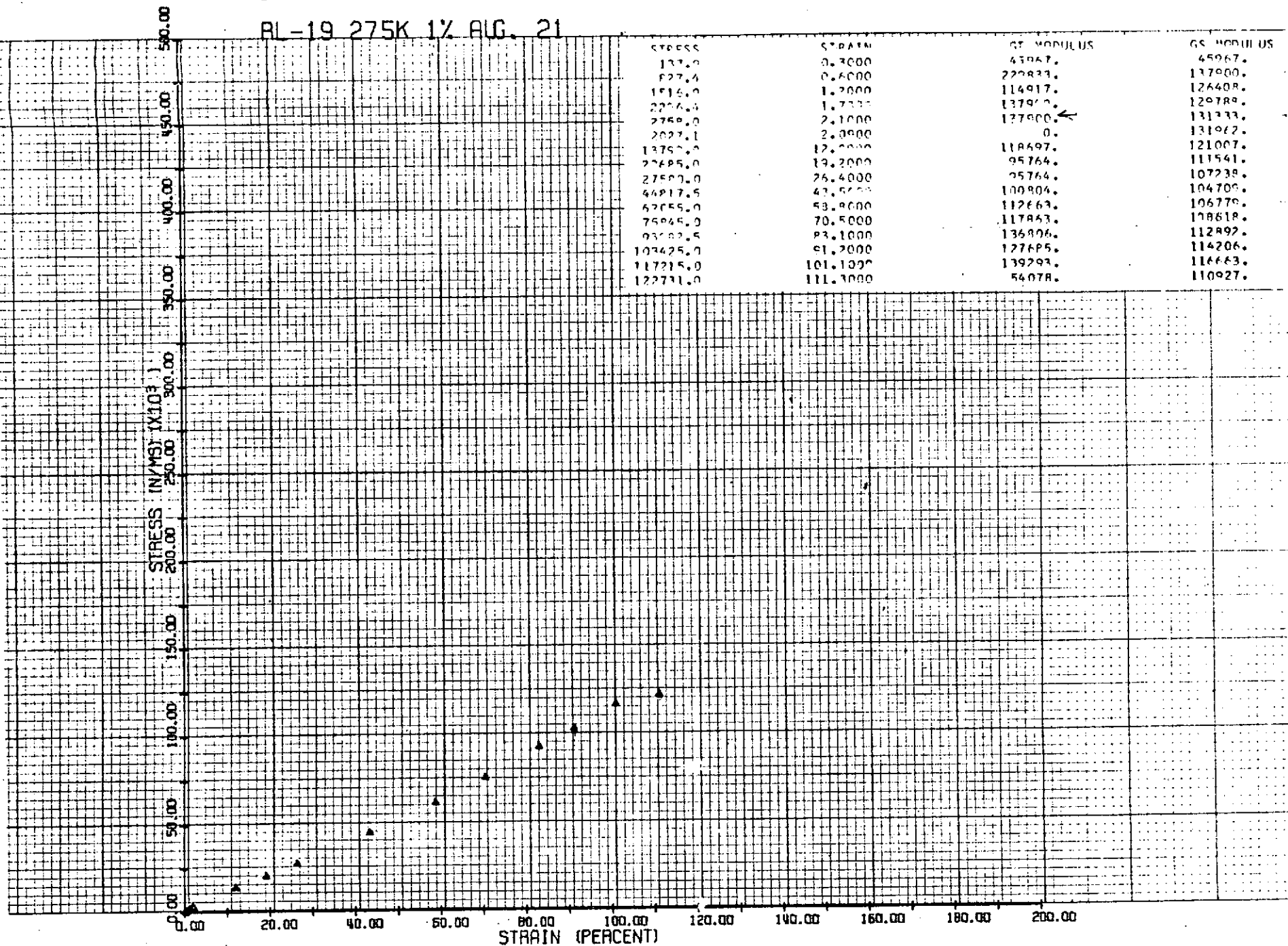
RL-28 250K 10% SEPT. 5



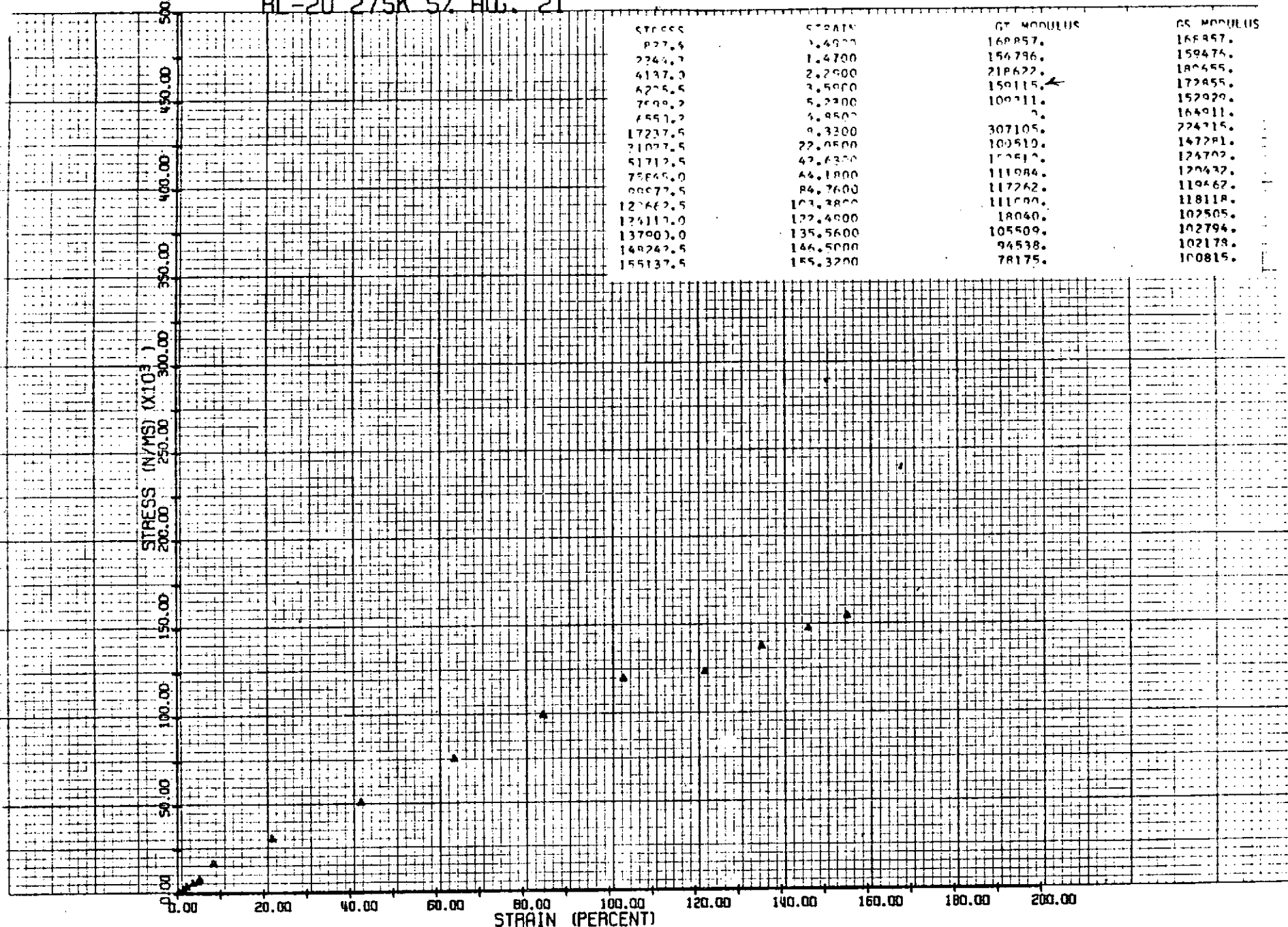


RL-19 275K 1X AUG. 21

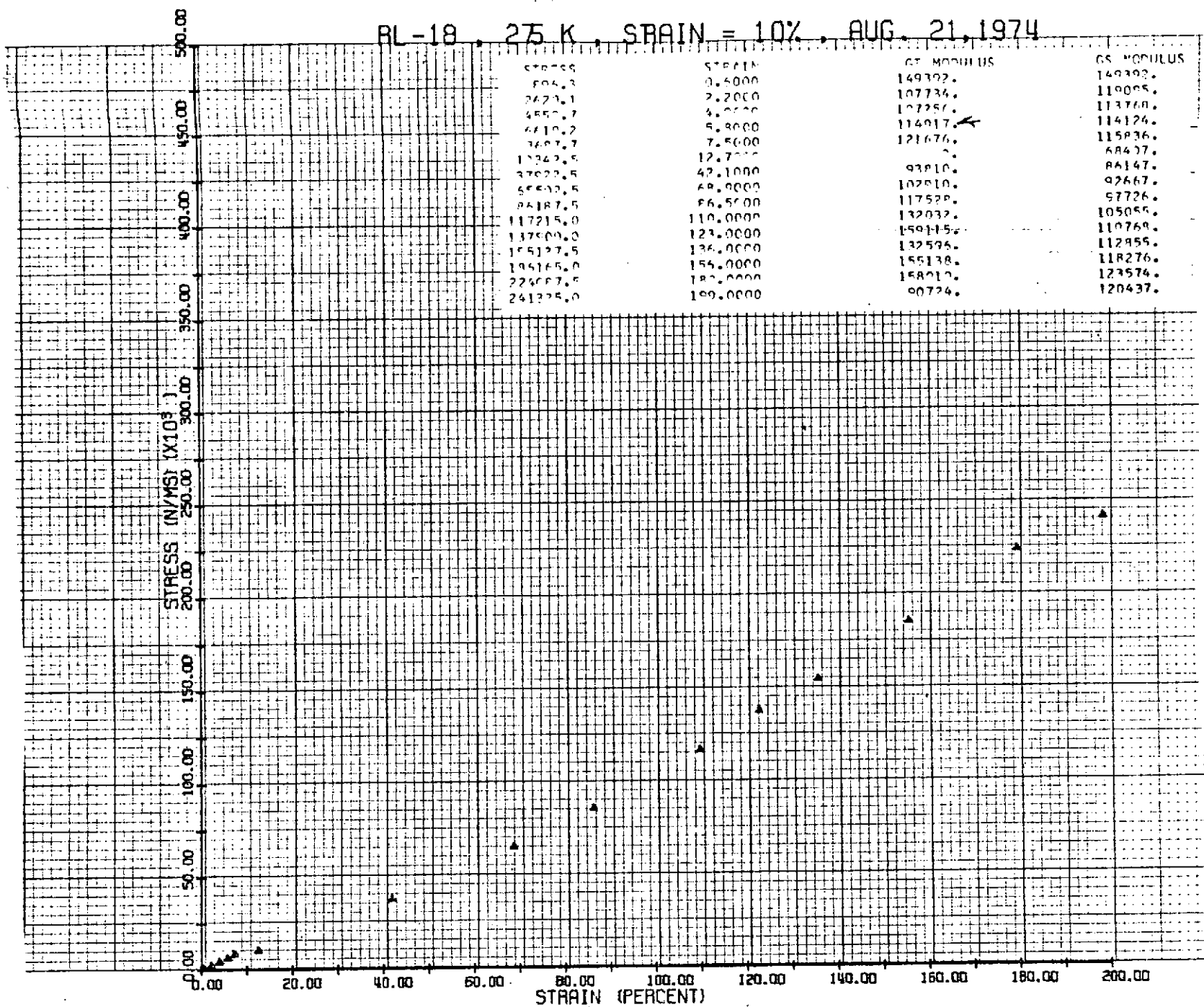
STRESS	STRAIN	G. MODULUS	G. MODULUS
137.0	0.3000	45067.	45067.
137.0	0.6000	220831.	137000.
1515.0	1.2000	114917.	126408.
2256.0	1.7000	13797.	120789.
2750.0	2.1000	127900.	131233.
2027.1	2.0000	0.	131922.
13757.0	12.0000	118697.	121007.
22685.0	19.2000	95764.	111541.
27507.0	26.4000	25764.	107238.
44817.5	47.5100	100804.	104700.
62055.0	53.8000	112663.	106776.
75945.0	70.5000	117853.	108618.
93182.5	93.1000	136804.	112892.
103425.0	91.2000	127685.	114206.
117215.0	101.1000	139293.	114663.
122731.0	111.3000	54078.	110927.



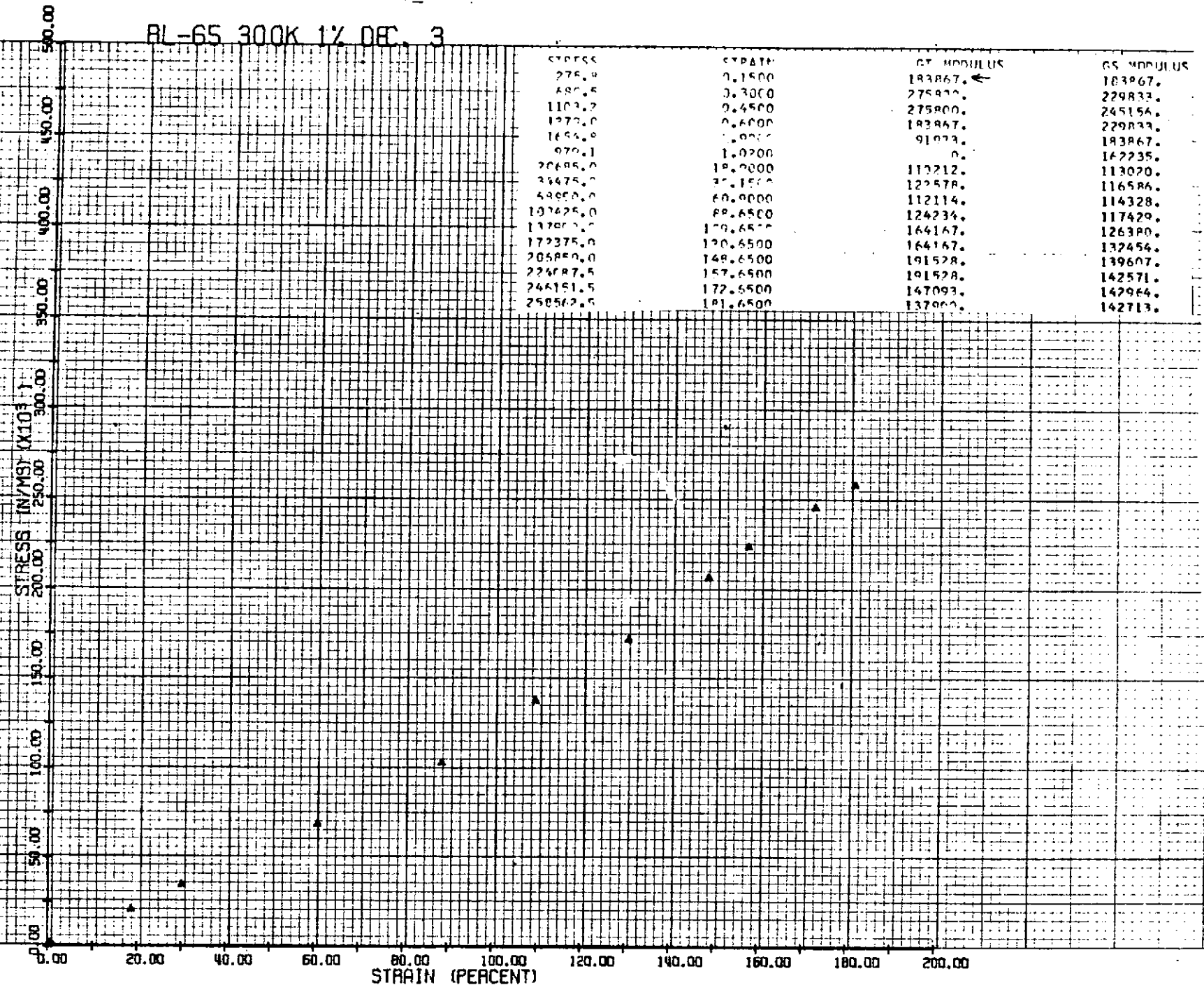
## RL-20 275K 5% ALG. 21



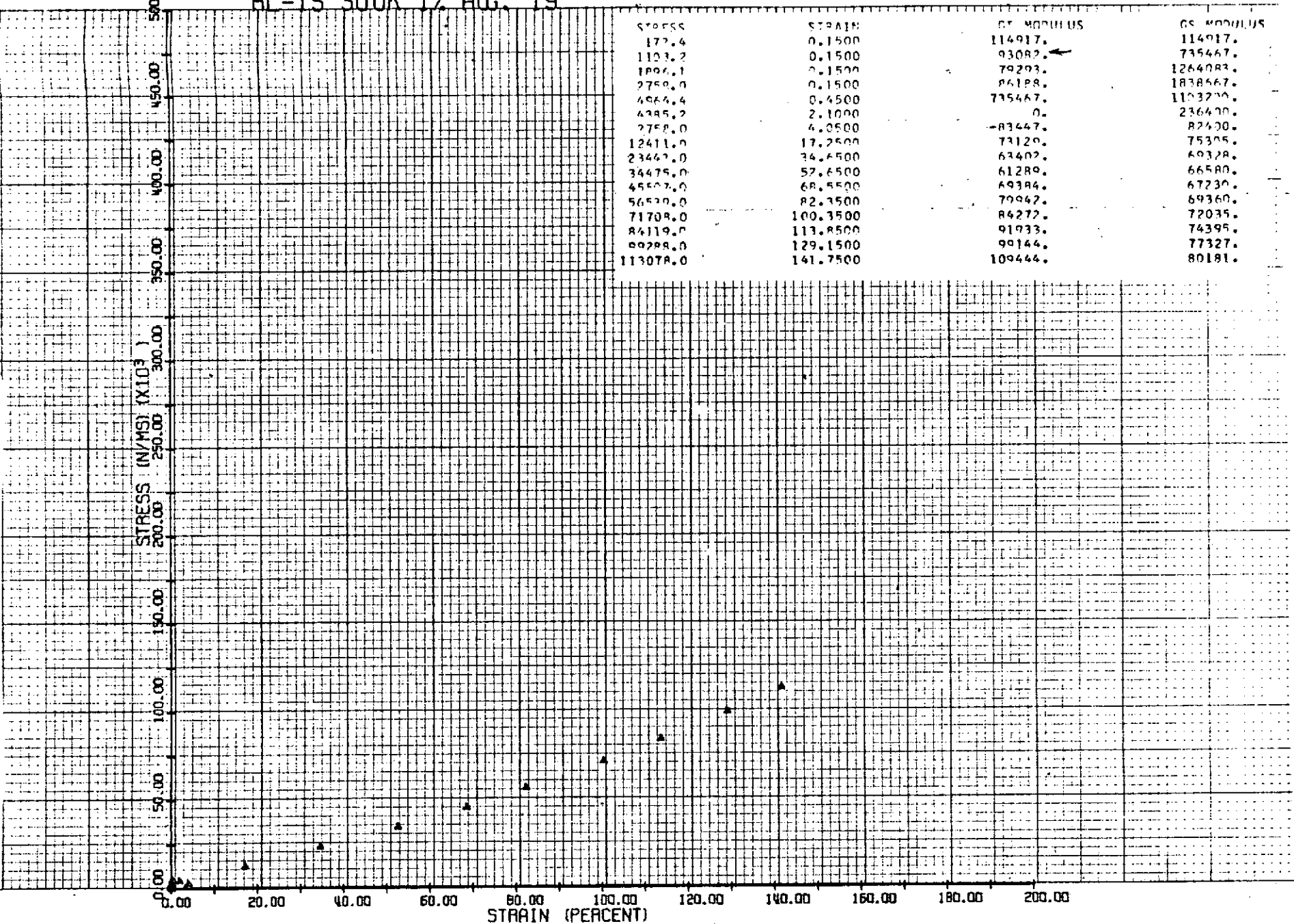
114 A



RL-65 300K 1% DEC. 3

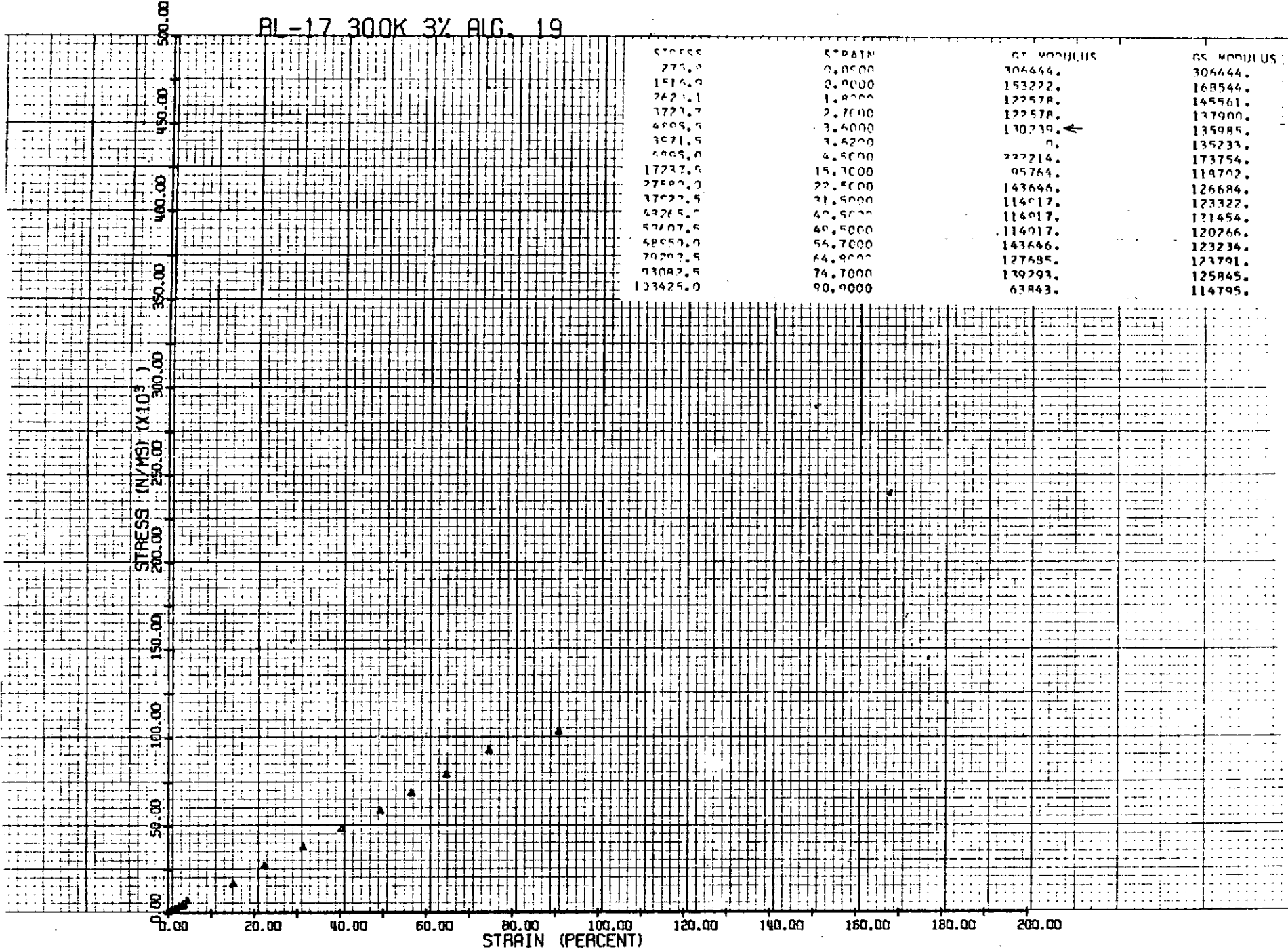


## RL-15 300K 1% ALG. 19



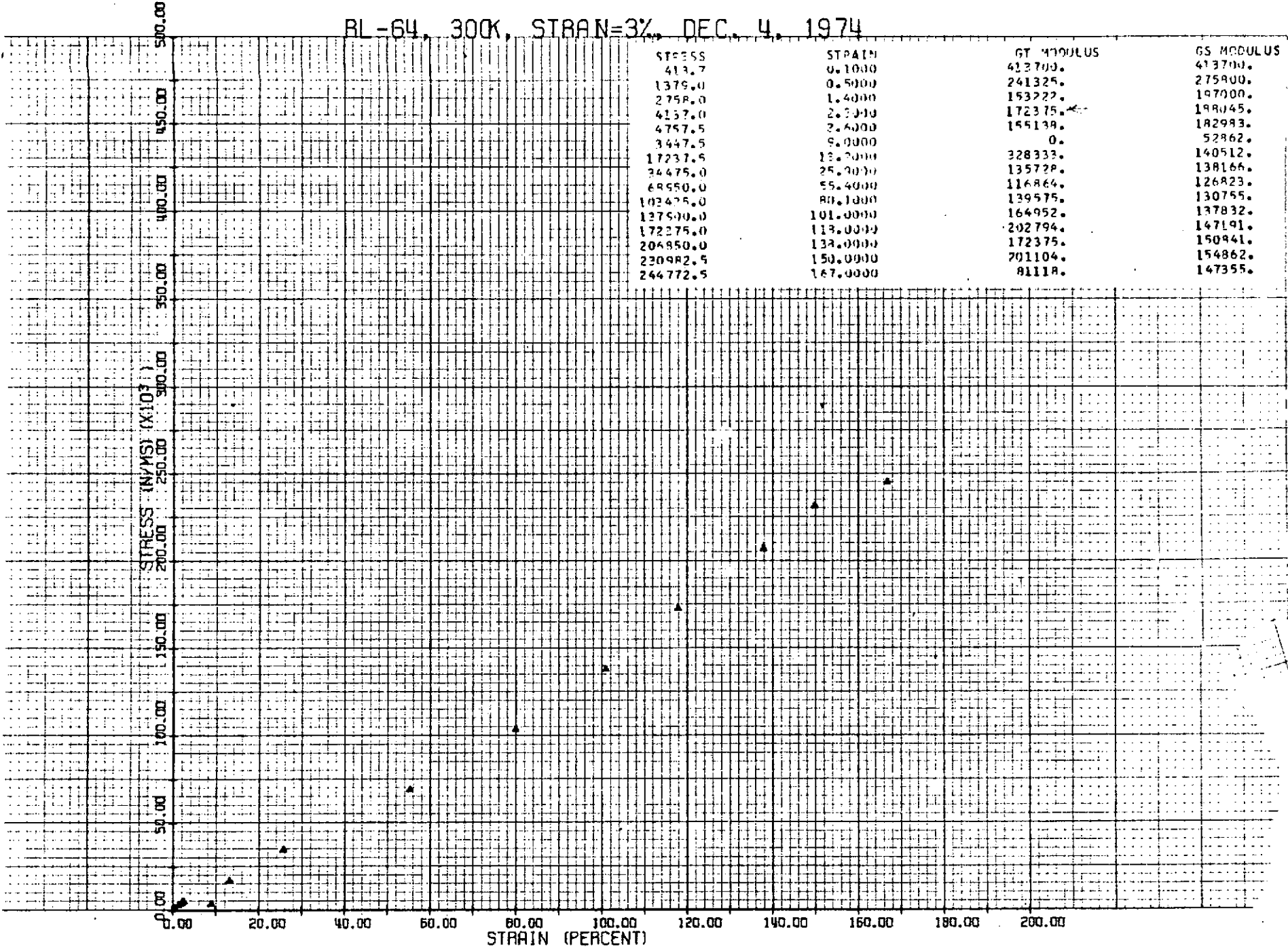
## BL-17 300K 3% ALG. 19

1C



RL-64, 300K, STRAN=3%, DEC. 4, 1974

STRESS	STRAIN	GT. HOOJUS	GS. HOOJUS
413.7	0.1000	413700.	413700.
1379.0	0.5000	241325.	275900.
2758.0	1.4000	153222.	197000.
4157.0	2.3040	172375.	198145.
4757.5	2.4000	145138.	182983.
3447.5	9.0000	0.	52862.
17237.5	13.2000	328333.	140512.
34475.0	25.2000	135728.	138166.
68550.0	55.4000	116864.	126823.
102475.0	80.1000	139575.	130755.
127500.0	101.0000	164952.	137832.
172275.0	113.0000	202794.	147191.
206850.0	132.0000	172375.	150841.
230982.5	150.0000	201104.	154862.
244772.5	167.0000	81118.	147355.



BL-5 300K 5% AUG 20

500.00

STRESS (IN.10<sup>3</sup>)

500.00

450.00

400.00

350.00

300.00

250.00

200.00

150.00

100.00

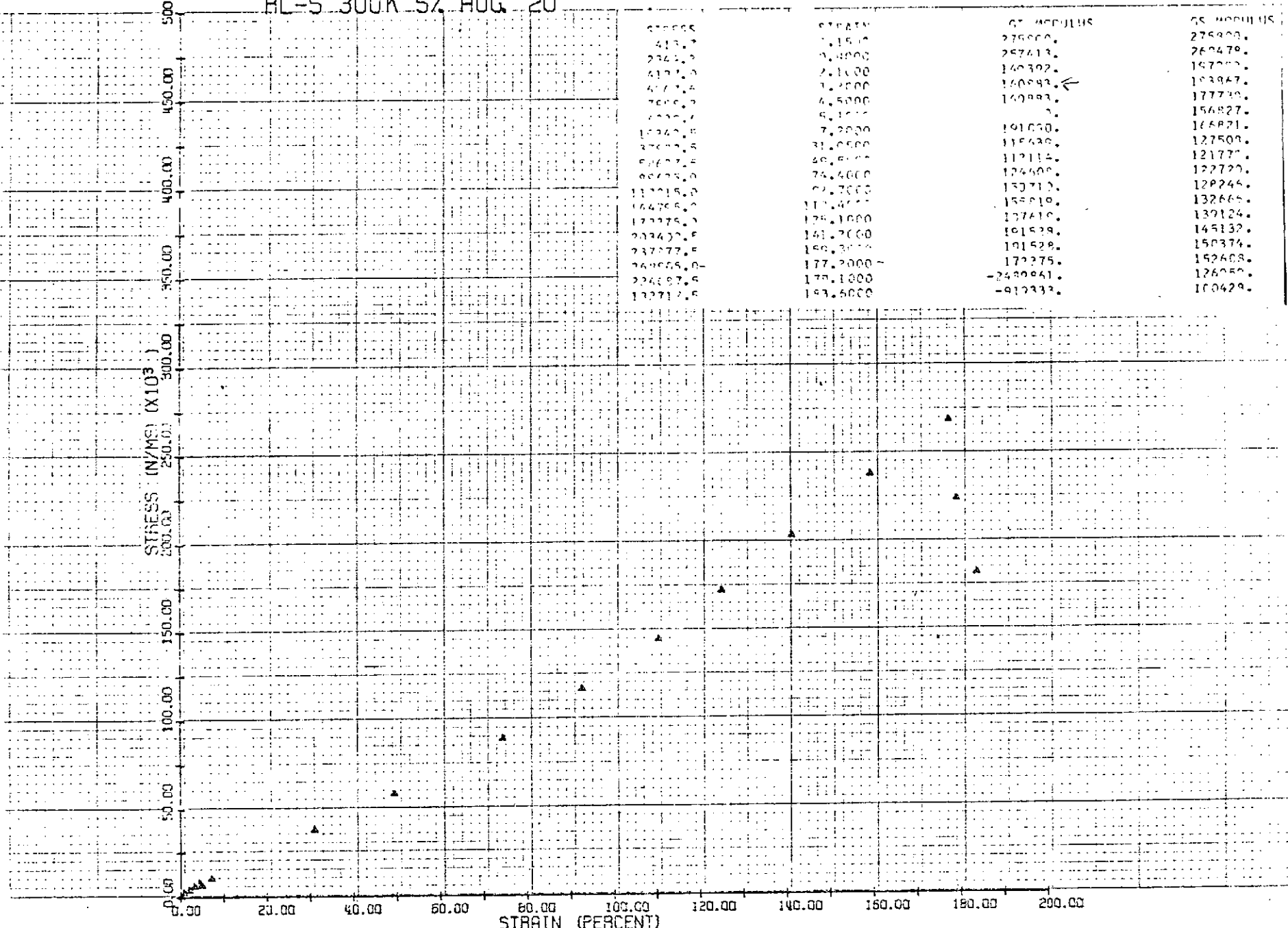
50.00

0.00

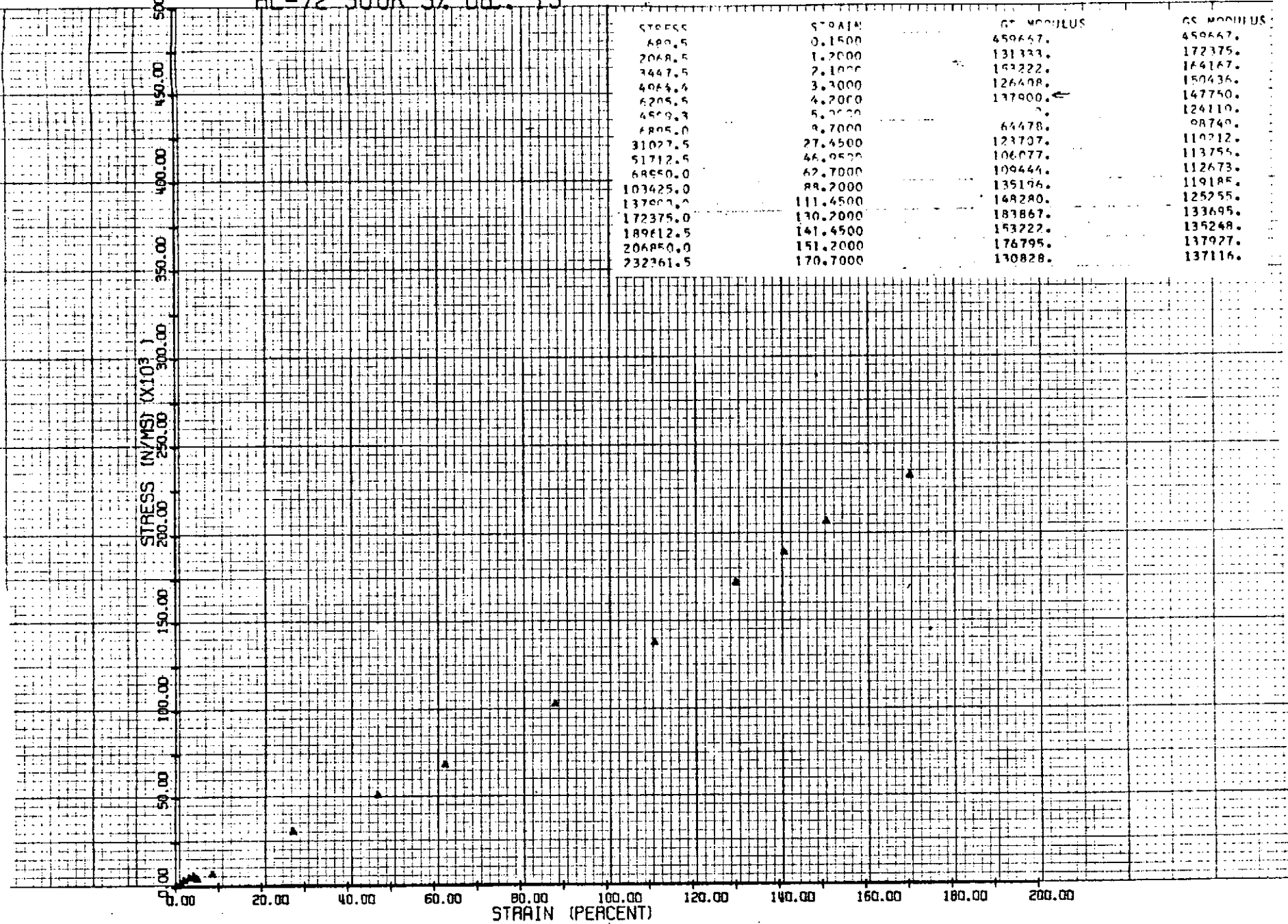
STRAIN (PERCENT)

STRAIN	G. MODULUS	G. MODULUS
0.151%	275000.	275000.
0.400%	257413.	262479.
0.600%	140392.	147207.
0.800%	140847.	143347.
1.000%	140883.	177710.
1.200%	140883.	156827.
1.400%	140883.	165821.
1.600%	140883.	127500.
1.800%	140883.	121777.
2.000%	140883.	122722.
2.200%	140883.	128244.
2.400%	140883.	132662.
2.600%	140883.	139124.
2.800%	140883.	145132.
3.000%	140883.	150374.
3.200%	140883.	152408.
3.400%	140883.	126053.
3.600%	140883.	100429.

V6TT



## BL-72 300K 5% DEC. 13



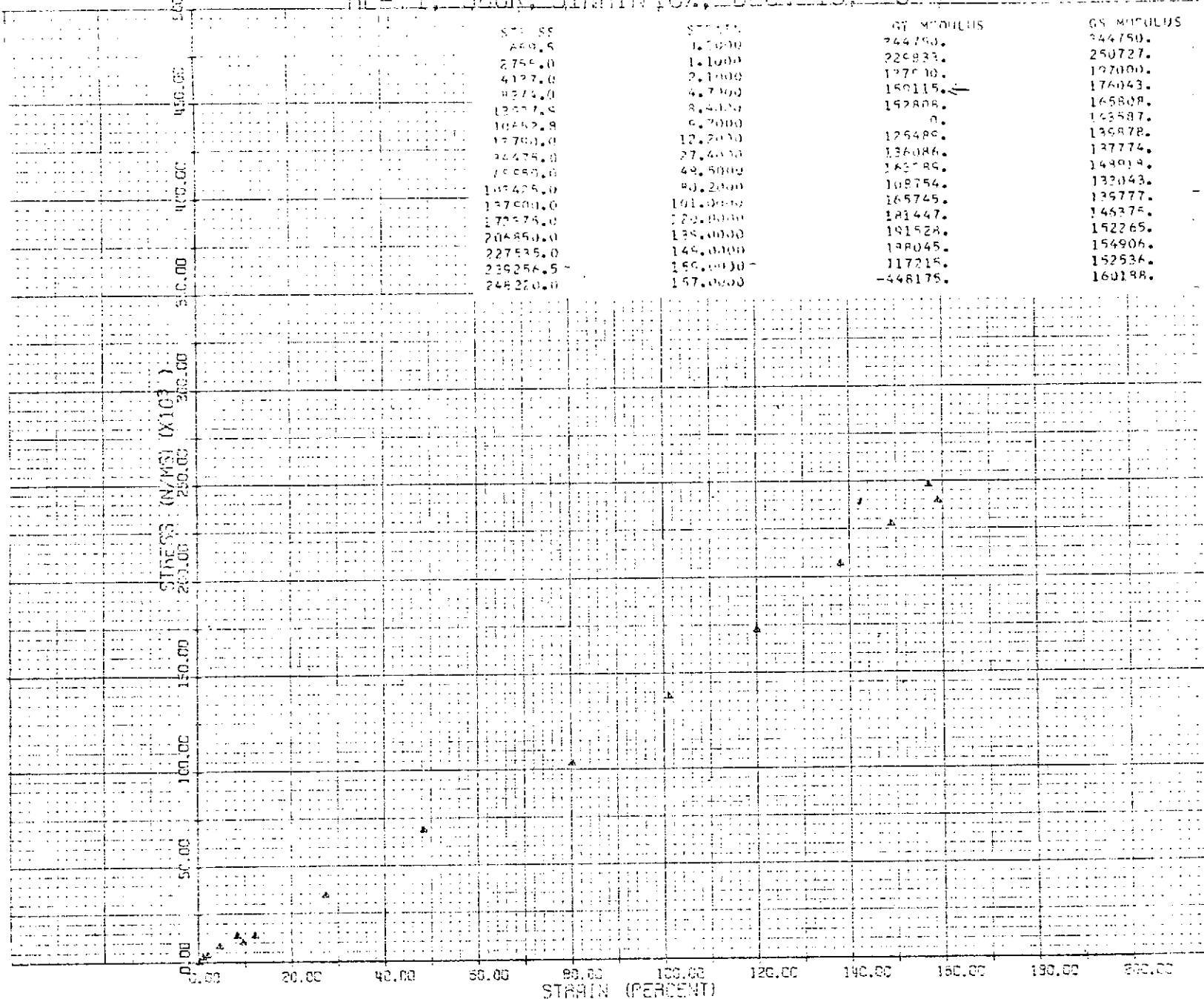
RL-9 300K 10% AUG. 20

STRAIN	STRESS (N/mm <sup>2</sup> )	STRESS (Kpsi)	GS. MODULUS
0.00	0.00	0.00	01033.
12.0	10.00	1.45	10153.
24.0	20.00	2.90	10222.
36.0	30.00	4.35	10277.
48.0	40.00	5.80	10327.
60.0	50.00	7.25	10375.
72.0	60.00	8.70	10421.
84.0	70.00	10.15	10467.
96.0	80.00	11.60	10511.
108.0	90.00	13.05	10554.
120.0	100.00	14.50	10598.
132.0	110.00	15.95	10642.
144.0	120.00	17.40	10686.
156.0	130.00	18.85	10730.
168.0	140.00	20.30	10774.
180.0	150.00	21.75	10818.
192.0	160.00	23.20	10862.
204.0	170.00	24.65	10906.
216.0	180.00	26.10	10950.
228.0	190.00	27.55	10994.
240.0	200.00	29.00	11038.
252.0	210.00	30.45	11082.
264.0	220.00	31.90	11126.
276.0	230.00	33.35	11170.
288.0	240.00	34.80	11214.
300.0	250.00	36.25	11258.
312.0	260.00	37.70	11302.
324.0	270.00	39.15	11346.
336.0	280.00	40.60	11390.
348.0	290.00	42.05	11434.
360.0	300.00	43.50	11478.
372.0	310.00	44.95	11522.
384.0	320.00	46.40	11566.
396.0	330.00	47.85	11610.
408.0	340.00	49.30	11654.
420.0	350.00	50.75	11698.
432.0	360.00	52.20	11742.
444.0	370.00	53.65	11786.
456.0	380.00	55.10	11830.
468.0	390.00	56.55	11874.
480.0	400.00	58.00	11918.
492.0	410.00	59.45	11962.
504.0	420.00	60.90	12006.
516.0	430.00	62.35	12050.
528.0	440.00	63.80	12094.
540.0	450.00	65.25	12138.
552.0	460.00	66.70	12182.
564.0	470.00	68.15	12226.
576.0	480.00	69.60	12270.
588.0	490.00	71.05	12314.
600.0	500.00	72.50	12358.
612.0	510.00	73.95	12402.
624.0	520.00	75.40	12446.
636.0	530.00	76.85	12490.
648.0	540.00	78.30	12534.
660.0	550.00	79.75	12578.
672.0	560.00	81.20	12622.
684.0	570.00	82.65	12666.
696.0	580.00	84.10	12710.
708.0	590.00	85.55	12754.
720.0	600.00	87.00	12798.
732.0	610.00	88.45	12842.
744.0	620.00	89.90	12886.
756.0	630.00	91.35	12930.
768.0	640.00	92.80	12974.
780.0	650.00	94.25	13018.
792.0	660.00	95.70	13062.
804.0	670.00	97.15	13106.
816.0	680.00	98.60	13150.
828.0	690.00	100.05	13194.
840.0	700.00	101.50	13238.
852.0	710.00	102.95	13282.
864.0	720.00	104.40	13326.
876.0	730.00	105.85	13370.
888.0	740.00	107.30	13414.
900.0	750.00	108.75	13458.
912.0	760.00	110.20	13502.
924.0	770.00	111.65	13546.
936.0	780.00	113.10	13590.
948.0	790.00	114.55	13634.
960.0	800.00	116.00	13678.
972.0	810.00	117.45	13722.
984.0	820.00	118.90	13766.
996.0	830.00	120.35	13810.
1008.0	840.00	121.80	13854.
1020.0	850.00	123.25	13898.
1032.0	860.00	124.70	13942.
1044.0	870.00	126.15	13986.
1056.0	880.00	127.60	14030.
1068.0	890.00	129.05	14074.
1080.0	900.00	130.50	14118.
1092.0	910.00	131.95	14162.
1104.0	920.00	133.40	14206.
1116.0	930.00	134.85	14250.
1128.0	940.00	136.30	14294.
1140.0	950.00	137.75	14338.
1152.0	960.00	139.20	14382.
1164.0	970.00	140.65	14426.
1176.0	980.00	142.10	14470.
1188.0	990.00	143.55	14514.
1200.0	1000.00	145.00	14558.

STRAIN (PERCENT) STRAIN (PERCENT) STRESS (N/mm<sup>2</sup>) STRESS (Kpsi)

STRAIN (PERCENT)

## RL-71, 300K, SIRAIN-10%, DEC. 13, 1971



122 A